Universidad Pública de Navarra
Nafarroako Unibertsitate Publikoa

Departamento de Ciencias del Medio Natural
Natur Ingurunearen Zientzien Saila

Tesis Doctoral

Drought stress responses in *Medicago truncatula* and *Glycine max*: system biology approaches

Memoria presentada por Dña. Amaia Seminario Huarriz para
optar al grado de Doctor con Mención de Doctor Internacional

Pamplona, marzo de 2017

upna

Universidad Pública de Navarra
Nafarroako Unibertsitate Publikoa

upna

Universidad Pública de Navarra
Nafarroako Unibertsitate Publikoa

This work was funded by "*Ministerio Español de Economía y Competitividad*" (AGL-2011-23738/AGR), "*Gobierno de Navarra*" (2016/PI013 LEGUMINOSAS) and "*Fundación Caja Navarra*" (FUNCAN, 07442).

Amaia Seminario Huarriz has been holder of a PhD fellowship from the Public University of Navarra and she has received two mobility grants from the same institution: "*Programa de ayudas de movilidad predoctoral*" (1710/2012, 1506/2013).

upna

Universidad Pública de Navarra
Nafarroako Unibertsitate Publikoa

AGRADECIMIENTOS-ACKNOWLEDGEMENTS

En primer lugar, me gustaría dar las gracias a mis directoras, las Dras Esther González y Estíbaliz Larrainzar, por haberme dado la oportunidad de realizar esta tesis doctoral. Gracias a las dos por vuestro tiempo, dedicación, consejos, apoyo… Esther, gracias por estar siempre disponible y dispuesta a escuchar y por haberme enseñado tanto. Gracias Esti por tu ayuda, por aportarme tantos conocimientos y por esos sabios consejos tanto profesionales como personales.

Gracias a todas las personas del departamento de Ciencias del Medio Natural y especialmente a aquellos pertenecientes al Área de fisiología vegetal. Eskerrik asko Iker por tus aportaciones en este trabajo. Gracias a Susana, Gustavo y Berta por compartir grandes momentos tanto en cafés como en comidas de tupper. Y también gracias a mis compañeros de despacho, Juan y Yueh-Hsin.

I would also like to thank Michael Udvardi from The Samuel Roberts Noble Foundation in Oklahoma, EEUU, for giving me the opportunity to participate in his experiments to improve my knowledge in plant science. My stay there was amazing thanks to Yun and to Ivone, Igor, Catalina, Lia and Shulan, who taught me a lot of things. It was a pleasure working with you!! Moreover, I want to thank Yanina, Alan, Bárbara, Ella, Mayra, Ewelina, Djordje and Pato for enjoying my life-besides-work, and making all the moments even more special. Pero sobre todo, gracias a la madrileña que conocí allá, muchas gracias Ana por explorar conmigo la ciencia y el estilo de vida de Ardmore. Hope to see you again!

La realización de esta tesis me ha permitido dirigir Trabajos Fin de Carrera, Máster, Grado… No me olvido de agradecer a todas las personas que han participado conmigo en experimentos y sus aportaciones en esta tesis: gracias a Maite Rodríguez, Ana Litago, Unai Pérez y Nahikari López.

Eskerrik asko Joseba por esos cafés y comidas tan productivos, por los buenos ratos pasados y por estar siempre al otro lado de la pared dispuesto a escuchar y ayudar. Especialmente gracias a Oskar, fue una suerte trabajar contigo y aprender de tí tanto en lo laboral como en lo personal. Erena…mila esker! Fue una pena no coincidir más tiempo contigo pero fuiste un ejemplo a seguir y aprendí de ti en otras facetas. Gracias por tu apoyo y por los momentos vividos fuera de la uni! Eskerrik asko Miriam por tu apoyo y ayuda en esta última etapa de la tesis, por tu compañía cuando más lo necesitaba y por los buenos ratos pasados... eskerrik asko por todo Txantxita!!

Gracias a Bea y Ane por empezar este camino de la mano y por los buenos momentos juntas durante el máster! Gracias David por esos buenismos ratos que en el último año me han ayudado a desconectar! Y gracias a Libertad también por hacer que esos ratos fueran especiales! Gracias también a todos los que han pasado por el departamento durante este tiempo; Laura, Cristina, Esti U., Maren, Sergio, Iván, Inma, Vero, Maitane, Raquel, Olaya, Karla, Amaia Z, Idoia, Janaina, Ester, Manu... y en especial a Maribel, Ainhoa e Irantzu, muchas gracias por todos los buenos ratos vividos!

Gracias a todos aquellos, ahora biólogos, que experimentaron conmigo mi etapa en la universidad. En especial, me gustaría agradecer su continuo apoyo a Jorge, María, Marijose, Javi y Ariane porque, a pesar de estar ahora cada uno en una punta, siempre nos quedarán los buenos momentos vividos juntos. Y en especial a Álvaro, por tu interés y continuo apoyo en estos años y por los momentos compartidos.

También me gustaría agradecer a ese grupo de chicas que finde a finde sacaba lo mejor de mí simplemente con la ayuda de un balón; risas y buenos momentos que merecen la pena! Eskerrik asko…Aupa Ostiralak!!!!

Después de haber intentado explicaros un montón de veces lo qué he estado haciendo en estos últimos años, espero que con esta tesis os quede un poco más claro. Iosune y Bea, gracias por esos raticos juntas, por vuestra amistad, por apoyarme a seguir adelante y por vuestro continuo interés. Gracias también a mis "Ojo avizor" Ainhoa, Itzi y Raquel, por las continuas risas y grandes momentos pasados juntas ayudándome a desconectar, eskerrik asko!!

Je tiens également à adresser mes sincères remerciements á la famille Baslam pour leur soutien constant et leur grand intérêt, même en étant à plusieurs kilomètres du Pampelune. Un trés gran MERCI à Fatiha, Lahcen, Badreddine et Abdel Mounaim.

Muchísimas gracias a Marouane!! Gracias por guiarme en este camino, por ser mi apoyo en todos los momentos, por tus ánimos a seguir hacia adelante, por tu visión para ver las cosas y sobre todo, por estar siempre a mi lado!

Gracias Abuela por ser un ejemplo a seguir, por tu cariño incondicional. Mención especial a tí abuelo, que allá donde estés, seguro me has seguido de cerca en esta etapa. Gracias a Tari, por estar siempre ahí y a Arantxa. Gracias también a Juanito, Jose e Igor. A mis primos Seminario y por último, a esa amplia familia zubiritarra. Eskerrik asko ere nire Urnietako familiari. Y en general, a toda la gente que me ha apoyado día tras día.

Y por último, gracias a mis padres Tere y Pedro, porque sin ellos no habría llegado hasta donde he llegado. Gracias por apoyarme en todo momento, por todo lo que he aprendido de vosotros y porque a pesar de no saber muy bien lo qué hacía, siempre me animabais a tirar para adelante. Gracias también a mi hermana Izaskun, por animarme y apoyarme en esta etapa. Gracias a los tres por estar siempre ahí!

MUCHAS GRACIAS A TODOS!!!

ABBREVIATIONS

AP2	Apetala2
AsA	Ascorbic Acid
AZ	Absorption zone
C	Control
D	Drought
D1	Drought 1
D2	Drought 2
DHA	Dehydroascorbic acid
DTT	Dithiothreitol
DW	Dry weight
ERF	Ethylene response factors
ETR	Electron transport rate through PSII
ETRc	Electron flow to the carboxylation reaction of Rubisco
ETRo	Electron flow to the oxygenation reaction of Rubisco
FW	Fresh weight
GABA	γ-aminobutyric acid
GalL	L-galactono-1,4-lactone
GalLDH	L-galactono-1,4-lactone dehydrogenase
GC-MS	Gas chromatography-mass spectrometry
GSH	Reduced Glutathione
GST	Glutathione S-transferase
LOX	Lipoxygenase
MD	Moderate drought
MDA	Malondialdehyde
MPa	Megapascal
MS	Mild stress
MSTFA	Methyltrimethylsilyltrifluoroacetamide
PEG	Polyethylene glycol
qRT-PCR	Quantitative reverse transcription polymerase chain reaction
QTL	Quantitive trait locus
RH	Root hair zone

RNA-Seq	Ribonucleic acid-sequencing
ROS	Reactive oxygen species
SD	Severe drought
SE	Standard error
TBA	Thiobarbituric acid
TCA	Trichloroacetic acid
TF	Transcription factor
TMSC	N-methyl-N-trimethylsilyltrifluoroacetamide
TRIS	Tris(hydroxymethyl)aminomethane
UHPLC	Ultra-high-performance liquid chromatography
VMS	Very mild stress
w/v	Weight by volume
WC	Water content
Ψw	Water potential

SUMMARY

After cereals, legumes are crops of great economic importance. However, legume plants are very sensitive to abiotic stresses, being drought one of the most harmful stress in terms of crop production. The general aim of the present work is to gain further insights into two legume species (*Medicago truncatula* and *Glycine max*) drought responses at the shoot and root level by using a combination of physiological, morphological, transcriptomic and metabolomic approaches.

Ascorbic acid (AsA) is one of the most abundant water-soluble antioxidant compound present in plant tissues involved in plant enzymatic and non-enzymatic detoxification mechanisms. Nevertheless, little is known on the regulation of this antioxidant biosynthesis pathway under drought stress. In chapter 1, through a combination of molecular and physiological approaches, we observed that AsA biosynthesis was severely affected by drought in soybean plants. These analyses showed that drought triggered multiple control points regulating AsA biosynthesis at the GDP-D-mannose pyrophosphorylase and GDP-D-mannose 3´, 5´-epimerase level of soybean plants. In parallel, these responses were also observed in the model legume *M. truncatula.*

In chapter 2, work presented here showed the tight link between above- and below-ground organs in *M. truncatula* plants and the fact that, under drought stress conditions, adult plants prioritized root growth over leaf development. Actually, different analyses showed responses which suggest a passive survival strategy for leaves coexisting with an active engagement of the root in drought-stressed plants.

New non-destructive and non-toxic protocols are needed to simulate drought conditions to better characterize plant responses under controlled conditions. To that end, in chapter 3, a new simple, efficient and reproducible method is presented to simulate *in vitro* drought stress conditions in *M. truncatula* seedlings grown on plates containing different agar concentrations. After validating of this method, it was observed that roots, rather than shoots, play a key role in plant adaptation to stress conditions. The relative simplicity of the method allows for its large-scale application in studies such as population screening for drought resistance traits in a variety of plants. Additionally, in chapter 4 we applied this method in combination with physiological, transcriptomic and metabolomic analyses in one of the most important parts of the root, the absorption zone, responsible for absorbing water and nutrients thus allowing the plant growth. Results led us to conclude that plants exhibited fast molecular responses under drought conditions; the metabolism of lipids, hormones, cell wall and secondary metabolism were some of the pathways most severely affected.

To sum up, work presented here provides new insights into the understanding of legume responses to water-limiting conditions and contributes towards elucidating water stress signals and gene networks controlling the response of legume plants to drought.

upna

Universidad Pública de Navarra
Nafarroako Unibertsitate Publikoa

RESUMEN

Las leguminosas, después de los cereales, son el cultivo de mayor importancia económica a nivel mundial. Sin embargo, estas plantas son muy sensibles a los estreses abióticos, siendo la sequía el que más afecta a su producción. El objetivo general del presente trabajo es ampliar los conocimientos sobre las respuestas a sequía de la parte aérea y la raíz de dos especies de leguminosas (*Medicago truncatula* y *Glycine max*) mediante la combinación de enfoques fisiológicos, morfológicos, transcriptómicos y metabolómicos.

El ácido ascórbico (AsA) es uno de los antioxidantes más abundantes en los tejidos vegetales que está involucrado en mecanismos enzimáticos y no enzimáticos de desintoxicación celular. Sin embargo, poco se sabe sobre la regulación de su biosíntesis bajo situaciones de estrés por sequía. En el capítulo 1 de este estudio, a través de una combinación de enfoques moleculares y fisiológicos, se observó que la biosíntesis del AsA está gravemente afectada por la sequía. Estos análisis mostraron que en plantas de soja sometidas a condiciones de estrés hídrico existen múltiples puntos de control que regulan la biosíntesis de AsA a nivel de la GDP-D-manosa pirofosforilasa y de la GDP-D-manosa 3 ', 5'-epimerasa. Estas respuestas también se observaron en la leguminosa modelo *M. truncatula*.

En el segundo capítulo de este trabajo se muestra el estrecho vínculo existente entre la parte aérea y la raíz de plantas de *M. truncatula.* Así, bajo condiciones de sequía, las plantas adultas priorizaron el crecimiento de las raíces frente al desarrollo foliar. Los diferentes análisis mostraron respuestas que sugieren una estrategia de supervivencia pasiva para las hojas coexistentes con un compromiso activo de la raíz en las plantas afectadas por la sequía.

Existe la necesidad de desarrollar nuevos protocolos no destructivos y no tóxicos que simulen condiciones de sequía para caracterizar mejor las respuestas de las plantas bajo condiciones controladas. En el capítulo 3 se presenta un nuevo método simple, eficiente y reproducible para simular condiciones *in vitro* de estrés por sequía en plántulas de *M. truncatula* crecidas en diferentes concentraciones de agar. Después de validar el uso de este método, se observó que las raíces desempeñan un papel clave en la adaptación de la planta a estas condiciones de estrés. La simplicidad de este método permite el análisis de poblaciones a gran escala para identificar rasgos de resistencia a la sequía en una variedad de plantas. Por último, en el capítulo 4, el método descrito en el capítulo anterior fue aplicado en combinación con análisis fisiológicos, transcriptómicos y metabolómicos al análisis de la zona de absorción de la raíz responsable de la absorción de agua y nutrientes para el crecimiento de la planta. Los resultados indicaron que las plantas mostraron rápidas respuestas moleculares bajo condiciones de sequía; el metabolismo de lípidos, hormonas, la composición de la pared celular y el metabolismo secundario se vieron muy afectados permitiendo a las plantas hacer frente a situaciones de estrés por sequía.

En resumen, este trabajo proporciona nuevas perspectivas en la comprensión de las respuestas de las leguminosas a las condiciones de limitación de agua y contribuye a aclarar las señales de estrés hídrico y las redes de genes que controlan la respuesta de las plantas leguminosas a la sequía.

upna

Universidad Pública de Navarra
Nafarroako Unibertsitate Publikoa

TABLE OF CONTENTS

upna

Universidad Pública de Navarra
Nafarroako Unibertsitate Publikoa

upna

Universidad Pública de Navarra
Nafarroako Unibertsitate Publikoa

» *GENERAL INTRODUCTION*

upna

Universidad Pública de Navarra
Nafarroako Unibertsitate Publikoa

GENERAL INTRODUCTION

A. LEGUMES

The legume family (Fabaceaea or Leguminosae) contains over 700 genera and 20,000 species, making it the third largest family of flowering plant, after orchids and sunflowers (Doyle and Luckow, 2003) and the second most important food crop after cereals (Liew et al., 2014). This family differs from most other plants in that they have the ability to fix atmospheric nitrogen in symbiosis with rhizobial bacteria and thus do not require nitrogen fertilizer for their growth and development allowing them to colonize soils with different nitrogen availability. In addition, the greatest benefit derived from this crop rotation is the role of legumes as a natural nitrogen fertilizer for the soil due to the process of biological nitrogen fixation and its high nitrogen content (Peoples et al., 2001). Hence, legumes contribute with many benefits to the soil being usually utilized as cover crop, intercropped with cereals and other staple crops. In rotation systems, legumes provide a source of nitrogen that contributes to sustainable cropping systems. Also, legumes improve soil quality by increasing soil organic matter and thus reducing soil erosion. The improvement in the production of these crops will therefore contribute substantially to better human nutrition and soil health (Popelka et al., 2004).

The economical relevance of legume crops is related to both their importance as a protein source for animal feed and human nutrition and their use as raw material in the industry (Edgerton et al., 2008). Depending on the use and destination of production of legumes, they can be divided into two groups: forage legumes of which the leaves and stems are used for animal feed, and grain legumes, whose main economic interest is in their dry seeds, which can be aimed at both animal and human feed. Forage legumes play an important role in dairy and meat production being sources of protein, fibre and energy. They are usually richer in protein, calcium and phosphorus than other non-legume forages, such as grasses, and they include clover (*Trifolium spp*.), alfalfa (*Medicago sativa*) and barrel medic (*Medicago truncatula*) as important livestock fodder plants. Grain legumes represent a major source of proteins in many developing countries and are rich in essential amino acids, thus supplementing the nutritional value of cereal and tuber diets (Graham and Vance, 2003) and including soybean (*Glycine max*), garden peas *(Pisum sativum*), peanuts (*Arachis hypogaea*), and broad beans (*Vicia faba*). Grain and forage legumes are grown on around 15% of the cultivated land area of the Earth and assumed the 27% of the world crop production and about 33% of the protein needed to meet human nutritional needs (Graham and Vance, 2003).

Among legumes, we can find two types: tropical and temperate legumes. A legume specie belonging to the first group is *G. max* (soybean) while *Medicago truncatula* is cultivated in warmer areas. Due to their agricultural and economic importance, scientists have carried out basic and applied research on legumes to better understand responses to abiotic stresses. Nevertheless, most legume species are poor models for experimental research because of their large genomes, difficulties to transformation and long generation times, among others (Cook, 1999). Of particular significance are the recently completed and annotated genomes of three legume species: *G. max* (soybean), *M. truncatula*, and *Lotus japonicus* (Young and Bharti, 2012) emphasizing comparisons among legume genomes. In this work, due to their agronomical and economical importance, we will focus on *G. max* and *M. truncatula*.

A.1 *Glycine max*

The grain legume soybean (*Glycine max* (L.) Merr.) is considered to be a very important crop world-wide. Due to its characteristics, soybean is used and appreciated in the world by consumers, the farming communities and commercial seed companies being its importance as a crop increased steadily during the last century (Qiu and Chang, 2010). This cultivated annual plant specie native of Asia (Pratap and Kumar, 2011) is one of the main crops cultivated for oil extraction apart from its uses in human and animal nutrition and industrial applications. Thereby, soybean is one of the most studied legumes from the agronomic perspective to improve cultivars for higher yield and resistance to biotic and abiotic stresses. Soybean economic importance and its large research community have contributed to develop molecular, genetic and genomic tools for this specie (Stacey et al., 2004) being its genome sequenced some years ago (Schmutz et al., 2010).

A.2 *Medicago truncatula*

The genus *Medicago* contains more than 54 characterized species, including both diploid annuals and tetraploid perennials (Lesins and Lesins, 1979). *M. truncatula*, also known by the common name “barrel medic”, is native to the Mediterranean basin and has long been cultivated as winter forage in Australia (Davidson and Davidson, 1993). From 1999, researchers have adopted *M. truncatula* as a model system to study legume genomics (Cook, 1999) due to it has a potential as a short-season annual crop to supply forage when traditional supplies are inadequate. The natural attributes of *M. truncatula* that make it desirable as an experimental system include its annual habit, diploid and self-fertile nature, short lifecycle, relatively small genome (~500Mb), abundant natural variation, and close phylogenetic relationships to the major crop legumes such as alfalfa (Cook, 1999).

Also, researchers have developed the tools and infrastructures for basic research in this specie including efficient transformation systems and a research network (http://www.medicago.org); (Benedito et al., 2008; Young et al., 2011). Consequently, knowledge of the genome organization and structure of both legume species will be useful to explore gene information of the other crop legume genomes to better understand plant responses under abiotic stress conditions.

B. WATER MOVEMENT IN PLANTS

In order to understand plant responses to abiotic stresses, we need first to analyze how water is transported in plants. Water transport in the soil-plant-atmosphere system is usually considered as a steady state flow driven by a water potential gradient and by the transpiration rate being essential the fact that there are no limitations on water absorption by the root system. Water from the soil enters plants via the roots and then it is transported to the roots xylem, passing through various morphological structures, such as the epidermis, the endodermis, the cortical cells and the walls of xylem vessels (Steudle and Peterson, 1998) to finally arrive to the shoot. With the water reaching the roots, the absorption process is directly dependent on the water potential gradient between the rhizosphere and the root xylem; when roots absorb water, there is a reduction in the water potential in the soil that is in contact with the roots (rhizosphere). This process establishes a water potential gradient between plants and soil which coordinates the water movement towards the roots of a transpiring plant. Therefore, water flows from soil to root at a rate depending on the water potential gradient between soil and plant which is affected by plant water need, hydraulic conductivity of the soil, soil type and soil water content (Chavarria and Pessoa dos Santos, 2012). There are two ways to establish this gradient, characterized by two absorption processes: 1) osmotically driven absorption, common in plants with low or restricted transpiration activity (for example, plants without leaves or with a limited vapour pressure deficit) where there is an accumulation of solutes in xylem thus reducing its water potential in relation to the soil water potential, and 2) passive absorption, which dominates in plants with high transpiration activity where the tension in the xylem vessels increases, stablishing a water potential gradient between the root xylem and the rhizosphere (Chavarria and Pessoa dos Santos, 2012).

Essentially, all water used by plants is absorbed by roots from the soil being this absorption related to roots surface directly in contact with soil. Thus, longer and younger roots with more root hairs are essential for increasing the contact surface thus improving the water absorption capacity of the roots. Moreover, the distribution and proportion of the roots is very important for meeting the water demand of a plant (Chavarria and Pessoa dos Santos, 2012); in humid regions,

plants usually do not require very extensive root systems but in dry regions, the plants invest more in their roots, decreasing the shoot:root ratio such that the roots can represent upper to 90% of a plant biomass in some species of a desert climate.

Water flows more efficiently through some parts of the plant than others. Upon absorption by the root, water first crosses the epidermis making its way toward the center of the root crossing the cortex and endodermis before arriving at the xylem. During absorption, water can flow by three ways into the root tissue in relation to the route of the epidermis to the endoderm of the root; apoplastic, symplastic and transmembrane pathways: 1) apoplastic, when water moves through the intercellular spaces and does not pass through any membranes, exclusively occupying the continuous network of the cell walls; 2) symplastic, where the water moves exclusively from one cell to another through plasmodesmata connections and remaining outside the vacuoles; and 3) transmembrane, when water crosses membranes to go from one cell to the next one. With regard to water absorption control in the roots, plants also present a family of membrane water transporter proteins (water-channel proteins) called aquaporins which have a critical role in water absorption and which are controlled by many endogenous and exogenous factors, such as environment factors that interfere in hydraulic conductance along the water flow by the plant (Chaumont et al., 2005; Maurel et al., 2008).

After travelling from roots to stems through the xylem, water enters leaves moving across the cells mainly via apoplastic (Sack et al., 2005). Once delivered to the leaves, water evaporates from the surface of the mesophyll cells into the air-filled substomatal cavity of the leaf. From there, water vapour diffuses via the stomata to the atmosphere surrounding the leaf, a process driven by the water vapour pressure difference between the interior air space of the leaf and the adjacent atmosphere. As a consequence, a decrease in the water potential of these cells results in a driving force for the movement of water from the xylem network of the leaf (Buckley, 2005). So stomata play a key role in the rapid regulation of water loss. However, abiotic factors can be equally disruptive to flow at various points along the water transport pathway.

C. DROUGHT

Climate change is multi-faceted, and includes changing concentrations of greenhouse gases in the atmosphere (like CO_2), rising temperatures, changes in precipitation patterns, and increasing frequency of extreme weather events, interacting all these processes on plant development and affecting these climate change factors plants at the level of molecular function, developmental processes, morphological traits, and physiology (Gray and Brady, 2016). Thus, Earth´s climate

is drastically changing leading to more intense and extended drought situations. Plants growing in many regions of the world will experience increasing water stress as a result of climate change. Already, the area affected by drought has increased substantially since the middle 20th century (Dai, 2011), and the frequency of droughts is predicted to increase in regions that are already dry by the end of the 21st century. Actually, drought observatories have estimated that around 40% of the land area is affected by drought and having an expectative in expansion due to the global climate change (Trenberth et al., 2013).

Despite the fact that water is a renewable resource, the world´s supply of fresh water is steadily decreasing due to the population growth, economic development and improved living standards. As a result, water resources for agricultural production are limited and diminishing. Among other consequences, drought is the most serious problem for global agriculture having an expectative in expansion due to the global climate change. A decrease in water availability affects primary productivity in the ecosystem and, more specifically, the growth of plants. Water does not only become limiting for plant communities as a result of inadequate rainfall, but also due to other environmental conditions like excessive salinity in the soil solution or as a consequence of freezing temperatures. To this end, predictions on an increasing world food demand and the rise in temperature at the global level led to investigate plant responses to drought to develop new varieties with improved water use efficiency and drought tolerance.

C.1 Plant responses to drought stress

Plants are exposed to a numerous environmental stresses under natural conditions, notably to drought, cold, heat, flooding or salt stress. Among them, drought is the most serious problem for global agriculture and a decrease in water availability affects primary productivity in the ecosystem (Boyer, 1982; Chaves and Oliveira, 2004), and more specifically, the growth of plants because water is the main plant compound comprising 80–95% of the biomass of leaves and roots in non-woody plants (Hirt and Shinozaki, 2004). Plant water management is a combination of increasing water uptake and reducing water loss during drought stress. While water uptake can only be increased by the development of specialized root structures, water loss can be avoided by various physiological mechanisms such as stomatal closure, reduction of leaf growth or production of specialized leaf surfaces to avoid transpiration (e.g. waxes, hairs or embedded stomata). Therefore, a constant water availability has crucial importance for plant survival.

Plants develop many complex responses to water deficit, involving adaptive changes and/or deleterious effects (Chaves et al., 2002). The strategies adopted by plants to cope with water scarcity under natural conditions can be generally

classified into drought escape, avoidance and tolerance. Particularly, drought tolerance is considered as the ability of plants to survive internal water deficits in dry environments. Therefore, the breeding of drought-tolerant and water use efficient crop varieties should be a global concern. Consequently, an understanding of the mechanisms by which plants can adapt to suboptimal watering conditions has become imperative for all plant researchers. Most research efforts have been devoted on the analyses of plant performance under drought stress focusing mainly on the aboveground organs whereas little attention has been given to root performance. In particular, in the area of legumes, the field remains largely unexplored and little is known about the role of roots in crop responsiveness despite these organs are responsible of nutrients and water acquisition and transport in plants. Then the drought responses will be generally described at the cellular level, then attending to the first stages of growth of the plant and finally to the shoot and root separately.

C.1.1 General plant drought responses at the cellular level

Several changes are found at cellular level in plants subjected to drought stress. The most relevant ones include the modification of the lipid membrane composition, some stress-signalling processes or the synthesis and accumulation of compatible osmoprotectants solutes such as sugars, polyamines, organic acids or amino acids (Fig. 1; (Hsiao, 1973; Bray, 1997)). It has been shown that these compounds accumulate in different plant tissues under drought stress conditions in order to maintain cell turgor by osmotic adjustment against the loss of water (Bartels and Sunkar, 2005; Krasensky and Jonak, 2012).

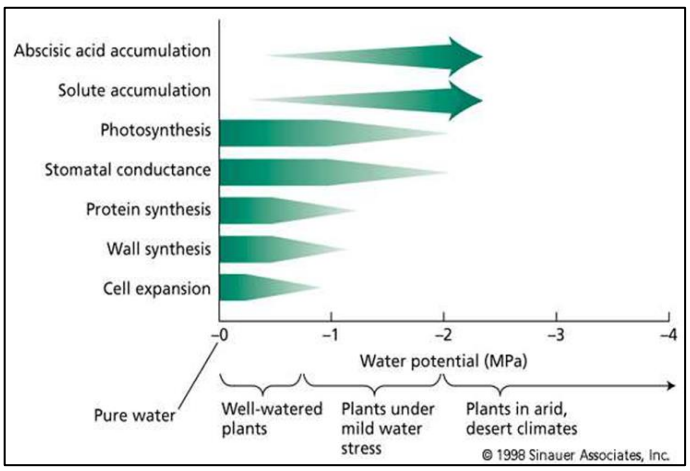

Figure 1. Effects of drought stress on some plant mechanisms. Adapted from Taiz and Zeiger, (2006).

These osmoprotectant solutes also act in the reduction of ROS production under conditions of stress in plants trying to maintain a steady homeostatic condition. ROS production increase can provoke oxidative stress by damaging membrane lipids, proteins, photosynthetic pigments and nucleic acids through oxidation process, and these are considerably amplified under drought stress. The singlet oxygen ($^1O_2$), the superoxide radical (O_2^-), hydrogen peroxide (H_2O_2) and the hydroxyl radical (OH^-) are produced from oxygen metabolism and play an important role as indicators in the stress process of water deficit. To cope with drought stress, plants acquire well-organized enzymatic and non-enzymatic antioxidants systems (Fig. 2). Among important antioxidants enzymes in plants we can find catalase, ascorbate peroxidase, glutathione peroxidase and so on. On the other hand, there are non-enzymatic antioxidant components such as ascorbic acid (AsA), glutathione (GSH), phenolic compounds or alkaloids. Thus, the enhanced activities of components of the antioxidant system decrease oxidative damage, and develop and improve the drought tolerance and resistance of plants.

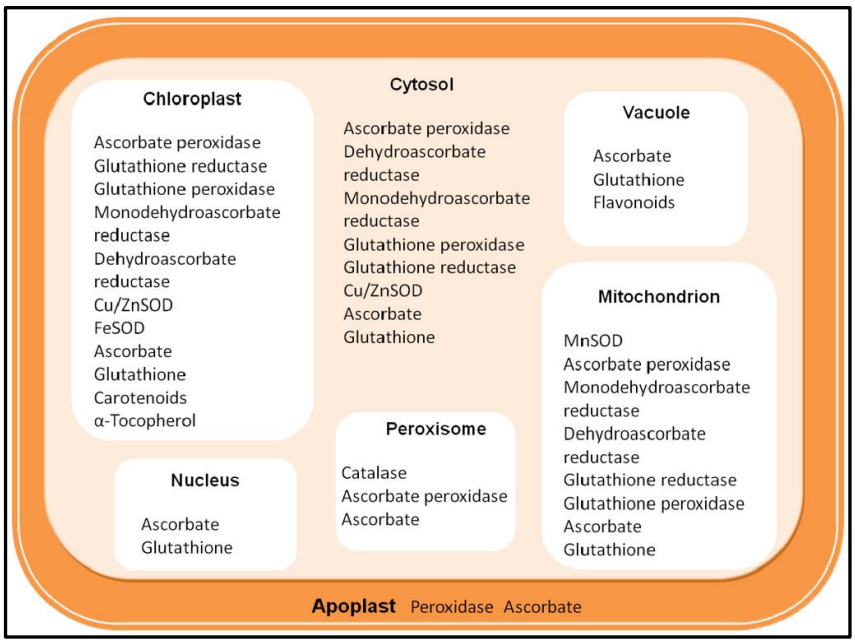

Figure 2. Distribution of the main enzymatic and non-enzymatic antioxidant resources in plant cells. Adapted from Racchi, (2013).

Particularly, AsA is one of the most abundant water-soluble reducing compound present in plant tissues, serving also as an electron donor in numerous reactions (Foyer and Noctor, 2011). AsA, also known as vitamin C, is an essential nutrient for some animals, including humans. Working as a ROS scavenger and as an

electron donor, AsA is oxidized to monodehydroascorbate and then to dehydroascorbate (DHA), which can be recycled by the AsA-GSH cycle, also known as "Foyer-Halliwell-Asada" pathway (Foyer and Halliwell, 1976; Asada, 1999). Although it is synthesized in mitochondria, AsA is present in all cellular compartments and it can represent more than 10% of the soluble carbohydrate fraction in plants (Noctor and Foyer, 1998; Fig. 3). Although alternative pathways have been described, the most studied biosynthetic route of AsA in plants is the Smirnoff-Wheeler (SW) pathway (Smirnoff and Wheeler, 2000). The last step in this pathway involves the conversion of L-galactono-1,4-lactone (GalL) to AsA in a reaction catalysed by the enzyme L-galactono-1,4-lactone dehydrogenase (GalLDH; EC 1.3.2.3). The enzyme, localized in inner mitochondrial membrane (Bartoli et al., 2000), has been characterized in several plant species although it has been barely studied in legumes.

C.1.2 Drought effects during the initial development stages of plants

Regarding the importance of limited water resources effects on crop yield, drought stress effects analysis in different plant growth stages is required. Plant communities are first shaped by seed dispersal and by the effect of environmental factors on seed survival, germination, seedling establishment and growth (Schupp and Fuentes, 1995). The first step of germination process is water absorption, where seeds swell and growth. If the water level is lower than desirable, water absorption is not completed and germination declines or stops. Taiz and Zeiger, (2010) observed a reduction in germination rates and stand stablishment under early drought conditions mainly due to reduced water uptake during the imbibition phase of germination. In previous studies, it was also reported that drought stress reduces germination and seedling stand of sunflower (Kaya et al., 2006), pea (Okçu et al., 2005) or alfalfa (Zeid and Shedeed, 2006) sedes. So seedling establishment might be one of the most decisive phases in the plant life-cycle. Once seeds germinate, survival and growth at early stages of plant development are major bottlenecks to successfully complete the reproductive cycle. So seed survival depends on the ability to cope with numerous environmental factors such as water availability, temperature, radiation… However, drought is the main reason for seedling mortality (Moles and Westoby, 2004). Two aspects are fundamental in order to ensure rapid seedlings establishment: prompt anchoring of juvenile seedlings to the substrate and immediate water absorption (Young and Martens, 1991). Given that high seedling survival is linked to larger biomass allocation to roots, a better water and nutrient uptake allows to explore larger volumes and deeper layers of soils (Padilla and Pugnaire, 2007).

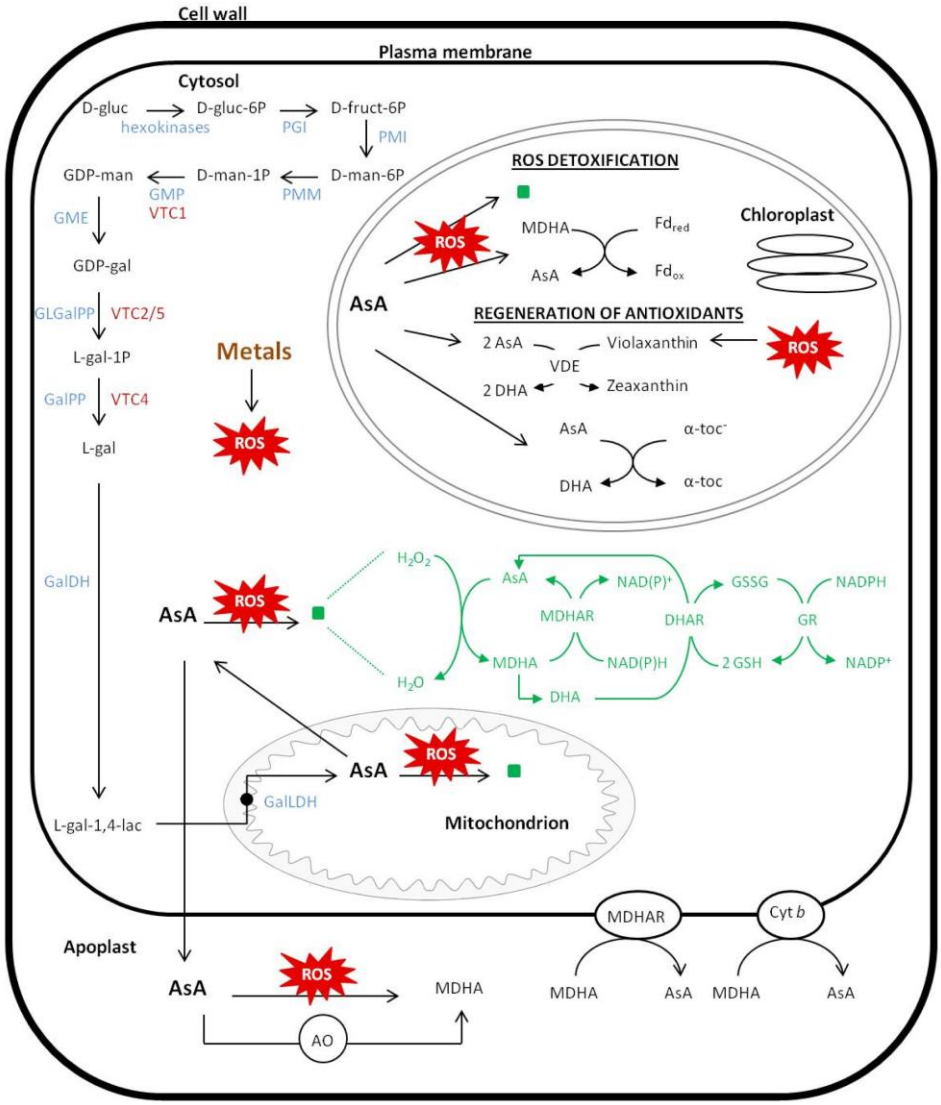

Figure 3. Representation of the biosynthesis, localization and antioxidant function of AsA. The biosynthesis of AsA takes place in the cytosol, except the last step occurs in the mitochondrion. AsA plays a role in the antioxidant defense scavenging ROS via the AsA-GSH cycle or by regenerating antioxidants such as α-tocopherol and zeaxanthin. Adapted from Bielen et al., (2013).

Also, the development of specialized tissues such as hypocotyls hairs during seedling emergence has positive effects involving facilitation of water uptake and providing seedling establishment (Aronne and De Micco, 2004). Thus, phenotypical evaluation at the seedling stage is regarded as an attractive approach because it is a high-throughput and low cost method that saves space and time (Meeks et al., 2013). Another advantage of using seedling drought screens is that phenotypical variation caused by experimental errors can be controlled better because the plants are much more uniform at an early seeding stage, compared to

other periods of plant development (Li et al., 2015; Wang et al., 2015). For this reason, studies carried out on seedlings in the early stages of growth are of great interest for further analysis in adult plants.

C.1.3 Drought responses at shoot level

Photosynthesis is the key process which contributes substantially to the plant growth and development by the conversion of light energy into a usable chemical form of energy. However, drought stress adversely affects the process of photosynthesis in plants (Hsiao, 1973) by altering the functionality of both PSII and PSI, the ultrastructure of the organelles (deterioration of thylakoid membranes; (Anjum et al., 2011)) thus reducing the carbon assimilation rate (Ashraf and Harris, 2013). To face water deficit stress, plants have developed adaptive responses to reduce drought induced damage to photosynthesis including thermal dissipation of light energy, the xanthophyll cycle, the water-water cycle, and dissociation of the light-harvesting complexes from photosynthetic reaction centers (Basu et al., 2016). Furthermore, the immediate response of plants on being exposed to drought stress is stomatal closure. The regulation of leaf stomatal conductance is crucial in plants as it is vital for both a prevention of desiccation (transpiration rates decrease) and CO_2 acquisition (Dodd et al., 2003). Stomata closure in response to drought generally occurs due to decreased leaf turgor and atmospheric vapor pressure along with root-generated chemical signals (Chaves et al., 2009). The stomata closure is generally considered to be the major factor of the photosynthetic rate decrease under stressful conditions attributed to the stomatal limitations for diffusion of gases, which ultimately alters photosynthesis and the mesophyll metabolism (Flexas et al., 2007; Chaves et al., 2009). Thus, all these adaptations in plants reduce the negative impacts of drought stress on photosynthesis and thereby have a positive effect on water use efficiency, which in turn will result in high yield potential and high yield (Basu et al., 2016).

Furthermore, the leaf cell expansion rate decrease observed under drought conditions provokes a reduction in the leaf area parameter and, on the other hand, the increase in the abscisic acid content promotes that the process of senescence is stimulated earlier causing leaf abscission (Fig. 4). Also, under pronounced water deficit situations, the tension of water in xylem becomes so high that dissolved air within water expands blocking xylem vessels thus activating embolism and impeding water and nutrient transport through the plant.

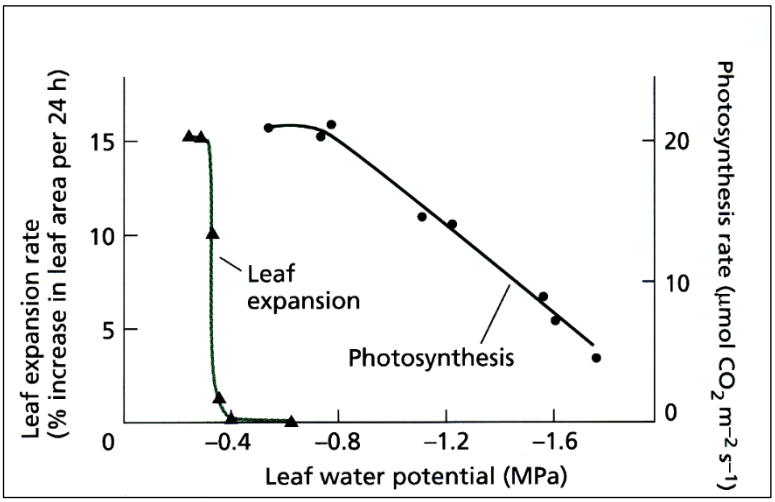

Figure 4. Effects of water stress on photosynthesis and leaf expansion in sunflower plants. Adapted from Taiz and Zeiger, (2010).

C.1.4 Drought responses at the root level

As mentioned earlier, most research efforts have been focused on studying how aerial parts contribute to plant drought tolerance being only a few studies focused on roots. As roots are the first organs sensing water deficit in soils directly interacting with water under the soil surface, drought responses of this organ are very important. Root systems have many functions in plants survival; anchorage and support to the soil, water and nutrients absorption or the establishment of biotic interactions at the rhizosphere storage (López-Bucio et al., 2003). For this reason, the anatomy of roots is complex with variable structures both between and within plant species, habitats and conditions. In the group of angiosperms, root growth is different between monocots and dicots plants; in contrast to monocots, dicots develop root systems with a main single root axis from which lateral roots develop to form an extensively branched root system. Internally, the apical region of the root is divided in three zones of activity: the meristematic, elongation and maturation zones, being this last also known as differentiation or absorption zone (AZ); (Fig. 5). The meristematic zone is the responsible for cell division and differentiation into the tissues of functional root and in the direction of the root apex (Clowes, 1975). Behind it is the zone of elongation, in which cells increase in size and in length through nutrient and water absorption and uptake into the vacuoles. Cells from this root zone undergo changes being differentiated in specific tissues. The vascular tissues of the root are surrounded by the pericycle; the phloem is characterized for transporting metabolites from the shoot to the root while xylem transports water and solutes to the shoot (Esau, 1977). In the third major root part

(maturation/differentiation/absorption zone) root hairs, which are themselves specialized projections from modified epidermal cells known as trichoblasts (Bibikova and Gilroy, 2002), are located to extend root absorbing surface thus increasing water and nutrient absorption. The whole root is surrounded by the outermost layer, the epidermis, being cortex cells involved in the movement of water from the epidermis.

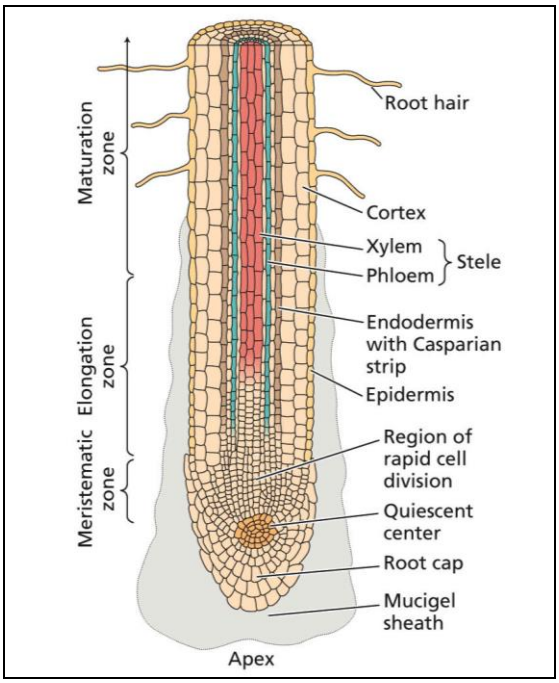

Figure 5. Longitudinal schematic root cellular organization. Adapted from Taiz and Zeiger, (2010).

Root development is strongly influenced by growing conditions such drought stress. However, root growth is usually less affected by drought stress than shoot growth (Sharp et al., 2004). Roots can always adjust their growth and biomass allocation to adapt water stress during plant growth and development stage and when they notice the lack of water in the soil, root morphological and physiological parameters are adjusted. Thus, a decrease in shoot:root ratio is a common observation under drought stress, which results either from an increase in root growth or from a relatively larger decrease in shoot growth than in root growth. Several factors have been described to affect root drought tolerance; root structure, diameter, density or length and their number (Comas et al., 2013), the presence of young roots for water uptaking (Peterson et al., 1993) and sufficient density and length of root hairs to ensure the maximal absorption surface between soils and

roots (Wasson et al., 2012) are parameters which can affect the ability of plants to adapt to limited soil moisture. Particularly, plants with longer roots may access moisture by growing deep into soil during periods of moisture stress. In this regard, root diameter and root density control the length and surface area of root systems (Fitter et al., 2002). Actually, a decrease in root diameter has been proposed as a trait for increasing plant acquisition of water and productivity under drought stress (Wasson et al., 2012). Few studies have been conducted on root architecture and scientists are constantly searching for mechanisms to model typical root growth outside of the field; genetic variation underlying root traits in response to moisture deficiency has been observed in many crops (Sharp et al., 2004). Gregory (2006) discusses the theory that thick roots can penetrate hardened soil more easily and reach soil moisture reserves deep in the soil profile. In addition to root diameter, xylem diameter also affects root hydraulic conductivity and can affect plant productivity under drought. Root depths of native vegetation in arid climates are consistently deeper than those in humid regions (Schenk and Jackson, 2002). So, root traits play a critical role for increasing crop yield under moisture stress (Tuberosa et al., 2002). Among these traits, root pulling force, the vertical force required to pull out the root system from the ground, could be an important trait in a drought-associated study being associated with drought tolerance and higher yield under moisture and nutrient stress in rice and maize. Root pulling force has been used as a tool for selection for drought adaptation in rice (Ekanayake et al., 1985). In this regard, several previous studies have focused on studying root system architecture modifications under drought stress in different plant species; soybean (Matsuo et al., 2013), *Arabidopsis thaliana* (van der Weele et al., 2000), rice (Uga et al., 2013) and *Medicago* (Fresnillo Fedorenko et al., 1995). Blum (2011) described several factors related to increased root growth under drought conditions: 1) root growth is less sensitive than leaf to drought stress due to its greater capacity to osmotic adjustment comparing with leaves (Ober and Sharp, 2007) by diverting proline and carbohydrates content to this organ, thus supporting osmotic adjustment and root growth. 2) The hormone abscisic acid (ABA) promotes root growth while it inhibits shoot growth. The role of ABA accumulation in roots in enhancing root growth in a drying soil has been clearly proven (Sharp et al., 2004; Ober and Sharp, 2007). 3) Cell wall expansion is an important factor in enhancing root growth in a drying soil. The importance of expansin proteins and the expression of expansin genes are crucial in root responses to drought situations

However, many are the physiological and molecular root mechanisms underlying adaptation to drought stress which remain largely unknown. So the understanding of regulatory molecular networks, and stress signaling mechanisms provide numerous advantages to improve drought stress responses in plants. To fill

this gap, several studies have been carried out in roots of a broad range of plants to characterize stress-related genes observing the change in their expression under low water availability situations and providing the opportunity to dissect the molecular response of roots to a drought stress (Micheletto et al., 2007; Zhang et al., 2014). Indeed, there are some studies focused on the analysis of differentially expressed genes in different root zones under drought stress (Ranjan et al., 2012; Opitz et al., 2015). In general, genes belonging to diverse functional groups such as transcription factors, protein kinases and phosphatases or secondary cell wall biosynthesis-related gene are differentially regulated in roots contributing to the signal transduction that occurs in plants in response to drought stress conditions. These studies allowed to obtain information that could be used to explore new strategies for developing drought tolerant plants through breeding.

C.2 Approaches to study drought stress

Compared to drought stress, salinity simulation under laboratory conditions is very simple to apply (by adding NaCl to the plant growth medium), easily to standardize and highly reproducible. However, the simulation of drought is more challenging. Under field conditions, drought effect studies are variable due to factors such as soil mixture, climate, temperature variations, precipitations or biotic stresses thus limiting the conclusions that can be obtained in this type of studies. Experiments with adult plants under controlled conditions are usually carried out using pot systems where drought stress is imposed by removing irrigation allowing a gradual depletion of water. Also, drought is simulated by extreme assays of detaching leaves (Qin and Zeevaart, 2002) or leaving plants in air to impose dehydration stress (Belamkar et al., 2014). In molecular biology studies, artificial growing system are usually employed as plant culture dishes, which usually apply several osmotic agents such as the artificial polymer polyethylene glycol (PEG); (Kang et al., 2015), sorbitol or natural osmolites such as mannitol to mimic a programmed level of drought stress conditions. Plants grown in these conditions show uniformity and reproducibility in typical drought responses. However, it has been shown that mannitol and PEG are absorbed by the plant, this latter causing a toxic effect (Emmert, 1974; Mexal et al., 1975; Munns et al., 1979). Therefore, the development of new non-destructive and non-toxic protocols are needed to study plant drought responses, allowing a better plant characterization.

Breeding strategies for drought tolerance have often focused on above ground aspects of plants such as reduced leaf area, stomatal conductance and transpiration rates or shorter flowering stages to limit time exposed to drought stress. However, due to the high importance of underground tissue in water absorption for plant

survival, different methodologies for root studies under drought conditions have been developed (Paez-Garcia et al., 2015). These authors described root architectural traits relevant to crop productivity, survey root phenotyping strategies and described their advantages, limitations and practical value for crop and forage breeding programs:

The analysis of root system in the field for phenotyping can be arduous and time consuming and in some cases can also involve use of expensive machinery. This strategy is referred to shovelomics characterized as a technique to visually phenotype roots (Trachsel et al., 2011). The goal was to identify root architectural traits important to plant productivity under edaphic stress. However, studies conducted in the laboratory, growth chambers or greenhouses have more controlled settings and attempt to study the relationship between roots and drought in greater detail. Many systems exist to study roots under controlled environmental conditions such as hydroponics, growth pouches (McMichael et al., 1985), minirhizotron system (Rellán-Álvarez et al., 2015), agar plates, slant tubes, aeroponic systems (Barker et al., 2006), mesocosm system (Chimungu et al., 2014) and various other containers to study young seedling plants. More methods for imaging, processing and data collection of roots have been developed like WinRHIZO, ROOTEDGE and SmartRoot softwares (Himmelbauer et al., 2004; Lobet et al., 2011). These programs assess parameters like root length, surface area, diameter, tips and branching (Himmelbauer et al., 2004).

D. "OMIC" APPROACHES TO UNDERSTAND PLANT DROUGHT RESPONSES

One of the goals in plant systems biology is to monitor and control cellular responses to genetic perturbation or environmental changes (Fukushima et al., 2009). Omic technologies offer the possibility to study these effects in plants. To understand the organization principle of cellular functions and to provide us with a detailed knowledge about the dynamic function of a plant molecular system, an integrative approach combining different tools including the detection of genes (genomics), mRNA (transcriptomics), proteins (proteomics) and metabolites (metabolomics) in a specific biological samples is needed (Horgan and Kenny, 2011; Fig. 6). Nowadays, plant researchers have been widely using these high-throughput omic technologies in the study of abiotic stress effects at different functional levels (Debnath et al., 2011). These multidisciplinary approaches have been applied in the field of drought stress responses in plants (Larrainzar et al., 2007; Gil-Quintana et al., 2015; Watson et al., 2015; Song et al., 2016). Proteomics is becoming a powerful tool to analyze biochemical pathways and to give insights into the complex molecular mechanisms underlying plant response to stress

(Timperio et al., 2008). Moreover, recent advances in genomics related techniques such as Quantitave Trait Locus (QTL) and Genome Wide Association (GWA) have greatly facilitated the understanding of plant responses against drought stress (Kang et al., 2015).

In the case of transcriptomics, a tool that provides a comprehensive analysis of the transcript levels in cells, one of the limitations is the highly dynamic nature of mRNA populations being these changes dependent on the developmental stage and environmental conditions. Latest advances in transcriptomic approaches show new techniques where gene expression is indirectly assessed in microarrays or chips using the principle of nucleic acid hybridization of mRNA or cDNA fragments (Tuteja et al., 2012). Among them, two are the main methods which are currently used; microarrays and RNA sequencing (RNA-Seq). Microarrays are considered one of the most powerful and widespread high throughput methods which has become an essential tool for studying the expression of all genes in the transcriptome simultaneously (Malone and Oliver, 2011). In the RNA-Seq method, complementary DNAs (cDNAs) generated from the RNA of interest are directly sequenced using next-generation sequencing technologies and several reads obtained from this can then be aligned to a reference genome in order to construct a whole-genome transcriptome map (Nagalakshmi et al., 2010). Comparing both transcriptomics methods, RNA-Seq is a most sensible technique which enables the detection of polymorphisms, splicing processes and that does not require a previous knowledge of the plant genome. However, both microarrays and RNA-Seq have disadvantages such as economical limitations (being higher in RNA-Seq technique) and the capacity to process a large amount of data.

Finally, since metabolites are the ultimate gene products, the associated field "metabolomics" provides an overview of the developmental and physiological state of an organism under defined conditions. The plant metabolome is defined as the full complement of low molecular weight molecules or metabolites and it is highly dynamic because metabolites represent the catabolic and anabolic activities inside the plant cells at a given time (Subudhi, 2011). Metabolites are classified in two groups: primary (those essential in carbon and nitrogen metabolisms) and secondary metabolites (several compounds involved in plant adaptation responses to environmental factors). In the plant kingdom, among 100,000-200,000 secondary metabolites are synthesized which are chemically diverse, often species specific and many are unknown for its physical details. When a comprehensive analysis of metabolites in terms of identification and quantification is needed, metabolomics is chosen to determine and quantify all possible identified or unknown compounds using a range of techniques such as Liquid Chromatography-Mass Spectrometry

(LC-MS), Gas Chromatography-Mass Spectrometry (GC-MS) or Nuclear Magnetic Resonance. The currently used analytical techniques in plant metabolic profiling is Mass Spectrometry often combined with chromatography; GC-MS is frequently used for detection of primary metabolites but LC-MS allows detection of wide range of diverse secondary metabolites such as phenols, flavonoids or phenylpropanoids. Thus, metabolomics is emerging as a useful tool in functional annotation analysis in plants response to environmental alterations being the relationship between metabolite contents and stress tolerance investigated on a large scale.

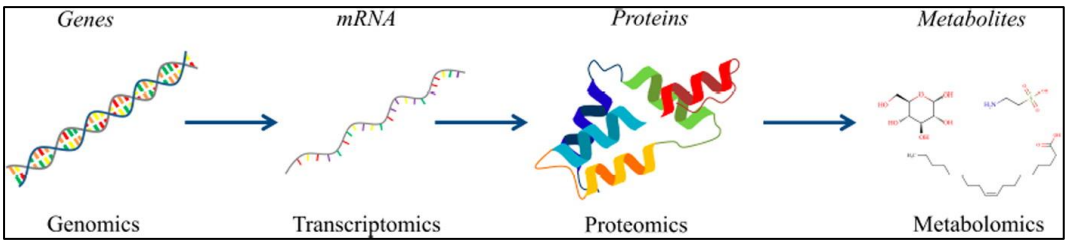

Figure 6. General schematic diagram showing the relationships among omics techniques. Adapted from Euceda et al. (2015).

Overall, challenges in integrating omics approaches such as transcriptomics and metabolomics could result in generating useful information about the genetic control of metabolite production under stress conditions (Gupta et al., 2013). In this context, the integrated approaches with multiple omics data should greatly contribute to the identification of key regulatory steps and to characterize the pathway interaction in various processes (Fukushima et al., 2009). Although diverse transcriptomic and metabolomic studies have been conducted in *M. truncatula* and soybean drought-stressed plants (Larrainzar et al., 2007; Zhang et al., 2014; Kang et al., 2015; Watson et al., 2015; Song et al., 2016), few have been analyzed these responses in different plant tissues in these stressed plants.

upna

Universidad Pública de Navarra
Nafarroako Unibertsitate Publikoa

GENERAL AIM

Although numerous studies have been focused on the analysis of plant drought responses, some important mechanisms responding to this stress require further investigation. So a better understanding of drought tolerant mechanisms by which plants cope with water deficit stress is necessary. In this work we focused on two legume species of great economic and agronomic importance all over the world. Previous research studies have mainly described defense mechanisms against drought stress in the aerial part of the plant while root responses have been barely studied. **Thus, the overall goal of this work was to gain further insights into the response to drought of two legume species (*Medicago truncatula* and *Glycine max*) at the shoot and root levels by using a combination of physiological, morphological, transcriptomic and metabolomic approaches.**

The general aim can be defined as summarized in the following four chapters:

1) To investigate the role of one of the main water soluble antioxidant in plant responses to drought stress by analyzing AsA metabolism in soybean (*G. max* L. Merr) plants.

2) To analyze the response of *M. truncatula* plants to drought stress in terms of the leaf-root partitioning carbon and nitrogen metabolism.

3) To describe a method for the standardized and reproducible simulation of drought conditions with different agar concentrations and to characterize drought stress responses of *M. truncatula* seedlings grown under these conditions.

4) To analyze the responses of the part of the root which contains root hairs (absorption zone) under low water availability in early developmental stages of *M. truncatula* plants at the transcriptomic and metabolomic level.

upna

Universidad Pública de Navarra
Nafarroako Unibertsitate Publikoa

» CHAPTER 1

Multiple regulation points control ascorbic acid biosynthesis in drought-stressed soybean plants

upna

Universidad Pública de Navarra
Nafarroako Unibertsitate Publikoa

1.1 INTRODUCTION

Drought stress is one of the main factors limiting plant productivity in agriculture. At the molecular level, drought provokes an increase in the formation of reactive oxygen species (ROS) in plants, leading to oxidative stress and cell damage (Hsiao, 1973). In order to cope with this increased ROS production, plant cells display a complex array of both enzymatic and non-enzymatic detoxification mechanisms. The latter group includes the production of low-molecular weight compounds such as ascorbic acid (AsA, vitamin C), glutathione (GSH), carotenoids or flavonoids (Mittler, 2002; Mittler et al., 2004; Szarka et al., 2012). AsA is one of the most abundant water-soluble reducing compound present in plant tissues, serving also as an electron donor in numerous reactions (Foyer and Noctor, 2011). Synthesised in mitochondria, AsA is present in all cellular compartments at concentrations up to 21 mM (Szarka et al., 2013) and it can represent more than 10% of the soluble carbohydrate fraction in plants (Noctor and Foyer, 1998). AsA is oxidised to monodehydroascorbate and then to dehydroascorbate (DHA), which can be recycled back to AsA by the AsA-GSH cycle, also known as the "Foyer-Halliwell-Asada" pathway (Foyer and Halliwell, 1976; Asada, 1999).

Although alternative pathways have been described, molecular genetic evidence from *Arabidopsis* indicates that the Smirnoff-Wheeler (SW) or D-mannose/L-galactose pathway is the primary route of AsA biosynthesis in plants (Wheeler et al., 1998; Conklin et al., 1999; Dowdle et al., 2007). Despite the importance of AsA in plants, knowledge on the mechanisms regulating its biosynthesis and metabolism is still limited. The steady state level of transcripts encoding several of the SW biosynthetic enzymes have been shown to correlate with exposure to light and AsA content (Gatzek et al., 2002; Tamaoki et al., 2003; Bartoli et al., 2006; Dowdle et al., 2007; Maruta et al., 2008; Yabuta et al., 2008; Bartoli et al., 2009; Fukunaga et al., 2010). Besides this light-dependent regulation, two genes have been identified as regulators of the pathway in *A. thaliana*: AMR1, a predicted F-box protein (Zhang et al., 2009) and VTC3, a protein kinase::protein phosphatase (Conklin et al., 2013).

Abiotic stresses are known to activate ROS-scavenging mechanisms such as superoxide dismutase, ascorbate peroxidase and catalase enzymes (Mittler, 2002). It could be expected that drought stress would trigger an increase in the biosynthesis of a major antioxidant compound like AsA. Consequently, plants with increased AsA levels might present improved tolerance to such stresses. This is particularly relevant in the case of legume crops, main source of protein for humans and cattle feed, which are highly sensitive to environmental constrains (Tuteja et al., 2012). Nevertheless, it remains unclear whether drought stress leads to an increased

production of AsA. For instance, AsA levels decreased in spinach but not in soybean leaves as water potential values dropped (Robinson and Bunce, 2000). Similarly, drought stress has been shown to cause increased AsA content in chloroplasts but a general reduction of AsA levels at the whole leaf level in several plant species (Munné-Bosch and Alegre, 2003). At the enzymatic level, AsA biosynthesis is found stimulated in mitochondria isolated from plants treated with gibberellic acid (Millar et al., 2003), a hormone inhibited during drought stress. Additionally, Bartoli and collaborators (2005) did not find a correlation between drought stress and AsA biosynthesis, being GalLDH activity and AsA content in wheat leaves independent on the stress tolerance of the cultivar.

1.2 OBJECTIVE

The aim of this work is to better understand drought effects on AsA biosynthesis pathway in one of the most economically relevant legume crops, soybean. For this purpose, we analyzed *in vivo* AsA biosynthesis and AsA levels in different plant tissues and queried RNA-seq databases to investigate the regulation of the biosynthesis pathway at various levels of stress.

1.3 MATERIALS AND METHODS

1.3.1 Plant growth conditions, drought treatments and water status characterization

Glycine max (L.) Merr. cv Oxumi seeds were sterilized as previously described (Labhilili et al., 1995); seeds were placed in 1% NaClO (v/v) and 0.01% SDS (w/v) for 40 minutes and after washing them with deionized water, they were placed in 0.01N HCL for 10 minutes. Seeds were germinated on trays with a mixture of perlite:vermiculite (1:1, v/v) for three days in the darkness at 26ºC. Seedlings were subsequently grown in 1-L pots containing 2:1 (v/v) vermiculite:perlite as rooting substrate in a controlled-environmental chamber (24ºC/18ºC day/night temperature, 60/70% day/night relative e humidity, and 16-h photoperiod). Plants were watered three times a week with a nutrient solution containing (values in g L^{-1}) K_2HPO_4 (0.2), $MgSO_4 \times 7H_2O$ (0.2), KCl (0.2), EDTA-Na_2Fe (0.025), $CaSO_4 \times 2H_2O$ (0.12); (values in mg L^{-1}) $NaMoO_4 \times 2H_2O$ (4), $FeCl_3 \times 2H_2O$ (1), $ZnSO_4 \times 7H_2O$ (1), H_3BO_3 (1), $MnSO_4 \times H_2O$ (0.08), $CuSO_4 \times 5H_2O$ (0.03), $AlCl_3 \times 6H_2O$ (0.05), $NiCl_2$ (0.03), KI (0.01); Rigaud and Puppo, 1975) supplemented with 5 mM KNO_3. Four-week-old plants were separated into two sets: control and drought. Control plants were supplied daily with the nutrient solution to field capacity, whereas drought was achieved by withholding water/nutrients. Two hours after the start of the photoperiod, leaf and root water potential (Ψ_w) were measured. Leaf Ψ_w was measured in the first fully expanded leaf using a pressure chamber (Soil Moisture Equipment, Santa Barbara, CA, USA; Scholander et al., 1966). Root Ψ_w was measured using C52 sample chambers coupled to a Wescor HR-33T Dew Point microvoltimeter (Wescor) and measurements were taken after at least 1 h. Soybean leaf water potential was daily monitored to classify plants into control (C; leaf Ψ_w = -0.23 ± 0.04 MPa), very mild stress (VMS; leaf Ψ_w = -0.54 ± 0.02 MPa) and mild stress (MS; leaf Ψ_w =-1.13 ± 0.1 MPa). Plant tissue fresh weight (FW) was measured and aliquots were collected, immediately frozen in liquid nitrogen and stored at –80ºC for analytical determinations. The remaining tissue was employed for dry weight (DW) determinations after drying for 48 h at 70ºC. Water content (WC) was calculated as follows: WC = (FW-DW)/(FW x 100).

1.3.2 Determination of total and reduced AsA content

AsA content was measured by high-performance capillary electrophoresis as previously described (Davey et al., 1996). Briefly, frozen leaf, stem and root samples (~0.2 g FW) were homogenised using a mortar and pestle under liquid nitrogen and mixed with 1.5 mL 2% (v/v) metaphosporic acid containing 1 mM ethylenediaminetetraacetate. Samples were centrifuged (12 min, 13000 *g*, 4ºC) and the filtered supernatant was used to determine antioxidants by capillary

electrophoresis (Herrero-Martínez et al., 1998) using a buffer containing 60 mM NAH_2PO_4, 60 mM NaCl (pH 7), and 0.0001% hexadimethrine bromide under the following conditions: −15 kV potential, 50 μm-internal diameter and 30/40.2 cm-long capillary tube with indirect UV detection at 256 nm. To obtain total AsA pools, samples were treated with dithiothreitol (DTT). Dehydroascorbic acid (DHA) levels were calculated as the difference between the total AsA pool and the reduced form.

1.3.3 *In vivo* AsA synthesis assay

In vivo biosynthesis of AsA was assayed as previously reported (Bartoli et al., 2000). Briefly, leaf and root samples (~0.1 g FW) were sliced and incubated for 3 h at 25ºC in a buffer containing 50 mM Tris-HCl (pH 8.0) either with or without 50 mM L-galactono-1,4-lactone (GalL) as a control. *In vivo* AsA synthesis capacity was estimated as the difference in AsA content between time 3 h vs. time 0 in untreated samples and samples supplemented with GalL.

1.3.4 Soybean and *M. truncatula* gene identification and expression analysis

To analyze the regulation of the AsA biosynthesis under drought conditions, the expression of genes encoding enzymes involved in the SW pathway route in soybean and *M. truncatula* was studied. Based on the pathway described in *Arabidopsis* plants by Linster and Clarke, (2008) and after Conklin et al., (2013) stablished the specific enzymatic reactions for AsA synthesis (from D-mannose-1-P to AsA as final product), in this study we focused on the analysis of those genes implied in this part of the pathway; *VTC1* (catalysed by GDP-D-mannose pyrophosphorylase), *GME* (GDP-D-mannose 3´,5´-epimerase), *VTC2/VTC5* (GDP-L-galactose phosphorylase), *VTC4* (L-galactose-1-P phosphatase), *L-GalDH* (L-galactose dehydrogenase) and *L-GalLDH* (L-galactono-1,4-lactone dehydrogenase). The putative orthologous genes implicated in SW pathway were identified by BLASTP using the Wm82.a1.v1.1 Soybean Knowledge Base genome version [http://soybase.org/GlycineBlastPages /blast_descriptions.php; (Joshi et al., 2014)] and the M. truncatula 4.0 genome version (http://www.medicagohapmap.org/tools/blastform). Only proteins with E-values $<1E^{-10}$ were further selected.

Soybean gene expression values were obtained using RNA-seq as previously described (Song et al., 2016). The expression profile of the orthologs was retrieved from the Medicago Gene Expression Atlas [http://mtgea.noble.org; (Benedito et al., 2008)], extended with data on drought stress responses (Zhang et al., 2014). The average from three biology replicates was used to calculate the fold change in gene

expression. Relative expression results were calculated as ratios taking expression values at day 0 as a reference. For soybean, genes with more or less than a 2-fold change compared to control and a P-value less than $5*10^{-5}$ were considered as significant differentially expressed genes. For *M. truncatula*, the criteria of genes changing more or less than a 2-fold compared to control was used with a significance of 95%.

1.4 RESULTS

1.4.1 Physiological characterization of soybean plants under drought stress

Soybean plants were subjected to progressive drought stress by withholding water/nutrients and leaf water potential (Ψw) was monitored to determine the level of stress. Plants were assigned to the following groups: well-watered plants were used as controls (C; leaf Ψw = -0.23 ± 0.04 MPa); three days after the onset of drought plants were classified as very mild stress (VMS; leaf Ψw = -0.54 ± 0.02 MPa) and seven days after the onset of drought plants were under mild stress conditions (MS; leaf Ψw =-1.13 ± 0.1 MPa; Fig. 1.1A). To better characterize the plant water status, we also measured root Ψw (Fig. 1.1A) and the relative water content (WC; Fig. 1.1B). A significant decline in Ψw was observed both in leaves and roots of plants subjected to progressive drought. In leaves, MS caused an almost five-fold decline in Ψw compared to C plants. In roots, Ψw values declined four-fold in VMS and six-fold in MS conditions, reaching more negative values compared to the aerial part. Leaf and root WC in C plants showed values around 80-90% throughout the study period (Fig. 1.1B). Water deprivation caused a gradual decrease in WC in both organs, which was more accused in roots (-63% vs. -26%; Fig. 1.1B). This response is consistent with the observed decline in Ψw values in the different drought treatments and provides a physiological context to the progressive drought stress imposed.

1.4.2 AsA content and *in vivo* AsA synthesis decline in leaves of drought-stressed soybean plants

To investigate whether the levels of AsA were affected by drought, the content of AsA and DHA were monitored in leaf, root and stem samples using high-performance capillary electrophoresis. Although spectrometry-based approaches are traditionally applied to the detection of AsA in plant extracts, capillary electrophoresis-based methods offer numerous advantages for a rapid and sensitive analysis of the levels of AsA in plants (Davey et al., 2000), and this technique has been successfully applied to measure AsA in various plant tissues (Davey et al., 1996; Fotsing et al., 1997; Herrero-Martínez et al., 1998; Zabalza et al., 2007).

Leaves showed a higher content of both AsA and DHA compared to stems under control conditions (4-fold and 2-fold higher, respectively; Fig. 1.2A-D), presenting also a higher reduced/total AsA ratio (0.76 vs. 0.54, respectively; Fig. 1.2E and 1.2F). Drought stress caused a progressive reduction of the levels of AsA in both aerial tissues (Fig. 1.2A and -B), while the content of DHA was only significantly reduced in stem samples (Fig. 1.2D). This suggests that the decline in AsA levels during drought is not explained by a conversion to DHA. Interestingly, the content

of AsA and DHA in soybean root samples was found under the detection limit of the technique (0.75 μmol g^{-1} DW).

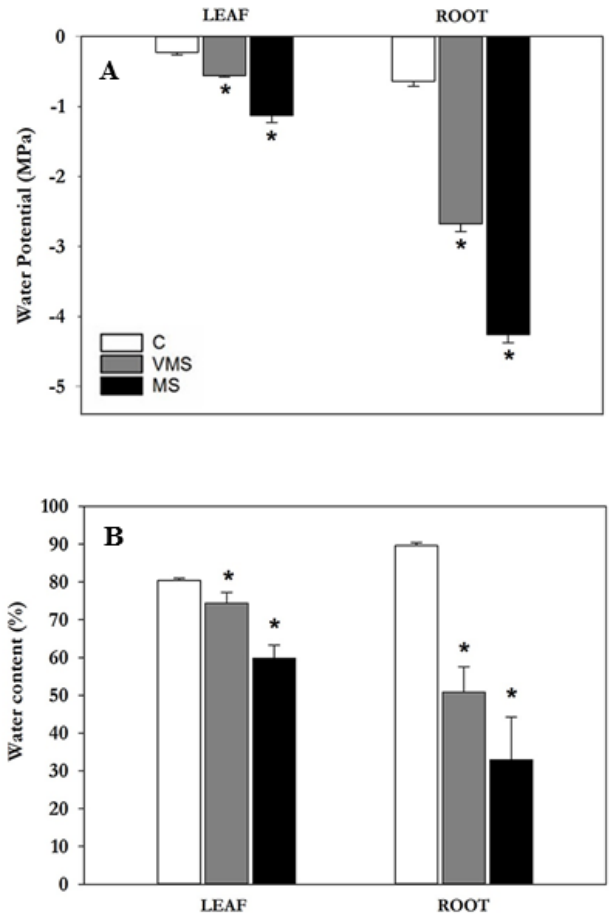

Figure 1.1 Effects of progressive drought stress on leaf and root water potentials (A) and water content (B) in soybean plants under well-watered control conditions (C), very mild stress (VMS) and mild stress (MS). Values represent the average ± SE (n=4 biological replicates). An asterisk (*) denotes significant differences ($p \leq 0.05$) with respect to C plants.

To test whether the observed decline in the levels of AsA could be explained by a reduction of AsA biosynthesis, AsA synthesis was investigated under *in vivo* conditions (Fig. 1.3). Again, activity was only detected in leaves and stems, but not in root tissue. Since activity in leaves and stems showed a similar pattern, only leaf AsA synthesis is shown. AsA biosynthesis was negatively affected by drought, showing a progressive decline as water potential values dropped (Fig. 1.3A).

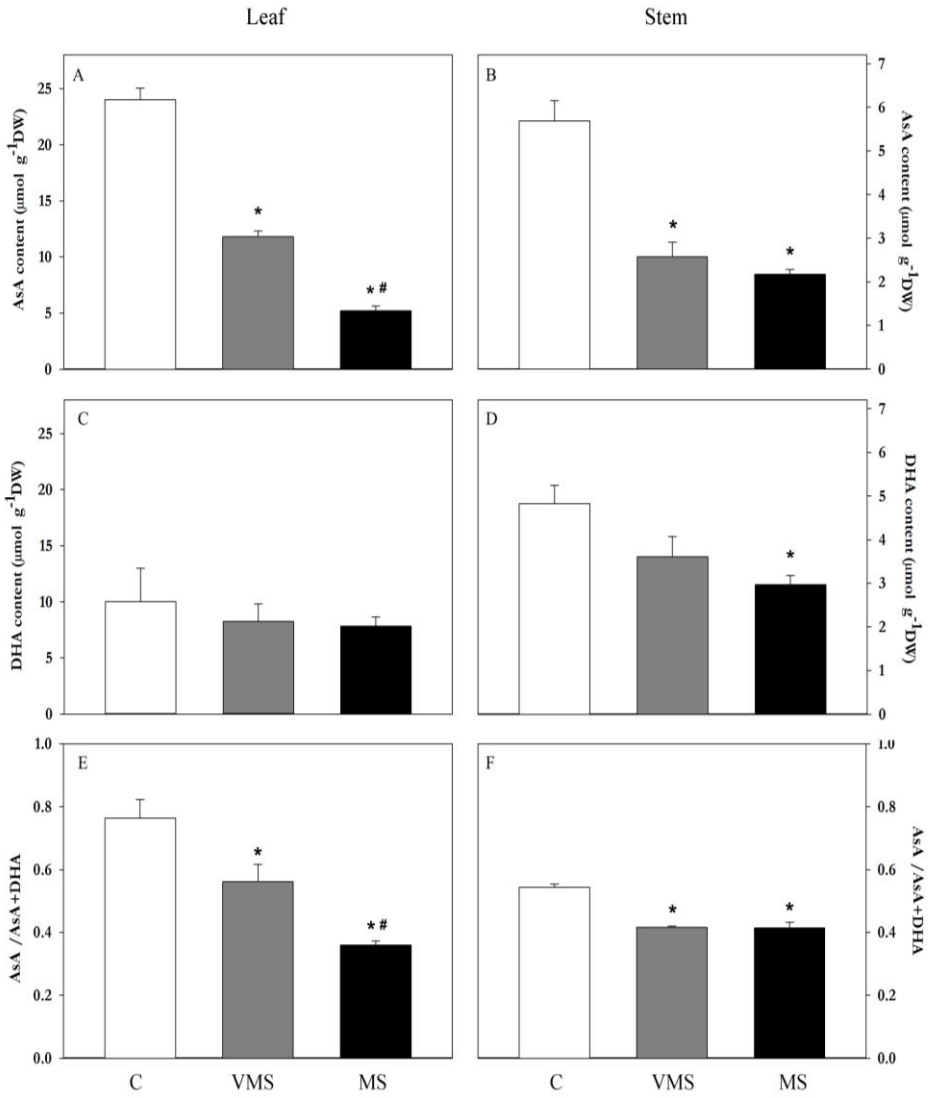

Figure 1.2. Variation on the levels of AsA, DHA and AsA/AsA+DHA on leaf (A, C, E) and stem (B, D, F) samples of soybean plants under control (C), very mild stress (VMS) and mild stress (MS) conditions. Values represent the average ± SE (n=3 biological replicates). An asterisk (*) denotes significant differences ($p \leq 0.05$) with respect to C plants.

To check whether there was a substrate limitation for GalLDH enzyme, activity was also measured adding the substrate of the reaction, GalL. In the presence of GalL, AsA biosynthesis increased in C plants around 78%, while drought stress led to a similar, progressive decline as the water deficit increased (Fig. 1.3B). These results show that the observed reduction in AsA biosynthesis under water deficit is not related to a substrate limitation, suggesting a possible regulation at the transcriptional or post-transcriptional level.

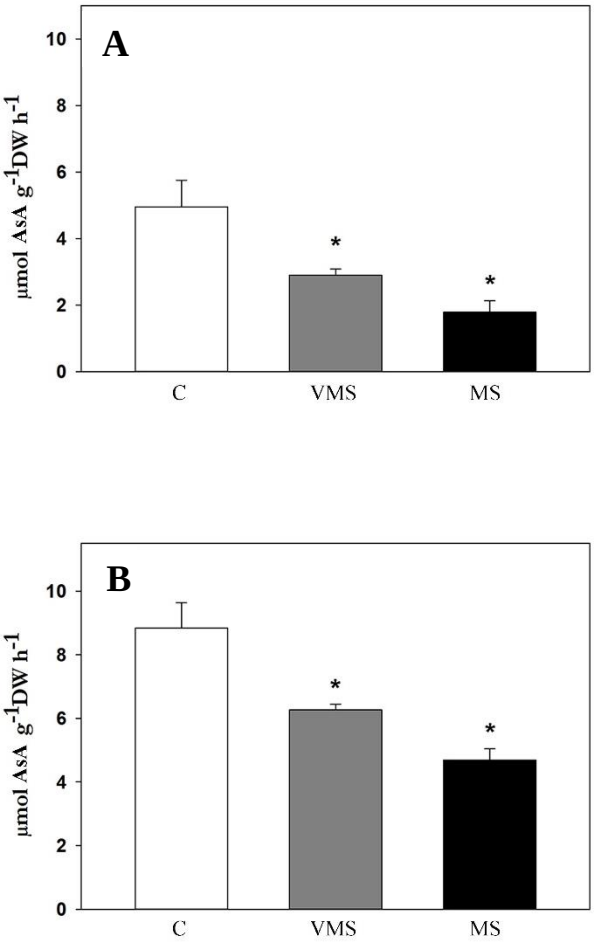

Figure 1.3. *In vivo* AsA biosynthesis rates in leaves of soybean plants under control (C), very mild (VMS) and mild (MS) stress conditions. Activity estimated as the difference in AsA content between at time 3 h vs. time 0 in untreated samples **(A)** and samples supplemented with GalL **(B)**. Values represent the average ± SE (n=3 biological replicates). An asterisk (*) denotes significant differences ($p \leq 0.05$) with respect to C plants.

1.4.3 Transcriptional regulation of AsA biosynthesis under drought stress

To gain further insights into the regulation of the biosynthesis of AsA at the transcriptional level, we analyzed the expression patterns of the genes involved in the pathway in soybean plants subjected to a progressive drought stress followed by a rewatering treatment (Song et al., 2016). Based on the SW pathway described for *A. thaliana*, we first searched for the putative orthologous genes in the soybean genome using a BLAST (Basic Local Alignment Search Tool; http://blast.ncbi.nlm.nih.gov) approach. Since the first steps in the pathway generate compounds also involved in other metabolic pathways, we focused our

analysis on the following enzymes: VTC1 (GDP-D-mannose pyrophosphorylase), GME (GDP-D-mannose 3´,5´-epimerase), VTC2/VTC5 (GDP-L-galactose phosphorylase), VTC4 (L-galactose-1-P phosphatase), GalDH (L-galactose dehydrogenase) and GalLDH (L-galactono-1,4-lactone dehydrogenase). Unlike the situation in *Arabidopsis*, the soybean genome contains multiple gene copies for each enzymatic step in the pathway (Fig. 1.4): four genes were found to code for VTC1 (Glyma02g41820, Glyma11g34550, Glyma14g07150 and Glyma18g03840), five genes for GME (Glyma01g09540, Glyma03g40720, Glyma10g30400, Glyma19g43410 and Glyma20g36740), the same set of four were retrieved when VTC2 and VTC5 were queried (Glyma02g46230, Glyma08g43200, Glyma14g02500 and Glyma18g10430), three for VTC4 (Glyma07g39620, Glyma09g01380 and Glyma15g12230), two for GalDH (Glyma07g30395 and Glyma08g06840) and two for GalLDH (Glyma02g27260 and Glyma10g17370). We also included in the analysis a known regulator of the pathway in *A. thaliana*, VTC3, for which only one candidate ortholog was found in the soybean genome, Glyma02g21970. Interestingly, the complete set of genes was found expressed both in shoot and in root tissue (Fig. 1.5).

In terms of drought responses, the mildest stress treatment showed one of the strongest responses in leaf tissue, with the down-regulation of most of the genes in the pathway. Three out of the five *GME* genes and two *VTC4* genes, however, were found up-regulated at later drought stages, a situation that was reverted upon rewatering of the plants. In contrast, the *GalLDH* genes, coding for the last enzyme in the pathway and supposedly one of the key regulators of the pathway, did not show a differential expression during drought (Fig. 1.5). In root tissue, however, drought stress caused a general up-regulation of the pathway, with the exception of the *GME* gene Glyma03g40720 and the *GalDH* gene Glyma08g06840, which were found significantly down-regulated. Interestingly, the *VTC4* gene Glyma09g01380 showed an induction under severe drought conditions, a similar expression pattern to this observed in leaf tissue (Fig. 1.5). Regarding *VTC3*, only in root tissue there was a drought-related response of this putative regulator, showing a mild down-regulation under water deficit, which was reverted by rewatering the plants.

To investigate whether this regulation at the transcriptional level was also found in other legume species, we performed a similar analysis in the pasture legume *M. truncatula*. After identification of the closest orthologs in the SW pathway, we queried their expression of genes in the Medicago Gene Atlas database [http://mtgea.noble.org; (Benedito et al., 2008)], which has been now extended with expression data corresponding to a progressive drought stress followed by a recovery treatment (Zhang et al., 2014). The list of genes in the pathway in *M.*

truncatula included two genes coding for VTC1 (Medtr3g069070 and Medtr5g080770), GME (Medtr1g080950 and Medtr7g115080), and VTC2/VTC5 (Medtr3g053020 and Medtr5g093390), and single copy genes for VTC4 (Medtr2g026060), GalDH (Medtr4g092750) and GalLDH (Medtr1g050360); (Fig. 1.4). Similarly to the case in soybean, the full pathway was found expressed in shoots and roots of the model legume (Fig. 1.6). However, there was a differential response to water deficit compared to this observed in soybean. For instance, in leaves progressive drought caused a gradual up-regulation of the expression of one of the *GME* gene, Medtr7g115080, while the *VTC1* gene Medtr5g080770 and the regulatory gene *VTC3* (Medtr1g050520) were down-regulated (Fig. 1.6). Interestingly, in roots drought induced the up-regulation of the expression of the same *GME* gene observed in leaves, along with the *VTC2* gene Medtr5g093390, being the two *VTC1* genes strongly down-regulated compared to controls (Fig. 1.6). It is worth noting that the two genes putatively coding for GME show an opposite pattern of expression both in roots and in leaves, suggesting a functional specialization of the genes.

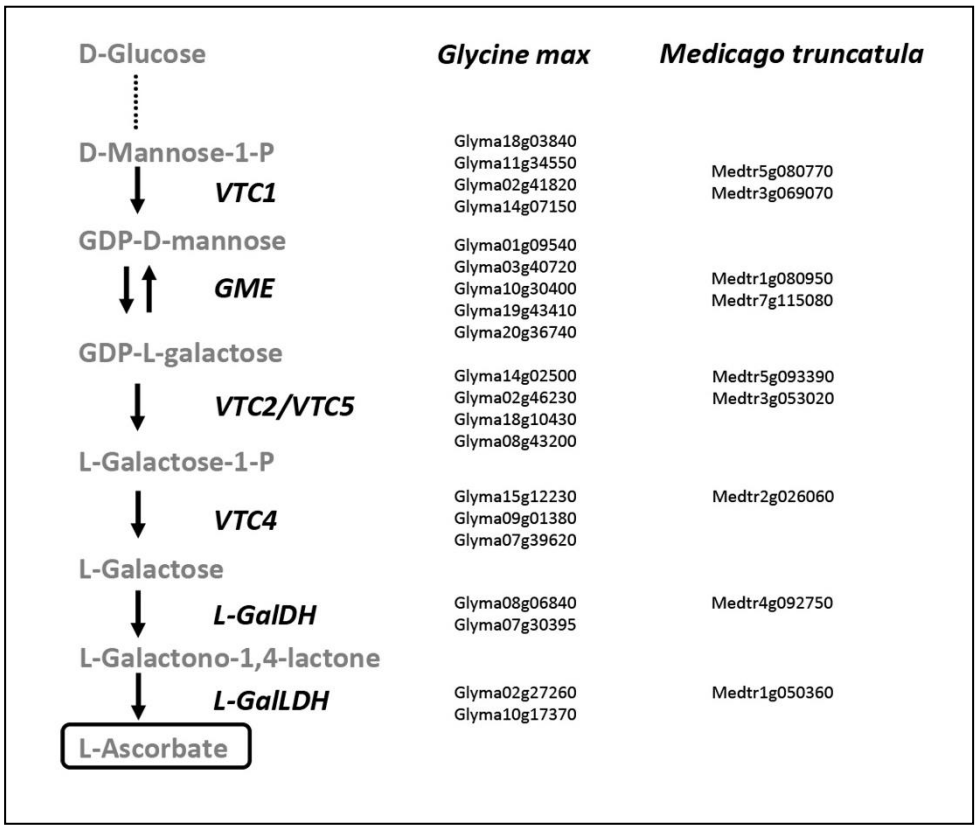

Figure 1.4. Identification of genes in the SW pathway in *G. max* and in *M. truncatula*.

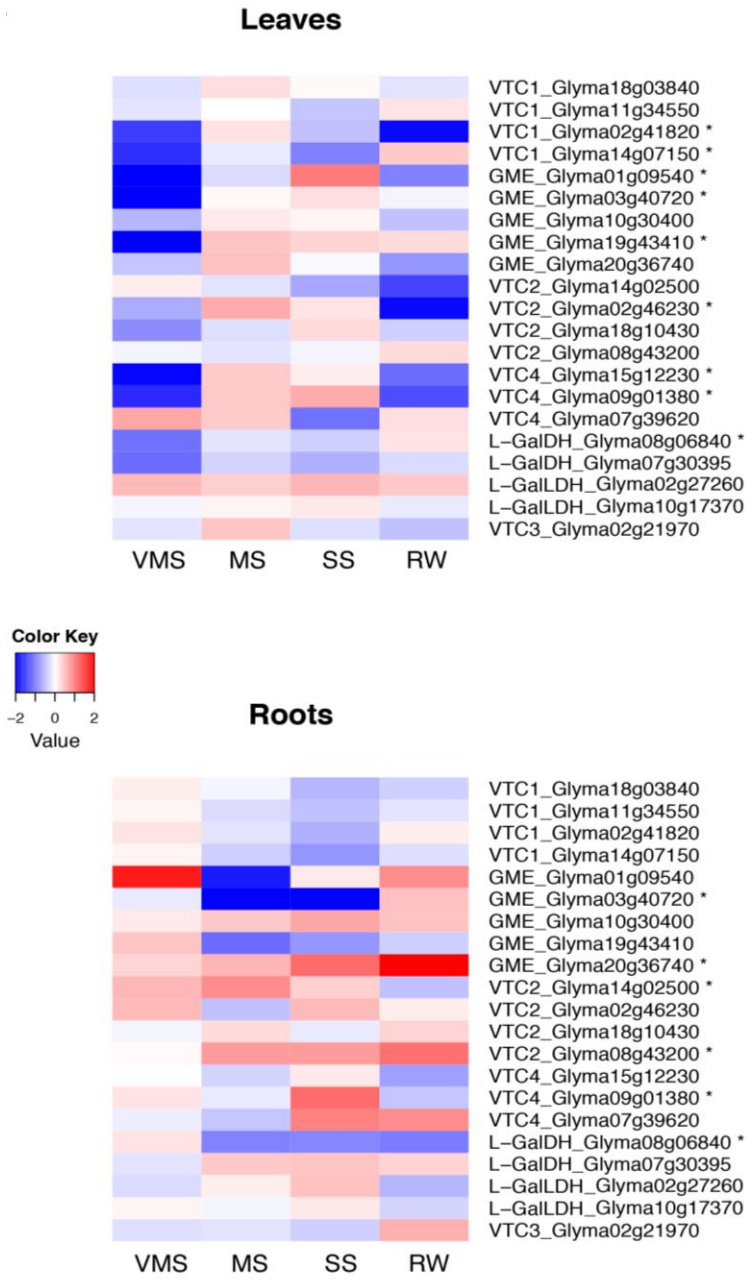

Figure 1.5. Expression of genes in the SW pathway in *Glycine max* leaves and roots. Hierarchical cluster representing the RNA-seq expression patterns of genes in the AsA biosynthetic pathway in leaf and root tissue under very mild (VMS), mild (MS), severe (SS) drought stress, and a subsequent recovery treatment (RW). An asterisk (*) denotes significant differences between treatments and control plants ($p < 5*10^{-5}$).

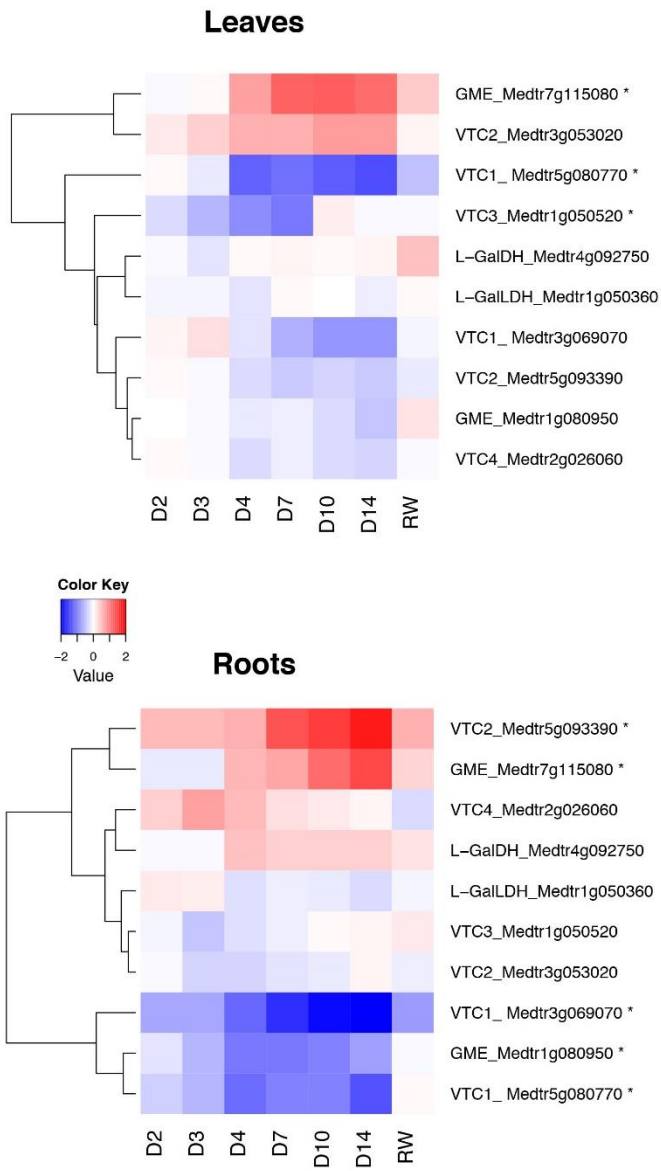

Figure 1.6. Expression of genes in SW pathway in *M. truncatula* leaves and roots**.** Hierarchical cluster representing the expression patterns of AsA biosynthetic pathway related genes in *M. truncatula* shoots and roots respectively under drought-stress at day 2 (D2), 3 (D3), 4 (D4), 7 (D7), 10 (D10), 14 (D14) and a rewatering treatment (RW) compared to well-watered control plants. An asterisk (*) denotes significant differences between treatments and control plants ($p < 0.05$).

1.5 DISCUSSION

In the current work, we analyzed the effects of drought stress in the biosynthesis of AsA in a crop of great economic relevance like soybean. The steady-state levels of AsA in a certain tissue are regulated via biosynthesis, degradation, recycling and transport of this antioxidant. Here we have measured the effects of drought stress in the regulation of biosynthesis both at the activity and transcriptional level, analyzing not only shoots, generally considered the main site of AsA biosynthesis in plants, but also root tissue. Knowledge on the AsA biosynthetic capacity of this underground organ is currently limited, despite being a key organ in terms of sensing a water deficit situation and triggering a response to drought stress. Through imposing a gradual water deficit, accompanied with a detailed plant physiological characterization (Fig. 1.1), we observed a reduction of the levels of AsA both in leaves (Fig. 1.2A) and stems (Fig. 1.2B) of soybean plants. Such drought-induced decline in the levels of AsA has been also observed in the leaves of wheat (Bartoli et al., 1999) and several *Labiatae* species (Munné-Bosch and Alegre, 2003), as well as in symbiotic root nodules (Marino et al., 2007; Naya et al., 2007; Zabalza et al., 2008), but not in pea leaves (Moran et al., 1994). This lower content of AsA, however, was not correlated to increased levels of DHA, suggesting that it may be related to a reduced biosynthesis or increased transport of AsA. Indeed, results on *in vivo* GalLDH activity showed a significant and progressive reduction in the rates of AsA biosynthesis as lower water potential values were reached (Fig. 1.3). Thus, although alternative routes cannot be ruled out, we found a correlation between the levels of AsA and GalLDH biosynthetic rates in leaves of drought-stressed soybean plants.

To check whether there was a regulation of the pathway at the transcriptional level, we analyzed the expression patterns of enzymes in the SW pathway, including putative orthologs described as regulators in other plant species, in soybean plants exposed to drought stress. Since the pathway has not been specifically described in legumes, we used the protein sequences of enzymes described for *A. thaliana* to identify the closest orthologous genes. Interestingly, we identified several genes encoding for each of the enzymes in the pathway in soybean (Fig. 1.4). This genetic redundancy can be explained by the fact that the soybean genome has undergone at least two polyploidy events, estimated to occur ~13 and ~59 million years ago, which has led to 75% of the genes in the soybean genome being present in multiple copies (Roulin et al., 2013). It is interesting to note, however, how these multiple gene copies show differential patterns of expression, as observed for the soybean *GME* and *VTC4* orthologs (Fig. 1.5), suggesting certain level of specialization at the functional level. These contrasting expression patterns

may be also explained by a differential localization of the gene expression at the tissue level, a dimension that is lost when harvesting the complete tissue.

Interestingly, the expression of genes coding for the full AsA biosynthetic pathway was detected not only in leaves but also in roots of both legume species. This suggests that although the vast majority of works in the literature have focused on AsA biosynthesis in leaves, roots have the potential of synthesizing this antioxidant compounds as well (Hancock et al., 2003; Liso et al., 2004), as shown in pea roots (Zabalza et al., 2007), *Lotus japonicus* root nodules (Matamoros et al., 2006), and a number of non-legume species.

GalLDH is considered one of the regulation points of AsA biosynthesis in plants (Yabuta et al., 2007). However, we did not observe significant changes on the expression levels of *GalLDH* genes in either soybean or *M. truncatula* plants under drought stress (Fig. 1.5 and Fig. 1.6, respectively). If *GalLDH* is not regulated at the transcriptional level under water deficit conditions, it could be hypothesized that the observed decline in GalLDH activity may be due to post-translational regulatory mechanisms. This is further supported by the fact that *in silico* prediction of phosphorylation sites [http://musite.net; (Gao et al., 2010)] identify two conserved Ser residues (Ser472 and 476, and Ser469 and 473 in Glyma.02G166300 and Glyma.10G104100, respectively; >99% specificity) as potential targets for phosphorylation in the predicted soybean proteins. Furthermore, several potential ubiquitylation sites are also found [support vector machine probability >0.83; http://bioinfo.ncu.edu.cn/ubiprober.aspx; (Chen et al., 2013)].

In contrast, drought induced the down-regulation of *VTC1* genes both in soybean and *M. truncatula*, while most *VTC2/VTC5* and *VTC4* genes showed an induction (Fig. 1.5 and Fig. 1.6). *A. thaliana* mutants in *VTC1*, which is encoded by a single gene, are deficient in AsA (Conklin et al., 1997; Conklin et al., 1999; Veljovic-Jovanovic et al., 2001) and the levels of expression of this gene have been correlated with the content of AsA in several other plant species (Badejo et al., 2007; Badejo et al., 2008; Wang et al., 2013). This correlation is also observed in the current work, which suggests that VTC1 may also play a role in the regulation of AsA biosynthesis in legumes. On the other hand, it has been hypothesized that GME in association with VTC2/VTC5 constitute a control point for the regulation of the AsA pathway in plants (Dowdle et al., 2007; Wolucka and Van Montagu, 2007; Linster and Clarke, 2008; Bulley et al., 2009). In legumes, the analysis of drought responses in the gene *GME* was complex, with several genes putatively coding for this enzyme in the pathway and each gene showing a differential response under drought conditions. For instance, in *M. truncatula* there was a clear induction of the *GME* gene Medtr7g115080 both in leaves and roots, while Medtr1g080950 was

strongly down-regulated in roots (Fig. 1.6). Further points of regulation in the pathway include *AMR1* (Zhang et al., 2009), for which there was not a good match in either the soybean or the *M. truncatula* genome, and *VTC3* (Conklin et al., 2013), which was found down-regulated only at early drought stages in soybean roots and *M. truncatula* leaves (Fig. 1.5 and Fig. 1.6).

In summary, the transcriptional regulation of the SW pathway in legumes under drought stress is complex, with multiple gene copies for each step in the pathway and a possible functional specialization of the paralogs. This complexity limits the applicability of the transfer of knowledge from other species and highlights the need of further research in legume species. Future lines may provide answers to questions such as the role of post-transcriptional regulatory mechanisms using targeted proteomic approaches (Wienkoop et al., 2008) or the tissue/functional specialization of the various paralog genes in the pathway, including their role in AsA biosynthesis and, ultimately, abiotic stress tolerance.

1.6 CONCLUSIONS

This study concludes that a progressive drought caused a decline in both *in vivo* AsA biosynthesis and AsA content in leaves of soybean plants. Furthermore, a complete gene set involved in the Smirnoff-Wheeler pathway is expressed in roots and leaves of both legume species, *G. max* and *M. truncatula*. Finally, drought stress responses highlighted multiple control points in the legume species analyzed; genes encoding GDP-D-mannose pyrophosphorylase (VTC1) emerge as strong candidates for the regulation of AsA biosynthesis in drought-stressed legume plants, while GDP-D-mannose 3´, 5´-epimerase (GME) genes appear to have undergone functional specialization.

upna

Universidad Pública de Navarra
Nafarroako Unibertsitate Publikoa

» CHAPTER 2

Medicago truncatula plants priotitize water for leaves and carbon and nitrogen for roots to face drought

upna

Universidad Pública de Navarra
Nafarroako Unibertsitate Publikoa

2.1 INTRODUCTION

Grain and forage legumes are grown on around 15% of the arable surface of the Earth, being the second most important crop after cereals attending to world primary crop production (Graham and Vance, 2003). The economical relevance of legume crops is related to both their importance as a protein source for animal feed and human nutrition and their use as raw material in the industry (Edgerton et al., 2008). Furthermore, the ability of legume plants to carry out nitrogen fixation in symbiosis with soil rhizobium bacteria provides an environmental-friendly source of reduced nitrogen in the biosphere, being an essential element in sustainable agriculture worldwide. Despite the numerous advantages of the cultivation of legumes, their yield is limited by the abiotic stress conditions, particularly drought.

Water stress is identified as a major environmental factor that constrains crop productivity (Araus et al., 2002). According to the different scenarios predicted by the Intergovernmental Panel on Climate Change (Alley, 2007), it is expected that there will be a reduction in precipitation and rising evapotranspiration rates. The perceived need to gain further understanding of photosynthesis, so as to alleviate practical problems such as crop yield under drought conditions, has increased interest in 'water stress physiology' (Lawlor and Tezara, 2009). The photosynthetic rates of plants exposed to drought decrease due to stomatal closure and non-stomatal processes (Lawlor and Cornic, 2002; Aranjuelo et al., 2007; Chaves et al., 2009; Lawlor and Tezara, 2009). While stomatal closure has been identified as a target factor conditioning photosynthetic performance under moderate water-limiting conditions (Chaves et al., 2002; Chaves et al., 2003), when water stress is more severe, metabolic impairment takes place (Medrano et al., 2002) associated with photooxidative damage (Lawlor and Tezara, 2009).

Most research efforts focused on the analyses of plant performance under drought stress have been traditionally focused on the aerial part of the plant, whereas, traditionally, little attention has been given to root performance. In particular, in the area of legumes, the field remains largely unexplored. Studies integrating the response of the above- and under-ground tissues under drought are scarce. In this regard, a further understanding of root responsiveness to water stress is essentially matter of great concern because roots play a target role in nutrient and water acquisition and transport. Increased nutrient and water uptake capacity may be achieved through better nitrogen and water transporters, more effective regulation of the transport system or better storage and assimilation of nutrients. Increasing the uptake capacity of roots is not simple because little is known about

its regulation. However, during the last decade, several root phenotyping studies highlight the relevance of root functioning in crop responsiveness to stressful growth conditions (Paez-Garcia et al., 2015). Roots are the first organ sensing the water deficit and signaling the variation of soil water status. However, few studies have specifically focused on legumes responses to water shortage at the root scale. For instance, Beebe et al. (2014) have revised some useful root traits for drought resistance in common bean while Zhang et al. (2014) have compared the transcriptomic and metabolomic responses of barrel medic shoots and roots under low water availability conditions. Recently, the strategies used to cope with environmental challenges in different legumes have been examined (Araújo et al., 2015), and the importance of the root system for the improvement of productivity has been studied in chickpea (Kashiwagi et al., 2015). In terms of quantitative loci traits (QTL), Quero et al. (2014) have identified a QTL for root growth under ionic–osmotic stress along with other related to shoot growth or shoot/root ratio in *Lotus*.

2.2 OBJECTIVE

This study aims to determine the response of *M. truncatula* plants to two progressive drought levels attending to the leaf-root partitioning target carbon and nitrogen metabolites involved in plant growth.

2.3 MATERIAL AND METHODS

2.3.1 Plant material, growth conditions and drought characterization

M. truncatula Gaertn cv. Jemalong A17 seeds were scarified and then sterilized using sulphuric acid 96% for 7 minutes. Then the acid was removed and seeds were washed using distilled water. Subsequently, 3.5% (v/v) NaClO was added for 5 minutes to sterilize the seeds. After washing, seeds were placed on 0.7% (w/v) agar plates and maintained one day at 4ºC for uniform germination. Plates were then incubated at 25ºC for two days to enable seed germination. After germinate, seeds were sown in 1-L pots containing a mixture of perlite:vermiculite (2:5, v/v) under controlled environmental conditions (14 h photoperiod; 400 µmol m^{-2} s^{-1} light intensity; 22ºC/16ºC day/night temperature; 60 to 70% relative humidity). Plants were watered to field capacity 3 times a week with Evans nutrient solution containing (values in mg L^{-1}): $MgSO_4 \cdot 7H_2O$ (493), K_2SO_4 (279), K_2HPO_4 (145), $CaCl_2$ (56), KH_2PO_4 (23), EDTA-Fe (17), H_3BO_3 (1.43), $CaSO_4 \cdot 2H_2O$ (1.03), $MnSO_4 \cdot 7H_2O$ (0.77), $ZnSO_4 \cdot 7H_2O$ (0.22), $CoCl_2 \cdot 6H_2O$ (0.12), $CuSO_4 \cdot 5H_2O$ (0.08), $NaMoO_4 \cdot 2H_2O$ (0.05); (Evans, 1981). This nutrient solution was supplemented with 5 mM NH_4NO_3.

Eight-week-old plants were randomly separated into two sets containing 6 biological replicates each. Controls (C) were supplied daily with a nutrient solution to field capacity and drought treatment was achieved by withholding water/nutrients. Water-stressed plants and their corresponding controls were harvested during the onset of drought in a 6-day-time period. During this period, leaf water potential values were measured in the first fully expanded leaf 2 h after the beginning of the photoperiod using a pressure chamber (Soil Moisture Equipment, Santa Barbara, CA, USA) as earlier described (Scholander et al., 1966) to classify plants according to their water status; these values declined gradually from control values, reaching progressively a stage of moderate drought (MD; Ψ_w -1.75 MPa) and severe drought (SD; Ψ_w -2.93 MPa). After that, leaf and root water potentials were measured in C52 sample chambers coupled to a Wescor HR-33T Dew Point Microvoltmeter (Wescor, Logan, UT, USA). Tissue aliquots (50 mg) were confined in a C52 chamber for 1h until temperature and vapour equilibration was reached. Leaf and root samples were harvested, immediately frozen in liquid nitrogen and stored at -80ºC for analytical determinations. Leaf and root water content (WC) was calculated as described in the section 1.3.1 of the Chapter 1, where FW corresponds to the fresh weight and DW, the dry weight of tissue samples after at least 48 h at 80ºC.

2.3.2 Gas exchange measurements

Transpiration rate was gravimetrically determined on a daily basis during the experimental period. Gas exchange measurements were carried out with a Li-COR 6400 portable gas exchange system (LI-COR, Lincoln, Nebraska, USA) in fully expanded leaves. Determinations were conducted between 2 h and 6 h after the onset of the photoperiod. The net photosynthetic rates were measured at 1000 µmol m^{-2} s^{-1} Photosynthetic Photon Flux Density (PPFD) with 400 µmol s^{-1}air flow rate, 25ºC and 60% relative humidity (Jauregui et al., 2016). The rate of electron transport through the photosystem II (ETR), electron flux for photosynthetic carbon reduction (ETRc) and the electron flux for photorespiratory carbon oxidation (ETRo) were measured as described by Epron et al. (1995).

2.3.3 Sucrose, starch and organic acids measurements

Frozen aliquots of root and leaf tissue (200 mg FW) were homogenized with 1.5 mL 80% (v/v) ethanol, being samples ultrasonicated for 30 minutes at 30ºC in an ultrasonic bath and after centrifuged at 7,500 *g* for 5 min at 4ºC (Fernández-Fernández et al., 2010). The same protocol was repeated twice and supernatants of the same sample were collected together. All the collected supernatant from ethanolic extracts was dried in a Turbovap® LV Evaporator (Zymark, Hopkinton, MA, USA) at 40ºC and 1.2 bar. When all the ethanol was evaporated, the dried sample was suspended in 1 mL of deionized water, mixed and centrifuged at 6,000 *g* for 10 min at 4ºC. After being filtered, the supernatant was collected in a new tube and stored at -20ºC until its utilization.

Ethanol non-soluble residues were extracted for starch content analysis as previously described (Gonzalez et al., 1998). The pellet obtained after the extraction of ethanol soluble sugars was dried at 70ºC for 24 h and after, it was suspended in 1 mL of deionized water. After the samples were boiled at 100ºC for 1 h in a water bath, 250 µL of 0.082% (w/v) amyloglucosidase dissolved in 8.55 mM acetate (pH 4.5) were added. This reaction was incubated at 50ºC overnight in darkness continuously shaking. Then, the mixture was centrifuged at 7,500 *g* for 15 min at 4ºC and the supernatant was collected and stored at -20ºC until it was used. Sucrose and starch-derived glucose were analyzed by high-performance capillary electrophoresis in a P/ACETM MDQ (Beckman Coulter Inc., Brea, CA, USA) according to Warren and Adams (2000). The background buffer consisted of 10 mM benzoate (pH 12.0) and 0.5 mM myristyltrimethylammonium bromide (MTAB). The applied potential was -15 kV, and the capillary tubing was 50 µm internal diameter and 31.4/38.4 cm long. The indirect UV detection wavelength was set at 225 nm.

The organic acid content, in this case malate and α-ketoglutarate, was determined according to the method of Wilson and Harris (1966). Frozen shoots and roots (0.1 g FW) were homogenized in a mortar with 1.5 mL 5% (w/v) trichloroacetic acid (TCA) and then centrifuged at 1750 *g* at 4ºC for 10 minutes. Supernatants were collected and washed thrice with ether-saturated water. The aqueous phase was bubbled for two minutes with helium and later filtered through 0.45 µm PVDF syringe membrane filters and stored at -20ºC until their use (Gálvez et al., 2005). Organic acids levels were determined by ion chromatography in a DX-500 system (Dionex Corporation, Sunnyvale, CS, USA) through gradient separation (from 0.2 mM NaOH to 35 mM NaOH and from 10% of methanol to 20% of methanol, in 27 min, at a flux of 2 mL min^{-1}) with a Dionex IonPack AG11+AS11 columns.

2.3.4 Protein and amino acid determination

Frozen leaves and roots (200 mg FW) were homogenized in a mortar and pestle with 3 volumes of extraction buffer (50 mM MOPS, 5 mM $MgCl_2$, 20 mM KCl, 1 mM Na_2EDTA, pH 7) and 1.5 mg mL^{-1} of DTT and 0.7 µL mL^{-1} of β-mercaptoethanol were freshly added. Homogenates were centrifuged at 20,500 *g* and 4ºC for 20 min. Protein was quantified using a Bradford-based dye-binding assay (Bio-Rad, Hercules, CA, USA) employing bovine serum albumin as standard (Bradford, 1976). Supernatants were then collected and diluted with deionized water and mixed with 200 µL BioRad Protein Assay Dye Reagent (Bio-Rad Laboratories Inc., Hercules, CA, USA) to quantify soluble protein. The samples were incubated at room temperature for 5 min and the absorbance was measured at 595 nm in a SinergyTM HT Multi-Detection Microplate Reader (BioTek Instruments Inc., Winooski, VT, USA).

For amino acid determination, frozen leaves and roots (200 mg FW) were ground to powder under liquid N_2 and subsequently homogenized in a mortar and pestle with 3 mL of 1 M HCl. Homogenates were transferred to glass tubes and incubated on ice for 10 min. Subsequently, extracts were centrifuged at 20,000 *g* and 4ºC for 10 min. Supernatants were neutralized to 7.0 - 8.0 pH with NaOH. For the free amino acids determination, known concentrations of internal standards norvaline and homoglutamic acid were added to the mixture.

Samples were then derivatized with 1 mM fluorescein isothiocyanate (FITC) dissolved in acetone and the homogenates were 5-fold diluted in 20 mM borate buffer (pH 10.0) and incubated at room temperature in the dark for 15 h. The content of free amino acids was determined using a Beckman Coulter capillary

electrophoresis PA-800 (Beckman Coulter Inc., USA) coupled to laser-induced fluorescence detection (argon laser at 488 nm), as described in Arlt et al. (2001) and Takizawa and Nakamura (1998) with minor modifications. A fused-silica capillary with 43/53.2 cm long and 50 µm internal diameter (Beckman Coulter Inc., USA) was employed. For amino acids separation, 45 mM α-cyclodextrin in 80 mM borax buffer (pH 9.2) was used. Analyses were performed at 20ºC and at a voltage of 20 kV. Total amino acid content is presented as the summation of single amino acids for each sample and expressed on a DW basis.

2.3.5 Statistical analysis

For all the variables determined in this study, we calculated the average as a central statistic and standard error as statistical of dispersion. Significant differences among control and treatments were determined with Student's t-test ($p \leq 0.05$).

2.4 RESULTS

2.4.1 Physiological characterization of M. truncatula plants under drought stress

Water content was determined in leaves and roots of *M. truncatula* plants exposed to drought stress (Fig. 2.1A). The water content of aerial parts was significantly affected only under severe drought (SD) decreasing 8% compared to control. However, root water content decreased around 33% and 39% in MD and SD, respectively. Besides determining leaf Ψ_w, plant water status was monitored by measuring water potential of leaf and root sections using a dew-point thermocouple psychrometer (Fig. 2.1B). Ψ_w showed a gradual decrease in MD and SD, in both leaves and roots, compared to C plants (Fig. 2.1B). Biomass of the whole plant was apparently not affected by the 6-day drought stress treatment applied in this study (Fig. 2.1C). However, photoassimilate partitioning between leaves and roots was significantly altered by drought, leading to a progressive and significant reduction of shoot biomass while root biomass exhibited an upward trend, only significant at moderate drought stress level (Fig. 2.1C). Consequently, the shoot:root ratio showed marked differences between control and drought treatments, being reduced to one-half when drought was applied (Fig. 2.1C).

2.4.2 Gas exchange parameters affected by low water availability conditions

Transpiration rates on a plant basis were reduced 50-55% under drought conditions compared to control values (Table 2.1). This decline was mainly due to stomatal closure as indicated by the stomatal conductance, which declined progressively to values around 26 and 6% of that exhibited by well-watered plants (Table 2.1). Photosynthesis was adversely affected in plants subjected to drought, decreasing progressively when increasing drought severity. Thus, photosynthesis of MD and SD plants was reduced a 46.29% and 79.60%, respectively (Table 2.1). This gradual decrease correlated with the reduction of the stomatal conductance and transpiration values. This suggests that the MD treatment applied in the current study represents an intermediate drought stress level at which parameters such as CO_2 level of the chloroplast, the flow of electrons crossing the photosystem II (ETR) or the values of maximum carboxylation of rubisco are still not affected (Table 2.1). Conversely, ETR was significantly reduced in SD treatment (Table 2.1). Although the ETR rate of oxygenation (ETRo) was unaffected, a significant decrease of electron flux for photosynthetic carbon reduction (ETRc) was observed supporting the slowdown of the Calvin cycle.

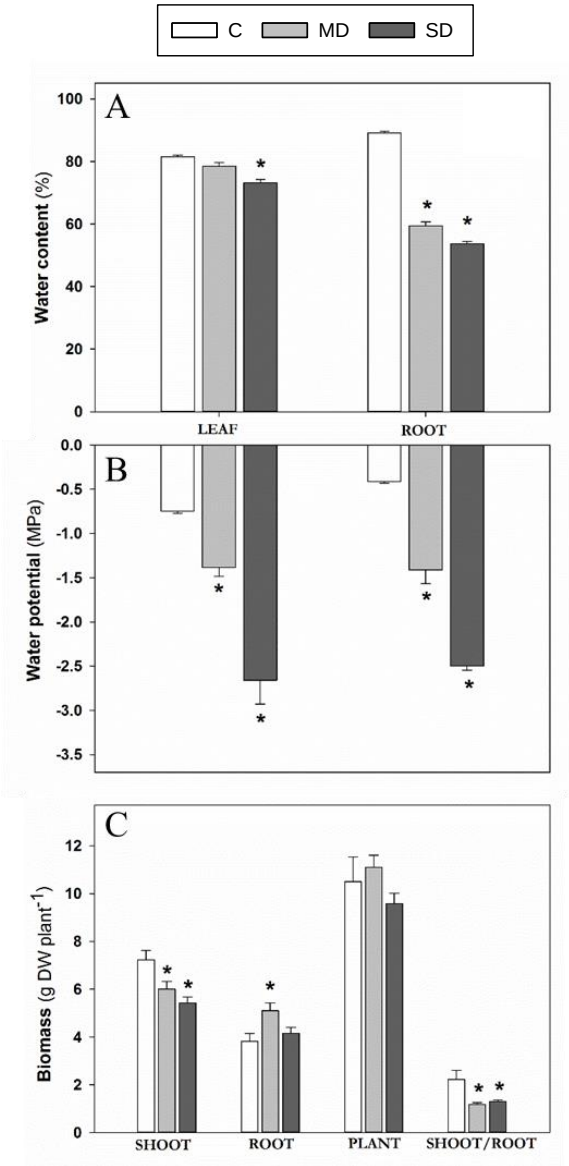

Figure 2.1. Effect of drought on leaf and root water content (A), water potential (B) and biomass (C) of *M. truncatula* plants under well-watered (C), Moderate Drought (MD) and Severe Drought (SD) conditions. Values represent mean ± SE (n=4 biological replicates). An asterisk (*) denotes significant differences ($p \leq 0.05$) with respect to C plants.

2.4.3 Metabolic changes in *M. truncatula* plants induced by drought stress

Leaf and root sucrose concentrations were not significantly affected by MD treatment but they showed a significant increase in both organs under SD stress, occurring to a higher extent in roots (Fig. 2.2A). Starch content under well-watered conditions was 19-fold higher in leaves (478 µmol g^{-1} DW) than in roots (25 µmol g^{-1} DW). Starch reserves values decreased 90% compared to control plants by the

imposition of drought (Fig. 2.2B). Under control conditions, the level of malate was 4 times higher in leaves than in roots (Fig. 2.2C). Drought stress induced the accumulation of this organic acid in both organs, being this effect only significant in SD roots (Fig. 2.2C). α-ketoglutarate content was significantly reduced in roots of MD and SD treatments, being unaffected in leaves which exhibited 5-fold higher values than roots (Fig. 2.2D).

Table 2.1. Gas exchange. Transpiration and photosynthesis rates, stomatal conductance, chloroplastic CO_2, ETR, ETRc, ETRo and maximum rate of carboxylation values of Control (C), Moderate Drought (MD) and Severe Drought (SD) plants. Values represent mean ± SE (n=3). For each parameter, an asterisk (*) denotes significant differences ($p \leq 0.05$) with respect to C plants and a hash (#) significant differences between MD and SD treatments.

GAS EXCHANGE			
	C	MD	SD
Transpiration rate ($g\ H_2O\ plant^{-1}\ day^{-1}$)	130.70 ± 7.02	36.89 ± 1.33 *	24.36 ± 1.52 *#
Photosynthesis rate ($\mu mol\ CO_2\ s^{-1}cm^{-2}$)	17.11 ± 1.41	9.19 ± 0.99 *	3.49 ± 0.86 *#
Stomatal conductance ($mmol\ H_2O\ m^{-2}\ s^{-1}$)	394.80 ± 34.31	101.89 ± 31.44 *	24.39 ± 14.32 *#
Chloroplastic CO_2 ($\mu mol\ mol^{-1}$)	194.99 ± 36.37	110.58 ± 8.35	68.28 ± 6.82 *
ETR ($\mu mol\ e^{-2}s^{-1}$)	114.83 ± 7.22	103.96 ± 8.11	75.65 ± 5.23 *
ETRc ($\mu mol\ e^{-2}s^{-1}$)	82.58 ± 5.23	58.06 ± 4.76 *	33.53 ± 4.18 *#
ETRo ($\mu mol\ e^{-2}s^{-1}$)	32.26 ± 7.91	45.90 ± 4.31	42.12 ± 1.10
Maximum rate of carboxilation ($\mu mol\ CO_2\ m^{-2}s^{-1}$)	58.96 ± 15.44	22.10 ± 2.69	nd

2.4.4 Amino acid metabolism changes in *M. truncatula* plants under drought stress

Regarding nitrogen metabolism, leaf protein content was progressively reduced at the different drought stress levels although this decrease was only significant in SD plants (Fig. 2.3A). Conversely, this parameter was maintained constant in the root system regardless of the water regime (Fig. 2.3A). The total amino acid content tended to increase significantly in leaves and roots under water stress, exhibiting a concomitant accumulation following the increase in drought severity in both organs (Fig. 2.3B).

Figure 2.4 presents the response of the 20 proteogenic amino acids and the non-protein γ-aminobutyric acid (GABA). Cysteine (Cys) showed a significant decline in MD leaves, reducing its content around 60% compared to controls, relieving this response under SD conditions. Meanwhile, Cys accumulated not significantly in roots. At the same time, glycine (Gly) co-eluting with serine (Ser) in the amino acid analysis increased around 25% in drought-stressed leaves being invariable in roots.

Phenylalanine (Phe) and tryptophan (Trp) showed a similar pattern, accumulating significantly in leaves of drought-stressed plants, increasing progressively from 4 to 10-20 fold with the severity of the stress. Both amino acids were significantly accumulated in roots, although the content in drought-stressed plants only duplicated the one of control plants. Tyrosine (Tyr) was only significantly accumulated in drought-stressed roots. Alanine (Ala) was slightly affected under SD, decreasing it content in leaves when significantly increasing in roots. The branched-chain amino acids, valine (Val), leucine (Leu) and isoleucine (Ile), together with methionine (Met), lysine (Lys), threonine (Thr), arginine (Arg) and histidine (His), were all notably accumulated in leaves and roots of drought-stressed plants. Proline (Pro), a known drought marker, showed the largest increase in drought treatments.

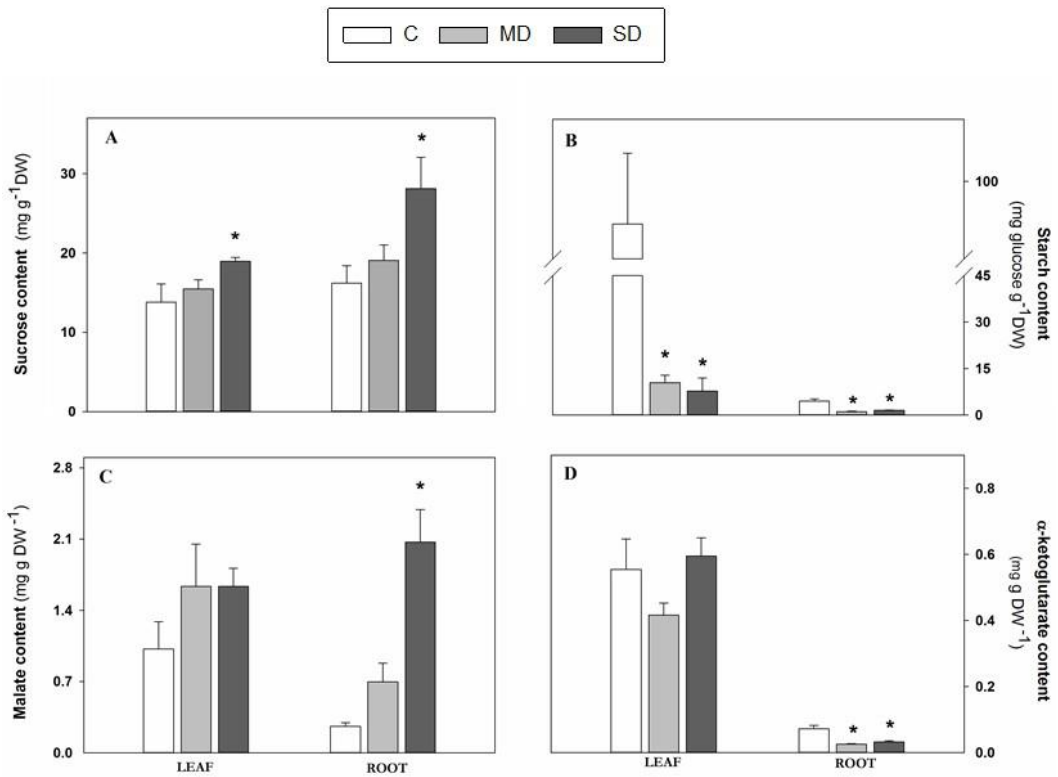

Figure 2.2. Effect of drought on starch (A), sucrose (B) and organic acids (C, D) content of *M. truncatula* plants under well-watered (C), Moderate Drought (MD) and Severe Drought (SD) conditions. Values represent mean ± SE (n=3 biological replicates). An asterisk (*) denotes significant differences ($p \leq 0.05$) with respect to C plants.

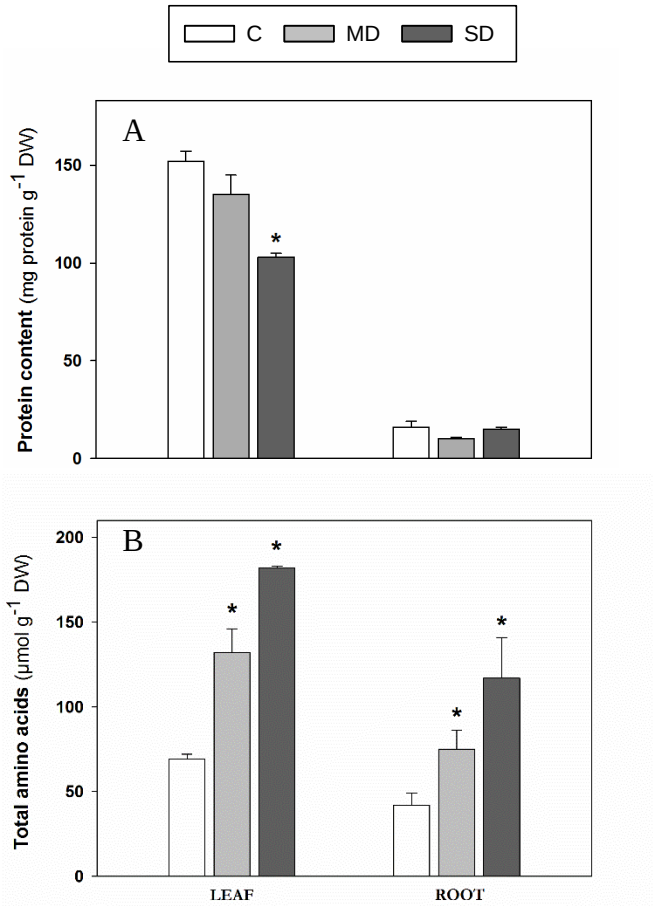

Figure 2.3. Effect of drought on protein (A) and total amino acids (B) content of *M.truncatula* plants under well-watered (C), Moderate Drought (MD) and Severe Drought (SD) conditions. Values represent mean ± SE (n=3 biological replicates). An asterisk (*) denotes significant differences ($p \leq 0.05$) with respect to C plants.

Interestingly, Pro accumulation was more pronounced in leaves as water content was more dramatically affected in roots (Fig. 2.1A). Conversely, the levels of GABA were unchanged under drought stress conditions in both organs. Glutamic (Glu) and aspartic acid (Asp) concentrations were not significantly affected by drought either in leaves or in roots. However, glutamine (Gln), the first form of organic nitrogen synthesized from ammonium and a-ketoglutarate, was significantly accumulated in leaves of MD and SD plants. Conversely, in roots, Gln content was significantly reduced under MD recovering control values in SD plants. Asparagine (Asn), the most abundant amino acid, synthesized from oxaloacetate and employing Gln as ammonium donor, showed an upward trend in leaves and roots, although differences were only significant in roots of SD plants, which doubled the Asn content of control plants. Summarizing, most of the amino acid

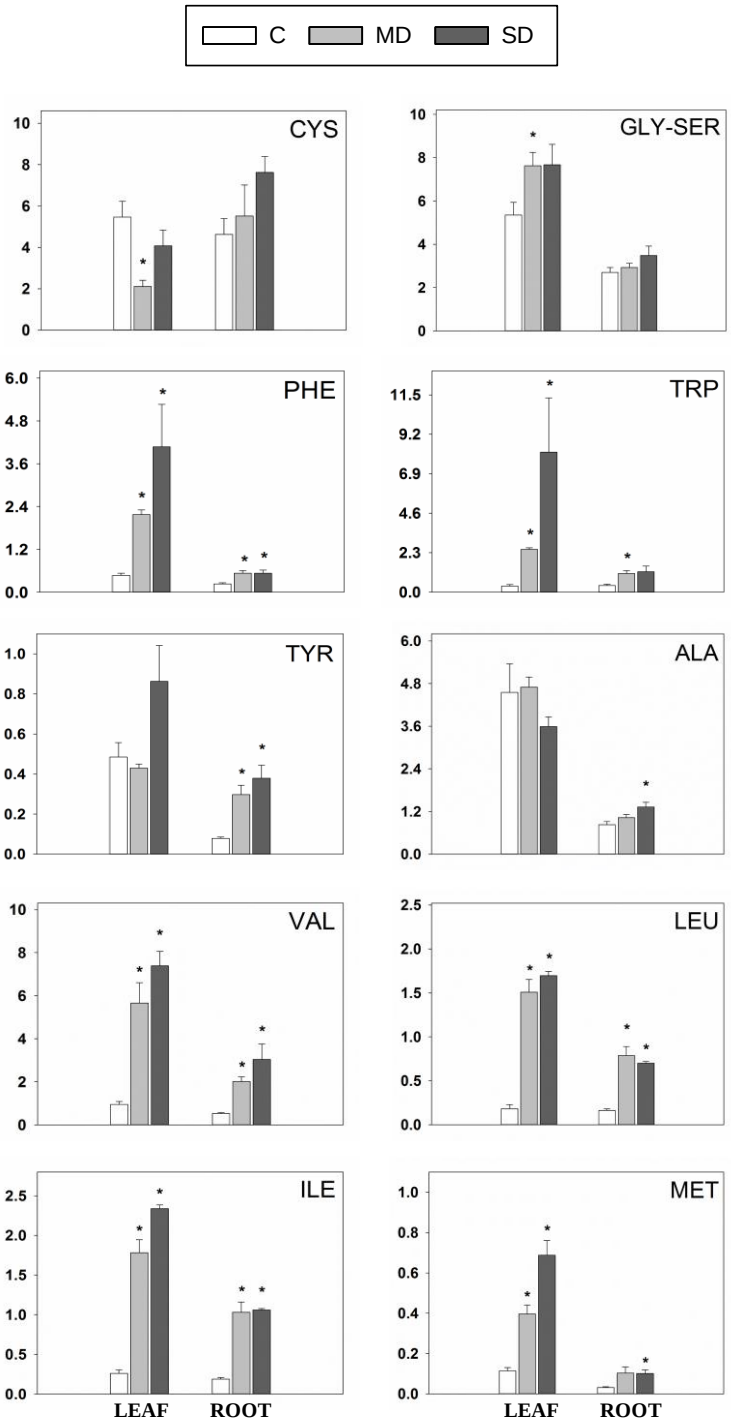

Figure 2.4. Effect of drought on individual amino acids content of *M. truncatula* plants under well-watered (C), Moderate Drought (MD) and Severe Drought (SD) conditions. Values in µmol g^{-1} DW represent mean ± SE (n=3 biological replicates). An asterisk (*) denotes significant differences ($p \leq 0.05$) with respect to C plants.

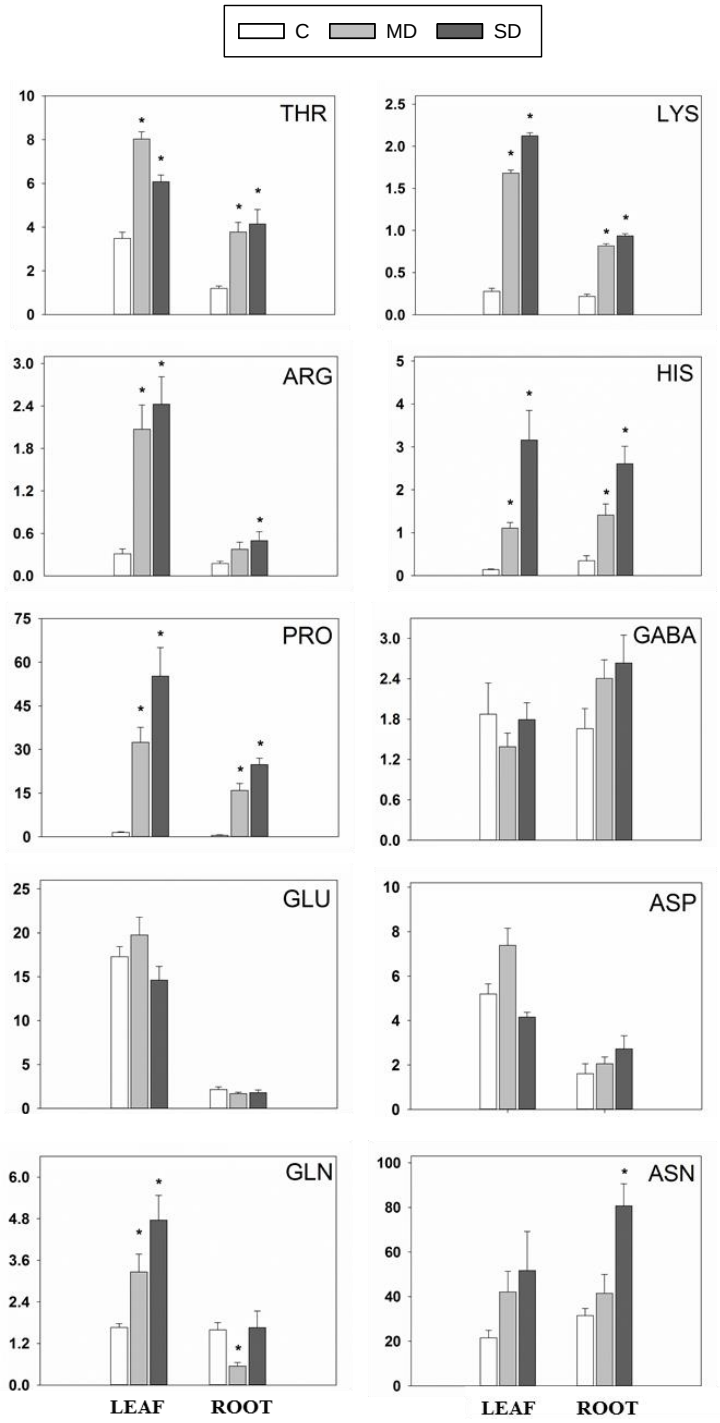

Figure 2.4 (*continued*). Effect of drought on individual amino acids content of *M. truncatula* plants under well-watered (C), Moderate Drought (MD) and Severe Drought (SD) conditions. Values in µmol g^{-1} DW represent mean ± SE (n=3 biological replicates). An asterisk (*) denotes significant differences ($p \leq 0.05$) with respect to C plants.

analyzed accumulated in leaves and roots of drought-stressed *M. truncatula* plants, only Cys declined significantly in leaves together with Gln in roots under MD conditions, recovering control values under SD conditions in both cases.

Figure 2.5 presents the change of the leaf to root ratio for each individual carbon and nitrogen compound analyzed occurring in both drought treatments compared to control plants. This change is expressed on a logarithmic basis to have an easy view of those compounds accumulating preferentially in leaves or in roots. The positive values [Log_2 (Drought/Control) >1] indicate a preferential accumulation in leaves explaining that leaf to root ratio was higher in drought than in control plants. On the contrary, the negative values [Log_2 (Drought/Control) <1] indicate a preferential accumulation in the root and, therefore, the leaf to root ratio of drought was lower than that of control. By analyzing this parameter, it can be observed that the main carbon compounds sucrose, starch and malate accumulated preferentially in the root of drought-stressed plants, exhibiting the aerial part a carbon deficit. Regarding the amino acids, the more abundant amino acid, Asn, accumulated to a similar extent in leaves and roots and therefore, its distribution between tissues did not vary in drought-stressed plants (Fig. 2.4). Similarly, Glu, which is mainly located in leaves, or Pro, whose concentration increased dramatically in both leaves and root, strictly maintained its distribution among aerial and underground organ under drought stress conditions (Fig. 2.4). However, the distribution pattern of some amino acid changed significantly under drought conditions: Cys and Tyr were preferentially accumulated in roots whilst Phe, Trp, Arg, His and Gln were accumulated in leaves (Fig. 2.5).

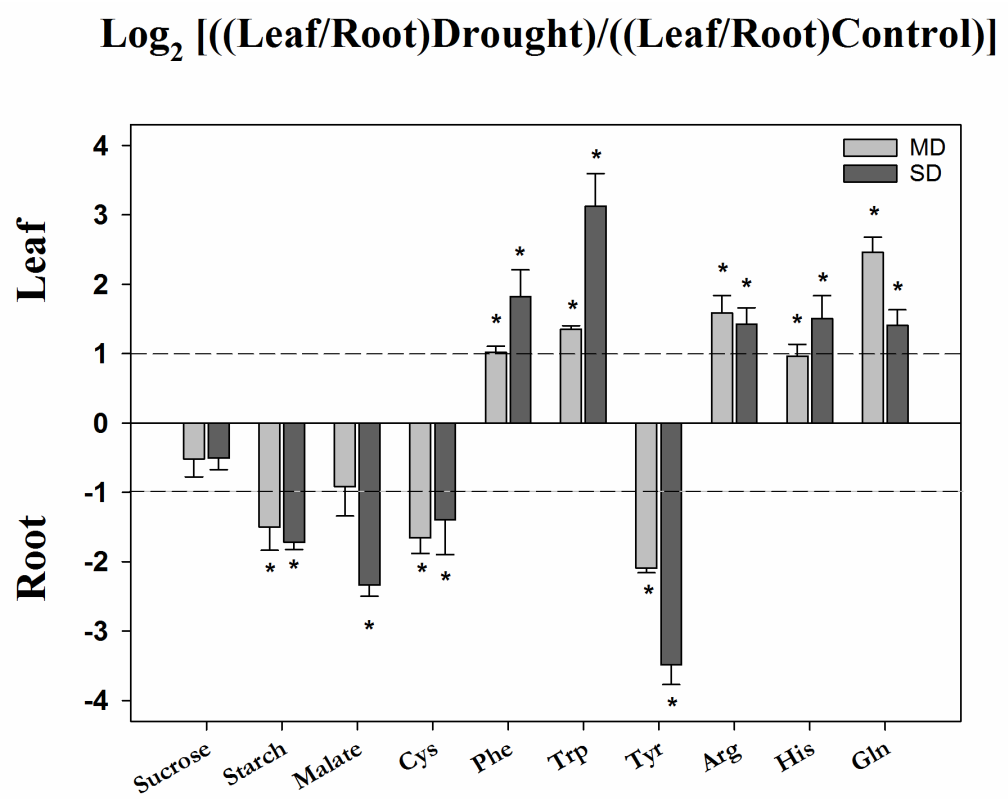

Figure 2.5. Schematic representation of significantly altered ($p \leq 0.05$) leaf to root ratios expressed on a logarithmic basis for different carbon and nitrogen compounds under both drought treatments (MD and SD) compared to control (C). Values represent mean ± SE (n=3 biological replicates). An asterisk (*) denotes significant differences ($p \leq 0.05$) with respect to C plants.

2.5 DISCUSSION

2.5.1 Plant growth: modifications in shoot/root ratio as a strategy to cope with water stress

Water availability has been identified as a strong inhibitor of plant growth (Aguirreolea and Sánchez-Díaz, 1989; Antolin and Sanchez-Diaz, 1992). Although at the plant level no significant differences were detected in terms of plant biomass, our study showed that drought stress had a significant impact on biomass production. Plants subjected to drought had a smaller shoot/root ratio, resulting mainly from a larger root biomass. Several authors have hypothesized that this response may be an adaptation to the Mediterranean dry summer season (Hilbert and Canadell, 1995; Lloret et al., 1999). Our results indicate that roots were able to maintain growth activity while shoot reduced its growth, leading to a reduction of the shoot/root ratio (Fig. 2.1C). This differential response seems to be a strategy to prevent excessive dehydration and it has been shown to be regulated by hormones (Sharp and Davies, 1989; Sharp, 2002; Wilkinson and Davies, 2010). The root to shoot Ψ_w gradient involved in regulation of water movement at the plant level was observed under control conditions but it seem not to be operative under drought stress. Nevertheless shoot WC was maintained much higher than that of roots (Fig. 2.1A). These results highlight the plant prioritization of shoot water content in detriment of the root under drought stress conditions.

2.5.2 Photosynthetic limitation is counteracted by starch degradation under drought stress

Root growth depends on an optimal supply of photoassimilates and, therefore, on an adequate rate of photosynthesis. Physiological characterization parameters revealed that diminishment of photosynthetic rates was strongly mediated by limitations in stomatal opening and the severe depletion in CO_2 diffusion through the mesophyll, especially in severely droughted plants. Similarly, data of the physiological characterization suggest that the Rubisco carboxylation rate (Vcmax) was also involved in the photosynthetic down-regulation of drought-stressed plants (Nunes et al., 2008). Interestingly, our study suggests the fact that despite the strong photosynthetic inhibition, sucrose content was not limiting in plants subjected to severe water stress. Moreover, leaves and roots have similar sucrose content in control conditions showing an accumulative trend under drought (Fig. 2.2A). Also, malate, the most abundant organic acid, accumulated up to 8-fold in roots of severe droughted plants compared to control (Fig. 2.2C), pointing out the importance of carbon compounds in the underground tissue to face drought. In agreement with previous findings, our study revealed that, under drought stress, a rapid starch

degradation occurred in both organs (Fig. 2.2B). Starch has been defined as a major integrator metabolite for plant growth (Sulpice et al., 2009) and its degradation in response to drought has been previously observed (Lee et al., 2008). Cuellar-Ortiz et al., (2008) showed that sucrose translocation occurs under drought stress from leaves to other parts of common bean plants, even when this does not occur under control conditions. In this regard, Durand et al. (2016) observed an enhance in C allocation to roots of *Arabidopsis* drought-stressed plants attending root C demand to maintain an efficient root system. An up-regulation of sucrose transporters involved in phloem loading at leaves was observed at the time the transcript levels of AtSUC2 and AtSWEET11 to AtSWEET15 increased in stressed roots. Kryvoruchko et al. (2016) also showed that MtSWEET13, a sugar efflux transporter up-regulated in leaves and roots in drought conditions, and those sucrose transporters genes described by Durand et al., 2016, cluster together in the same clade suggesting its role in drought stress responses. In this regard, Gargallo-Garriga et al. (2014) provided clear evidence of the high capacity of plants to vary the allocation of nutrients and metabolites. These authors observed in two common grass species that primary metabolites concentrations are higher in leaves than in roots under control conditions but a shift of these towards the roots in detriment of the leaves was observed under drought conditions.

In conclusion, leaf starch metabolization supplied carbon skeletons avoiding any carbon limitation in leaves and roots when photosynthetic activity dropped in water-stressed plants. Previous studies have shown that under drought growth is constrained by tissue level processes and active stress signaling rather than by provision of photoassimilates (Muller et al., 2011; Körner, 2015).

2.5.3 Above- and below-ground tissues activate different stress signaling and tolerance responses linked to amino acid metabolism

As mentioned above, the accumulation of stress metabolites such as specific amino acids has been described in leaves and roots of plants exposed to water stress (Aranjuelo et al. 2011; Gil-Quintana et al., 2013). Under unfavorable conditions, the mobilization of N from leaf proteins has been described to contribute by increasing the availability of amino acids (Feller et al., 2008). In *M. truncatula*, leaves seem to be the main soluble protein reservoir and this was significantly reduced in SD plants (Fig. 2.3A). This could be related to the decline of Rubisco protein concentration in accordance with that observed in *Arabidopsis* plants grown under elevated CO_2 conditions (Jauregui et al., 2016) linked to the decrease of photosynthesis (Table 2.1). Proteolytic activities have been described to be enhanced by drought stress (Mosolov and Valueva, 2011). The main biological

function related to proteases has been observed to be focused on the degradation of nonfunctional proteins releasing free amino acids (van der Hoorn, 2008). Kohli et al. (2012) suggested a role of proteases on the nitrogen status by mobilizing internal and external nitrogen sources under drought stress conditions, although a correlation has not been observed in other experimental systems (Gil-Quintana et al., 2013) suggesting that this may not be the main mechanism behind the amino acid accumulation. Recently, Lyon et al. (2016) examined in deep the proteome response to severe drought in shoot and roots of *M. truncatula*, concluding that functional groups related to protein turnover (synthesis and degradation) play a key role in drought stress response with a different pattern in shoot and root. This study reveals the complexity of drought response regarding protein metabolism, highlighting the differential processes associated to drought stress responses versus recovery in shoots and roots.

Considering the different roles of the individual amino acids (Häusler et al., 2014), special attention should be paid to their pool size, which depends not only on a particular amino acid biosynthesis and degradation but also on synthesis, and breakdown of cell proteins. In the present study we analyzed the drought induced changes in the leaf:root ratio of different amino acids as a tool to identify organ specific patterns. For the most abundant amino acids, the distribution did not vary in response to drought stress and therefore, the leaf:root ratio of the most abundant amino acids such as Asn and Pro were not altered by drought stress. We first discuss the amino acids preferentially accumulated in the aerial part in detriment of the root part (Fig. 2.5). The modulation of Arg biosynthesis has been shown to determine the water stress tolerance in *Arabidopsis* throughout an effect on reactive oxygen species production (Shi et al., 2013). In the present study the preferential accumulation of Arg in the leaves may respond to the large ETR/An ratio detected in plants exposed to drought conditions (Table 2.1) which imply an increase in the proton gradient, with the consequent susceptibility to generate ROS. Besides, Arg is the natural precursor of polyamines in plants, compounds playing a key role on abiotic stress responses (reviewed by (Liu et al., 2015a)). Although polyamines are widely distributed in plants, its biosynthesis has been described as organ specific and thus putrescine is mostly synthetized in roots whilst spermine and spermidine biosynthesis occurs in the shoot in *Nicotiana tabacum* (Moschou et al., 2008).

On the other hand, Phe and Trp, are closely interlinked with the shikimate pathway and participate in the biosynthesis of innumerable aromatic secondary metabolites with important roles in plant defense against abiotic stresses (Maeda and Dudareva, 2012). Corea et al. (2012) described that carbon flux throughout shikimate pathway increased from 20 to 50% under stress conditions. In contrast,

shikimate pathway seems to be preferentially deviated towards Tyr in the roots being this amino acid preferentially accumulated in this tissue when exposed to drought (Fig. 2.4 and 2.5). These three amino acids serve as precursors of a wide variety of products that play crucial roles in abiotic stress responses and thus, Phe is the `precursor of numerous phenolic compounds as lignin and Trp is the precursor of alkaloids as well as the plant hormone auxin whereas Tyr is mainly derive to quinones (Kutchan, 1995).

His biosynthesis has been reviewed by Stepansky and Leustek (2006) remarking the interaction with other metabolic pathways as purine biosynthesis and its role as chelators and transporters of metal ions. Although an important His accumulation has been observed in different plants systems (Larrainzar et al., 2009) as it is observed in the present study, its metabolism has not yet been investigated at all in plants (Hildebrandt et al., 2015).

Summarizing, the differential partitioning of Arg and aromatic amino acids between shoot and root support the activation of specific cell protection pathways in above- and below-ground organs in response to drought.

2.5.4 Leaf:root partitioning of glutamine and cysteine is modulated under water stress

Gln is the primary product of nitrogen assimilation from inorganic nitrogen sources and a central metabolite in nitrogen metabolism in plants. This is the major amino donor for synthesis of other amino acids and nitrogen compounds and play a key role in protein and nucleotide biosynthesis (Forde and Lea, 2007). In control plants, the concentration of Gln in leaf and root was very similar around 1.6 µmol g^{-1} DW, whilst in drought-stressed plants it accumulated significantly in leaves, triplicating its concentration compared to roots (Fig. 2.4). Besides, Gln is the unique amino acid decreasing transiently its concentration in roots exposed to moderate drought suggesting a decline in primary nitrogen assimilation (Fig. 2.4). Despite its major role on protein synthesis, no correlation with the soluble protein concentration is observed, presenting the root tissue a reduced concentration of soluble protein compared to leaf (Fig. 2.3) when both organs exhibited the same Gln content (Fig. 2.4). This lack of correlation is also observed in response to drought stress when protein content decreased significantly despite the Gln accumulation (Fig. 2.4). Most studies on glutamine in plants have focused on its role as the primary amino acid derived from the assimilation of inorganic nitrogen (Miller et al., 2007), although the bulk content of this amino acid seem to be more related to the drought effect on differential protein turnover regulation of shoot and

root under drought (Lyon et al., 2016). Besides, increasing evidence about Gln role on sensing and signaling pathways in plants is coming out (Chellamuthu et al., 2014). A large battery of transcription factors, kinases and stress related genes are shown to be induced by Gln in rice roots (Kan et al., 2015) suggesting a signaling role for this amino acid in plants as it has been widely shown in human metabolism (Curi et al., 2007). The differential pattern of Gln accumulation in leaf and root suggest this amino acid play a role in drought response at the whole plant, although further research need to be carried out.

Cys was preferentially located in the root of drought-stressed plants (Fig. 2.5). Leaves showed a decrease of Cys concentration in MD conditions whilst a slight increase was observed in roots (Fig. 2.4), suggesting a limitation of sulfur transport from root to leaves. In accordance with our data, Larrainzar et al. (2014) showed that sulfate accumulates in roots of drought -stressed *M. truncatula* plants. Lee et al. (2016) found that PEG induced drought limits the translocation of absorbed sulfate from roots to leaves, thus causing a reduction of flux through the pathway. Although scarce studies have been focused on the study of the regulation of sulfur assimilation under this abiotic stress, this nutrient has been suggested to be a key component in helping plants to cope with drought (Chan et al., 2013). Sulfur assimilation pathway appears to be connected with drought stress response, not only for the production of the antioxidant molecule glutathione but, for instance, it has been shown that some abscisic acid functions are sulfate-dependent (Ernst et al., 2010). Besides, Cys acts as a precursor or donor of reduced S for a range of S-compounds such as methionine, which control key stress-metabolites such as ethylene through its first derivative S-adenosylmethionine. In this context, down-regulation of methionine biosynthesis pathway have been found associated with drought stress (Irar et al., 2014), natural senescence (Matamoros et al., 2013) and in ROS induced-senescence (Marino et al., 2009).

2.6 CONCLUSIONS

Under water stress, roots of *M. truncatula* plants reduce notably their water content to values around 60%, prioritizing the maintenance of leaf water status. At the same time, plants prioritize carbon exportation, coming mainly from starch degradation, toward this organ in order to promote root growth. Regarding nitrogen, although root nitrogen primary assimilation seems to be affected at Gln level under moderate drought conditions, leaf protein degradation is partly allocated to the root contributing to maintain the leaf-root ratio for most of the amino acids. On the contrary, the low Cys levels observed at the leaf level suggest a drought effect on sulfur transport at the whole plant level.

upna

Universidad Pública de Navarra
Nafarroako Unibertsitate Publikoa

» *CHAPTER 3*

In vitro simulation of drought stress in Medicago truncatula seedlings

upna

Universidad Pública de Navarra
Nafarroako Unibertsitate Publikoa

3.1 INTRODUCTION

Drought is considered one of the most serious problems in agriculture worldwide affecting around 40% of the land area and with a significant potential of expansion as a consequence of climate change (Trenberth et al., 2013). Salinity is the second largest limiting the productivity of crops, affecting 7% of the world arable zones (Rozema and Flowers, 2008). Although salt and drought stress trigger some common reactions in plants, especially at early stages, salinity implies an important ionic stress due to high intracellular sodium and chloride concentrations, which are absent in drought-stressed plants (Bartels and Sunkar, 2005).

Although under field conditions crop plants are exposed to multifactorial abiotic stresses and eventually results need to be validated in the field (Ribaut, 2008), growing plants under controlled growth conditions facilitates the identification of the molecular processes underpinning plant stress responses. Under laboratory conditions, salinity stress is usually simulated by adding NaCl to the growth medium at different concentrations depending on the plant species involved (Munns and Tester, 2008). The simulation of drought stress under *in vitro* conditions is more challenging, though different strategies can be found in the literature. For instance, drought responses have been analyzed by exposing plants to direct air flux (Belamkar et al., 2014; de Ollas et al., 2015), which causes a rapid reduction in the water content of the plant tissues that is unlikely to occur under physiological conditions. Alternatively, water deficit has been simulated by applying different osmotic compounds including PEG (van der Weele et al., 2000; Kang et al., 2015), sorbitol (Antoni et al., 2013) or mannitol (Luo et al., 2009; Sassi et al., 2010; Liu et al., 2015b), among others. However, these osmotic agents are absorbed by plants causing undesirable secondary effects such as cell toxicity (Lawlor, 1970; Emmert, 1974; Mexal et al., 1975; Munns et al., 1979; Ranjan et al., 2012), oxygen diffusion limitation in roots (Verslues et al., 1998) and transport inhibition in roots (Plaut and Federman, 1985).

Drought responses have been thoroughly studied in adult plants being scarcely analyzed in the early stages of development. In this regard, new not destructive and not toxic protocols are needed to simulate drought conditions to better characterize plant responses under controlled conditions. In this regard, in the current work we describe a method for the standardized and reproducible simulation of drought stress conditions in Petri dishes using growth media containing different agar concentrations. To validate the protocol, we characterized the growth, water status and drought stress responses of *M. truncatula*, a model legume cultivated as an annual forage in several regions worldwide (Michaud et al., 1988) and

phylogenetically related to some of the most important European legume crops (Aubert et al., 2006; Phan et al., 2007). Three different agar concentrations were used simulating control (C), mild drought (D1) and moderate drought (D2) conditions. Additionally, the protocol was applied for the identification of metabolic plant responses to water deficit at the root and shoot level. The method described here represents a useful alternative to the use of polyols to simulate drought stress under *in vitro* conditions with potential applications to a wide range of plant species and up scalability.

3.2 OBJECTIVES

The aims of this work were to describe a new simple and efficient method for the standardized and reproducible simulation of drought conditions with different agar concentrations and to characterize drought stress responses of *M. truncatula* seedlings grown under these conditions.

3.3 MATERIALS AND METHODS

3.3.1 Plant materials and growth conditions

M. truncatula Gaertn. cv Jemalong ecotype A17 plants growth conditions are the same as detailed in the section 2.3.1 of the Chapter 2 of the present thesis. However, the only difference with the previously method described is that 0.7% (w/v) agar plates were incubated at room temperature for 36 hours instead of for two days. In this way, we obtained seedlings having rootlets of around 0.5 cm. Plates containing seedlings were placed in a growth chamber growing during 4 days at 25ºC, 16 h photoperiod, 150 µmol m^{-2} s^{-1} light intensity and 60–70% relative humidity.

3.3.2 Experimental design and drought stress treatment

Different agar (Becton-Dickinson Bacto-Agar 214010) amounts were dissolved in the same volume of modified Fahräeus culture medium: 0.5 mM $MgSO_4$, 0.7 mM KH_2PO_4, 0.8 mM Na_2HPO_4, 50 µM FeEDTA, 1 mM $CaCl_2$, including 0.1 mg L^{-1} of the following microelements: $MnSO_4$, $CuSO_4$, $ZnSO_4$, H_3BO_3, and Na_2MoO_4 at pH 6.5 (Vincent, 1970). Culture medium was poured in square Petri dishes (12 x 12 cm) under aseptic conditions.

After germination, seedlings having rootlets of around 0.5 cm were transferred to Petri dishes containing agar of the different concentrations. Following Sauviac et al. method (Sauviac et al., 2005), a filter paper was laid onto solid agar surface, in order to avoid direct root contact with the medium but allowing water and nutrient uptake by the seedlings and being cotyledons in contact with the agar. Around eight seedlings were laid per plate and a drop of water was applied to the root tip to promote seed adhesion to the medium. Petri dishes were sealed using a surgical tape belt (3M Micropore) allowing gas exchange, maintaining sterile conditions and limiting drying out of the agar. The zone supporting root system of the Petri dishes was covered with aluminum foil to keep roots in darkness simulating natural growing conditions, thus allowing better illumination of the leaves within a stack of plates. Petri plates were placed partially (30º) inclined from the vertical. After growing stage, plant tissue aliquots from each treatment were collected and immediately frozen in liquid nitrogen, being stored at -80ºC for analytical determinations. Root and shoot fresh weight (FW) aliquots were dried for 48 hours at 80ºC to determinate dry weight (DW).

3.3.3 Water status and biomass determination

To estimate the water availability for the plants in the different agar plates, the amount of water absorbed by the filter paper in direct contact with the root was

determined gravimetrically, monitoring the maximum weight gained by paper disks exposed to the plates containing different agar concentrations. Similarly, the Ψ_w of these paper disks were measured using C52 sample chambers coupled to a Wescor HR-33T Dew Point Microvoltmeter (Wescor, Logan, UT, USA) as described in the section 2.3.1 of the Chapter 2. Also, shoot ($\Psi_{w\ shoot}$) and root ($\Psi_{w\ root}$) water potentials were measured with the above-mentioned microvoltimeter two hours after the beginning of the photoperiod. The osmotic potential was determined using the Wescor 5500 Vapor Pressure Osmometer (Logan, Utah, USA) as described González et al. (2002); the tissue sap was collected by centrifugation (2300 *g*) of fresh leaf and root material which was previously heated at 100ºC for 5 min. Root and shoot FW and DW were used to calculate biomass and water content (WC) as was described in the section 1.3.1 of the Chapter 1.

3.3.4 Determination of proline, free amino acid content and lipid peroxidation

These leaf and root ethanol extractions were similar to that described in section 2.3.3 of the Chapter 2 with slight modifications which will be detailed as follows. Frozen root and shoot tissues (0.1 g FW) were ground to powder under liquid N_2 and then homogenized with 1.5 mL of 80% (v/v) ethanol, boiled for 30 seconds and centrifuged at 5000 *g*, 4ºC for five minutes to collect the supernatant. This process was repeated three times in order to perform an exhaustive extraction of soluble osmolites. A final wash was carried out with cold ethanol. The whole volume was dried in a Turbovap LV evaporator (Zymark Corp, Hopkinton, MA, USA) at 40ºC and 1.2 bar. Dry residues were resuspended in 1 mL of deionized water, sonicated for 10 minutes and centrifuged at 2300 *g*, 4ºC for 10 minutes. The supernatants were stored at -80ºC for further analysis.

Free proline content was measured spectrophotometrically employing a ninhydrin-base assay as described Bates et al. (1973). A total of 0.3 mL 6M phosphoric acid, 0.6 mL ninhydrin solution (12.5 mL glacial acetic acid and 0.5 g ninhydrin acid) and 0.2 mL of ethanolic extract were mixed and boiled for 60 min. When the reaction mixtures reached room temperature, 3 mL of toluene were added. The samples were centrifuged at 5000 *g* for 1 minute to separate the phase with the chromophore and its absorbance was measured at 515 nm using a standard curve of L-proline.

Total free amino acid pool was measured spectrophotometrically in leaves and roots of *M. truncatula* plants according to the method proposed by Yemm and Cocking (1955). The same extracts obtained for ethanol extraction were used here. A total of 500 µL of citrate buffer (0.88 M citric acid + 1.6 M NaOH) and 430 µL of ninhydrin reactive (1.25 g ninhydrin in 125 mL 2-methoxyethanol + 50 mg AsA

in 5 mL H_2O) were mixed with 20 µL of the ethanolic extracts. The mixture was boiled at 100ºC for 20 min and after cooling, 1 mL of ethanol 60% was added to the tubes and stirred vigorously. The absorbance of the mixture was measured at 570 nm in a SinergyTM HT Multi-Detection Microplate Reader (BioTek Instruments Inc., Winooski, VT, USA) using a glycine (Gly) standard being the results expressed as µmol Gly per g^{-1} DW.

Lipid peroxidation level was measured by the thiobarbituric acid (TBA) test as described Hodges et al. (Hodges et al., 1999) with minor modifications, determining the amount of MDA as the end product of lipid peroxidation process. Shoot and root samples (0.05 g) were homogenized with 1 mL pre-chilled 0.1% (w/v) TCA. The homogenates were centrifuged at 20,000 *g* for 5 min at 4ºC. After, 750 µL of supernatant were mixed with 750 µL of reagent solution (20% (w/v) TCA + 0.01% butylhydroxytoluene + 0.65% TBA) and mixed vigorously. After heating at 95ºC for 25 min in a water bath, the reaction was stopped on ice before being centrifuged at 13200 g 4ºC for five minutes. The absorbance of supernatants was determined with a SinergyTM HT Multi-Detection Microplate Reader (BioTek Instruments Inc., Winooski, VT, USA) at 440 (sugar absorbance), 532 (maximum absorbance of pinkish-red chromagen, product of the reaction of MDA with TBA) and 600 nm (turbidity) using 0.1% (w/v) TCA as blank.

The MDA contents were estimated by the following formula:

MDA equivalents (nmol mL^{-1}) = [(A–B)/157 000] x 106

where A = [(Abs 532RSII – Abs 600RSII)] and B = [(Abs 440 RSII – Abs 600 RSII) x 0.0571].

MDA equivalents (nmol g^{-1} FW) = MDA equivalents (nmol mL^{-1}) x total volume of the extracts (mL) / g FW.

3.3.5 Measurements of root morphology

Root morphology was examined after four days exposure to the different agar concentrations. Total root length together with the position of each root section (upper root (UR), root hair zone (RH) and root tip (considering elongation zone and tip; RT), were determined

Root morphological parameters (volume and diameter) were determined by using the SmartRoot software. This is a semi-automated image analysis software, which analyzes digital images and streamlines the quantification of root growth and architecture for complex root systems (Lobet et al., 2011). SmartRoot is an

operating system independent freeware, based on ImageJ, which uses cross-platform standards for communication with data analysis software.

3.3.6 Determination of total root respiration rates

Root respiration oxygen consumption was measured using a Clark-type O_2 electrode (Hansatech Oxygraph, H. Sabur Laborbedarf, Reutlingen, Deutschland) connected to constant temperature circulating water baths (25ºC). Seedling roots (0.015 g) of each treatment were cut into small pieces and placed into Oxygraph chambers containing 1 mL of buffer (25 mM Imidazole-HCl, pH 6.5). The decrease of the oxygen in the chambers was measured under continuous stirring to promote oxygen diffusion within the chamber. The total root respiration rate was calculated by using the slope of the oxygen consumption rates.

3.3.7 Measurement of soluble carbohydrates

Fructose, glucose, and sucrose amounts were determined by capillary electrophoresis as it was previously described in the section 2.3.3 of the Chapter 2.

3.3.8 Organic acid determination

The organic acids content, in this case the malate, citrate, α-ketoglutarate and succinate, was measured according to the previously described method in the section 2.3.3 of the Chapter 2.

3.3.9 Statistical analysis

For all the variables determined in this study, we calculated the average as a central statistic and standard error as statistical of dispersion. For measurements of soluble carbohydrates, organic acids and drought stress markers a pool of roots was used due to the material shortage and three technical replicates were measured for each parameter. Significant differences among treatments were determined with Student's t-test ($p \leq 0.05$).

3.4 RESULTS

3.4.1 Plants grown under increased agar concentrations present reduced water potential values and levels of water status associated to drought stress

The growth of plantlets on agar plates is a common technique in molecular biology studies when tightly controlled growth conditions are required or large plant populations need to be screened (Sauviac et al., 2005; Barker et al., 2006; Pacheco-Villalobos and Hardtke, 2012; Petti et al., 2013; Xu et al., 2013). A common protocol for growing *M. truncatula* seedlings on plates suggests using agar concentrations in the 0.7-1.5% (w/v) range in Fahräeus medium (Barker et al., 2006). The quality of the agar is an important factor in this type of experiments since alterations in root growth has been shown to occur due to the presence of inhibitory compounds in certain commercial agars (Barker et al., 2006). Taking this into account and to define the optimal agar concentrations simulating drought conditions, we initially tested a range of concentrations from 1.5 to 12.5% of Becton-Dickinson bacto-agar, one of the recommended brands. Since growth of *M. truncatula* in direct contact with the agar surface is not recommended either, a piece of filter paper was laid onto each plate. To monitor whether increased agar concentrations induced drought stress responses, we measured the water potential (Ψ_w) of plants, the universally accepted and most common method of expression of water status in plant physiology (Siddique et al., 2000; Zhang et al., 2014). Preliminary tests using agar concentrations >7% were found to inhibit seedling development and were therefore excluded. In contrast, concentrations in the 3-5% range allowed seedling growth while reducing root Ψ_w. Based on the Ψ_w measurements, three treatments were established: plates containing 1.5% agar were defined as control (C) conditions, plates containing 3% agar were considered as the first level of drought stress (mild drought, D1) and plates containing 5% agar plates were defined as the second level of drought stress (moderate drought, D2; Fig. 3.1).

Once the agar concentrations were established, we carried out a detailed characterization of the water status of the plants under the three treatments. Given that a layer of filter paper is direct contact with the plant root system, we quantified the water availability in the media by measuring the levels of Ψ_w and the amount of water absorbed by the papers of plates at the three agar concentrations (Fig. 3.2A). There was a negative correlation between the concentration of agar and the values of water potential and water absorbed by the filter papers; Ψ_w values declined from -0.15 ± 0.01 MPa at 1.5% agar to -0.60 ± 0.04 MPa at 5% agar, whereas the amount of water absorbed was reduced from 19.26 ± 0.28 mg/cm^2 to 3.34 ± 0.24 mg/cm^2, respectively (Fig. 3.2A). Therefore, these results show that minimal variations in

the concentration of agar in plated medium lead to a decrease in the amount of water available for the plants through a reduction of the water absorbed by the paper in direct contact with the root system.

Regarding the levels of Ψ_w in shoots and roots and in agreement with our initial measurements, an increase in the agar concentration of the medium led to a decline in Ψ_w values in both organs, being only significant in plants grown under 5% agar (i.e., D2 plants; Fig. 3.2B).

Another key indicator of the plant water status closely related to Ψ_w is water content (Nunes et al., 2008). Again, both D1 and D2 plants showed a progressive reduction of water content compared to C plants both shoots and roots (Fig. 3.2C). To investigate the contribution of solutes in the decline of in Ψ_w values, we also measured osmotic potential (Ψ_s) of shoots and roots. Ψ_s was significantly reduced in the two levels of stress, being more pronounced in roots (-34%) than in the aerial tissue (-22%; Fig. 3.2D).

Taken together, the physiological parameters analyzed show that the plant water status is altered as a consequence of increased agar concentrations, presenting water status values characteristic of plants under water-limiting conditions both at the level of shoots and roots.

3.4.2 Analysis of drought stress markers

Proline accumulation is a widely known marker of drought stress in plants. This amino acid has been shown to play an osmoprotective role under osmotic stress conditions, acting also as a reactive oxygen species (ROS) scavenger and redox regulator (reviewed in (Szabados and Savouré, 2010)). Besides proline accumulation, another general response of plant exposed to abiotic stresses is an overall increase in the levels of free amino acids (Handa et al., 1983; Rhodes et al., 1986; Usadel et al., 2008; Gil-Quintana et al., 2009; Larrainzar et al., 2009; Widodo et al., 2009; Gil-Quintana et al., 2013). Thus, to check whether the experimental set up described here also led to these stress responses, the levels of proline and free amino acids were measured in roots and shoots of *M. truncatula* plants grown under different agar concentrations. Limited water availability led to a significant increase in the content of proline under D1 and D2 conditions in both organs, with contents between 1.5- and 2-fold those of C plants (Fig. 3.3A). Total amino acids were also found to accumulate in both drought treatments, with a more gradual and pronounced accumulation in root tissue (Fig. 3.3B).

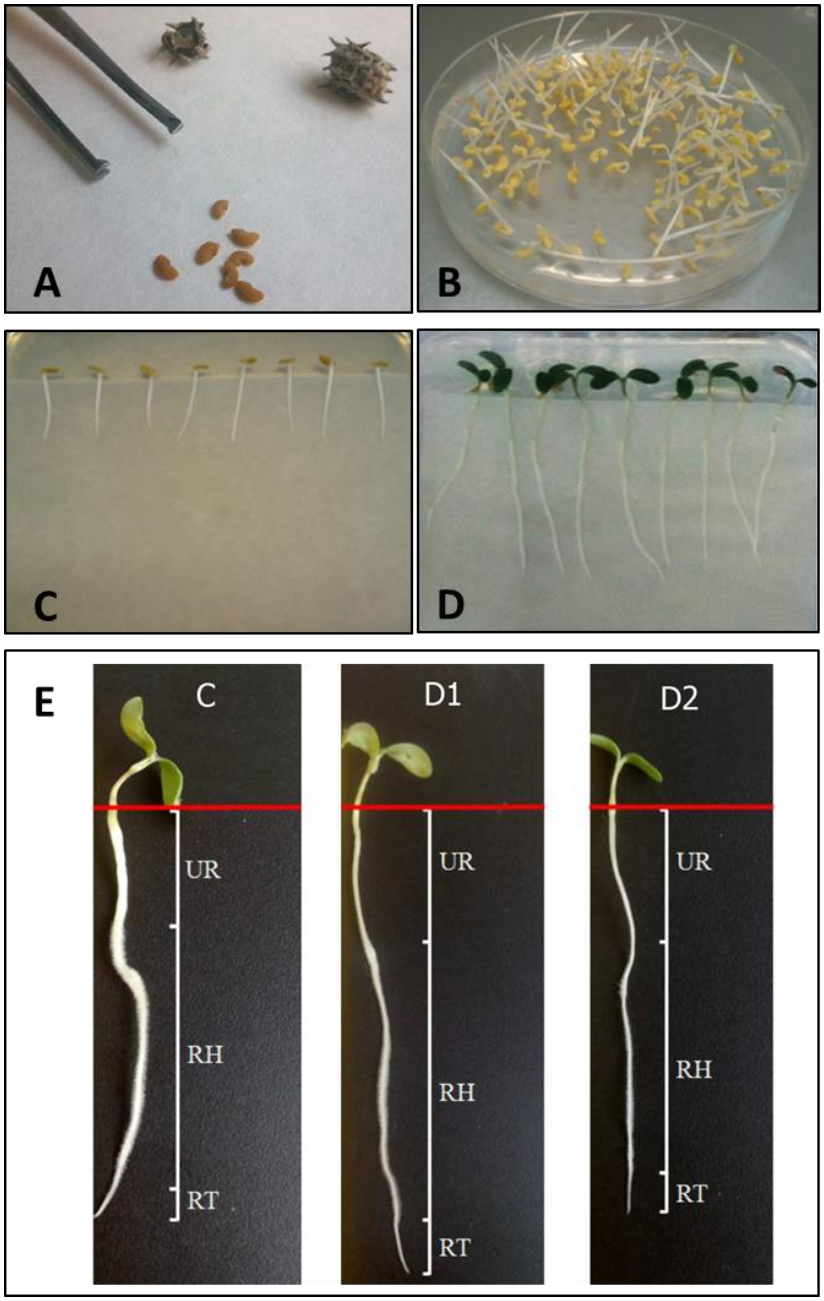

Figure 3.1. Different stages of *M. truncatula* seedlings development. **A)** Seeds of *M. truncatula* separated from mature pods. (**B**) Germinated seeds in 0.7% (w/v) agar plates after being incubated at 4ºC for 24 hours and 36 hours at room temperature. (**C**) Germinated seeds transferred to corresponding agar plate to be cultured for 4 days in a controlled conditions growth room. (**D**) Front view of seedlings growth after 4 days of treatment showing fully expanded cotyledons and root elongation. (**E**) Plant growth after four-day exposure to different water availability treatments C: Control, D1: Drought 1 and D2: Drought 2. UR: Upper Root, RH: Root Hair zone, RT: Root Tip zone.

Drought stress is usually associated with oxidative damage in plant tissues. To determine whether *M. truncatula* plants grown under this method were also exposed to oxidative stress, the levels of malondialdehyde (MDA), a product of membrane lipid peroxidation, were quantified (Fig. 3.4). Increased agar concentration caused a gradual accumulation of MDA in shoot tissue (+50% and +100% in D1 and D2 plants, respectively), although only D2 induced lipid peroxidation in roots, a tissue that showed a lower content of MDA compared to shoots.

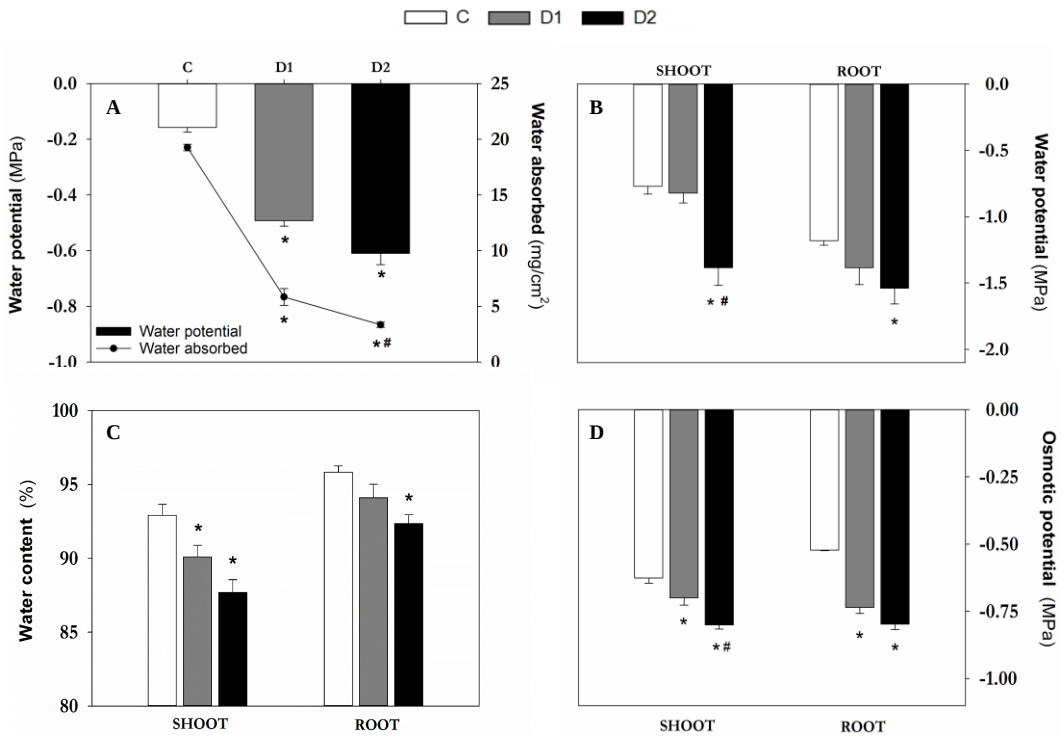

Figure 3.2. Physiological determination of water status. Measurement of the amount of water absorbed (n=25) and water potential values (n=7) of the filter paper in direct contact with roots in plates containing 1.5 (control plants, C), 3 (drought 1, D1) and 5% (drought 2, D2) (w/v) agar in Fahräeus medium **(A).** Shoot and root water potential (B), water content (C) and osmotic potential (D) on control (C), Drought 1 (D1) and Drought 2 (D2) plants. Values represent mean ± SE (n=3, unless otherwise stated). An asterisk (*) denotes significant differences ($P \leq 0.05$) with respect to C plants; a hash (#) indicates significant differences between D1 and D2 treatments.

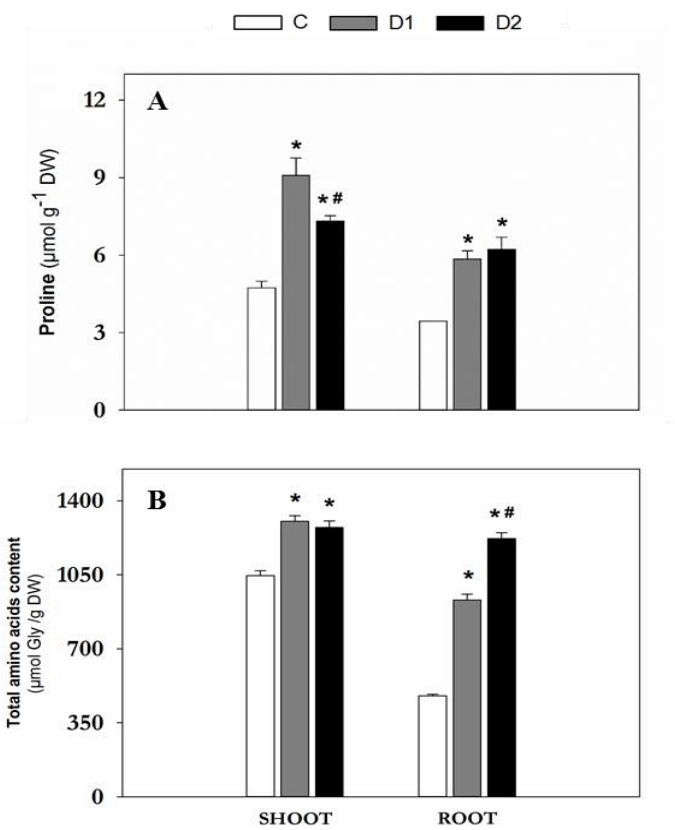

Figure 3.3. Drought stress markers. Effects of drought on proline **(A)** and total amino acids **(B)** contents in shoots and roots of control (C), Drought 1 (D1) and Drought 2 (D2) plants. Values represent mean ± SE (n=3). An asterisk (*) denotes significant differences ($P \leq 0.05$) with respect to C plants; a hash (#) indicates significant differences between D1 and D2 treatments.

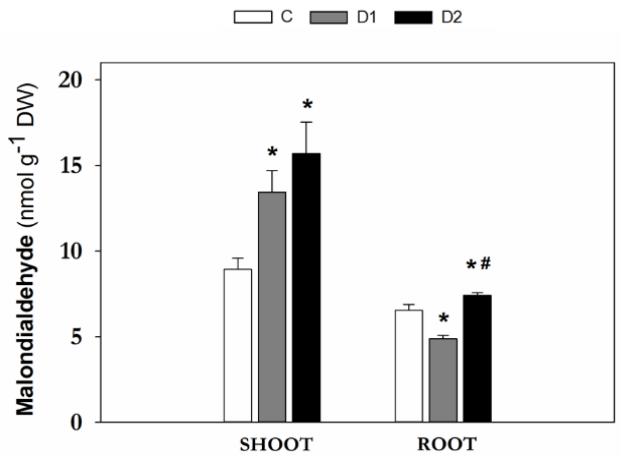

Figure 3.4. Lipid peroxidation. Effects of drought in malondialdehyde (MDA) content in shoots and roots of control (C), Drought 1 (D1) and Drought 2 (D2) plants. Values represent mean ± SE (n=3). An asterisk (*) denotes significant differences ($P \leq 0.05$) with respect to C plants; a hash (#) indicates significant differences between D1 and D2 treatments.

Table 3.1. Root morphology. Total length and length of the different sections, average diameter, volume, biomass and density of control (C), Drought 1 (D1) and Drought 2 (D2) plants. Values represent mean ± SE (n=6). An asterisk (*) indicates significant differences ($p \leq 0.05$) between control and drought treatments; hash (#) indicates significant differences between D1 and D2 plants.

	C	D1	D2
Total root length (mm)	51.9 ± 2.2	61.3 ± 2.1 *	50.7 ± 1.7 #
Upper root (mm)	20.7 ± 1.2	23.6 ± 0.8 *	23.5 ± 1.0
Root hair (mm)	23.3 ± 1.9	28.4 ± 1.5 *	19.3 ± 1.2 #
Root tip (mm)	7.9 ± 1.1	9.3 ± 0.8	7.9 ± 0.7
Root average diameter (mm)	0.90 ± 0.03	0.70 ± 0.01 *	0.58 ± 0.02 *#
Root volume (mm^3)	39.1 ± 2.7	26.8 ± 1.5 *	14.7 ± 1.3 *#
Root biomass (mg DW $plant^{-1}$)	2.7 ± 0.1	2.0 ± 0.1	2.2 ± 0.2
Root density (mg cm^{-3})	74.80 ± 4.05	82.38 ± 1.66	170.01 ± 14.12 *#

3.4.3 Morphological and metabolic changes in roots of *M. truncatula* induced by water deficit

To further characterize the physiological effects of growing plants under reduced water availability, several root growth parameters were measured (Table 3.1). Although plant biomass did not show significant differences at the various treatments, changes in root growth and morphology were observed. To measure root length, roots were divided into upper root, AZ containing root hairs and elongation/root tip zone. Mild water limitation (D1) induced total root growth, particularly in the upper root and zone of absorption. In contrast, the most severe treatment, D2, provoked a slight reduction in root length, most noticeable in the zone of root hair growth. Interestingly, both treatments produced a decrease in the diameter of roots (22% and 35%, in D1 and D2, respectively), leading to a significant increase in single root density (mg cm^{-3}) in D2.

Plant carbon status is dependent on the balance between photosynthesis and respiration (Flexas et al., 2006), being the amount of carbon lost through respiration up to 50% of the daily carbon gain by photosynthesis (Morgan and Austin, 1983). To analyze how total oxygen consumption was affected by limited water availability in the medium, root respiration rates were determined. Compared to control plants, total respiration rates remained relatively constant in roots of D1 plants but significantly decreased in D2 roots (Fig. 3.5A).

Plant carbon partitioning is highly altered by drought stress due to changes in the source–sink relations (Lemoine et al., 2013; Osorio et al., 2014; Xu et al., 2015). To better understand the mobilization of carbon reserves under the different treatments, the content of the main carbon compounds was measured in root and shoot tissue (Fig. 3.5 and 3.6, respectively). In general, we observed a higher content of carbon compounds in roots compared to shoots, which suggests that the underground organ represents a significant source of carbon reserves at this growth stage. The content of sucrose, the main carbon compound transported through the plant, declined both in D1 and D2 roots (Fig. 3.5B). In contrast, only fructose levels increased significantly in D1 roots (Fig. 3.5C) Furthermore, the levels of the organic acids malate, citrate, α-ketoglutarate and succinate were also measured. The content of malate -the most abundant organic acid in roots-, citrate and α-ketoglutarate showed a significant reduction in roots of D1 and D2 plants compared to controls (Fig. 3.5E-G), while succinate did not show significant variations in roots (Fig. 3.5H). Unlike roots, shoots did not show significant changes in the levels of sucrose (Fig. 3.6A), which suggests that the drought stress imposed did not limit carbon availability in the aerial part. However, the levels of malate significantly decreased (Fig. 3.6D), while citrate was progressively accumulated (Fig. 3.6E) as water deficit became more intense. The content of fructose, glucose, succinate and α-ketoglutarate significantly increased in shoots of D1 plants but went back to control values under D2 conditions (Fig. 3.6B-C, F-G).

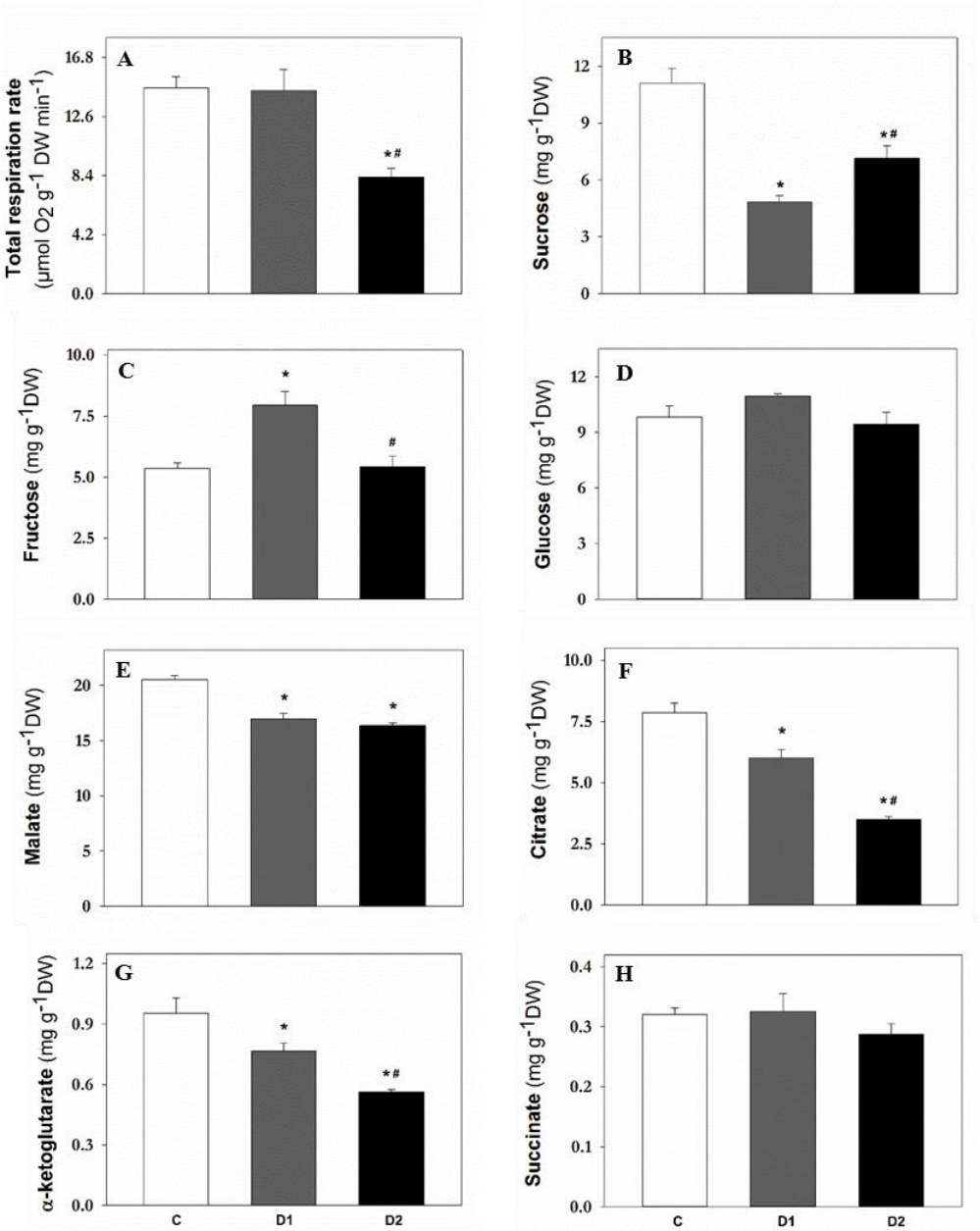

Figure 3.5. Root carbon metabolism. Effects of drought on total root respiration rate **(A)** and on carbon compounds levels [sucrose **(B)**, fructose **(C)**, glucose **(D),** malate **(E)**, citrate **(F)**, α-ketoglutarate **(G)** and succinate **(H)**] in roots of control (C), Drought 1 (D1) and Drought 2 (D2) plants. Values represent mean ± SE (n=3). An asterisk (*) indicates significant differences ($p \leq 0.05$) between control and drought treatments; hash (#) indicates significant differences between D1 and D2 plants.

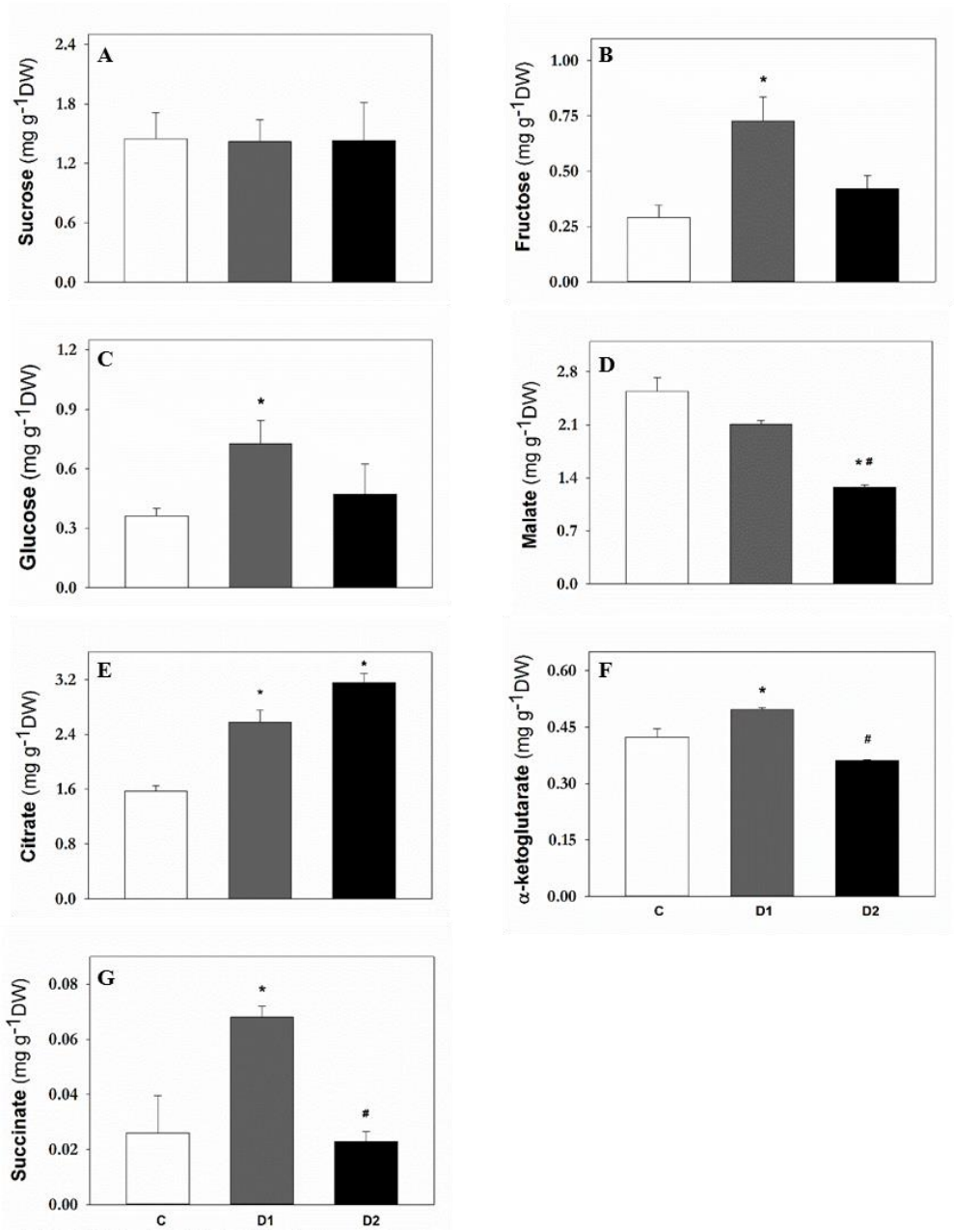

Figure 3.6. Shoot carbon metabolism. Effects of drought on carbon compounds levels sucrose **(A)**, fructose **(B)**, glucose **(C),** malate **(D)**, citrate **(E)**, α-ketoglutarate **(F)** and succinate **(G)**] in shoots of control (C), Drought 1 (D1) and Drought 2 (D2) plants. Values represent mean ± SE (n=3). An asterisk (*) indicates significant differences ($p \leq 0.05$) between control and drought treatments; hash (#) indicates significant differences between D1 and D2 plants.

3.5 DISCUSSION

3.5.1 Variations in the concentration of agar in plates is a useful method to simulate drought stress conditions *in vitro*

The current work presents a simple method for the analysis of plant drought stress responses under in vitro conditions based on the use of different concentrations of agar, a widely used polymer for plant tissue culture. Agar is the generic term used to designate a pool of molecules derived from agarobiose, which has been employed as a solidifying agent for microorganism and tissue culture during more than a century. The method described in the current work is based on the fact that applying agar at concentrations above the usual 0.7-1.5% range increases the number of water molecules withheld within the polymer network, reducing the water absorbed by the filter paper in direct contact with the roots and, accordingly, the filter water potential values (Fig. 3.2A). This leads to a limitation of water available for the plant, creating drought stress conditions, as confirmed by multiple measurements of the plant water status (Fig. 3.2B-2D). M. truncatula seedlings grown under this method present physiological parameters and water status markers comparable to previous drought stress studies where adult plants were grown in perlite:vermiculite pots and subjected to a gradual water deficit (Larrainzar et al., 2007; Gil-Quintana et al., 2009; Larrainzar et al., 2009; Yousfi et al., 2010; Aranjuelo et al., 2011; Planchet et al., 2014; Larrainzar et al., 2014; Zhang et al., 2014). Addition of a paper interface between the agar and the roots seems to be a key element to simulate water-deficit conditions, since previous studies did not observe significant changes in the matric potential of the agar gels when using concentrations of agar in the range employed here (Spomer and Smith, 1996).

Osmotic adjustment is one of the main physiological strategies used by plants to respond to water deficit situations (Greenway and Munns, 1980; Morgan, 2003). Small osmolytes such as polyol sugars or amino acids typically accumulate in tissues to limit cell damage and act as signaling compounds, among other roles (Hare et al., 1998; Szabados and Savouré, 2010). Drought stress has been shown to cause an increase in the content of amino acids in several plants (Voetberg and Sharp, 1991; Mohammadkhani and Heidari, 2008; Larrainzar et al., 2009; Widodo et al., 2009; Lugan et al., 2010; Gil-Quintana et al., 2013; Zhang et al., 2014). Similarly, we observed an accumulation of proline and free amino acids in seedlings exposed to increased agar concentrations (Fig. 3.3). This amino acid accumulation may be attributed to either the activation of protein degradation mechanisms or *de novo* amino acid biosynthesis under stress conditions. Interestingly, the increase in amino acid content observed in root tissue was more pronounced than this of shoots, in agreement with previous developmental studies (Glevarec et al., 2004). This

response suggests that it is the underground organ the one showing a stronger drought stress response at these early stages of seedling development.

In terms of lipid peroxidation, most studies have focused on leaves or aerial parts of plants and there is little information about the variations of MDA content at the root level. Stresses such as herbicide treatment have been reported to increase MDA levels in roots of another legume plant, pea (Zabalza et al., 2007). However, exposure to cadmium had the opposite effect in *M. truncatula* radicles (Rahoui et al., 2014). In this work, we observed that MDA content strongly increased in shoots of D1 and D2 plants, similarly to observed in *M. sativa* nodules (Naya et al., 2007), but showed a differential response in roots, decreasing in D1 and increasing in D2 (Fig. 3.4).

3.5.2 Root elongation is prioritized over enlargement under mild drought conditions: the role of respiration and carbon reserve mobilization.

Besides validating the experimental method, we analyzed the response of *M. truncatula* roots to different levels of drought stress. Roots are the first organs detecting water limitation in soils and their response is essential to counteract stressful conditions. Therefore, detailed analysis of root parameters provides insight into the role of this tissue under water deficit conditions.

During seedling development there is a significant reactivation of metabolism, cell division, elongation and differentiation processes. However, cell growth is one the processes most affected by drought stress (Hsiao, 1973). Interestingly, under water limiting conditions roots challenge this general theory by increasing growth rate, which can be interpreted as an attempt to reach deeper soil layers where water availability is higher (Sharp et al., 1988). When grown on plates, intermediate agar concentrations (D1) provoked an increase in root length, which was more moderate in D2 plants (Fig. 3.1E, Table 3.1). This response may be partly due to modulation of the root system architecture by changes in the proportion of root cell division and differentiation in the root tip (Silva-Navas et al., 2015) or by changes in the local hexose concentration in the growing zone of roots (Freixes et al., 2002), indicating the importance of carbon supply in this tissue. van der Weele et al, 2000 (van der Weele et al., 2000) also observed an increase in the length of *Arabidosis thaliana* seedling roots under water deficit conditions caused by a stimulation of root elongation along with a high rate of cell production. Root elongation was also observed in rootlets of *M. truncatula* under low temperature and water deficit stress conditions (Youssef et al., 2016) and in water-stressed *M. sativa* (Zeid and Shedeed, 2006). In the present study, a clear decrease in root thickness was observed in plants

grown on increased agar concentrations (Table 3.1). Previous studies showed this effect in maize plants roots (Sharp et al., 1988), which become thinner as water potential decrease. Also, Wasson et al. (2012) found a decrease in root diameter as a strategy to improve wheat root systems for water uptake under water deficit conditions. This response has been interpreted as a strategy of the root system to explore efficiently the soil water reserves at a minimum cost (Sharp et al., 1988), modifying its architecture and morphology (Comas et al., 2013). Li et al. (2015) observed changes in root architecture of maize seedlings under drought conditions affecting root length, area, diameter, and volume. In D2 plants, a significant increase of the root tissue density was observed (Table 3.1), which may increase the strength of roots to face soil impedance. In this regard, it has been reported an increase in the root thickness in *Nerium oleander* plants under drought stress conditions (Bañon et al., 2006), what could be related to the mechanical impedance to root penetration in compact substrates described in different plant species (Materechera et al., 1991). Root elongation in soils is a complex process affected not only by soil mechanical strength or water reserves location but also by shoot-root signaling and plant metabolic responses (Jin et al., 2013). Our experimental system provides an experimental set up in which water is homogenously available, thus avoiding gradients and facilitating studies without the interference of other factors such as soil impedance. Under these conditions, primary root elongation seems to be a constitutive response of plants under mild drought stress, being this effect reverted under more severe drought stress.

Cuellar-Ortiz et al. (2008) showed that drought resistance is linked to modifications in the plant carbon metabolism in legumes, as it is the case in cereals. In the seedling system employed in current study, it is highlighted the key role of roots at this first stage of plant development, concentrating most of the carbohydrates and organic acid reserves (Fig. 3.5 and 3.6). Unlike adult *M. truncatula* plants where leaves are the main starch reservoir (86.29 µmol glucose g^{-1} DW in leaves versus 4.3 µmol glucose g^{-1} DW in roots; Seminario et al., unpublished observations, seedlings have reduced starch reserves (7.6 µmol glucose g^{-1} DW). Indeed, starch content showed similar basal levels between seedling shoots and roots displaying no significant differences in any of both organs with no regard to water availability (data not shown). However, the sucrose content decreased significantly in roots under D1 conditions together with the content of the main organic acids (Fig. 3.5). Pinheiro et al. (2004) observed a similar response in drought-stressed *Lupinus albus* plants. This decrease could be related to the increased energy requirements to maintain respiration rates (Fig 3.5A) and to fuel root elongation processes (Table 3.1; Sharp et al., 1988; Muller et al., 1998; Muller

et al., 2011). Under water stress conditions, photosynthesis is reduced but respiration is the process that provides energy and intermediates for cell growth and maintenance, and so cell respiration is directly involved on plant productivity (Flexas et al., 2005). The critical question remains: how do drought-stressed plants regulate root respiration rates to survive under water deficit situations? Indeed, under mild stress conditions, root elongation was activated while respiration was maintained. Similar drops in respiration under drought stress have been also observed in wheat (Liu and Li, 2005). One possibility is that under water limiting conditions respiration rates are lowered due to ROS damage in mitochondria or a decrease in the rates of ion uptake and associated energy demand (Atkin and Macherel, 2009).

Taken together, these results show that aerial tissues and roots respond differently to water deficit. The analysis of root metabolism indicates that during the first stages of plant development roots have a crucial role in plant establishment and growth. The observations and metabolic analysis performed on *M. truncatula* seedlings suggest that roots alter their functionality and morphology to cope with the imposed water deficit.

3.6 CONCLUSIONS

The current simple method presented here for simulation of drought stress under *in vitro* conditions mimics water deficit conditions. Furthermore, this method facilitates the standardization of drought studies across laboratories by increasing the reproducibility and the fine-tuning of the level of stress applied. Besides being validated this protocol, we conclude that *M. truncatula* seedlings were affected at the morphological, physiological and metabolic level when they were grown under these conditions.

upna

Universidad Pública de Navarra
Nafarroako Unibertsitate Publikoa

upna

Universidad Pública de Navarra
Nafarroako Unibertsitate Publikoa

» CHAPTER 4

Root lipid, cell wall and secondary metabolism play a key role in the response to drought of Medicago truncatula *seedlings*

upna

Universidad Pública de Navarra
Nafarroako Unibertsitate Publikoa

4.1 INTRODUCTION

Legumes are the second most consumed crop across the world after cereals, being a valuable source of protein for human nutrition and for animal feed. The temperate legume *M. truncatula* has been selected as a model legume for molecular and genetic studies because of its small diploid genome size, the fact that it is self-fertile and relatively easy to transform (Cook, 1999; Barker et al., 2006). This specie is phylogenetically related to some of the most important European legume crops such as pea or alfalfa (Aubert et al., 2006; Phan et al., 2007). Despite the advantage given by their capacity to establish symbiosis with N_2-fixing soil bacteria, legume production is adversely affected by environmental stresses, being drought one of the main constraints limiting plant growth and crop yield (Boyer, 1982; Chaves and Oliveira, 2004; Daryanto et al., 2015).

Tolerance to abiotic stresses is associated with modifications of morphological and physiological traits; these include changes in plant architecture, variation in leaf cuticle thickness, stomatal regulation, germination, antioxidant capacity, hormonal regulation, membrane and protein stability, maintenance of photosynthesis and root morphology (Edmeades et al., 2000). In some situations like inadequate rainfall, excessive salinity in the soil or as a consequence of freezing temperatures, water becomes limited for plant communities. This limitation can negatively impact plant growth causing adaptive changes and/or deleterious effects (Chaves et al., 2002), forcing plants to develop different strategies for better growth under adverse water conditions (Li et al., 2015). It is well known that the process mainly affected by water deficit is plant cell growth; the more severe the water deficit, the larger the number of cellular processes affected (Hsiao, 1973). Plants have mechanisms for osmotic adjustment by synthesizing compatible solutes and accumulating them in response to drought stress (Chen and Jiang, 2010); sugars, amino acids or amines are described to accumulate in different plant tissues under drought stress or desiccation conditions (Voetberg and Sharp, 1991). Involvement of other pathways and protection mechanisms, including a battery of cellular proteins such as late embryogenesis abundant, heat shock proteins and aquaporins, have been reported to play important roles in the plant response to drought stress (Bartels and Sunkar, 2005).

Roots are the first plant organs detecting soil water shortage, being their architecture the result of continuous dynamic developmental processes (Hodge et al., 2009). Under water availability limited conditions, the architecture of the root system undergoes modifications such as changes in lateral roots, which developing deeper and more highly branched root systems to improve water absorption

efficiency (Malamy, 2005). This parameter is, therefore, important for the study of plant growth responses under environmental stress conditions. The roots of dicotyledonous plants consist of a main taproot from which secondary roots emerge (Waisel et al., 2002). According to their structure, different sections can be distinguished in the primary root; namely, the root cap, the apical meristematic section, the elongation section and the maturation section, known as absorption zone (AZ), where cells start to differentiate and root hairs are more abundant for water and nutrient uptake (Ishikawa and Evans, 1995). Root hairs are single tubular cell projections emerging from root epidermal cells (Grierson et al., 2014), which allow the study of a single cell plant system being one of the best characterized cell types in plant biology (Hossain et al., 2015). Root hairs increase the ground contact of the root and presumably increase root absorptive surface area, providing a mechanism for adaptation under water shortage situations. With a few exceptions (Ramos and Bisseling, 2003), there number of studies focused on root hairs is limited, most likely due to the difficulties of obtaining samples, which is limiting for most of applications.

Seed germination is the first interface of material exchange between the plant development cycle and the environment. Thus, a better understanding of seedling responses against stressful environments is one of the first steps towards the discovery of new genes and identification of functional pathways underlying those responses (Cordeiro et al., 2014). In addition, seedling phenotyping methods are useful and successful when it comes to saving costs, space and time. Wang et al. (2015) also indicated that plants are much more uniform at early seeding stages, with less phenotypic variation caused by experimental errors. In this context, Galvan-Ampudia and Testerink (2011) reviewed salt stress signals shaping plant root and concluded that seedling root development is crucial for plant survival by determining water absorption capacity. Similar studies with seedlings under water deficit conditions have been carried out with other species like maize (Li et al., 2015) and *A. thaliana* (van der Weele et al., 2000) indicating the importance of these early developmental stages plant studies in determining the structure and dynamics of plant populations. Several studies of seed germination under desiccation have been carried out in *Medicago sativa* (Wu et al., 2013; Castroluna Ruiz et al., 2014). However, to our knowledge, there are only few studies in *M. truncatula* plants focused on the study of seedlings under low water availability (Boudet et al., 2006; Planchet et al., 2011; Planchet et al., 2014; Watson et al., 2015). In the case of Boudet et al. (2006), they compared *M. truncatula* radicles with desiccation tolerance at proteomic level and Watson et al. (2015) analyzed *M.*

truncatula root tip border cells by metabolomics and transcriptomics in young seedlings.

4.2 OBJECTIVE

In this context, the present work is focused on analyzing drought responses at the transcriptomic and metabolomic level in the AZ of the root under low water availability conditions in early developmental stages of *M. truncatula* in order to identify the key metabolic pathways in seedlings grown in a medium with different agar concentrations (as described in Chapter 3) which simulates water deficit conditions.

4.3 MATERIALS AND METHODS

4.3.1 Plant materials, growth conditions and drought stress treatment.

M. truncatula Gaertn. cv Jemalong ecotype A17 plants were grown as detailed in the section 3.3.1 of the Chapter 3 of the present thesis with minor modifications. Seeds were treated with concentrated sulfuric acid for eight minutes, and rinsed several times with cold sterile distilled water. Then seeds were sterilized with 3.5% sodium hypochlorite (v/v) and 0.1% Tween-20 for 10 minutes, incubated at room temperature in distilled water and kept in the dark overnight. After imbibition, seeds were placed on wet filter paper in a petri dish and vernalized at 4ºC for 2 days to synchronize germination. Afterwards, seeds were placed at room temperature for 24 hours.

As it was shown in Chapter 3, ranges from 1.5 to 5% agar in Fahräeus medium allowed to mimic stress responses associated with limited water availability. Thus, two treatments were established: seeds grown in plates containing 1.5% agar were defined as control (C) and plants grown on 5% agar plates were considered as drought (D). Therefore, upon germination, seedlings presenting rootlets of around 0.5 cm were transferred to Petri dishes containing at the above mentioned concentrations of agar (Becton-Dickinson Bacto-Agar, ref. 214010) dissolved in Fahräeus nutrient solution [0.5 mM $MgSO_4$, 0.7 mM KH_2PO_4, 0.8 mM Na_2HPO_4, 1 mM ferric citrate, 1 mM $CaCl_2$, including 0.1 mg L^{-1} of the following microelements: $MnSO_4$, $CuSO_4$, $ZnSO_4$, H_3BO_3, and Na_2MoO_4 at pH 6.5, (Vincent, 1970)]. Forty-two mL of agar medium were poured into square Petri dishes (12x12 cm) and a layer of sterile filter paper was placed on top of it under aseptic conditions (Sauviac et al., 2005). Plates were sealed with a surgical tape belt (3M Micropore), covered with aluminum foil to keep roots in the dark and placed in a growth chamber growing during 4 days as previously described in the section 3.3.2 of the Chapter 3. Plates containing the seedlings were placed partially (30º) inclined to direct root straight growth. Four days after transplanting, root and shoot tissue was collected for seedling growth and water status determination. The root absorption zone (AZ) containing the bulk of root hairs was collected separately, immediately frozen in liquid nitrogen and stored at -80ºC for further transcriptomic and metabolomic analysis.

4.3.2 Plant physiological characterization; biomass, water content, root length and leaf area determination.

Root and shoot tissue fresh weight (FW) was measured and dry weight (DW) was determined after drying for 48 h at 70ºC. Water Content (WC) was calculated as described in section 1.3.1 of the Chapter 1. For seedling morphology analysis,

total root length was manually measured using a ruler and leaf area was determined by using the Li-3000A (LI-COR) portable area meter.

4.3.3 RNA isolation and microarray analysis.

Root AZ total RNA was extracted using TRIZOL reagent [Life Technologies; (Chomczynski and Mackey, 1995)]. Isolated RNA was digested with RNase-free DNase1 (Ambion) following manufacturer's recommendations, and further column purified with an RNeasyMinElute CleanUp kit (Qiagen). Ribonucleic acid was quantified using a NanoDrop Spectrophotometer ND-100 (NanoDrop Technologies) and the purity assessed with a Bioanalyzer 2100 (Agilent Technologies). Three independent biological replicates were included and hybridized to the Medicago Genome Array-Affymetrix GeneChip. Array hybridization was done according to the manufacturer's recommendations (Affymetrix), and scanning of arrays was performed as described previously (Benedito et al., 2008). Microarray data were submitted to MIAMExpress with accession number E-MEXP-3723. Raw data were normalized by robust multichip averaging, as described earlier (Irizarry et al., 2003). Presence and absence calls for probe sets were obtained using the dCHIP algorithm (Li and Wong, 2001). The ranking method employed was based on fold change (FC) cut-off for expression using a cut-off value of 2-fold up- or 0.5-fold down-regulated. Transcript expression values were loaded to Mapman software (Thimm et al., 2004; Usadel et al., 2005) to visualize the expression pattern of genes onto metabolic pathways. For an overview of the main transcript changes, a heatmap was generated using normalized expression values to the average control values with R statistical software analysis.

4.3.4 Primer design and qRT-PCR conditions.

Reverse transcription was performed with 1 µg of total RNA using SuperScript III Reverse Transcriptase (Invitrogen) and oligo-dT_{20} (Invitrogen GmbH, Karlsruhe, Germany). PCR reactions were carried out in an ABI PRISM® 7900 HT Sequence Detection System (Applied Biosystems, Foster City, CA, USA). SYBR® Green was used to quantify dsDNA synthesis. Five-µl reactions were performed in an optical 384-well plate containing 2.5 µL 2 × SYBR® Green Power Master Mix reagent (Applied Biosystems), 10 ng cDNA and 200 nM of each gene-specific primer. Amplified templates followed the standard PCR protocol: 50ºC for 2 min; 95ºC for 10 min; 40 cycles of 95ºC for 15 sec and 60ºC for 1 min, and SYBR® Green fluorescence was measured continuously. Melting curves were generated after 40 cycles by heating the sample up to 95ºC for 15 sec followed by cooling

down to 60ºC for 15 s and heating the samples to 95ºC for 15 sec and primer PCR efficiencies were assessed using the LinReg software. Transcript levels were normalized using the geometric mean of three plant housekeeping genes, PTB (TC111751), UBC9 (TC106312) and Mt-EXON (Livak and Schmittgen, 2001). All the primers which were designed previously with "Primer express 3.0" software (Thermofisher, MA, USA) are listed in Table 4.1.

Table 4.1. List of primer sequences used for qRT-PCR validation of microarray data.

	Annotation (Gene ID)	Forward Primer sequence	Reverse Primer sequence
DOWN-REGULATED	Glutathione S-transferase GST 19 (TC102103)	AATAGGAGGACTGAGTGTGTGTTTGT	AGCGACTCGCCGTGATTC
	Dehydration-induced protein RD22-like protein 2 (TC95843)	GAGTGTGAAGACGCAGCCATT	CCATGGATTCAAGCGAGGTT
UP-REGULATED	Nonspecific lipid-transfer protein precursor (LTP) (TC94138)	CGTCAGGCTGCATGCAACT	GCAGCGGTATTCAAACCTGAA
	Anthocyanidin synthase (BM812824)	GCCCAAGACACCTGCTGATT	TGCTAGCTAGGACTCTTAATTCCTTTG
	WRKY44 transcription factor (TC97762)	AGACTGGGTTATTTACTTTCTGTTGCA	CAAACCAACACCAAATTCCAAGA
	AP2 domain transcription factor-like (TC110781)	CGGCGATGTTTTGCTTACG	TTGGTGGATCATTAGGGAGGTT
HOUSEKEEPING GENES	MT.ubi-exon (Mt-EXON)	GCAGATAGACACGCTGGGA	AACTCTTGGGCAGGCAATAA
	MT.PTB (-393, -496) (TC111751)	CGCCTTGTCAGCATTGATGTC	TGAACCAGTGCCTGGAATCCT
	MT.UBC9 (-547, -622) (TC106312)	GGTTGATTGCTCTTCTCTCCCC	TTTTGGCATTGCTGCAAGC

4.3.5 Metabolomic analysis.

Root AZ tissue was lyophilized and then homogenized into fine powder. Extraction and metabolite analysis was performed as described before (Broeckling et al., 2005) with slight modifications. Briefly, three biological replicates of 10 mg were used for extraction with 1 mL 80% methanol containing umbelliferone as internal standard. After sonication, agitation and centrifugation, 0.5 mL of supernatant extract was separated and kept at -20ºC until further Ultra-High-Performance Liquid Chromatography-quadrupole Time of Flight-Mass Spectrometry (UHPLC–qTOF-MS) use. The remaining extract was mixed with 1.5 mL of chloroform containing docosanol as internal standard and incubated for 45 minutes at 50ºC followed by another incubation with 1mL of water containing ribitol. Next samples centrifugation allowed for the phase separation: upper phase (polar metabolites extracted) was dried with speed vac and lower phase (non-polar metabolites fraction) was dried using nitrogen. Dried and methoxyamine hydrochlorides in pyridine resuspended polar extracts were firstly vigorously stirred and then sonicated, repeating this process thrice. Finally, 50 µL of methyltrimethylsilyltrifluoroacetamide (MSTFA) and 1% N-methyl-N-trimethylsilyltrifluoroacetamide (TMSC) were added to polar metabolites extracts, incubating them for 1 hour at 50ºC. 0.8 mL of chloroform were added to resuspend

non-polar dried metabolites and later 0.5 mL of 1.25 M HCL in methanol was added for metabolites hydrolysis at 50ºC for 4 hours. After samples were completely evaporated with nitrogen, 70 µL of pyridine and 30 µL of MSTFA + 1% TMSC were added to resuspend and to derivatize respectively the samples, being these incubated during 1 hour at 50ºC.

Polar and non-polar extracts were analyzed onto a Hewlett Packard Agilent 6890 Gas Chromatograph System (HP 6890 GC, Agilent Technologies, Santa Clara, CA, USA) equipped with a 60 M DB-5-MS column (J&W Scientific, Folsom, CA, USA) coupled to a HP 5973 MS as previously described (Broeckling et al., 2005; Zhang et al., 2014). Compound derivative identification and quantification were conducted using the MET-IDEA software (Broeckling et al., 2005). The relative abundance of each compound was normalized to the internal standards and then used in statistical analyses. Finally, identified metabolites were classified according to their functional category with KEGG database (Kanehisa and Goto, 2000; Kanehisa et al., 2015).

4.3.6 Supplemental data

All the results obtained in transcriptomic and metabolomics analyses are included in the following files presented at the end of this work.

Table S4.1. List of all induced genes in root absorption zone of *M. truncatula* seedlings under drought treatment (≥2-fold, $p \leq 0.05$).

Table S4.2. List of all repressed genes in root absorption zone of *M. truncatula* seedlings under drought treatment (≤0.5-fold, $p \leq 0.05$).

Table S4.3. List of all GC-MS identified polar metabolites significantly regulated in root absorption zone of *M. truncatula* seedlings under drought treatment ($p \leq 0.05$).

Table S4.4. List of all GC-MS identified nonpolar metabolites significantly regulated in root absorption zone of *M. truncatula* seedlings under drought treatment ($p \leq 0.05$).

Table S4.5. List of all UHPLC-QTOF-MS identified metabolites significantly regulated in root absorption zone of *M. truncatula* seedlings under drought treatment ($p \leq 0.05$).

4.4 RESULTS

4.4.1 Physiological responses of *M. truncatula* seedlings grown under water deficit conditions

For the characterization of seedling drought responses, water content and biomass were determined. Attending to seedling DW, shoot and root biomass did not show significant differences between control and drought treatments (Fig. 4.1A). In addition, water content decreased significantly in shoots and roots; the decline was more pronounced in shoots, while in roots this parameter decreased from almost 92% to 90% (Fig. 4.1B). Furthermore, changes in root morphology were observed; water limitation induced root elongation in seedlings subjected to this treatment. Interestingly, drought treatment produced a significant increase (40%) in root length compared to control plants (Fig. 4.1C). This root growth is also obvious in figure 4.1E, where drought-stressed plantlets grew thinner and longer than controls. However, leaf area showed a significant reduction as water restriction became higher; from 0.85 cm^2 in control plants to 0.65 cm^2 in drought plants (Fig. 4.1D).

4.4.2 Gene expression analysis in the root absorption zone of *M. truncatula* seedlings

To identify genes induced or repressed when seedlings are subjected to water deficit, we carried out a transcriptomic analysis using the Medicago Genome Array-Affymetrix GeneChip. A comparison of control and drought-stressed root samples showed a total of 314 genes differentially regulated, 168 induced (≥2-fold, $p \leq 0.05$; Table S4.1 and 146 repressed (≤0.5-fold, $p \leq 0.05$; Table S4.2) when compared to control seedling roots. Additionally, to visualize the effects of the water deficit treatment in the significantly regulated genes, a heatmap was generated (Fig. 4.2).

To have a broader perspective about which genes were involved in response to the treatments, a comparison of functional gene categories have been carried out (Fig. 4.3). Firstly, 101 out of the 314 probesets were unknown sequences. Attending to the number of genes involved, the functional group containing the largest number of genes was secondary metabolism, followed by functional groups such as hormones, lipid, and cell wall metabolism (Fig. 4.3). Special attention deserves the hormone metabolism category, which contained 17 genes differentially regulated by water deficit in root AZ of *M. truncatula* seedlings (Fig. 4.3). Furthermore, almost twice as many of these hormone metabolism-related genes were found up-regulated compared to down-regulated genes. A special mention should be also

given to those functional groups which are represented by less genes but that are important in the analysis of drought effects, including transcription factors, stress regulation, signaling or transport related genes (67 genes).

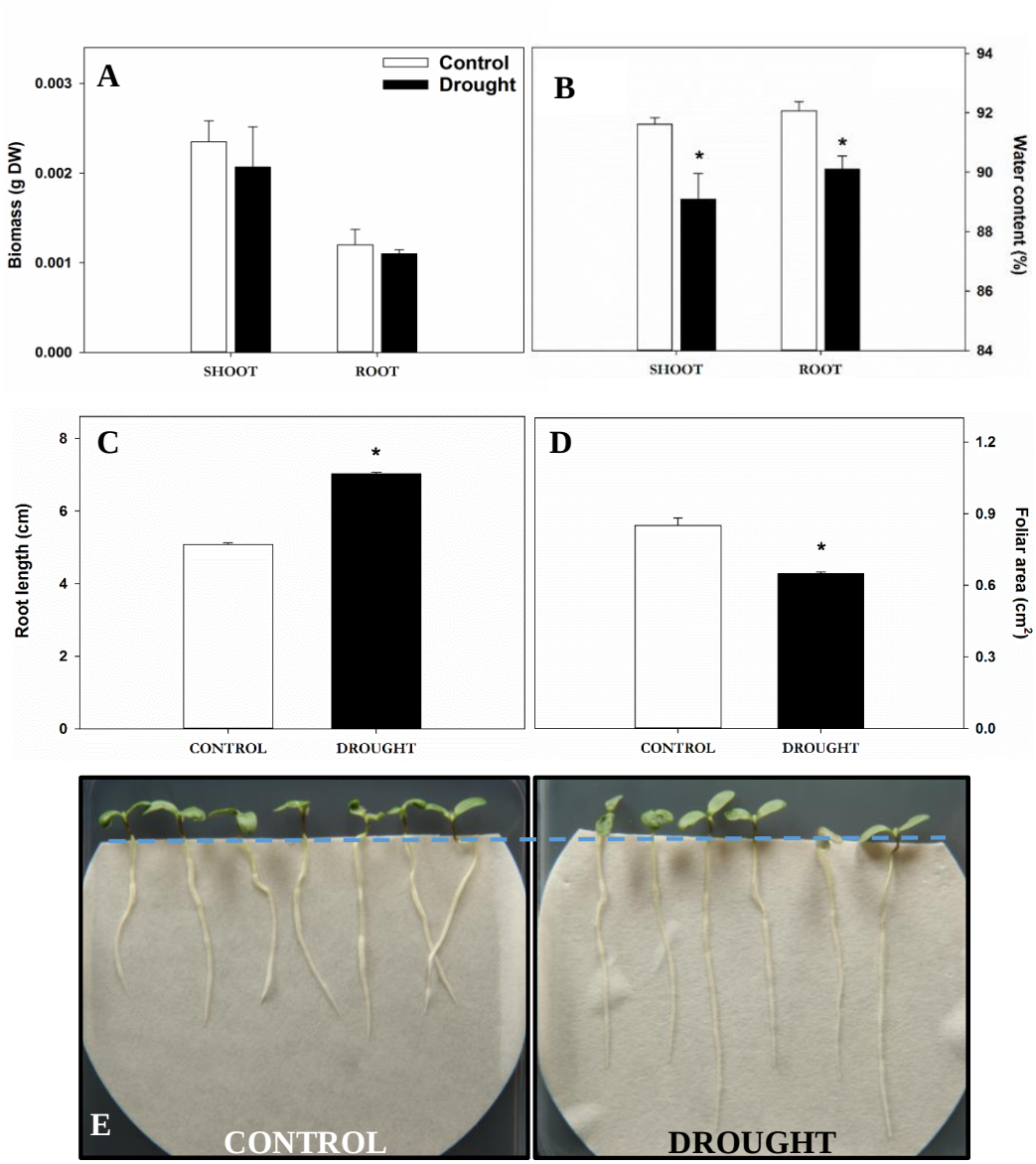

Figure 4.1. Effects of different water availability conditions on shoot and root biomass (A), water content (B), root length (C) and leaf area (D) of 4-day old seedlings of *M. truncatula*. Values represent the average ± SE (n=3 biological replicates for biomass and water content, n= 18 for root length and leaf area). An asterisk (*) denotes significant differences ($p \leq 0.05$; Student's t-test) with respect to control plants. (C) and (D) represent 4-days old *M. truncatula* seedlings growth under control and drought conditions respectively.

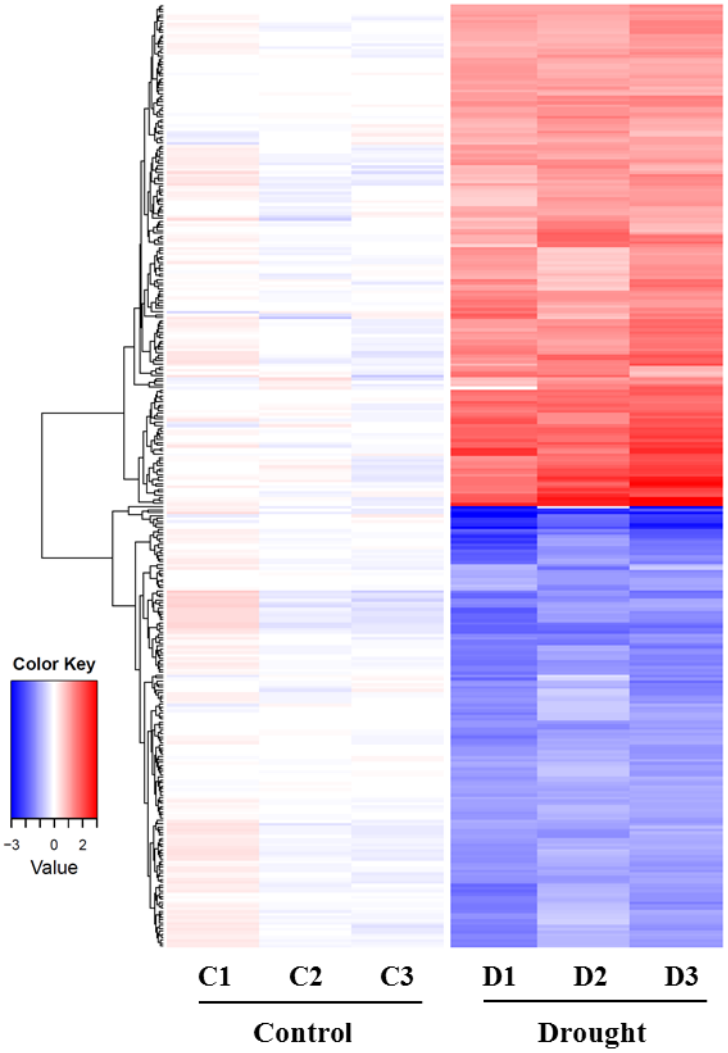

Figure 4.2. Heat map for the mRNA profiles of 314 genes differentially expressed between two treatments. Red color represents high expression while blue color represents low expression.

To summarize and functionally analyze the gene expression changes observed, the bioinformatics tool Mapmap was used (Fig. 4.4). Although differentially expressed genes were found in basically all the functional groups, three Mapman sections contain >75% of the genes: cell wall, lipids and secondary metabolism. In the cell wall section, most of the genes (around 80%) were up-regulated under water deficit stress treatment, while the other two sections contained both up- and down-regulated genes (Fig. 4.4). Genes involved in lipid breakdown and in fatty acid synthesis were significantly induced under low water availability conditions, being most of them lipases and fatty acid condensing enzymes (Fig. 4.4, Table 4.2). In terms of secondary metabolism, genes related to terpene, flavonoid and

phenylpropanoid metabolism were also found significantly expressed, with similar number of genes up- and down-regulated. Although to a lesser extent, other metabolic sections also were affected by the water deficit, such as amino acid, nucleotide and carbohydrate metabolism.

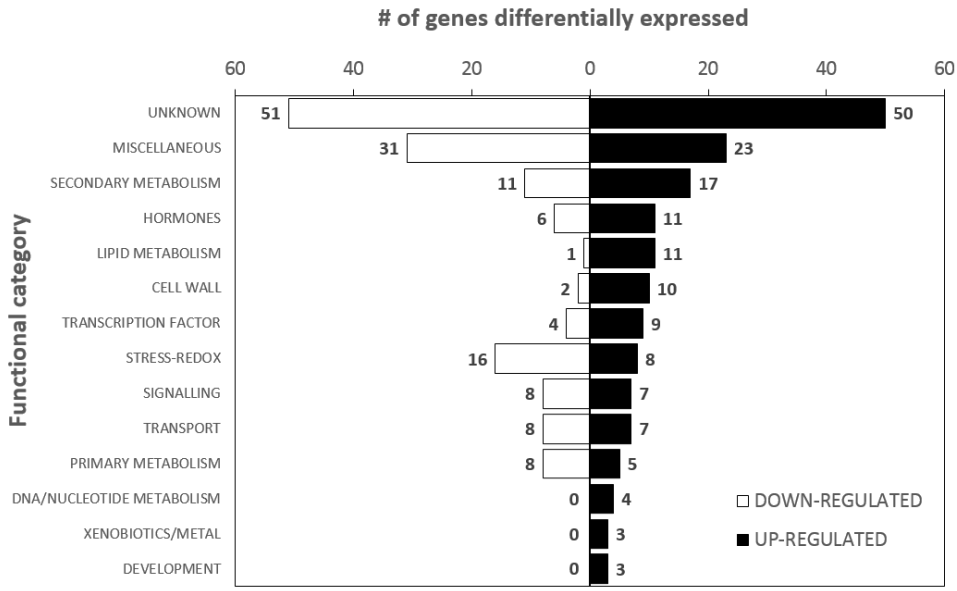

Figure 4.3. Comparison of the transcriptional up and down regulation of gene families in root absortion zone of *M. truncatula* seedlings (≥2-fold up- or ≤0.5-fold down-regulated, $p \leq 0.05$).

To identify which genes show the largest relative expression changes, the ratio between expression values under water deficit and control samples (D/C) was calculated. Tables 4.2 and 4.3 show the top-ten up- and down-regulated genes respectively based on the D/C ratio representing fold change. Interestingly, lipid and secondary metabolism related genes predominate in these lists of top-ten up and down regulated genes. Genes related to cell wall metabolism are not so well represented in tables 4.2 and 4.3 since their expression was altered to a lower ratio than lipid and secondary metabolism genes (Tables S4.1 and S4.2). The relative expression of genes such as a probable glutathione S-transferase (heat shock protein (TC105598) and an extracellular lipase EXL3 (TC95982) was increased more than 6-fold when the plants were grown under water deficit conditions. Also, an anthocyanin-related gene and one transcription factor were significantly upregulated (4-fold) in water deficit treatment (Table 4.2). Conversely, histidine decarboxylase decreased its expression more than 7-fold in drought conditions compared to controls as well as two terpene-related genes, which reduced five- and

three-fold respectively their expressions as plants were subjected to low water availability conditions (Table 4.3).

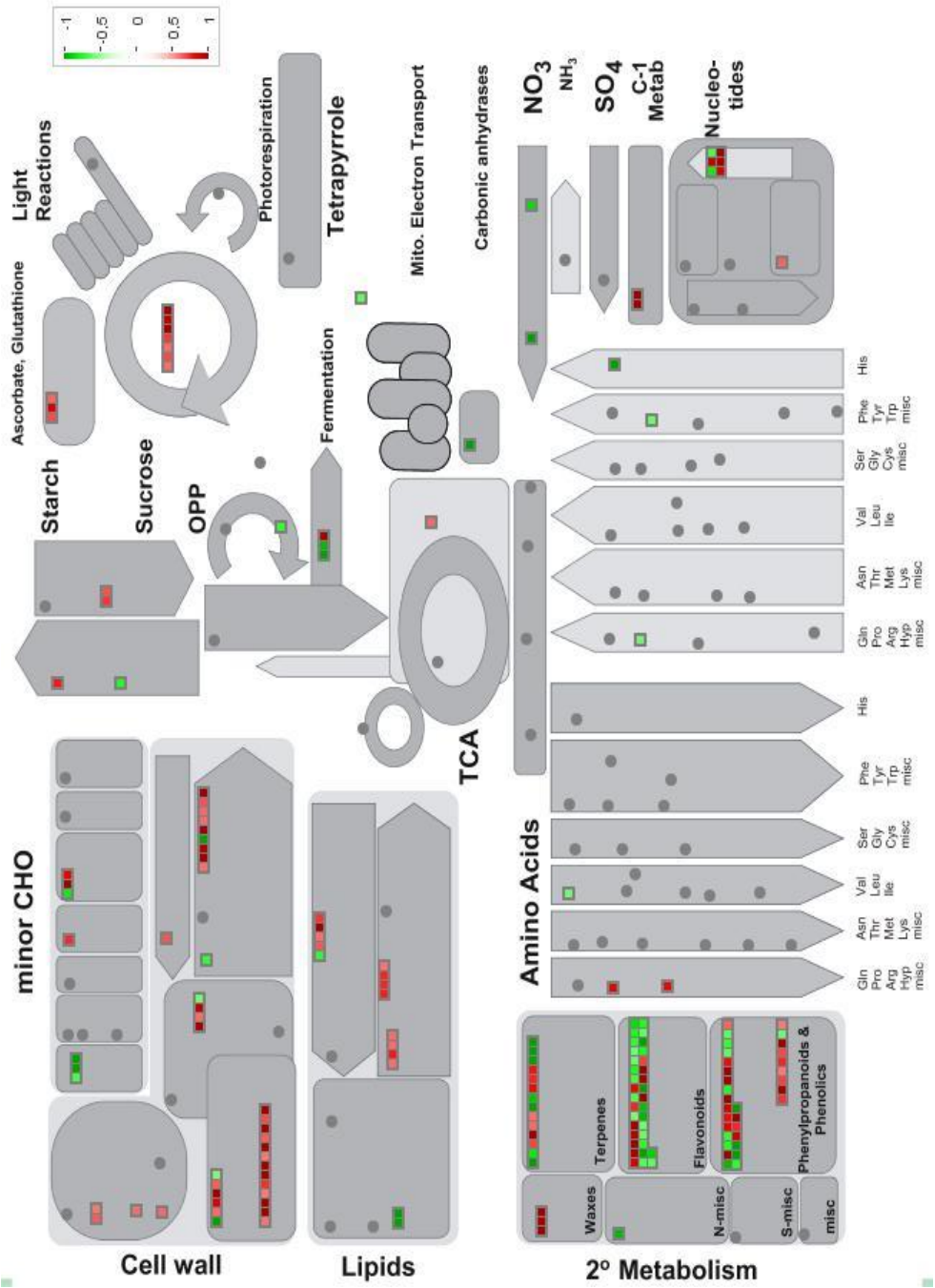

Figure 4.4. Mapman overview of changes of transcript levels in the root AZ of 4-day old seedlings of *M. truncatula* under different water availability stress. Every functional category is represented and red and green represent an increase and decrease of gene expression respectively relative to control values. A color scale was used corresponding an intense color with a high degree of expression difference and viceversa.

Table 4.2. List of top 10 most up-regulated genes in the root AZ of *M. truncatula* seedlings under drought conditions (≥2-fold, $p \leq 0.05$).

Probesets ID	EST ID	Target Description	Control AV ± SE	Drought AV ± SE	Ratio (D/C)	Functional category
Mtr.39734.1.S1_at	TC105598	Probable glutathione S-transferase (Heat shock protein 26A)	375.8 ± 40.1	2441.0 ± 217.2	6.5	Gluthatione S-transferase
Mtr.12797.1.S1_at	TC95982	Family II extracellular lipase EXL3	38.6 ± 3.9	245.8 ± 53.7	6.4	GDSL motif-lipase
Mtr.12258.1.S1_at	TC94140	Nonspecific lipid-transfer protein precursor (LTP)	590.6 ± 55.4	3544.0 ± 703.1	6.0	Lipid metabolism
Msa.1549.1.S1_at	iMsa.1549	Family II lipase EXL3	55.9 ± 6.6	280.5 ± 51.5	5.0	GDSL motif-lipase
Mtr.42933.1.S1_x_at	TC94143	Nonspecific lipid-transfer protein precursor (LTP)	670.1 ± 76.9	3296.9 ± 723.0	4.9	Lipid metabolism
Mtr.28774.1.S1_at	BM812824	Anthocyanidin synthase	34.9 ± 1.6	164.0 ± 30.2	4.7	Secondary metabolism
Mtr.39293.1.S1_at	TC104602	Unkown	32.5 ± 1.4	146.6 ± 29.6	4.5	Not assigned
Mtr.8427.1.S1_at	TC100141	Lipoxygenase 1	707.4 ± 47.6	3177.9 ± 442.8	4.5	Hormones metabolism
Mtr.28742.1.S1_at	BI312233	Very-long-chain fatty acid condensing enzyme cuticular 1 (CUT1)	62.0 ± 7.2	277.5 ± 61.4	4.5	Lipid metabolism
Mtr.44034.1.S1_at	TC96563	Pathogenesis-related and ethylene-responsive transcriptional factor	11.7 ± 1.7	51.3 ± 10.5	4.4	Transcription factor

Table 4.3. List of top 10 most down-regulated genes in the root AZ of *M. truncatula* seedlings under drought conditions (<0.5-fold, $p \leq 0.05$).

Probesets ID	EST ID	Target Description	Control AV ± SE	Drought AV ± SE	Ratio (D/C)	Functional category
Mtr.39734.1.S1_at	TC105598	Probable glutathione S-transferase (Heat shock protein 26A)	375.8 ± 40.1	2441.0 ± 217.2	6.5	Gluthatione S-transferase
Mtr.12797.1.S1_at	TC95982	Family II extracellular lipase EXL3	38.6 ± 3.9	245.8 ± 53.7	6.4	GDSL motif-lipase
Mtr.12258.1.S1_at	TC94140	Nonspecific lipid-transfer protein precursor (LTP)	590.6 ± 55.4	3544.0 ± 703.1	6.0	Lipid metabolism
Msa.1549.1.S1_at	iMsa.1549	Family II lipase EXL3	55.9 ± 6.6	280.5 ± 51.5	5.0	GDSL motif-lipase
Mtr.42933.1.S1_x_at	TC94143	Nonspecific lipid-transfer protein precursor (LTP)	670.1 ± 76.9	3296.9 ± 723.0	4.9	Lipid metabolism
Mtr.28774.1.S1_at	BM812824	Anthocyanidin synthase	34.9 ± 1.6	164.0 ± 30.2	4.7	Secondary metabolism
Mtr.39293.1.S1_at	TC104602	Unkown	32.5 ± 1.4	146.6 ± 29.6	4.5	Not assigned
Mtr.8427.1.S1_at	TC100141	Lipoxygenase 1	707.4 ± 47.6	3177.9 ± 442.8	4.5	Hormones metabolism
Mtr.28742.1.S1_at	BI312233	Very-long-chain fatty acid condensing enzyme cuticular 1 (CUT1)	62.0 ± 7.2	277.5 ± 61.4	4.5	Lipid metabolism
Mtr.44034.1.S1_at	TC96563	Pathogenesis-related and ethylene-responsive transcriptional factor	11.7 ± 1.7	51.3 ± 10.5	4.4	Transcription factor

The microarray expression results were then validated by performing quantitative real-time PCR (qRT-PCR) on a set of 6 genes up- or down-regulated by drought stress (Fig. 4.5). In all cases, the trends observed in the microarray analysis were confirmed by qRT-PCR. Among these selected genes transcription factors belonging to the AP2/ERF (Fig. 4.5A) and WRKY family (WRKY44, Fig. 4.5B), which were both markedly up-regulated. According to the importance of the secondary and lipid metabolism functional groups in the drought response, a nonspecific lipid-transfer protein precursor (Fig. 4.5C) and the anthocyanidin synthase (Fig. 4.5D) relative expression levels are presented to illustrate the up-regulation of these pathways by water deficit. The opposite trend was observed for the glutathione S-transferase GST 19 and the dehydration-induced protein RD22-like protein, which were down-regulated under limited water situations (Figs. 4.5E-F).

4.4.3 Metabolomic overview of water deficit effects in *M. truncatula* seedlings

In order to identify which metabolites are involved in the response of M. truncatula seedlings to water deficit, two types of metabolomic analysis were carried out. First, both polar and nonpolar compounds were analyzed by gas chromatography coupled to mass spectrometry (GC-MS; Table S4.3 and S4.4, respectively). Second, secondary metabolites were examined by ultra-high performance liquid chromatography coupled to quadrupole time-of-flight mass spectrometry (UHPLC; Table S4.5).

Table 4.4. Total number (and corresponding percentage) of known and unknown significantly regulated metabolites identified in the AZ of *M. truncatula* 4-days old seedlings under drought treatment conditions ($p \leq 0.05$).

METABOLITES	GC-MS		UPLC-QTOF-MS	TOTAL
	POLAR	NONPOLAR		
	# (%)	# (%)	# (%)	#
KNOWN	134 (67)	45 (47.4)	776 (99.7)	**955**
UNKNOWN	66 (33)	50 (52.6)	2 (0.3)	**188**
TOTAL	**200**	**95**	**778**	**1073**

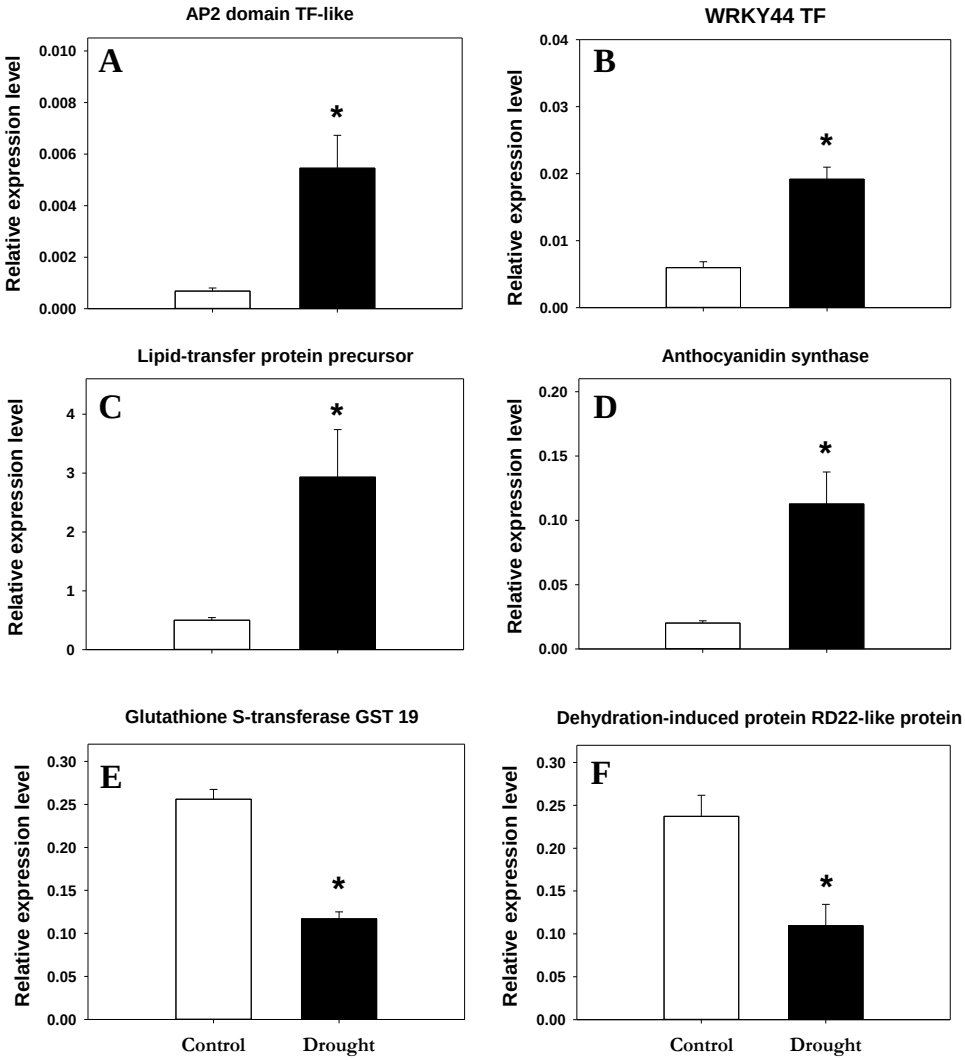

Figure 4.5. qRT-PCR analysis of *M. truncatula* genes in root AZ of 4-day old seedlings. X-axis represents the different treatments of water availability stress while Y-axis represents average values of relative mRNA levels of genes. Error bars show the standard error between values from three each biological and technical replicates. An asterisk (*) denotes significant differences ($p \leq 0.05$; Student's t-test) with respect to control plants.

In the GC-MS analysis, the levels of 200 polar and 95 nonpolar compounds were found to change differentially ($p \leq 0.05$) under stress conditions, with a fraction of them unknown (33% and 53%, respectively; Table 4.4). In order to further select which metabolites had a higher impact in the metabolic profile changes, only those showing a ≥2 D/C ratio ≤0.5 were analyzed in detail and functionally classified (Fig. 4.6). This led to 36 metabolites showing a significant change in relative

content, corresponding mostly to polar compounds. The only nonpolar metabolite regulated by drought was arachinyl alcohol, a compound related to lipid metabolism (Fig. 4.6). The group of polar metabolites includes compounds mostly related to amino acid (38%) and carbohydrate metabolism (18%). Some of the main plant proteinogenic amino acids were accumulated under the water deficit treatment including alanine, asparagine, histidine, leucine, valine and phenylalanine, along with some compounds with an osmotic role such as pinitol and ononitol (Fig. 4.7). In contrast, the relative levels of the organic acid citrate decreased together with the non-proteinogenic amino acid canavanine.

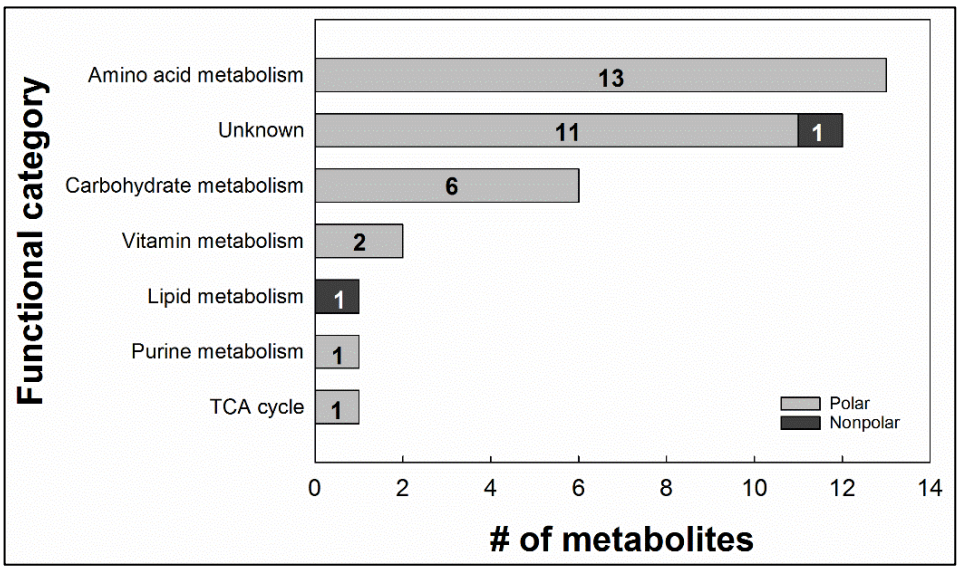

Figure 4.6. Distribution of polar and nonpolar GC-MS identified metabolites in the AZ of *M. truncatula* seedlings into functional categories (≥2-fold or ≤0.5-fold, $p \leq 0.05$).

Regarding the UHPLC analysis, it led to the identification of 778 metabolites mostly involved in secondary metabolism, with few unknown compounds (0.3%). Among them, 146 metabolites were significantly affected by drought ($p \leq 0.05$; Table S4.5). Similarly to the GC-MS analysis, we further selected those showing a ≥2 D/C ratio ≤0.5 and a p value ≤ 0.01, narrowing down the list to a total of 19 and 21 metabolites whose levels increased and decreased, respectively, upon the treatment (Table 4.5). In terms of compounds accumulating under water deficit, one of the largest group included metabolites related to saponin metabolism such as

soyasapogenol E. On the other side, luteolin or kaempferol-related metabolites, both belonging to flavonoid group, were down-regulated in drought-stressed plants.

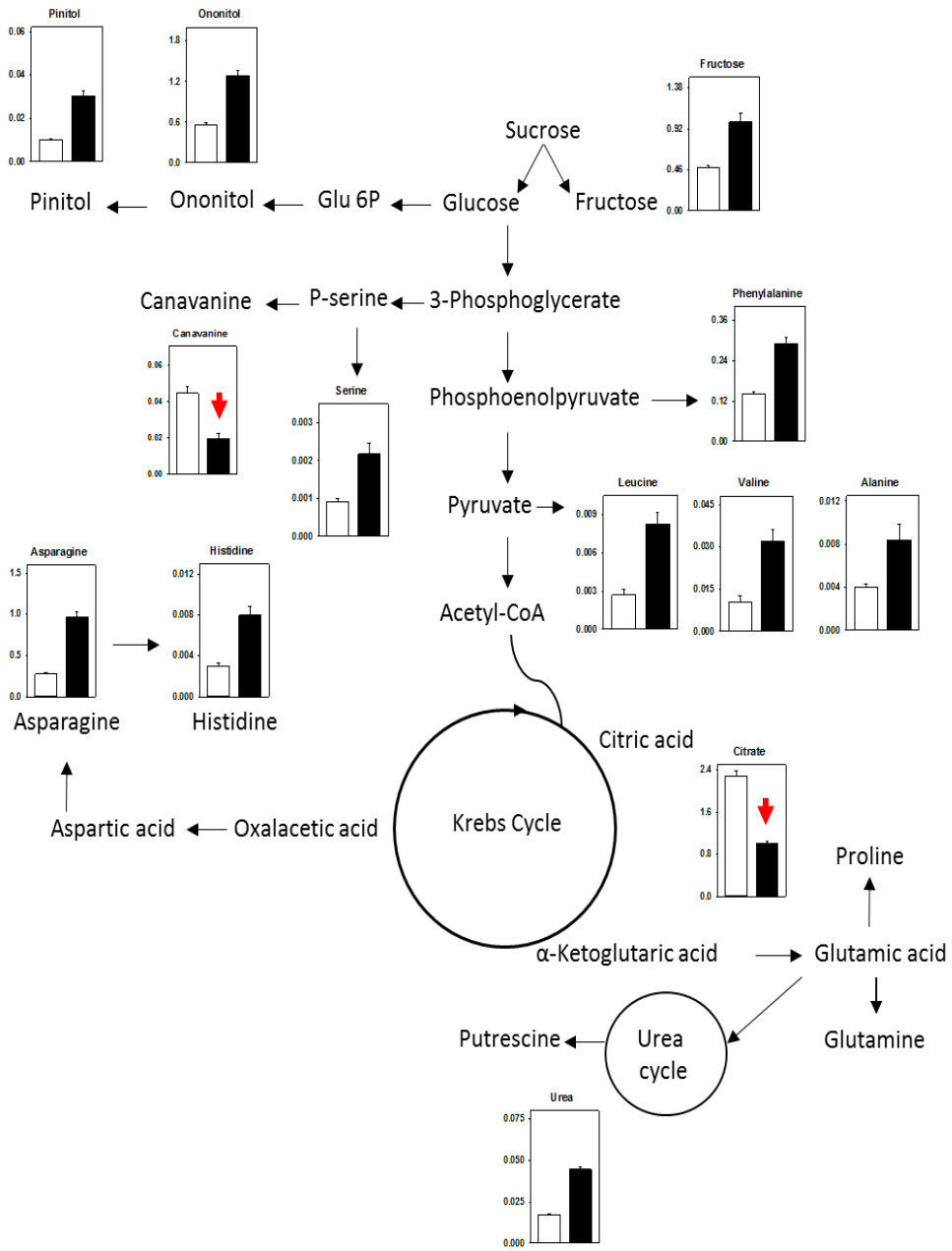

Figure 4.7. Changes in relative levels of polar metabolites of the AZ of *M. truncatula* seedlings in drought stress (black bars) as compared to control levels (white bars) (≥2-fold or ≤0.5-fold, $p \leq 0.05$). Red arrows show those metabolites which decreased their relative levels. Values represent the average ± SE (n=3 biological replicates).

Table 4.5. List of dysregulated UPLC metabolites significantly affected by drought treatment in the root AZ of *M. truncatula* plants (≥2-fold or ≤0.5-fold, $p \leq 0.01$).

METABOLITE	Control (AV ± SE) (*10^{-4})	Drought (AV ± SE) (*10^{-4})	p-value	Fold change
Gypsogenic acid	29 ± 11	140 ± 10	0.002	4.9
Sinapic acid	3 ± 1	11 ± 1	0.001	3.9
Glycyrrhetinic acid, 18 alpha-	2 ± 1	6 ± 0	0.006	3.2
Glycyrrhetinic acid, 18 beta-	2 ±1	6 ± 0	0.006	3.2
Glycyrrhetinic acid	2 ± 1	6 ± 0	0.006	3.1
Aglycone triterpene C30H48O4	51 ± 2	149 ± 11	0.001	3
Echinocystic acid	16 ± 1	42 ± 5	0.006	2.7
Hederagenin	26 ± 0	67 ± 6	0.002	2.6
Hederagenin	26 ± 0	67 ± 5	0.001	2.6
Soyasapogenol E	70 ± 7	182 ± 13	0.002	2.6
Oleanolic acid	70 ± 7	181 ± 13	0.001	2.6
Ursolic acid	71 ± 6	181 ± 13	0.001	2.6
Rha-hexose-hexose-hexose-Bayogenin	6 ± 1	15 ± 1	0.004	2.5
Epicatechin-3-Glucoside	107 ± 9	246 ± 23	0.005	2.3
Hexose-Quillaic acid	11 ± 1	25 ± 2	0.005	2.2
Quillaic acid	54 ± 5	116 ± 7	0.002	2.1
Gal-GlcA-SoyB	108 ± 11	220 ± 4	0.001	2
Gypsogenin	16 ± 2	33 ± 0	0.002	2
Dehydrosoyasaponin	326 ± 17	656 ± 51	0.004	2
Isorhoifolin	95 ± 4	40 ± 2	0.000	0.4
Saponari	533 ± 20	219 ± 11	0.000	0.4
Isorhoifolin (Apigenin-7-O-rutinoside)	96 ± 4	39 ± 2	0.000	0.4
Luteolin-3'-7-di-O-glucoside	14 ± 0	6 ± 1	0.000	0.4
Sakuranin	9 ± 1	4 ± 0	0.001	0.4
Lignoceric acid	5 ± 0	2 ± 1	0.007	0.4
Irisolidone	5 ± 1	2 ± 0	0.007	0.4
Kaempferol	4 ± 0	1 ± 0	0.001	0.3
Liquiritigenin	87 ± 5	29 ± 1	0.000	0.3
Liquiritigenin	87 ± 5	28 ± 1	0.000	0.3
Coumestrol	249 ± 14	78 ± 3	0.000	0.3
Quercitrin	127 ± 6	33 ± 3	0.000	0.3
(3',4'-Dimethoxyphenyl)-7-hydroxycoumarin	6 ± 1	2 ± 0	0.005	0.3
3',4'-Methoxy-phenylo-7-OH-Coumarin	6 ± 1	2 ± 0	0.005	0.3
Pelargonidin-3-glucoside	1237 ± 44	304 ± 151	0.004	0.2
Orientin (Luteolin 8-C-glucoside)	10 ± 1	2 ± 1	0.004	0.2
Orientin (Luteolin 8-C-glucoside)	10 ± 1	2 ± 1	0.004	0.2
5,6-dihydroxy-3',4'-dimethoxy-flavanone	8 ± 0	2 ± 1	0.000	0.2
7,3',4'-Trihydroxyisoflavone Precursor	709 ± 15	150 ± 44	0.000	0.2
7,3',4'-Trihydroxyisoflavone Precursor	709 ± 15	150 ± 44	0.000	0.2
8-Methylsulfinyl-n-octyl glucosinolate	5 ± 1	1 ± 0	0.003	0.2

4.5 DISCUSSION

4.5.1 Global metabolism is affected by drought in the AZ of *M. truncatula* roots

Drought stress affects several processes in plants, particularly plant growth and development (Farooq et al., 2012). Roots, as first organs sensing water shortage in soils, play a key role in the first stages of plant responses to water deficit conditions. Despite the fact that cell growth is one of the process firstly inhibited by drought (Hsiao, 1973), root tissue apparently contradicts this general theory by increasing growth rate through morphologic modifications (Comas et al., 2013), which can be interpreted as an attempt to reach deeper soil layers where water availability is higher (Sharp et al., 1988). In the experimental system employed in the present work, the root systems were grown in a Petri dish with homogeneous water availability but, even so, root length increased under increased agar concentrations (Fig. 4.1C; 4.1E). Similar responses have been observed in other plants when grown on plates containing polyethylene glycol as osmotic agent (van der Weele et al., 2000; Zeid and Shedeed, 2006; Youssef et al., 2016). Conversely, seedling leaf area showed a significant reduction in the water stress treatment (Fig. 4.1D), indicating a differential response of the aerial plant tissues by prioritizing root growth to face drought (Gargallo-Garriga et al., 2014).

Various research groups have exhaustively analyzed *M. truncatula* root transcriptomic and metabolomic profiles. Zhang et al. (2014) analyzed the transcriptomic and metabolomics of roots of adult *M. truncatula* plants and showed the expression profile of a large number of transcripts tightly coupled to the plant water potential. Dealing with seedlings, Watson et al. (2015) identified substantial metabolic differences between distinct and spatially segregated root regions as root tip and seedling border cells, highlighting the need of detailed transcriptomic and metabolomics studies to understand root biology properly (Wang et al., 2012; Opitz et al., 2015). In the present study, the number of transcripts altered by the water deficit applied was limited; it should be noted that the experimental approach applied provoked a mild water stress during a short period of time and in a specific section of the root, the AZ, thus not including meristematic, a section with high transcriptional activity in roots. Summarizing, the genes identified as differentially expressed in the present study can be considered as primary responses to drought associated to the root AZ. In this sense, the number of up-regulated genes affected by low water availability conditions in root AZ of *M. truncatula* seedlings was slightly higher than down-regulated ones.

Regarding the GS-MS analysis, the number of significantly regulated metabolites (Table 4.4; 134 polar + 45 nonpolar) did not differ substantially from other studies analyzing root tissue of adult *M. truncatula* plants as Zhang et al. (2014), who found 100 and 70 known polar and nonpolar metabolites, respectively. Among them, those significantly altered by drought were mainly polar compounds related to primary metabolism of nitrogen and carbon (Fig. 4.6 and 4.7) which have been suggested to prevent damage in stressed plants as amino acids or carbohydrates such as ononitol and pinitol (Bartels and Sunkar, 2005; Staudinger et al., 2012). The mild changes in important drought markers as the amino acid proline (significant at 95% but D/C ratio lower than 2-fold) indicate that drought applied treatment is moderate but even under these conditions other metabolic pathways less notorious are being activated by drought. Indeed, the UPLC analysis identified a higher amount of metabolites than GC-MS (Table 4.4), being most of them related to secondary metabolism, especially to terpenes and flavonoids. Particularly related to terpene metabolism, saponins are glycosylated triterpenic or steroidal compounds with protection properties widely distributed in many plant species (Confalonieri et al., 2009); for example, it has been described to be in a high amounts in legumes (Huhman and Sumner, 2002; Dixon and Sumner, 2003; Huhman et al., 2005) and especially abundant in the genus *Medicago*. Many of the UPLC identified compounds like hederagenin, soyasapogenol E or medicagenic acid (Table 4.5, Table S4.5) were linked to saponins. Watson et al. (2015) attributed the elevated biosynthesis of these terpene-related compounds with defense function in plants. Similar drought studies carried out in potato or in grapevine analyzed the metabolic profile finding similar compounds that were altered due to water shortage (Evers et al., 2010; Hochberg et al., 2013; Gong et al., 2015).

In agreement with this response, the majority of the transcripts altered by drought were involved in four functional groups related to lipid, hormones, cell wall and secondary metabolisms (Figs. 4.2 and 4.3). Interestingly, as a part of early responses to water restriction stress, genes related to secondary metabolism such as terpenoids, flavonoids, waxes and phenylpropanoids involved in defense and protection systems were mainly regulated, as previously observed in alfalfa roots (Chen et al., 2008). Also, the identification of many lipid and cell wall metabolism-related genes in respond to drought stress was in agreement with other studies carried out in young maize roots subjected to this stress situations (Voothuluru et al., 2016). Studies focused on transcriptomic analysis in other legume species such as chickpea and soybean have detected that genes associated to key hormone metabolism or that several transcription factors regulate root growth and responses under water-deficit conditions (Garg et al., 2016; Song et al., 2016).

In summary, transcriptomic and metabolomic analysis performed under mild drought conditions disclose the activation of metabolic pathways related to lipid, hormones, cell wall and secondary metabolism in the AZ of the root as primary responses.

4.5.2 Drought up-regulated genes involved in lipid, fatty acid and hormone metabolisms in roots

Drought stress up-regulated genes involved in lipid and fatty acid metabolism in roots including several lipases and lipid-transfer proteins (Table 4.2) affecting cell biological membranes integrity and fluidity. Firstly, a total of 11 lipoxygenases (LOXs) genes were identified in the present study being 9 of them strongly up-regulated in roots under drought conditions (Tables 4.2 and S4.1). LOXs are non-heme iron-containing dioxygenases ubiquitous in the animal and plant kingdoms and are involved in various physiological processes such as seed development and germination (Brash, 1999; Porta and Rocha-Sosa, 2002) and responses to stresses such as drought (Porta et al., 1999). Recently, LOX6, has been shown to be essential for drought stress-induced jasmonate accumulation in *Arabidopsis* roots (Grebner et al., 2013). The first step in jasmonate biosynthesis is catalyzed by a total of 13 lipoxygenases (LOXs; Feussner and Wasternack, 2002; Maalekuu et al., 2006) by deoxygenation of linoleic (methyl 9,12-octadecadienoate) and linolenic acids (octadecatrienoic acid methylester, 9,12,15), whose content decreased significantly in drought-stressed roots to a fold change of 0.71 and 0.77, respectively (Table S4.4). Being linolenic acid the most abundant fatty acid in plant membranes, the decrease observed in drought-stressed roots may be related to membrane reorganization occurring in plant cells to counteract the metabolic slowdown (Upchurch, 2008). Similar responses have been observed in other plant systems (Dakhma et al., 1995; Zhang et al., 2005), suggesting that plant drought tolerance is dependent on the level of fatty acid unsaturation and/or the ability to maintain or adjust fatty acid unsaturation (Berberich et al., 1998; Mikami and Murata, 2003).

Lipases, transcripts coding for a fatty acid condensing enzyme (CUT1) and a nonspecific lipid-transfer protein precursor were also found significantly overexpressed under drought conditions (Tables 4.2, S4.1). Lipases are one of the lipid hydrolyzing enzymes in plants and their overexpression has been closely associated with morphogenesis and development (Matsui et al., 2004). Particularly, phospholipases have been described to act as a signaling drought response in plants (Hong et al., 2010). In addition, nonspecific lipid transfer proteins are small proteins that are ubiquitously distributed throughout the plant kingdom which has been related to lipid mobilization during post-germinative growth (Pagnussat et al.,

2015) and in defense reactions against abiotic stress (Wei and Zhong, 2014), particularly under drought conditions in *Arabidopsis* (Guo et al., 2013). In this regard, drought responses of these precursors were validated by quantitative real-time PCR (qRT-PCR), finding that they increased their expression level more than three-fold under water-deficit conditions (Fig. 4.5C). All these results could indicate that an enhanced lipid metabolism in roots might also contribute to enhance drought tolerance in *M. truncatula*.

Among the transcripts regulated under low water availability conditions (Tables 4.2 and 4.3), there were several oxidoreductases (2-oxoglutarate/Fe (II)-oxygenase proteins) which have been associated with ethylene biosynthesis (Farrow and Facchini, 2014). In addition, the cytochrome P450 enzymes family was highly represented by 19 down-regulated genes (Table S4.2), which play an essential role in numerous plant metabolic pathways (Schuler, 1996; Werck-Reichhart et al., 2002; Nielsen and Møller, 2005; Li et al., 2007; Pan et al., 2009; Nelson and Werck-Reichhart, 2011). It has been suggested that cytochrome P450 monooxygenases are related to the terpene metabolism (Suzuki et al., 2002; Confalonieri et al., 2009; Watson et al., 2015), which is highly affected by drought at the transcript (with the two terpene synthases highly down-regulated (Table 4.3)) and metabolic level, with a reduced content of saponins observed in drought-stressed roots (Table S4.5; (Huhman et al., 2005)) together with an accumulation of hederagenin and soyasapogenol E (Table 4.5; (Tava et al., 2010)).

4.5.3 Cell wall modifications to tackle drought situations

Notably, cell wall associated genes were highly overexpressed in drought conditions, most likely affecting cell wall modification and degradation as Mapman software indicates (Fig. 4.4). The elongation of roots observed when plants were grown in low water availability conditions (Fig. 4.1C) supports the hypothesis of expansion of cell walls as part of the mechanism of exploration of deeper substrate areas to facilitate water uptake. This suggests that seedling growth is a coordinated work between water uptake and cell wall enlargement leading to cell expansion (Cosgrove, 1993). In this experiment we found several genes encoding cell-wall biosynthesis enzymes which may contribute to root elongation such as cellulose synthase, α-expansin and xyloglucan endotransglycosylases/hydrolase (Table S4.1). All of them have been reported to play a role on root adaptation to low water availability conditions by participating in cell extension (Wu et al., 1994; Wu and Cosgrove, 2000; Wu et al., 2001). Additionally, these enzymes have been related to root hair initiation (Vissenberg et al., 2001), which agrees with the observed activation in the root AZ of *M. truncatula* roots. Further evidence supporting the

idea that plant cells walls are altered is the overexpression of glycine-rich proteins (Table S4.1), which has been already reported to be induced under different abiotic stresses in *A. thaliana* seedlings (Kim et al., 2008) and whose activation has been related to root cell elongation (Mangeon et al., 2009). Similarly, proline-related proteins have been associated to growing regions indicating that cell wall modifications are induced in actively growing cells in response to drought (Yoshiba et al., 1997; Battaglia et al., 2007; Szabados and Savouré, 2010; Kavi Kishor et al., 2015), as well as to root hair growth and elongation in *A. thaliana* plants (Velasquez et al., 2011; Boron et al., 2014). These findings suggest that drought stress provokes changes in root seedling cell walls promoting their elongation to cope with stress conditions.

4.5.4 The phenylpropanoid pathway is severely modulated under mild drought conditions

The phenylpropanoid pathway serves as a rich source of metabolites in plants by the production of many important compounds such as flavonoids, coumarins, and lignans. Flavonoids represent a major component of secondary metabolism in plants being extensively described as defense metabolites which are synthesized in response to both abiotic and biotic stresses. Among flavonoid biosynthesis enzymes, anthocyanidin synthase participates in the synthesis of anthocyanins. Particularly, anthocyanidin synthase gene is present in the top 10 up-regulated genes table (Table 4.2), followed by transcripts with lower D/C ratio as those related to flavonoids or phenylpropanoids (Table S4.1), indicating the importance of anthocyanins in drought responses at root level. Also, anthocyanidin synthase expression level was analyzed by qRT-PCR showing nearly 5-fold increment under drought conditions (Fig. 4.5D). It has been previously described that anthocyanins are osmoregulators which their accumulation is stimulated by environmental stresses, particularly by drought; thus acting as antioxidants by reducing damage and protecting against oxidation (Rabino and Mancinelli, 1986; Chalker-Scott, 1999; Steyn et al., 2002). Related to this point, especially relevant is the amino-acid phenylalanine (precursor of phenylpropanoids), whose levels increased considerably (Fig. 4.7), leading to an increase in products derived from this pathway (such as flavonoids) to cope with drought stress. Several flavonoid-related genes changed considerably its expression under drought conditions. Fini et al. (2011) deduced that flavonoid biosynthesis is transcriptionally induced in response to drought stress while, in agreement with this point, Maloney et al. 2014 suggested that flavonols play a major role as antioxidants in roots. Through UHPLC analysis, we detected important secondary metabolites such as daidzein (Table S4.5), which

is associated with isoflavone metabolism and was also identified in *M. truncatula* seedling roots (Staszków et al., 2011) and kaempferol, a constituent compound in the biosynthesis of flavonols.

4.5.5 Antioxidant responses activated in roots

The second group is associated with antioxidant responses to water scarcity conditions highlighting the importance of oxidative stress and detoxification of reactive oxygen species. In this regard, glutathione metabolism is a pathway that is involved in the antioxidative system of plants. As in humans, plant gluthatione S-tranferases (GST) enzymes are induced by diverse environmental stimuli to maintain cell redox homeostasis and protect organisms against oxidative stress by metabolizing a wide variety of toxic exogenous compounds via the tripeptide glutathione (GSH) conjugation. Apart from their detoxification function, they also participate in processes such as flavonoid transport (Zhao and Dixon, 2010). According to the amino acid sequence and to the conservation of intron:exon placement, three types of plant GSTs are described: type I, II, II and then, unknown GSTs (Marrs, 1996). In our transcriptomic analysis, we found a probable glutathione S-transferase (heat shock protein 26A) transcript, which significantly increased its expression under drought conditions. In addition, more transcripts related to GST were regulated with drought treatment (Tables S4.1 and S4.2); in particular, the expression levels of GST19 were validated by RT-PCR in Fig. 4.5E, results that verified that this gene is down-regulated under drought. This and above discussed issue are related since GSTs are implicated to secondary metabolism since phenylpropanoids are substrates of plant GSTs (Marrs, 1996); changes in secondary metabolism could lead in higher drought tolerance of these plants.

4.5.6 Transcription factors regulated under drought conditions

It is now well established that alteration in the expression of several types of transcription factors (TFs) can provide increased drought tolerance enabling plants to withstand unfavorable conditions (Singh and Laxmi, 2015; Joshi et al., 2016). The current work identifies several TFs differentially regulated at the transcriptional level and Mapman analysis displayed a total of 13 differentially-expressed genes linked to TFs, being most of them up-regulated (Fig. 4.4). Additionally, the relative expression of some of these TFs was validated by qRT-PCR (Figs. 4.5A-B). WRKY TFs have been described to play an important role in plant stress responses (Chen et al., 2012) being particularly WRKY44 a gene overexpressed under salinity and drought stress conditions in *Arabidopsis* plants (Claeys and Inzé, 2013). Also, one of the largest groups of plant-specific TFs is the AP2 /ERF superfamily. Members of this family are involved in numerous

biological processes such as plant growth and development and in the responses of plants to abiotic stresses (Mizoi et al., 2012). In our study, an AP2/ERF TF shows a high fold-change expression ratio (4.4) (Table 4.2). In agreement with our work, Sharoni et al. (2012) described the induction of AP2/ERF expression levels under drought conditions in rice plants, showing a six-fold increase in the drought-tolerant line compared with the drought-susceptible line in the root. Similarly to our study, Shu et al., 2015 (Shu et al., 2016) ranked the differentially expressed AP2/ERF TFs according to the tissues in which such expression changed and to the response to various stresses in adult *M. truncatula* plants.

In addition to above described TFs, transcripts associated with APETALA3, MYB, LBD and Zn-finger TFs were also differentially regulated in this experiment. Specifically, MYB TFs have been described to participate in very-long-chain fatty acids and in cuticular wax biosynthesis regulation in wheat plants; so the overexpression of these MYB-related proteins could be associated with the observed activation of wax biosynthesis (Fig. 4.3), compounds with a relevant role in terms of plant responses to environmental stresses like drought (Bi et al., 2016). Seo et al. (2011) proposed that the regulation of the expression of *RD22* gene was carried out by MYB TFs at stomatal movements modulation level under drought conditions; however, this differs from the expression pattern of dehydration-induced protein RD22-like, which was down-regulated as drought became more intense (Fig. 4.5F and Table S4.2).

4.6 CONCLUSIONS

In this chapter, we showed that plants have rapid molecular responses upon changes in the levels of available water; in the case of *M. truncatula* roots, lipid, hormone, cell wall and secondary metabolisms appear as relevant factors enabling plants to cope with drought stress situations. Also, results presented here identify several TFs which may be involved in the regulation of gene expression in response to drought. Finally, these results suggest that the AZ of roots is very active tissue rapidly responded to changes in water levels even during the early stages of *M. truncatula* plant development.

upna

Universidad Pública de Navarra
Nafarroako Unibertsitate Publikoa

upna

Universidad Pública de Navarra
Nafarroako Unibertsitate Publikoa

» *GENERAL OVERVIEW*

upna

Universidad Pública de Navarra
Nafarroako Unibertsitate Publikoa

GENERAL OVERVIEW

The overall goal of this work is to gain further insights into drought responses in plants of two legume species of great agronomical importance; the tropical legume *G. max* and the temperate model legume *M. truncatula*. To address this general aim, this work is divided in four chapters where results have been presented.

In **chapter 1**, we observed that drought stress negatively affected AsA biosynthesis in the aerial part of soybean plants both at the AsA content and enzymatic level. In roots the levels of this antioxidant were found under detection limits, while a decrease was observed in leaves of drought-stressed plants, demonstrating that plant tissues respond differently to drought stress; this differential response at the tissue level was also observed in terms of gene expression via RNA-Seq analysis. Furthermore, this differential pattern of gene expression was also observed in plants of *M. truncatula* as water deficit became more intense. These results suggest that the last step of the AsA biosynthesis pathway (catalyzed by GAlLDH) is not the only point involved in the control of AsA content under drought stress conditions. Genes encoding GDP-D-mannose pyrophosphorylase (VTC1) emerge as strong candidates for the regulation of AsA biosynthesis in drought-stressed legume plants, while several steps in the pathway such as GDP-D-mannose 3´, 5´-epimerase (GME) genes appear to have undergone functional specialization in soybean.

Chapter 2 presents a detailed characterization of plants subjected to two levels of progressive drought stress. Changes in biomass and in water parameters indicate that these plants prioritize the maintenance of leaf water status and that they modify biomass shoot/root ratio as a strategy to cope with water stress. Also, gas exchange parameters such as stomatal conductance, photosynthesis and transpiration rates were limited by the low water availability. Concomitantly, plants prioritize carbon exportation, coming mainly from starch degradation in leaves, supplying carbon skeletons toward root in order to promote its growth. Regarding nitrogen metabolism, protein degradation was found activated in leaves as a stress signal being amino acids partly allocated in both organs. Altogether, responses observed here exhibit different behavior patterns present in different plant tissues under this stress; a passive survival strategy for the leaf is suggested coexisting with an active engagement of the root organ in drought-stressed plants

Drought responses have been thoroughly studied in plant adult stages but little is known about responses at the early stages of development. Responses at these stages could affect drought tolerance in subsequent episodes of low water

availability. In addition, methods of analysis of the effects of drought in plants have been carried out through deprivation of water or the use of polyols that simulate osmotic stress, with unwanted secondary effects in terms of plant physiology. For that reason, in **chapter 3**, a new *in vivo* method for simulating drought conditions was developed by using different concentrations of agar in the medium thus allowing lowering water availability for plants. The water deficit imposed caused reproducible reductions in water potential and other physiological parameters in agreement with previous studies in adult plants confirming the validity of the new *in vivo* method. Also, this protocol allows a better characterization of root metabolism. These results highlight the key role of this organ during the first plant development stages concentrating most of the carbon reserves of the plants. An intensive root examination was carried out under two drought levels finding that root architecture and morphology are strongly affected by water scarcity. All these findings conclude that this method is suitable to simulate different drought stress levels under highly controlled conditions in a variety of plant seedlings.

The focus of **chapter 4** is the study the drought stress response of the part of the root known as "maturation, differentiation or absorption zone" using transcriptomic and metabolomic techniques. This zone corresponds to the area where root hairs are present and is the root zone in charge of carrying out the absorption of nutrients and water. Analysis presented here showed that root lipid, hormones, cell wall and secondary metabolism play a key role in the response of plants to low water availability conditions. These factors enable plants to face drought stress situations through the expression of genes such as transcription factors or cell wall-related genes. Also, several metabolites, mostly amino acids, accumulate in roots, which could be related to an activation of plant signaling responses under drought conditions. Results presented here show that root tissue is very active under drought conditions at the early stages of development in *M. truncatula* plants.

In conclusion, this work contributes towards our understanding of legume responses to drought stress, particularly at the root level, with potential implications for improved plant tolerance to environmental constrains. Results also provide new insights of potential mechanisms for water deficit signal transduction and gene networks controlling the response of roots to drought, contributing to support the crucial role of roots in situations of drought stress.

upna

Universidad Pública de Navarra
Nafarroako Unibertsitate Publikoa

upna

Universidad Pública de Navarra
Nafarroako Unibertsitate Publikoa

» *BIBLIOGRAPHY*

upna

Universidad Pública de Navarra
Nafarroako Unibertsitate Publikoa

BIBLIOGRAPHY

Aguirreolea J, Sánchez-Díaz M (1989) CO_2 evolution by nodulated roots in *Medicago sativa* L. under water stress. J Plant Physiol **134**: 598–602

Alley RB (2007) Wally was right: predictive ability of the north atlantic "Conveyor Belt" hypothesis for abrupt climate change. Annu Rev Earth Planet Sci **35**: 241–272

Anjum S, Farooq M, Wang L, Xue L, Wang S, Wang L, Zhang S, Chen M (2011) Gas exchange and chlorophyll synthesis of maize cultivars are enhanced by exogenously-applied glycinebetaine under drought conditions. Plant, Soil Environ **57**: 326–331

Antolin MC, Sanchez-Diaz M (1992) Photosynthetic nutrient use efficiency, nodule activity and solute accumulation in drought stressed alfalfa plants. Photosynthetica **27**: 595–604

Antoni R, Gonzalez-Guzman M, Rodriguez L, Peirats-Llobet M, Pizzio GA, Fernandez MA, De Winne N, De Jaeger G, Dietrich D, Bennett MJ, et al (2013) PYRABACTIN RESISTANCE1-LIKE8 plays an important role for the regulation of abscisic acid signaling in root. Plant Physiol 161: 931–941

Aranjuelo I, Irigoyen JJ, Sánchez-Díaz M (2007) Effect of elevated temperature and water availability on CO_2 exchange and nitrogen fixation of nodulated alfalfa plants. Environ Exp Bot **59**: 99–108

Aranjuelo I, Molero G, Erice G, Avice JC, Nogués S (2011) Plant physiology and proteomics reveals the leaf response to drought in alfalfa (*Medicago sativa* L.). J Exp Bot **62**: 111–123

Araújo SS, Beebe S, Crespi M, Delbreil B, González EM, Gruber V, Lejeune-Henaut I, Link W, Monteros MJ, Prats E, et al (2015) Abiotic stress responses in legumes: Strategies used to cope with environmental challenges. CRC Crit Rev Plant Sci **34**: 237–280

Araus JL, Slafer GA, Reynolds MP, Royo C (2002) Plant breeding and drought in C3 cereals: What should we breed for? Ann Bot **89**: 925–940

Arlt K, Brandt S, Kehr J (2001) Amino acid analysis in five pooled single plant cell samples using capillary electrophoresis coupled to laser-induced fluorescence detection. J Chromatogr A **926**: 319–325

Aronne G, De Micco V (2004) Hypocotyl features of *Myrtus communis* (Myrtaceae): A many-sided strategy for possible enhancement of seedling establishment in the Mediterranean environment. Bot J Linn Soc **145**: 195–202

Asada K (1999) The water-water cycle in chloroplasts: scavenging of active oxygens and dissipation of excess photons. Annu Rev Plant Physiol Plant Mol Biol **50**: 601–639

Ashraf M, Harris PJC (2013) Photosynthesis under stressful environments: An overview. Photosynthetica **51**: 163–190

Atkin OK, Macherel D (2009) The crucial role of plant mitochondria in orchestrating drought tolerance. Ann Bot **103**: 581–597

Aubert G, Morin J, Jacquin F, Loridon K, Quillet MC, Petit A, Rameau C, Lejeune-Hénaut I, Huguet T, Burstin J (2006) Functional mapping in pea, as an aid to the candidate gene selection and for investigating synteny with the model legume *Medicago truncatula*. Theor Appl Genet **112**: 1024–1041

Badejo AA, Jeong ST, Goto-Yamamoto N, Esaka M (2007) Cloning and expression of GDP-D-mannose pyrophosphorylase gene and ascorbic acid content of acerola (*Malpighia glabra* L.) fruit at ripening stages. Plant Physiol Biochem **45**: 665–672

Badejo AA, Tanaka N, Esaka M (2008) Analysis of GDP-D-mannose pyrophosphorylase gene promoter from acerola (*Malpighia glabra*) and increase in ascorbate content of transgenic tobacco expressing the acerola gene. Plant Cell Physiol **49**: 126–132

Bañon S, Ochoa J, Franco JA, Alarcón JJ, Sánchez-Blanco MJ (2006) Hardening of oleander seedlings by deficit irrigation and low air humidity. Environ Exp Bot **56**: 36–43

Barker D, Pfaff T, Moreau D, Groves E, Ruffel S, Lepetit M, Whitehand S, Maillet F, Nair R, Journet E (2006) Growing *Medicago truncatula*: choice of substrates and growth conditions. *Medicago truncatula* Handb.

Bartels D, Sunkar R (2005) Drought and salt tolerance in plants. CRC Crit Rev Plant Sci **24**: 23–58

Bartoli CG, Guiamet JJ, Kiddle G, Pastori GM, Di Cagno R, Theodoulou FL, Foyer CH (2005) Ascorbate content of wheat leaves is not determined by maximal L-galactono-1,4-lactone dehydrogenase (GalLDH) activity under drought stress. Plant, Cell Environ **28**: 1073–1081

Bartoli CG, Pastori GM, Foyer CH (2000) Ascorbate biosynthesis in mitochondria is linked to the electron transport chain between complexes III and IV. Plant Physiol **123**: 335–344

Bartoli CG, Simontacchi M, Tambussi E, Beltrano J, Montaldi E, Puntarulo S (1999) Drought and watering-dependent oxidative stress: effect on antioxidant content in *Triticum aestivum* L. leaves. J Exp Bot **50**: 375–383

Bartoli CG, Tambussi EA, Diego F, Foyer CH (2009) Control of ascorbic acid synthesis and accumulation and glutathione by the incident light red/far red ratio in *Phaseolus vulgaris* leaves. FEBS Lett **583**: 118–122

Bartoli CG, Yu J, Gómez F, Fernández L, McIntosh L, Foyer CH (2006) Inter-relationships between light and respiration in the control of ascorbic acid synthesis and accumulation in *Arabidopsis thaliana* leaves. J Exp Bot **57**: 1621–1631

Basu S, Ramegowda V, Kumar A, Pereira A (2016) Plant adaptation to drought stress. F1000Research **5**: 1554

Bates LS, Waldren RP, Teare ID (1973) Rapid determination of free proline for water-stress studies. Plant Soil **39**: 205–207

Battaglia M, Solórzano RM, Hernández M, Cuéllar-Ortiz S, García-Gómez B, Márquez J, Covarrubias AA (2007) Proline-rich cell wall proteins accumulate in growing regions and phloem tissue in response to water deficit in common bean seedlings. Planta **225**: 1121–1133

Beebe SE, Rao IM, Devi MJ, Polania J (2014) Common beans, biodiversity, and multiple stresses: Challenges of drought resistance in tropical soils. Crop Pasture Sci **65**: 667–675

Belamkar V, Weeks NT, Bharti AK, Farmer AD, Graham MA, Cannon SB (2014) Comprehensive characterization and RNA-Seq profiling of the HD-Zip transcription factor family in soybean (*Glycine max*) during dehydration and salt stress. BMC Genomics **15**: 950

Benedito VA, Torres-Jerez I, Murray JD, Andriankaja A, Allen S, Kakar K, Wandrey M, Verdier J, Zuber H, Ott T, et al (2008) A gene expression atlas of the model legume Medicago truncatula. Plant J 55: 504–513

Berberich T, Harada M, Sugawara K, Kodama H, Iba K, Kusano T (1998) Two maize genes encoding omega-3 fatty acid desaturase and their differential expression to temperature. Plant Mol Biol **36**: 297–306

Bi H, Luang S, Li Y, Bazanova N, Morran S, Song Z, Perera MA, Hrmova M, Borisjuk N, Lopato S (2016) Identification and characterization of wheat drought-responsive MYB transcription factors involved in the regulation of cuticle biosynthesis. J Exp Bot **67**: 5363–5380

Bibikova T, Gilroy S (2002) Root Hair Development. J Plant Growth Regul **21**: 383–415

Bielen A, Remans T, Vangronsveld J, Cuypers A (2013) The influence of metal stress on the availability and redox state of ascorbate, and possible interference with its cellular functions. Int J Mol Sci **14**: 6382–6413

Blum A (2011) Plant breeding for water-limited environments. doi: 10.1007/978-1-4419-7491-4

Boron AK, Van Orden J, Nektarios Markakis M, Mouille G, Adriaensen D, Verbelen JP, Höfte H, Vissenberg K (2014) Proline-rich protein-like PRPL1 controls elongation of root hairs in *Arabidopsis thaliana*. J Exp Bot **65**: 5485–5495

Boudet J, Buitink J, Hoekstra FA, Rogniaux H, Larré C, Satour P, Leprince O (2006) Comparative analysis of the heat stable proteome of radicles of *Medicago truncatula* seeds during germination identifies late embryogenesis abundant proteins associated with desiccation tolerance. Plant Physiol **140**: 1418–1436

Boyer JS (1982) Plant productivity and environment. Science **218**: 443–448

Bradford MM (1976) A rapid and sensitive method for the quantitation of microgram quantities of protein utilizing the principle of protein-dye binding. Anal Biochem **72**: 248–254

Brash AR (1999) Lipoxygenases: Occurrence, functions, catalysis, and acquisition of substrate. J Biol Chem **274**: 23679–23682

Bray EA (1997) Plant responses to water deficit. Trends Plant Sci **2**: 48–54

Broeckling CD, Huhman D V, Farag MA, Smith JT, May GD, Mendes P, Dixon RA, Sumner LW (2005) Metabolic profiling of *Medicago truncatula* cell cultures reveals the effects of biotic and abiotic elicitors on metabolism. J Exp Bot **56**: 323–336

Buckley TN (2005) The control of stomata by water balance. New Phytol **168**: 275–292

Bulley SM, Rassam M, Hoser D, Otto W, Schünemann N, Wright M, MacRae E, Gleave A, Laing W (2009) Gene expression studies in kiwifruit and gene over-expression in *Arabidopsis* indicates that GDP-L-galactose guanyltransferase is a major control point of vitamin C biosynthesis. J Exp Bot **60**: 765–778

Castroluna Ruiz OM, Quiroga AM, Pedgranzani HE (2014) Effects of salinity and drought stress on germination, biomass and growth in three varieties of *Medicago sativa* L. Av en Investigocion Agropecu **18**: 39–50

Chalker-Scott L (1999) Environmental significance of anthocyanins in plant stress responses. Photochem Photobiol **70**: 1–9

Chan KX, Wirtz M, Phua SY, Estavillo GM, Pogson BJ (2013) Balancing metabolites in drought: the sulfur assimilation conundrum. Trends Plant Sci **18**: 18–29

Chaumont F, Moshelion M, Daniels MJ (2005) Regulation of plant aquaporin activity. Biol Cell **97**: 749–764

Chavarria G, Pessoa dos Santos H (2012) Plant water relations: absorption, transport and control mechanisms. Adv. Sel. Plant Physiol. Asp.105–132

Chaves MM, Flexas J, Pinheiro C (2009) Photosynthesis under drought and salt stress: regulation mechanisms from whole plant to cell. Ann Bot **103**: 551–560

Chaves MM, Maroco JP, Pereira JS (2003) Understanding plant responses to drought - from genes to the whole plant. Funct Plant Biol **30**: 239–264

Chaves MM, Oliveira MM (2004) Mechanisms underlying plant resilience to water deficits: prospects for water-saving agriculture. J Exp Bot **55**: 2365–2384

Chaves MM, Pereira JS, Maroco J, Rodrigues ML, Ricardo CPP, Osório ML, Carvalho I, Faria T, Pinheiro C (2002) How plants cope with water stress in the field. Photosynthesis and growth. Ann Bot 89: 907–916

Chellamuthu VR, Ermilova E, Lapina T, Lüddecke J, Minaeva E, Herrmann C, Hartmann MD, Forchhammer K (2014) A widespread glutamine-sensing mechanism in the plant kingdom. Cell 159: 1188–1199

Chen D, Liang MX, DeWald D, Weimer B, Peel MD, Bugbee B, Michaelson J, Davis E, Wu Y (2008) Identification of dehydration responsive genes from two non-nodulated alfalfa cultivars using *Medicago truncatula* microarrays. Acta Physiol Plant **30**: 183–199

Chen H, Jiang JG (2010) Osmotic adjustment and plant adaptation to environmental changes related to drought and salinity. Environ Rev **18**: 309–319

Chen L, Song Y, Li S, Zhang L, Zou C, Yu D (2012) The role of WRKY transcription factors in plant abiotic stresses. Biochim Biophys Acta - Gene Regul Mech **1819**: 120–128

Chen X, Qiu JD, Shi SP, Suo SB, Huang SY, Liang RP (2013) Incorporating key position and amino acid residue features to identify general and species-specific ubiquitin conjugation sites. Bioinformatics **29**: 1614–1622

Chimungu JG, Brown KM, Lynch JP (2014) Large root cortical cell size improves drought tolerance in maize. Plant Physiol **166**: 2166–2178

Chomczynski P, Mackey K (1995) Modification of the TRI reagent procedure for isolation of RNA from polysaccharide- and proteoglycan-rich sources. Biotechniques **19**: 942–945

Claeys H, Inzé D (2013) The agony of choice: how plants balance growth and survival under water-limiting conditions. Plant Physiol **162**: 1768–79

Clowes FAL (1975) The cessation of mitosis at the margins of a root meristem. New Phytol **74**: 263–271

Comas LH, Becker SR, Cruz VM, Byrne PF, Dierig DA (2013) Root traits contributing to plant productivity under drought. Front Plant Sci **4**: 442

Confalonieri M, Cammareri M, Biazzi E, Pecchia P, Fevereiro PM, Balestrazzi A, Tava A, Conicella C (2009) Enhanced triterpene saponin biosynthesis and root nodulation in transgenic barrel medic (*Medicago truncatula* Gaertn.) expressing a novel β -amyrin synthase (AsOXA1) gene. Plant Biotechnol J **7**: 172–182

Conklin PL, DePaolo D, Wintle B, Schatz C, Buckenmeyer G (2013) Identification of *Arabidopsis* VTC3 as a putative and unique dual function protein kinase::protein phosphatase involved in the regulation of the ascorbic acid pool in plants. J Exp Bot **64**: 2793–2804

Conklin PL, Norris SR, Wheeler GL, Williams EH, Smirnoff N, Last RL (1999) Genetic evidence for the role of GDP-mannose in plant ascorbic acid (vitamin C) biosynthesis. Proc Natl Acad Sci U S A **96**: 4198–4203

Conklin PL, Pallanca JE, Last RL, Smirnoff N (1997) L-ascorbic acid metabolism in the ascorbate-deficient arabidopsis mutant *vtc1*. Plant Physiol **115**: 1277–1285

Cook DR (1999) *Medicago truncatula* - a model in the making! Curr Opin Plant Biol **2**: 301–304

Cordeiro MA, Moriuchi KS, Fotinos TD, Miller KE, Nuzhdin S., von Wettberg EJ, Cook DR (2014) Population differentiation for germination and early seedling root growth traits under saline conditions in the annual legume *Medicago truncatula* (Fabaceae). Am J Bot **101**: 488–498

Corea ORA, Ki C, Cardenas CL, Kim SJ, Brewer SE, Patten AM, Davin LB, Lewis NG (2012) Arogenate dehydratase isoenzymes profoundly and differentially modulate carbon flux into lignins. J Biol Chem **287**: 11446–11459

Cosgrove DJ (1993) Water uptake by growing cells: an assessment of the controlling roles of wall relaxation, solute uptake, and hydraulic conductance. Int J Plant Sci **154**: 10–21

Cuellar-Ortiz SM, De La Paz Arrieta-Montiel M, Acosta-Gallegos J, Covarrubias AA (2008) Relationship between carbohydrate partitioning and drought resistance in common bean. Plant Cell Environ **31**: 1399–1409

Curi R, Newsholme P, Procopio J, Lagranha C, Gorjão R, Pithon-Curi TC (2007) Glutamine, gene expression, and cell function. Front Biosci 344–357

Dai A (2011) Drought under global warming: a review. Wiley Interdiscip Rev Clim Chang **2**: 45–65

Dakhma WS, Zarrouk M, Cherif A (1995) Effects of drought-stress on lipids in rape leaves. Phytochemistry **40**: 1383–1386

Daryanto S, Wang L, Jacinthe PA (2015) Global synthesis of drought effects on food legume production. PLoS One **10**: e0127401

Davey MW, Bauw G, Montagu M (1996) Analysis of ascorbate in plant tissues by high-performance capillary zone electrophoresis. Anal Biochem **239**: 8–19

Davey MW, Van Montagu M, Inze D, Sanmartin M, Kanellis A, Smirnoff N, Benzie IJJ, Strain JJ, Favell D, Fletcher J (2000) Plant L-ascorbic acid: Chemistry, function, metabolism, bioavailability and effects of processing. J Sci Food Agric **80**: 825–860

Davidson B, Davidson H (1993) Legumes, the Australian experience : the botany, ecology, and agriculture of indigenous and immigrant legumes. Research Studies Press Ltd., Taunton, UK

Debnath M, Pandey M, Bisen PS (2011) An omics approach to understand the plant abiotic stress. Omi A J Integr Biol **15**: 739–762

Dixon RA, Sumner LW (2003) Legume natural products: understanding and manipulating complex pathways for human and animal health. Plant Physiol **131**: 878–885

Dodd IC, Tan LP, He J (2003) Do increases in xylem sap pH and/or ABA concentration mediate stomatal closure following nitrate deprivation? J Exp Bot **54**: 1281–1288

Dowdle J, Ishikawa T, Gatzek S, Rolinski S, Smirnoff N (2007) Two genes in *Arabidopsis thaliana* encoding GDP-l-galactose phosphorylase are required for ascorbate biosynthesis and seedling viability. Plant J **52**: 673–689

Doyle JJ, Luckow MA (2003) The Rest of the iceberg. Legume diversity and evolution in a phylogenetic context. Plant Physiol **131**: 900–910

Durand M, Porcheron B, Hennion N, Maurousset L, Lemoine R, Pourtau N (2016) Water deficit enhances C export to the roots in *A. thaliana* plants with contribution of sucrose transporters in both shoot and roots. Plant Physiol **170**: 1460–1479

Edgerton SA, MacCracken MC, Jacobson MZ, Ayala A, Whitman CE, Trexler MC (2008) Prospects for future climate change and the reasons for early action. J Air Waste Manag Assoc **58**: 735–786

Edmeades GO, Cooper M, Lafitte R, Zinselmeier C, Ribaut JM, Habben JE, Löffler C, Bänziger M (2000) Abiotic stresses and staple crops. Crop Sci. Prog. Prospect. Pap. Present. Third Int. Crop Sci. Congr. CABI, Wallingford, UK, pp 137–154

Ekanayake IJ, Garrity DP, Masajo TM, O'Toole JC (1985) Root pulling resistance in rice: Inheritance and association with drought tolerance. Euphytica **34**: 905–913

Emmert FH (1974) Inhibition of phosphorus and water passage across intact roots by polyethylene glycol and phenylmercuric acetate. Plant Physiol **53**: 663–665

Epron D, Godard D, Cornic G, Genty B (1995) Limitation of net CO_2 assimilation rate by internal resistances to CO_2 transfer in the leaves of two tree species (*Fagus sylvatica* L. and *Castanea sativa* Mill.). Plant, Cell Environ **18**: 43–51

Ernst L, Goodger JQD, Alvarez S, Marsh EL, Berla B, Lockhart E, Jung J, Li P, Bohnert HJ, Schachtman DP (2010) Sulphate as a xylem-borne chemical signal precedes the expression of ABA biosynthetic genes in maize roots. J Exp Bot **61**: 3395–3405

Esau K (1977) Anatomy of seed plants, 2d ed.

Euseda LR, Giskeødegård GF, Bathen TF (2015) Preprocessing of NMR metabolomics data. Scand J Clin Lab Invest **75**:193-203

Evans HJ (1981) Symbiotic nitrogen fixation in legume nodules. TC Moore, Ed, Res. Exp. Plant Physiol. Ed 1.

Evers D, Lefevre I, Legay S, Lamoureux D, Hausman JF, Rosales ROG, Marca LRT, Hoffmann L, Bonierbale M, Schafleitner R (2010) Identification of drought-responsive compounds in potato through a combined transcriptomic and targeted metabolite approach. J Exp Bot **61**: 2327–2343

Farooq M, Hussain M, Wahid A, Siddique KHM (2012) Drought stress in plants: An overview. Plant Responses to Drought Stress From Morphol to Mol Featur. doi: 10.1051/agro:2008021

Farrow SC, Facchini PJ (2014) Functional diversity of 2-oxoglutarate/Fe(II)-dependent dioxygenases in plant metabolism. Front Plant Sci **5**: 524–538

Feller U, Anders I, Demirevska K (2008) Degradation of rubisco and other chloroplast proteins under abiotic stress. Gen Appl Plant Physiol **34**: 5–18

Fernández-Fernández R, López-Martínez JC, Romero-González R, Martínez-Vidal JL, Alarcón Flores MI, Garrido Frenich A (2010) Simple LC–MS determination of citric and malic acids in fruits and vegetables. Chromatographia 72: 55–62

Feussner I, Wasternack C (2002) The lipoxygenase pathway. Annu Rev Plant Biol **53**: 275–297

Fini A, Brunetti C, Di Ferdinando M, Ferrini F, Tattini M (2011) Stress-induced flavonoid biosynthesis and the antioxidant machinery of plants. Plant Signal Behav **6**: 709–711

Fitter A, Williamson L, Linkohr B, Leyser O (2002) Root system architecture determines fitness in an *Arabidopsis* mutant in competition for immobile phosphate ions but not for nitrate ions. Proc R Soc B Biol Sci **269**: 2017–2022

Flexas J, Bota J, Galmés J, Medrano H, Ribas-Carbó M (2006) Keeping a positive carbon balance under adverse conditions: responses of photosynthesis and respiration to water stress. Physiol Plant **127**: 343–352

Flexas J, Galmes J, Ribas-Carbo M, Medrano H (2005) The effects of water stress on plant respiration. Plant Respir. Springer-Verlag, Berlin/Heidelberg, pp 85–94

Flexas J, Ortuño MF, Ribas-Carbo M, Diaz-Espejo A, Flórez-Sarasa ID, Medrano H (2007) Mesophyll conductance to CO_2 in *Arabidopsis thaliana*. New Phytol **175**: 501–511

Forde BG, Lea PJ (2007) Glutamate in plants: metabolism, regulation, and signalling. J Exp Bot **58**: 2339–2358

Fotsing L, Fillet M, Bechet I, Hubert P, Crommen J (1997) Determination of six water-soluble vitamins in a pharmaceutical formulation by capillary electrophoresis. J Pharm Biomed Anal **15**: 1113–1123

Foyer CH, Halliwell B (1976) The presence of glutathione and glutathione reductase in chloroplasts: A proposed role in ascorbic acid metabolism. Planta **133**: 21–25

Foyer CH, Noctor G (2011) Ascorbate and glutathione: the heart of the redox hub. Plant Physiol **155**: 2–18

Freixes S, Thibaud MC, Tardieu F, Muller B (2002) Root elongation and branching is related to local hexose concentration in *Arabidopsis thaliana* seedlings. Plant, Cell Environ **25**: 1357–1366

Fresnillo Fedorenko DE, Fernández OA, Busso CA (1995) The effect of water stress on top and root growth in *Medicago minima*. J Arid Environ **29**: 47–54

Fukunaga K, Fujikawa Y, Esaka M (2010) Light regulation of ascorbic acid biosynthesis in rice via light responsive cis-elements in genes encoding ascorbic acid biosynthetic enzymes. Biosci Biotechnol Biochem **74**: 888–891

Fukushima A, Kusano M, Redestig H, Arita M, Saito K (2009) Integrated omics approaches in plant systems biology. Curr Opin Chem Biol **13**: 532–538

Galvan-Ampudia CS, Testerink C (2011) Salt stress signals shape the plant root. Curr Opin Plant Biol **14**: 296–302

Gálvez L, González EM, Arrese-Igor C (2005) Evidence for carbon flux shortage and strong carbon/nitrogen interactions in pea nodules at early stages of water stress. J Exp Bot **56**: 2551–2561

Gao J, Thelen JJ, Dunker AK, Xu D (2010) Musite, a tool for global prediction of general and kinase-specific phosphorylation sites. Mol Cell Proteomics **9**: 2586–2600

Garg R, Shankar R, Thakkar B, Kudapa H, Krishnamurthy L, Mantri N, Varshney RK, Bhatia S, Jain M (2016) Transcriptome analyses reveal genotype- and developmental stage-specific molecular responses to drought and salinity stresses in chickpea. Sci Rep **6**: 19228–19242

Gargallo-Garriga A, Sardans J, Pérez-Trujillo M, Rivas-Ubach A, Oravec M, Vecerova K, Urban O, Jentsch A, Kreyling J, Beierkuhnlein C, et al (2014) Opposite metabolic responses of shoots and roots to drought. Sci Rep 4: 6829–6835

Gatzek S, Wheeler GL, Smirnoff N (2002) Antisense suppression of l-galactose dehydrogenase in *Arabidopsis thaliana* provides evidence for its role in ascorbate synthesis and reveals light modulated l-galactose synthesis. Plant J **30**: 541–553

Gil-Quintana E, Aldasoro J, Ladrera R, Arrese-Igor C, González EM (2009) Transpiration rate and amino acid distribution in water stressed *Medicago truncatula* plants. Acta Hortic **846**: 339–344

Gil-Quintana E, Larrainzar E, Arrese-Igor C, González EM (2013) Is N-feedback involved in the inhibition of nitrogen fixation in drought-stressed *Medicago truncatula*? J Exp Bot **64**: 281–292

Gil-Quintana E, Lyon D, Staudinger C, Wienkoop S, González EM (2015) *Medicago truncatula* and *Glycine max*: Different drought tolerance and similar local response of the root nodule proteome. J Proteome Res **14**: 5240–5251

Glevarec G, Bouton S, Jaspard E, Riou MT, Cliquet JB, Suzuki A, Limami AM (2004) Respective roles of the glutamine synthetase/glutamate synthase cycle and glutamate dehydrogenase in ammonium and amino acid metabolism during germination and post-germinative growth in the model legume *Medicago truncatula*. Planta **219**: 286–297

Gong L, Zhang H, Gan X, Zhang L, Chen Y, Nie F, Shi L, Li M, Guo Z, Zhang G, et al (2015) Transcriptome profiling of the potato (*Solanum tuberosum* L.) Plant under drought stress and water-stimulus conditions. PLoS One **10**: e0128041

Gonzalez EM, Aparicio-Tejo PM, Gordon AJ, Minchin FR, Royuela M, Arrese-Igor C (1998) Water-deficit effects on carbon and nitrogen metabolism of pea nodules. J Exp Bot **49**: 1705–1714

González EM, Arrese-Igor C, Aparicio-Tejo PM, Royuela M, Koyro HW (2002) Solute heterogeneity and osmotic adjustment in different leaf structures of semi-leafless pea (*Pisum sativum* L.) subjected to water stress. Plant Biol **4**: 558–566

Graham PH, Vance CP (2003) Legumes: importance and constraints to greater use. Plant Physiol **131**: 872–877

Gray SB, Brady SM (2016) Plant developmental responses to climate change. Dev Biol **419**: 64–77

Grebner W, Stingl NE, Oenel A, Mueller MJ, Berger S (2013) Lipoxygenase6-Dependent oxylipin snthesis in roots is required for abiotic and biotic stress resistance of *Arabidopsis*. Plant Physiol **161**: 2159–2170

Greenway H, Munns R (1980) Mechanisms of salt tolerance in nonhalophytes. Annu Rev Plant Physiol **31**: 149–190

Gregory PJ (2006) Plant roots : growth, activity, and interaction with soils. Blackwell Pub, Oxford

Grierson C, Nielsen E, Ketelaarc T, Schiefelbein J (2014) Root hairs. Arab. B. p e0172

Guo L, Yang H, Zhang X, Yang S (2013) Lipid transfer protein 3 as a target of MYB96 mediates freezing and drought stress in *Arabidopsis*. J Exp Bot **64**: 1755–1767

Gupta B, Sengupta A, Saha J, Gupta K (2013) Plant Abiotic Stress:"Omics" Approach. J Plant Biochem Physiol. doi: 10.4172/2329-9029.1000e108

Hancock RD, McRae D, Haupt S, Viola R (2003) Synthesis of L-ascorbic acid in the phloem. BMC Plant Biol **3**: 7–19

Handa S, Bressan RA, Handa AK, Carpita NC, Hasegawa PM (1983) Solutes contributing to osmotic adjustment in cultured plant cells adapted to water stress. Plant Physiol **73**: 834–843

Hare PD, Cress WA, Van Staden J (1998) Dissecting the roles of osmolyte accumulation during stress. Plant, Cell Environ **21**: 535–553

Häusler RE, Ludewig F, Krueger S (2014) Amino acids – A life between metabolism and signaling. Plant Sci **229**: 225–237

Herrero-Martínez JM, Simó-Alfonso E, Deltoro VI, Calatayud A, Ramis-Ramos G (1998) Determination of l-Ascorbic Acid and total ascorbic acid in vascular and nonvascular plants by capillary zone electrophoresis. Anal Biochem **265**: 275–281

Hilbert D, Canadell J (1995) Biomass partitioning and resource allocation of plants from mediterranean-type ecosystems: possible responses to elevated atmospheric CO_2. *In* JM Moreno, WC Oechel, eds, Glob. Chang. Mediterr. Ecosyst. Springer New York, New York, NY, pp 76–101

Hildebrandt TM, Nunes Nesi A, Araújo WL, Braun HP (2015) Amino acid catabolism in plants. Mol Plant **8**: 1563–1579

Himmelbauer ML, Loiskandl W, Kastanek F (2004) Estimating length, average diameter and surface area of roots using two different Image analyses systems. Plant Soil **260**: 111–120

Hirt H, Shinozaki K (2004) Plant responses to abiotic stress. Springer

Hochberg U, Degu A, Toubiana D, Gendler T, Nikoloski Z, Rachmilevitch S, Fait A (2013) Metabolite profiling and network analysis reveal coordinated changes in grapevine water stress response. BMC Plant Biol **13**: 184

Hodge A, Berta G, Doussan C, Merchan F, Crespi M (2009) Plant root growth, architecture and function. Plant Soil **321**: 153–187

Hodges DM, DeLong JM, Forney CF, Prange RK (1999) Improving the thiobarbituric acid-reactive-substances assay for estimating lipid peroxidation in plant tissues containing anthocyanin and other interfering compounds. Planta **207**: 604–611

Hong Y, Zhang W, Wang X (2010) Phospholipase D and phosphatidic acid signalling in plant response to drought and salinity. Plant Cell Environ **33**: 627–635

van der Hoorn RAL (2008) Plant proteases: from phenotypes to molecular mechanisms. Annu Rev Plant Biol **59**: 191–223

Horgan RP, Kenny LC (2011) "Omic" technologies: genomics, transcriptomics, proteomics and metabolomics. Obstet Gynaecol **13**: 189–195

Hossain MS, Joshi T, Stacey G (2015) System approaches to study root hairs as a single cell plant model: current status and future perspectives. Front Plant Sci **6**: 1–7

Hsiao TC (1973) Plant responses to water stress. Ann Rev Plant Physiol **24**: 519–570

Huhman D, Berhow MA, Sumner LW (2005) Quantification of saponins in aerial and subterranean tissues of *Medicago truncatula*. J Agric Food Chem **53**: 1914–1920

Huhman D, Sumner LW (2002) Metabolic profiling of saponins in *Medicago sativa* and *Medicago truncatula* using HPLC coupled to an electrospray ion-trap mass spectrometer. Phytochemistry **59**: 347–360

Irar S, González EM, Arrese-Igor C, Marino D (2014) A proteomic approach reveals new actors of nodule response to drought in split-root grown pea plants. Physiol Plant **152**: 634–645

Irizarry RA, Hobbs B, Collin F, Beazer-Barclay YD, Antonellis KJ, Scherf U, Speed TP (2003) Exploration, normalization, and summaries of high density oligonucleotide array probe level data. Biostatistics **4**: 249–264

Ishikawa H, Evans ML (1995) Specialized zones of development in roots. Plant Physiol **109**: 725–727

Jauregui I, Aparicio-Tejo PM, Avila C, Cañas R, Sakalauskiené S, Aranjuelo I (2016) Root-shoot interactions explain the reduction of leaf mineral content in *Arabidopsis* plants grown under elevated [CO_2] conditions. Physiol Plant **158**: 65–79

Jin K, Shen J, Ashton RW, Dodd IC, Parry MAJ, Whalley WR (2013) How do roots elongate in a structured soil ? **64**: 4761–4777

Joshi R, Wani SH, Singh B, Bohra A, Dar ZA, Lone AA, Pareek A, Singla-Pareek SL (2016) Transcription factors and plants response to drought stress: Current understanding and future directions. Front Plant Sci **7**: 1029

Joshi T, Fitzpatrick MR, Chen S, Liu Y, Zhang H, Endacott RZ, Gaudiello EC, Stacey G, Nguyen HT, Xu D (2014) Soybean knowledge base (SoyKB): a web resource for integration of soybean translational genomics and molecular breeding. Nucleic Acids Res **42**: D1245-52

Kan CC, Chung TY, Juo YA, Hsieh MH (2015) Glutamine rapidly induces the expression of key transcription factor genes involved in nitrogen and stress responses in rice roots. BMC Genomics **16**: 731–745

Kanehisa M, Goto S (2000) KEGG: kyoto encyclopedia of genes and genomes. Nucleic Acids Res **28**: 27–30

Kanehisa M, Sato Y, Kawashima M, Furumichi M, Tanabe M (2015) KEGG as a reference resource for gene and protein annotation. Nucleic Acids Res **44**: 457–462

Kang Y, Sakiroglu M, Krom N, Stanton-Geddes J, Wang M, Lee YC, Young ND, Udvardi M (2015) Genome-wide association of drought-related and biomass traits with HapMap SNPs in *Medicago truncatula*. Plant Cell Environ **38**: 1997–2011

Kashiwagi J, Krishnamurthy L, Purushothaman R, Upadhyaya HD, Gaur PM, Gowda CLL, Ito O, Varshney RK (2015) Scope for improvement of yield under drought through the root traits in chickpea (*Cicer arietinum* L.). F Crop Res **170**: 47–54

Kavi Kishor PB, Hima Kumari P, Sunita MSL, Sreenivasulu N (2015) Role of proline in cell wall synthesis and plant development and its implications in plant ontogeny. Front Plant Sci **6**: 544–560

Kaya MD, Okçu G, Atak M, Çıkılı Y, Kolsarıcı Ö (2006) Seed treatments to overcome salt and drought stress during germination in sunflower (*Helianthus annuus* L.). Eur J Agron **24**: 291–295

Kim JS, Jung HJ, Lee HJ, Kim KA, Goh CH, Woo Y, Oh SH, Han YS, Kang H (2008) Glycine-rich RNA-binding protein 7 affects abiotic stress responses by regulating stomata opening and closing in *Arabidopsis thaliana*. Plant J **55**: 455–466

Kohli A, Narciso JO, Miro B, Raorane M (2012) Root proteases: reinforced links between nitrogen uptake and mobilization and drought tolerance. Physiol Plant **145**: 165–179

Körner C (2015) Paradigm shift in plant growth control. Curr Opin Plant Biol **25**: 107–114

Krasensky J, Jonak C (2012) Drought, salt, and temperature stress-induced metabolic rearrangements and regulatory networks. J Exp Bot **63**: 1593–1608

Kryvoruchko IS, Sinharoy S, Torres-Jerez I, Sosso D, Pislariu CI, Guan D, Murray J, Benedito VA, Frommer WB, Udvardi MK (2016) MtSWEET11, a nodule-specific sucrose transporter of *Medicago truncatula*. Plant Physiol 171: 554–565

Kutchan TM (1995) Alkaloid biosynthesis-The basis for metabolic engineering of medicinal plants. Plant Cell **7**: 1059–1070

Labhilili M, Joudrier P, Gautier MF (1995) Characterization of cDNAs encoding *Triticum durum* dehydrins and their expression patterns in cultivars that differ in drought tolerance. Plant Sci **112**: 219–230

Larrainzar E, Molenaar JA, Wienkoop S, Gil-Quintana E, Alibert B, Limami AM, Arrese-Igor C, González EM (2014) Drought stress provokes the down-regulation of methionine and ethylene biosynthesis pathways in *Medicago truncatula* roots and nodules. Plant Cell Environ **37**: 2051–2063

Larrainzar E, Wienkoop S, Scherling C, Kempa S, Ladrera R, Arrese-Igor C, Weckwerth W, González EM (2009) Carbon metabolism and bacteroid functioning are involved in the regulation of nitrogen fixation in *Medicago truncatula* under drought and recovery. Mol Plant Microbe Interact **22**: 1565–1576

Larrainzar E, Wienkoop S, Weckwerth W, Ladrera R, Arrese-Igor C, González EM (2007) *Medicago truncatula* root nodule proteome analysis reveals differential plant and bacteroid responses to drought stress. Plant Physiol **144**: 1495–1507

Lawlor D (1970) Absorption of polyethylene glycols by plants and their effects on plant growth. New Phytol **69**: 501–513

Lawlor DW, Cornic G (2002) Photosynthetic carbon assimilation and associated metabolism in relation to water deficits in higher plants. Plant Cell Environ **25**: 275–294

Lawlor DW, Tezara W (2009) Causes of decreased photosynthetic rate and metabolic capacity in water-deficient leaf cells: A critical evaluation of mechanisms and integration of processes. Ann Bot **103**: 561–579

Lee BR, Jin YL, Jung WJ, Avice JC, Morvan-Bertrand A, Ourry A, Park CW, Kim TH (2008) Water-deficit accumulates sugars by starch degradation--not by *de novo* synthesis--in white clover leaves (*Trifolium repens*). Physiol Plant **134**: 403–411

Lee BR, Zaman R, Avice JC, Ourry A, Kim TH (2016) Sulfur use efficiency is a significant determinant of drought stress tolerance in relation to photosynthetic activity in *Brassica napus* cultivars. Front Plant Sci **7**: 1–11

Lemoine R, La Camera S, Atanassova R, Dédaldéchamp F, Allario T, Pourtau N, Bonnemain JL, Laloi M, Coutos-Thévenot P, Maurousset L, et al (2013) Source-to-sink transport of sugar and regulation by environmental factors. Front Plant Sci 4: 272–292

Lesins KA, Lesins I (1979) Genus *Medicago* (Leguminosae) A taxogenetic study. doi: 10.1007/978-94-009-9634-2_1

Li C, Wong WH (2001) Model-based analysis of oligonucleotide arrays: expression index computation and outlier detection. Proc Natl Acad Sci U S A **98**: 31–36

Li L, Cheng H, Gai J, Yu D (2007) Genome-wide identification and characterization of putative cytochrome P450 genes in the model legume *Medicago truncatula*. Planta **226**: 109–123

Li R, Zeng Y, Xu J, Wang Q, Wu F, Cao M, Lan H, Liu Y, Lu Y (2015) Genetic variation for maize root architecture in response to drought stress at the seedling stage. Breed Sci **65**: 298–307

Liew LC, Singh MB, Bhalla PL (2014) Unique and conserved features of floral evocation in legumes. J Integr Plant Biol **56**: 714–728

Linster CL, Clarke SG (2008) L-Ascorbate biosynthesis in higher plants: the role of VTC2. Trends Plant Sci **13**: 567–573

Liso R, De Tullio MC, Ciraci S, Balestrini R, La Rocca N, Bruno L, Chiappetta A, Bitonti MB, Bonfante P, Arrigoni O (2004) Localization of ascorbic acid, ascorbic acid oxidase, and glutathione in roots of *Cucurbita maxima* L. J Exp Bot **55**: 2589–2597

Liu HS, Li FM (2005) Root respiration, photosynthesis and grain yield of two spring wheat in response to soil drying. Plant Growth Regul **46**: 233–240

Liu JH, Wang W, Wu H, Gong X, Moriguchi T (2015a) Polyamines function in stress tolerance: from synthesis to regulation. Front Plant Sci **6**: 827–836

Liu M, Li M, Liu K, Sui N (2015b) Effects of drought stress on seed germination and seedling growth of different maize varieties. J Agric Sci **7**: 231–240

Livak KJ, Schmittgen TD (2001) Analysis of relative gene expression data using real-time quantitative PCR and the 2(-Delta Delta C(T)) Method. Methods **25**: 402–408

Lloret F, Casanovas C, Penuelas J (1999) Seedling survival of Mediterranean shrubland species in relation to root:shoot ratio, seed size and water and nitrogen use. Funct Ecol **13**: 210–216

Lobet G, Pages L, Draye X (2011) A novel image-analysis toolbox enabling quantitative analysis of root system architecture. Plant Physiol **157**: 29–39

López-Bucio J, Cruz-Ramírez A, Herrera-Estrella L (2003) The role of nutrient availability in regulating root architecture. Curr Opin Plant Biol **6**: 280–287

Lugan R, Niogret MF, Leport L, Guégan JP, Larher FR, Savouré A, Kopka J, Bouchereau A (2010) Metabolome and water homeostasis analysis of *Thellungiella salsuginea* suggests that dehydration tolerance is a key response to osmotic stress in this halophyte. Plant J **64**: 215–229

Luo Y, Bo Liu Y, Xiu Dong Y, Gao XQ, Sheng Zhang X (2009) Expression of a putative alfalfa helicase increases tolerance to abiotic stress in *Arabidopsis* by enhancing the capacities for ROS scavenging and osmotic adjustment. J Plant Physiol **166**: 385–394

Lyon D, Castillejo MA, Mehmeti-Tershani V, Staudinger C, Kleemaier C, Wienkoop S (2016) Drought and recovery: independently regulated processes highlighting the importance of protein turnover dynamics and translational regulation in *Medicago truncatula*. Mol Cell Proteomics **15**: 1921–1937

Maalekuu K, Elkind Y, Leikin-Frenkel A, Lurie S, Fallik E (2006) The relationship between water loss, lipid content, membrane integrity and LOX activity in ripe pepper fruit after storage. Postharvest Biol Technol **42**: 248–255

Maeda H, Dudareva N (2012) The shikimate pathway and aromatic amino acid biosynthesis in plants. Annu Rev Plant Biol **63**: 73–105

Malamy JE (2005) Intrinsic and environmental response pathways that regulate root system architecture. Plant, Cell Environ **28**: 67–77

Malone JH, Oliver B (2011) Microarrays, deep sequencing and the true measure of the transcriptome. BMC Biol **9**: 34–42

Maloney GS, DiNapoli KT, Muday GK (2014) The anthocyanin reduced tomato mutant demonstrates the role of flavonols in tomato lateral root and root hair development. Plant Physiol **166**: 614–631

Mangeon A, Magioli C, Menezes-Salgueiro AD, Cardeal V, de Oliveira C, Galvão VC, Margis R, Engler G, Sachetto-Martins G (2009) AtGRP5, a vacuole-located glycine-rich protein involved in cell elongation. Planta 230: 253–265

Marino D, Frendo P, Ladrera R, Zabalza A, Puppo A, Arrese-Igor C, González EM (2007) Nitrogen fixation control under drought stress. Localized or systemic? Plant Physiol **143**: 1968–1974

Marino D, Pucciariello C, Puppo A, Frendo P (2009) The redox state, a referee of the legume–rhizobia symbiotic game. Adv Bot Res **52**: 115–151

Marrs KA (1996) The functions and regulation of glutathione s-transferases in plants. Annu Rev Plant Physiol Plant Mol Biol **47**: 127–158

Maruta T, Yonemitsu M, Yabuta Y, Tamoi M, Ishikawa T, Shigeoka S (2008) *Arabidopsis* phosphomannose isomerase 1, but not phosphomannose isomerase 2, is essential for ascorbic acid biosynthesis. J Biol Chem **283**: 28842–28851

Matamoros MA, Fernández-García N, Wienkoop S, Loscos J, Saiz A, Becana M (2013) Mitochondria are an early target of oxidative modifications in senescing legume nodules. New Phytol **197**: 873–885

Matamoros MA, Loscos J, Coronado MJ, Ramos J, Sato S, Testillano PS, Tabata S, Becana M (2006) Biosynthesis of ascorbic acid in legume root nodules. Plant Physiol 141: 1068–1077

Materechera SA, Dexter AR, Alston AM (1991) Penetration of very strong soils by seedling roots of different plant species. Plant Soil **135**: 31–41

Matsui K, Fukutomi S, Ishii M, Kajiwara T (2004) A tomato lipase homologous to DAD1 (LeLID1) is induced in post-germinative growing stage and encodes a triacylglycerol lipase. FEBS Lett **569**: 195–200

Matsuo N, Takahashi M, Fukami K, Tsuchiya S, Tasaka K (2013) Root growth of two soybean [*Glycine max* (L.) Merr.] cultivars grown under different groundwater level conditions. Plant Prod Sci **16**: 374–382

Maurel C, Verdoucq L, Luu DT, Santoni V (2008) Plant Aquaporins: membrane channels with multiple integrated functions. Annu Rev Plant Biol **59**: 595–624

McMichael BL, Burke JJ, Berlin JD, Hatfield JL, Quisenberry JE (1985) Root vascular bundle arrangements among cotton strains and cultivars. Environ Exp Bot **25**: 23–30

Medrano H, Escalona JM, Bota J, Gulías J, Flexas J (2002) Regulation of photosynthesis of C3 plants in response to progressive drought: Stomatal conductance as a reference parameter. Ann Bot **89**: 895–905

Meeks M, Murray S, Hague S, Hays D (2013) Measuring maize seedling drought response in search of tolerant germplasm. Agronomy **3**: 135–147

Mexal J, Fisher JT, Osteryoung J, Reid CP (1975) Oxygen availability in polyethylene glycol solutions and its implications in plant-water relations. Plant Physiol **55**: 20–24

Michaud R, Lehman WF, Rumbaugh MD (1988) Alfalfa and alfalfa improvement. Alfalfa Alfalfa Improv. doi: 10.2134/agronmonogr29.c2

Micheletto S, Rodriguez-Uribe L, Hernandez R, Richins RD, Curry J, O'Connell MA (2007) Comparative transcript profiling in roots of *Phaseolus acutifolius* and *P. vulgaris* under water deficit stress. Plant Sci **173**: 510–520

Mikami K, Murata N (2003) Membrane fluidity and the perception of environmental signals in cyanobacteria and plants. Prog Lipid Res **42**: 527–543

Millar AH, Mittova V, Kiddle G, Heazlewood JL, Bartoli CG, Theodoulou FL, Foyer CH (2003) Control of ascorbate synthesis by respiration and its implications for stress responses. Plant Physiol **133**: 443–447

Miller AJ, Fan X, Shen Q, Smith SJ (2007) Amino acids and nitrate as signals for the regulation of nitrogen acquisition. J Exp Bot **59**: 111–119

Mittler R (2002) Oxidative stress, antioxidants and stress tolerance. Trends Plant Sci **7**: 405–410

Mittler R, Vanderauwera S, Gollery M, Van Breusegem F (2004) Reactive oxygen gene network of plants. Trends Plant Sci **9**: 490–498

Mizoi J, Shinozaki K, Yamaguchi-Shinozaki K (2012) AP2/ERF family transcription factors in plant abiotic stress responses. Biochim Biophys Acta **1819**: 86–96

Mohammadkhani N, Heidari R (2008) Drought-induced accumulation of soluble sugars and proline in two maize varieties. World Appl Sci J 3 **3**: 448–453

Moles AT, Westoby M (2004) What do seedlings die from and what are the implications for evolution of seed size? Oikos **106**: 193–199

Moran J, Becana M, Iturbe-Ormaetxe I, Frechilla S, Klucas R, Aparicio-Tejo P (1994) Drought induces oxidative stress in pea plants. Planta 194: 346–352

Morgan CL, Austin RB (1983) Respiratory loss of recently assimilated carbon in wheat. Ann Bot **51**: 85–95

Morgan J (2003) Plants, osmotic adjustment, In : Encyclopedia of Water Science. CRC Press, New York

Moschou PN, Paschalidis KA, Delis ID, Andriopoulou AH, Lagiotis GD, Yakoumakis DI, Roubelakis-Angelakis KA (2008) Spermidine exodus and oxidation in the apoplast induced by abiotic stress is responsible for H_2O_2 signatures that direct tolerance responses in Tobacco. Plant Cell **20**: 1708–1724

Mosolov VV, Valueva TA (2011) Inhibitors of proteolytic enzymes under abiotic stresses in plants. Appl Biochem Microbiol **47**: 453–459

Muller B, Pantin F, Génard M, Turc O, Freixes S, Piques M, Gibon Y (2011) Water deficits uncouple growth from photosynthesis, increase C content, and modify the relationships between C and growth in sink organs. J Exp Bot **62**: 1715–1729

Muller B, Stosser M, Tardieu F (1998) Spatial distributions of tissue expansion and cell division rates are related to irradiance and to sugar content in the growing zone of maize roots. Plant, Cell Environ **21**: 149–158

Munné-Bosch S, Alegre L (2003) Drought-induced changes in the redox state of alpha-tocopherol, ascorbate, and the diterpene carnosic acid in chloroplasts of Labiatae species differing in carnosic acid contents. Plant Physiol **131**: 1816–1825

Munns R, Brady C, Barlow E (1979) Solute accumulation in the apex and leaves of wheat during water stress. Aust J Plant Physiol **6**: 379–389

Munns R, Tester M (2008) Mechanisms of salinity tolerance. Annu Rev Plant Biol **59**: 651–681

Nagalakshmi U, Waern K, Snyder M (2010) RNA-Seq: A method for comprehensive transcriptome analysis. Curr. Protoc. Mol. Biol. John Wiley & Sons, Inc., Hoboken, NJ, USA, p 89:II:4.11:4.11.1–4.11.13.

Naya L, Ladrera R, Ramos J, González EM, Arrese-Igor C, Minchin FR, Becana M (2007) The response of carbon metabolism and antioxidant defenses of alfalfa nodules to drought stress and to the subsequent recovery of plants. Plant Physiol **144**: 1104–1114

Nelson D, Werck-Reichhart D (2011) A P450-centric view of plant evolution. Plant J **66**: 194–211

Nielsen KA, Møller BL (2005) Cytochrome P450s in Plants. *In* PRO de Montellano, ed, Cytochrome P450 Struct. Mech. Biochem., Springer U. Kluwer Academic/Plenum Publishers, New York, pp 553–583

Noctor G, Foyer CH (1998) Ascorbate and gluthatione: keeping active oxygen under control. Annu Rev Plant Physiol Plant Mol Biol **49**: 249–279

Nunes C, de Sousa Araújo S, da Silva JM, Fevereiro MPS, da Silva AB (2008) Physiological responses of the legume model *Medicago truncatula* cv. Jemalong to water deficit. Environ Exp Bot **63**: 289–296

Ober ES, Sharp RE (2007) Regulation of root growth responses to water deficit. *In* MA Jenks, PM Hasegawa, SM Jain, eds, Adv. Mol. Breed. Towar. Drought Salt Toler. Crop., Springer N. Springer Netherlands, Dordrecht, pp 33–53

Okçu G, Kaya MD, Atak M (2005) Effects of salt and drought stresses on germination and seedling growth of Pea (*Pisum sativum* L.). Turk J Agric For **29**: 237–242

de Ollas C, Arbona V, Gómez-Cadenas A (2015) Jasmonoyl isoleucine accumulation is needed for abscisic acid build-up in roots of *Arabidopsis* under water stress conditions. Plant, Cell Environ **38**: 2157–2170

Opitz N, Marcon C, Paschold A, Malik WA, Lithio A, Brandt R, Piepho HP, Nettleton D, Hochholdinger F (2015) Extensive tissue-specific transcriptomic plasticity in maize primary roots upon water deficit. J Exp Bot **67**: 1095–1107

Osorio S, Ruan YL, Fernie AR (2014) An update on source-to-sink carbon partitioning in tomato. Front Plant Sci **5**: 516–526

Pacheco-Villalobos D, Hardtke CS (2012) Natural genetic variation of root system architecture from *Arabidopsis* to *Brachypodium*: towards adaptive value. Philos Trans R Soc Lond B Biol Sci **367**: 1552–1558

Padilla FM, Pugnaire FI (2007) Rooting depth and soil moisture control Mediterranean woody seedling survival during drought. Funct Ecol **21**: 489–495

Paez-Garcia A, Motes C, Scheible WR, Chen R, Blancaflor E, Monteros M (2015) Root Traits and Phenotyping Strategies for Plant Improvement. Plants **4**: 334–355

Pagnussat LA, Oyarburo N, Cimmino C, Pinedo ML, de la Canal L (2015) On the role of a Lipid-Transfer Protein. *Arabidopsis* ltp3 mutant is compromised in germination and seedling growth. Plant Signal Behav **10**: e1105417

Pan Y, Michael TP, Hudson ME, Kay SA, Chory J, Schuler MA (2009) Cytochrome P450 monooxygenases as reporters for circadian-regulated pathways. Plant Physiol **150**: 858–878

Peoples MB, Baldock JA, Peoples MB, Baldock JA (2001) Nitrogen dynamics of pastures: nitrogen fixation inputs, the impact of legumes on soil nitrogen fertility, and the contributions of fixed nitrogen to Australian farming systems. Aust J Exp Agric **41**: 327–346

Peterson C, Murrmann M, Steudle E (1993) Location of the major barriers to water and ion movement in young roots of *Zea mays* L. Planta **190**: 127–136

Petti C, Shearer A, Tateno M, Ruwaya M, Nokes S, Brutnell T, Debolt S (2013) Comparative feedstock analysis in *Setaria viridis* L. as a model for C4 bioenergy grasses and Panicoid crop species. Front Plant Sci **4**: 181

Phan HTT, Ellwood SR, Hane JK, Ford R, Materne M, Oliver RP (2007) Extensive macrosynteny between *Medicago truncatula* and *Lens culinaris* ssp. *culinaris*. Theor Appl Genet **114**: 549–558

Pinheiro C, Passarinho JA, Ricardo CP (2004) Effect of drought and rewatering on the metabolism of *Lupinus albus* organs. J Plant Physiol **161**: 1203–1210

Planchet E, Rannou O, Ricoult C, Boutet-Mercey S, Maia-Grondard A, Limami AM (2011) Nitrogen metabolism responses to water deficit act through both abscisic acid (ABA)-dependent and independent pathways in *Medicago truncatula* during post-germination. J Exp Bot **62**: 605–615

Planchet E, Verdu I, Delahaie J, Cukier C, Girard C, Morere-Le Paven MC, Limami AM (2014) Abscisic acid-induced nitric oxide and proline accumulation in independent pathways under water-deficit stress during seedling establishment in *Medicago truncatula*. J Exp Bot **65**: 2161–2170

Plaut Z, Federman E (1985) A simple procedure to overcome polyethelene glycol toxicity on whole plants. Plant Physiol **79**: 559–561

Popelka JC, Terryn N, Higgins T (2004) Gene technology for grain legumes: can it contribute to the food challenge in developing countries? Plant Sci **167**: 195–206

Porta H, Rocha-Sosa M (2002) Plant lipoxygenases. Physiological and molecular features. Plant Physiol **130**: 15–21

Porta H, Rueda-Benítez P, Campos F, Colmenero-Flores JM, Colorado JM, Carmona MJ, Covarrubias AA, Rocha-Sosa M (1999) Analysis of lipoxygenase mRNA accumulation in the common bean (*Phaseolus vulgaris* L.) during development and under stress conditions. Plant Cell Physiol **40**: 850–858

Pratap A, Kumar J (2011) Biology and breeding of food legumes. Wallingford, UK: CABI

Qin X, Zeevaart JAD (2002) Overexpression of a 9-cis-epoxycarotenoid dioxygenase gene in *Nicotiana plumbaginifolia* increases abscisic acid and phaseic acid levels and enhances drought tolerance. Plant Physiol **128**: 544–551

Qiu L, Chang R (2010) The origin and history of soybean. *In* G Singh, ed, soybean Bot. Prod. uses. CABI, Wallingford, pp 1–23

Quero G, Gutíerrez L, Lascano R, Monza J, Sandal N, Borsani O (2014) Identification of QTLs for shoot and root growth under ionic–osmotic stress in Lotus, using a RIL population. Crop Pasture Sci **65**: 139–149

Rabino I, Mancinelli AL (1986) Light, temperature, and anthocyanin production. Plant Physiol **81**: 922–924

Racchi LM (2013) Antioxidant defenses in plants with attention to *Prunus* and *Citrus* spp. Antioxidants **2**: 340–369

Rahoui S, Ben C, Chaoui A, Martinez Y, Yamchi A, Rickauer M, Gentzbittel L, El Ferjani E (2014) Oxidative injury and antioxidant genes regulation in cadmium-exposed radicles of six contrasted *Medicago truncatula* genotypes. Environ Sci Pollut Res Int **21**: 8070–8083

Ramos J, Bisseling T (2003) A method for the isolation of root hairs from the model legume *Medicago truncatula*. J Exp Bot **54**: 2245–2250

Ranjan A, Pandey N, Lakhwani D, Dubey NK, Pathre U, Sawant S (2012) Comparative transcriptomic analysis of roots of contrasting *Gossypium herbaceum* genotypes revealing adaptation to drought. BMC Genomics **13**: 680–701

Rellán-Álvarez R, Lobet G, Lindner H, Pradier PL, Sebastian J, Yee MC, Geng Y, Trontin C, LaRue T, Schrager-Lavelle A, et al (2015) GLO-Roots: an imaging platform enabling multidimensional characterization of soil-grown root systems. Elife **4**: 393–399

Rhodes D, Handa S, Bressan RA (1986) Metabolic changes associated with adaptation of plant cells to water stress. Plant Physiol **82**: 890–903

Ribaut J (2008) Drought Adaptation in Cereals. CRC Press

Rigaud J, Puppo A (1975) Indole-3-acetic acid catabolism by soybean bacteroids. J Gen Microbiol **88**: 223–228

Robinson JM, Bunce JA (2000) Influence of drought-induced water stress on soybean and spinach leaf ascorbate-dehydroascorbate level and redox status. Int J Plant Sci **161**: 271–279

Roulin A, Auer PL, Libault M, Schlueter J, Farmer A, May G, Stacey G, Doerge RW, Jackson SA (2013) The fate of duplicated genes in a polyploid plant genome. Plant J 73: 143–153

Rozema J, Flowers T (2008) Ecology. Crops for a salinized world. Science **322**: 1478–1480

Sack L, Tyree MT, Holbrook NM (2005) Leaf hydraulic architecture correlates with regeneration irradiance in tropical rainforest trees. New Phytol **167**: 403–413

Sassi S, Aydi S, Hessini K, Gonzalez EM, Arrese-Igor C, Abdelly C (2010) Long-term mannitol-induced osmotic stress leads to stomatal closure, carbohydrate accumulation and changes in leaf elasticity in *Phaselous vulgaris* leaves. African J Biotechnol **9**: 6061–6069

Sauviac L, Niebel A, Boisson-Dernier A, Barker DG, De Carvalho-Niebel F (2005) Transcript enrichment of Nod factor-elicited early nodulin genes in purified root hair fractions of the model legume *Medicago truncatula*. J Exp Bot **56**: 2507–2513

Schenk HJ, Jackson RB (2002) Rooting depths, lateral root spreads and below-ground/above-ground allometries of plants in water-limited ecosystems. J Ecol **90**: 480–494

Schmutz J, Cannon SB, Schlueter J, Ma J, Mitros T, Nelson W, Hyten DL, Song Q, Thelen JJ, Cheng J, et al (2010) Genome sequence of the palaeopolyploid soybean. Nature 463: 178–183

Scholander PF, Bradstreet ED, Hammel HT, Hemmingsen EA (1966) Sap concentrations in halophytes and some other plants. Plant Physiol **41**: 529–532

Schuler MA (1996) The role of cytochrome P450 monooxygenases in plant-insect interactions. Plant Physiol **112**: 1411–1419

Schupp EW, Fuentes M (1995) Spatial patterns of seed dispersal and the unification of plant population ecology. Écoscience **2**: 267–275

Seo PJ, Lee SB, Suh MC, Park MJ, Go YS, Park CM (2011) The MYB96 transcription factor regulates cuticular wax biosynthesis under drought conditions in *Arabidopsis*. Plant Cell **23**: 1138–1152

Sharoni AM, Nuruzzaman M, Satoh K, Moumeni A, Attia K, Venuprasad R, Serraj R, Kumar A, Leung H, Islam Akmr, et al (2012) Comparative transcriptome analysis of AP2/EREBP gene family under normal and hormone treatments, and under two drought stresses in NILs setup by Aday Selection and IR64. Mol Genet Genomics **287**: 1–19

Sharp RE (2002) Interaction with ethylene: changing views on the role of abscisic acid in root and shoot growth responses to water stress. Plant Cell Environ **25**: 211–222

Sharp RE, Davies WJ (1989) Regulation of growth and development of plants growing with a restricted supply of water. *In* H Jones, T Flowers, M Jones, eds, Plant under Stress. Cambridge, pp 71–93

Sharp RE, Poroyko V, Hejlek LG, Spollen WG, Springer GK, Bohnert HJ, Nguyen HT (2004) Root growth maintenance during water deficits: physiology to functional genomics. J Exp Bot **55**: 2343–2351

Sharp RE, Silk WK, Hsiao TC (1988) Growth of the maize primary root at low water potentials : I. Spatial distribution of expansive growth. Plant Physiol **87**: 50–57

Shi H, Ye T, Chen F, Cheng Z, Wang Y, Yang P, Zhang Y, Chan Z (2013) Manipulation of arginase expression modulates abiotic stress tolerance in *Arabidopsis*: effect on arginine metabolism and ROS accumulation. J Exp Bot **64**: 1367–1379

Shu Y, Liu Y, Zhang J, Song L, Guo C (2016) Genome-Wide analysis of the AP2/ERF superfamily genes and their responses to abiotic stress in *Medicago truncatula.* Front Plant Sci **6**: 1247–1263

Siddique MRB, Hamid A, Islam MS (2000) Drought stress effects on water relations of wheat. Bot Bull Acad Sin **41**: 35–39

Silva-Navas J, Moreno-Risueno MA, Manzano C, Pallero-Baena M, Navarro-Neila S, Téllez-Robledo B, Garcia-Mina JM, Baigorri R, Gallego FJ, del Pozo JC (2015) D-Root: a system for cultivating plants with the roots in darkness or under different light conditions. Plant J 84: 244–255

Singh D, Laxmi A (2015) Transcriptional regulation of drought response: a tortuous network of transcriptional factors. Front Plant Sci **6**: 1–11

Smirnoff N, Wheeler GL (2000) Ascorbic acid in plants: biosynthesis and function. Crit Rev Biochem Mol Biol **35**: 291–314

Song L, Prince S, Valliyodan B, Joshi T, Maldonado Dos Santos J, Wang J, Lin L, Wan J, Wang Y, Xu D, et al (2016) Genome-wide transcriptome analysis of soybean primary root under varying water-deficit conditions. BMC Genomics **17**: 57–73

Spomer LA, Smith M (1996) Direct measurement of water availability in gelled plant tissue culture media. In Vitro Cell Dev Biol Plant.**32**: 210–215

Stacey G, Vodkin L, Parrott WA, Shoemaker RC (2004) National Science Foundation-sponsored workshop report. Draft plan for soybean genomics. Plant Physiol **135**: 59–70

Staszków A, Swarcewicz B, Banasiak J, Muth D, Jasiński M, Stobiecki M (2011) LC/MS profiling of flavonoid glycoconjugates isolated from hairy roots, suspension root cell cultures and seedling roots of *Medicago truncatula*. Metabolomics **7**: 604–613

Staudinger C, Mehmeti V, Turetschek R, Lyon D, Egelhofer V, Wienkoop S (2012) Possible role of nutritional priming for early salt and drought stress responses in *Medicago truncatula*. Front Plant Sci **3**: 285–297

Stepansky A, Leustek T (2006) Histidine biosynthesis in plants. Amino Acids **30**: 127–142

Steudle E, Peterson CA (1998) How does water get through roots? J Exp Bot **49**: 775–788

Steyn WJ, Wand SJE, Holcroft DM, Jacobs G (2002) Anthocyanins in vegetative tissues: a proposed unified function in photoprotection. New Phytol **155**: 349–361

Subudhi PK (2011) Omics approaches for abiotic stress tolerance in plants. Omi Plant Abiotic Stress Toler. doi: 10.2174/97816080505811110101

Sulpice R, Pyl ET, Ishihara H, Trenkamp S, Steinfath M, Witucka-Wall H, Gibon Y, Usadel B, Poree F, Piques MC, et al (2009) Starch as a major integrator in the regulation of plant growth. Proc Natl Acad Sci U S A 106: 10348–10353

Suzuki H, Achnine L, Xu R, Matsuda SPT, Dixon RA (2002) A genomics approach to the early stages of triterpene saponin biosynthesis in *Medicago truncatula*. Plant J **32**: 1033–1048

Szabados L, Savouré A (2010) Proline: a multifunctional amino acid. Trends Plant Sci **15**: 89–97

Szarka A, Bánhegyi G, Asard H (2013) The inter-relationship of ascorbate transport, metabolism and mitochondrial, plastidic respiration. Antioxid Redox Signal **19**: 1036–1044

Szarka A, Tomasskovics B, Bánhegyi G (2012) The ascorbate-glutathione-α-tocopherol triad in abiotic stress response. Int J Mol Sci **13**: 4458–4483

Taiz L, Zeiger E (2006) Plant Physiology, Fourth edition. Sinauer Associates, Sunderlan, MA

Taiz L, Zeiger E (2010) Plant Physiology, Fifth edition. Sinauer Associates, Sunderlan, MA

Takizawa K, Nakamura H (1998) Separation and determination of fluorescein isothiocyanate-labeled amino acids by capillary electrophoresis with laser-induced fluorescence detection. Anal Sci **14**: 925–928

Tamaoki M, Mukai F, Asai N, Nakajima N, Kubo A, Aono M, Saji H (2003) Light-controlled expression of a gene encoding L-galactono-γ-lactone dehydrogenase which affects ascorbate pool size in *Arabidopsis thaliana*. Plant Sci **164**: 1111–1117

Tava A, Scotti C, Avato P (2010) Biosynthesis of saponins in the genus *Medicago*. Phytochem Rev **10**: 459–469

Thimm O, Bläsing O, Gibon Y, Nagel A, Meyer S, Krüger P, Selbig J, Müller LA, Rhee SY, Stitt M (2004) MAPMAN: a user-driven tool to display genomics data sets onto diagrams of metabolic pathways and other biological processes. Plant J **37**: 914–939

Timperio AM, Egidi MG, Zolla L (2008) Proteomics applied on plant abiotic stresses: Role of heat shock proteins (HSP). J Proteomics **71**: 391–411

Trachsel S, Kaeppler SM, Brown KM, Lynch JP (2011) Shovelomics: high throughput phenotyping of maize (*Zea mays* L.) root architecture in the field. Plant Soil **341**: 75–87

Trenberth KE, Dai A, van der Schrier G, Jones PD, Barichivich J, Briffa KR, Sheffield J (2013) Global warming and changes in drought. Nat Clim Chang 4: 17–22

Tuberosa R, Sanguineti MC, Landi P, Michela Giuliani M, Salvi S, Conti S (2002) Identification of QTLs for root characteristics in maize grown in hydroponics and analysis of their overlap with QTLs for grain yield in the field at two water regimes. Plant Mol Biol **48**: 697–712

Tuteja N, Gill SS, Tiburcio AF, Tuteja R (2012) Improving crop resistance to abiotic stress. doi: 10.1002/9783527632930

Uga Y, Sugimoto K, Ogawa S, Rane J, Ishitani M, Hara N, Kitomi Y, Inukai Y, Ono K, Kanno N, et al (2013) Control of root system architecture by DEEPER ROOTING 1 increases rice yield under drought conditions. Nat Genet **45**: 1097–1102

Upchurch RG (2008) Fatty acid unsaturation, mobilization, and regulation in the response of plants to stress. Biotechnol Lett **30**: 967–977

Usadel B, Bläsing OE, Gibon Y, Retzlaff K, Höhne M, Günther M, Stitt M (2008) Global transcript levels respond to small changes of the carbon status during progressive exhaustion of carbohydrates in *Arabidopsis* rosettes. Plant Physiol **146**: 1834–1861

Usadel B, Nagel A, Thimm O, Redestig H, Blaesing OE, Palacios-Rojas N, Selbig J, Hannemann J, Piques MC, Steinhauser D, et al (2005) Extension of the visualization tool MapMan to allow statistical analysis of arrays, display of corresponding genes, and comparison with known responses. Plant Physiol **138**: 1195–1204

Velasquez SM, Ricardi MM, Dorosz JG, Fernandez P V, Nadra AD, Pol-Fachin L, Egelund J, Gille S, Harholt J, Ciancia M, et al (2011) O-glycosylated cell wall proteins are essential in root hair growth. Science 332: 1401–1403

Veljovic-Jovanovic SD, Pignocchi C, Noctor G, Foyer CH (2001) Low ascorbic acid in the *vtc-1* mutant of *Arabidopsis* is associated with decreased growth and intracellular redistribution of the antioxidant system. Plant Physiol **127**: 426–435

Verslues PE, Ober ES, Sharp RE (1998) Root growth and oxygen relations at low water potentials. Impact of oxygen availability in polyethylene glycol solutions. Plant Physiol **116**: 1403–1412

Vincent JM (1970) A Manual for the Practical Study of Root-nodule Bacteria.

Vissenberg K, Fry SC, Verbelen JP (2001) Root hair initiation is coupled to a highly localized increase of xyloglucan endotransglycosylase action in *Arabidopsis* roots. Plant Physiol **127**: 1125–1135

Voetberg GS, Sharp RE (1991) Growth of the maize primary root at low water potentials : III. Role of increased proline deposition in osmotic adjustment. Plant Physiol **96**: 1125–1130

Voothuluru P, Anderson JC, Sharp RE, Peck SC (2016) Plasma membrane proteomics in the maize primary root growth zone: novel insights into root growth adaptation to water stress. Plant Cell Environ **39**: 2043–2054

Waisel Y, Eshel A, Kafkafi U (2002) Plant roots - the hidden half, 3rd ed. doi: 10.1093/aob/mcf252

Wang J, Zhang Z, Huang R (2013) Regulation of ascorbic acid synthesis in plants. Plant Signal Behav **8**: e24536

Wang L, Liu K, Mao S, Li Z, Lu Y, Wang J, Liu Y, Wei Y, Zheng Y (2015) Large-scale screening for *Aegilops tauschii* tolerant genotypes to phosphorus deficiency at seedling stage. Euphytica **204**: 571–586

Wang X, Liu Y, Jia Y, Gu H, Ma H, Yu T, Zhang H, Chen Q, Ma L, Gu A, et al (2012) Transcriptional responses to drought stress in root and leaf of chickpea seedling. Mol Biol Rep **39**: 8147–8158

Warren CR, Adams MA (2000) Capillary electrophoresis for the determination of major amino acids and sugars in foliage: application to the nitrogen nutrition of *Sclerophyllous* species. J Exp Bot **51**: 1147–1157

Wasson AP, Richards RA, Chatrath R, Misra SC, Prasad SVS, Rebetzke GJ, Kirkegaard JA, Christopher J, Watt M (2012) Traits and selection strategies to improve root systems and water uptake in water-limited wheat crops. J Exp Bot **63**: 3485–3498

Watson BS, Bedair MF, Urbanczyk-Wochniak E, Huhman D, Yang DS, Allen SN, Li W, Tang Y, Sumner LW (2015) Integrated metabolomics and transcriptomics reveal enhanced specialized metabolism in *Medicago truncatula* root border cells. Plant Physiol **167**: 1699–1716

van der Weele CM, Spollen WG, Sharp RE, Baskin TI (2000) Growth of *Arabidopsis thaliana* seedlings under water deficit studied by control of water potential in nutrient-agar media. J Exp Bot **51**: 1555–1562

Wei K, Zhong X (2014) Non-specific lipid transfer proteins in maize. BMC Plant Biol **14**: 281–298

Werck-Reichhart D, Bak S, Paquette S (2002) Cytochromes p450. Arab B **1**: e0028

Wheeler GL, Jones MA, Smirnoff N (1998) The biosynthetic pathway of vitamin C in higher plants. Nature **393**: 365–369

Widodo, Patterson JH, Newbigin E, Tester M, Bacic A, Roessner U (2009) Metabolic responses to salt stress of barley (*Hordeum vulgare* L.) cultivars, Sahara and Clipper, which differ in salinity tolerance. J Exp Bot **60**: 4089–4103

Wienkoop S, Larrainzar E, Glinski M, Gonzalez EM, Arrese-Igor C, Weckwerth W (2008) Absolute quantification of *Medicago truncatula* sucrose synthase isoforms and N-metabolism enzymes in symbiotic root nodules and the detection of novel nodule phosphoproteins by mass spectrometry. J Exp Bot **59**: 3307–3315

Wilkinson S, Davies WJ (2010) Drought, ozone, ABA and ethylene: new insights from cell to plant to community. Plant Cell Environ **33**: 510–525

Wilson AM, Harris GA (1966) Hexose-, inositol-, and nucleoside phosphate esters in germinating seeds of crested wheatgrass. Plant Physiol **41**: 1416–1419

Wolucka BA, Van Montagu M (2007) The VTC2 cycle and the *de novo* biosynthesis pathways for vitamin C in plants: An opinion. Phytochemistry **68**: 2602–2613

Wu C, Wang Q, Xie B, Wang Z, Cui J, Hu T (2013) Effects of drought and salt stress on seed germination of three leguminous species. African J Biotechnol **10**: 17954–17961

Wu Y, Cosgrove D (2000) Adaptation of roots to low water potentials by changes in cell wall extensibility and cell wall proteins. J Exp Bot **51**: 1543–1553

Wu Y, Spollen WG, Sharp RE, Hetherington PR, Fry SC (1994) Root growth maintenance at low water potentials (increased activity of xyloglucan endotransglycosylase and its possible regulation by abscisic acid). Plant Physiol **106**: 607–615

Wu Y, Thorne ET, Sharp RE, Cosgrove DJ (2001) Modification of expansin transcript levels in the maize primary root at low water potentials. Plant Physiol **126**: 1471–9147

Xu W, Cui K, Xu A, Nie L, Huang J, Peng S (2015) Drought stress condition increases root to shoot ratio via alteration of carbohydrate partitioning and enzymatic activity in rice seedlings. Acta Physiol Plant **37**: 9–19

Xu W, Ding G, Yokawa K, Baluška F, Li QF, Liu Y, Shi W, Liang J, Zhang J (2013) An improved agar-plate method for studying root growth and response of *Arabidopsis thaliana*. Sci Rep **3**: 1273–1279

Yabuta Y, Maruta T, Nakamura A, Mieda T, Yoshimura K, Ishikawa T, Shigeoka S (2008) Conversion of L-Galactono-1,4-lactone to L-Ascorbate is regulated by the photosynthetic electron transport chain in *Arabidopsis*. Biosci Biotechnol Biochem **72**: 2598–2607

Yabuta Y, Mieda T, Rapolu M, Nakamura A, Motoki T, Maruta T, Yoshimura K, Ishikawa T, Shigeoka S (2007) Light regulation of ascorbate biosynthesis is dependent on the photosynthetic electron transport chain but independent of sugars in *Arabidopsis*. J Exp Bot **58**: 2661–2671

Yemm EW, Cocking EC, Ricketts RE (1955) The determination of amino-acids with ninhydrin. Analyst **80**: 209

Yoshiba Y, Kiyosue T, Nakashima K, Yamaguchi-Shinozaki K, Shinozaki K (1997) Regulation of levels of proline as an osmolyte in plants under water stress. Plant Cell Physiol **38**: 1095–1102

Young JA, Martens E (1991) Importance of hypocotyl hairs in germination of *Artemisia* seeds. J Range Manag **44**: 438–442

Young ND, Bharti AK (2012) Genome-enabled insights into legume biology. Annu Rev Plant Biol **63**: 283–305

Young ND, Debellé F, Oldroyd GED, Geurts R, Cannon SB, Udvardi MK, Benedito VA, Mayer KFX, Gouzy J, Schoof H, et al (2011) The *Medicago* genome provides insight into the evolution of rhizobial symbioses. Nature 480: 520–524

Yousfi N, Slama I, Ghnaya T, Savouré A, Abdelly C (2010) Effects of water deficit stress on growth, water relations and osmolyte accumulation in *Medicago truncatula* and *M. laciniata* populations. C R Biol **333**: 205–213

Youssef C, Aubry C, Montrichard F, Beucher D, Juchaux M, Ben C, Prosperi JM, Teulat B (2016) Cell length instead of cell number becomes the predominant factor contributing to hypocotyl length genotypic differences under abiotic stress in *Medicago truncatula*. Physiol Plant **156**: 108–124

Zabalza A, Gálvez L, Marino D, Royuela M, Arrese-Igor C, González EM (2008) The application of ascorbate or its immediate precursor, galactono-1,4-lactone, does not affect the response of nitrogen-fixing pea nodules to water stress. J Plant Physiol **165**: 805–812

Zabalza A, Gaston S, Sandalio LM, del Río LA, Royuela M (2007) Oxidative stress is not related to the mode of action of herbicides that inhibit acetolactate synthase. Environ Exp Bot **59**: 150–159

Zeid IM, Shedeed ZA (2006) Response of alfalfa to putrescine treatment under drought stress. Biol Plant **50**: 635–640

Zhang JY, Cruz DE Carvalho MH, Torres-Jerez I, Kang Y, Allen SN, Huhman D, Tang Y, Murray J, Sumner LW, Udvardi MK (2014) Global reprogramming of transcription and metabolism in *Medicago truncatula* during progressive drought and after rewatering. Plant Cell Environ **37**: 2553–2576

Zhang M, Barg R, Yin M, Gueta-Dahan Y, Leikin-Frenkel A, Salts Y, Shabtai S, Ben-Hayyim G (2005) Modulated fatty acid desaturation via overexpression of two distinct omega-3 desaturases differentially alters tolerance to various abiotic stresses in transgenic tobacco cells and plants. Plant J **44**: 361–371

Zhang W, Lorence A, Gruszewski HA, Chevone BI, Nessler CL (2009) *AMR1*, an *Arabidopsis* gene that coordinately and negatively regulates the mannose/l-galactose ascorbic acid biosynthetic pathway. Plant Physiol **150**: 942–950

Zhao J, Dixon RA (2010) The “ins” and “outs” of flavonoid transport. Trends Plant Sci **15**: 72–80

upna

Universidad Pública de Navarra
Nafarroako Unibertsitate Publikoa

» *SUPPLEMENTAL DATA*

upna

Universidad Pública de Navarra
Nafarroako Unibertsitate Publikoa

Table S4.1. List of all induced genes in root absorption zone of *M. truncatula* seedlings under drought treatment (≥2-fold, $p \leq 0.05$).

	UP-REGULATED		CONTROL (C)			DROUGHT (D)			AVE C	SE C	AVE D	SE D	P-VALUE	Ratio (D/C)
Probesets	Target Description	Representative Public ID	#1	#2	#3	#1	#2	#3						
Mtr.46426.1.S1_s_at	Cellulose synthase	1767.m00041	227.51	166.95	186.37	306.38	409.11	446.46	193.61	17.85	387.31	41.88	0.013	2.00
Mtr.50397.1.S1_at	Protein of unknown function DUF588	IMGAG|971.m00010	201.07	168.07	185.65	310.11	387.79	412.37	184.93	9.53	370.09	30.82	0.005	2.00
Mtr.9873.1.S1_at	Thioredoxin H2	TC104708	133.65	128.13	154.54	265.49	303.63	264.28	138.77	8.04	277.80	12.92	0.001	2.00
Mtr.36889.1.S1_s_at	NIP3	CX540431	136.01	106.20	130.07	241.92	202.29	301.13	124.09	9.11	248.45	28.72	0.015	2.00
Mtr.36347.1.S1_at	MXA21_90	BE320554	15.06	16.94	14.56	35.20	28.88	29.19	15.52	0.72	31.09	2.06	0.002	2.00
Mtr.13198.1.S1_at	PHAP2B protein	TC97243	15.23	18.27	19.00	31.99	34.66	38.51	17.50	1.16	35.05	1.89	0.001	2.00
Mtr.42503.1.S1_at	Isoflavonoid glucosyltransferase	TC111703	88.74	62.13	76.68	119.49	166.13	170.86	75.85	7.69	152.16	16.39	0.014	2.01
Mtr.40121.1.S1_at	Peroxidase 1C precursor	TC106551	518.72	516.86	474.59	975.58	1033.36	1021.27	503.39	14.41	1010.07	17.59	0.000	2.01
Mtr.38699.1.S1_at	NADH dehydrogenase subunit 2	TC103343	457.54	402.96	391.85	780.05	787.39	953.29	417.45	20.30	840.24	56.56	0.002	2.01
Mtr.13559.1.S1_s_at	LOB domain protein 38	TC98397	171.59	138.17	171.59	326.44	336.65	306.32	160.45	11.14	323.14	8.91	0.000	2.01
Mtr.19019.1.S1_at	No apical meristem (NAM) protein	IMGAG|969.m00019	382.37	332.77	301.54	639.77	805.85	611.96	338.89	23.53	685.86	60.53	0.006	2.02
Mtr.16234.1.S1_at	Allergen V5/Tpx-1 related	IMGAG|818.m00026	56.85	41.27	40.92	104.40	70.10	106.96	46.35	5.25	93.82	11.88	0.022	2.02
Mtr.44569.1.S1_at	Peroxidase precursor	TC97623	1461.29	1147.34	1045.52	2166.57	2432.46	2799.72	1218.05	125.12	2466.25	183.55	0.005	2.02
Mtr.7451.1.S1_at	Unknown	TC112337	28.51	28.78	36.51	56.95	71.77	62.05	31.26	2.62	63.59	4.35	0.003	2.03
Mtr.4723.1.S1_at	Unknown	AL378019	100.29	81.65	108.96	145.39	219.78	227.55	96.97	8.06	197.57	26.19	0.021	2.04
Mtr.40106.1.S1_s_at	Ripening-related protein	TC106511	1222.75	1144.11	975.35	2485.67	1805.87	2524.11	1114.07	72.98	2271.88	233.27	0.009	2.04
Mtr.10910.1.S1_at	Probable xyloglucan endotransglucosylase/hydrolase protein 33 precursor	TC108325	113.75	79.06	90.63	188.36	187.33	202.78	94.48	10.20	192.82	4.99	0.001	2.04
Mtr.1516.1.S1_at	S-receptor kinase-like protein 2	AW257197	30.95	14.97	21.76	37.05	56.94	44.48	22.56	4.63	46.16	5.80	0.034	2.05
Mtr.9617.1.S1_at	Auxin induced proline rich protein	TC103864	21.40	31.18	37.54	51.43	67.24	66.13	30.04	4.69	61.60	5.10	0.010	2.05
Mtr.25983.1.S1_s_at	Pectinesterase 2 precursor	1475.m00044	105.55	99.06	90.93	224.07	156.84	225.50	98.51	4.23	202.14	22.65	0.011	2.05
Mtr.38808.1.S1_at	Class III peroxidase	TC103581	53.51	48.25	48.78	76.93	108.52	123.79	50.18	1.67	103.08	13.80	0.019	2.05
Mtr.12696.1.S1_at	Dimethylaniline monooxygenase (N-oxide-forming)-like protein	TC95640	2276.79	2335.80	2338.46	4996.13	4742.60	4543.01	2317.01	20.13	4760.58	131.11	0.000	2.05
Mtr.45327.1.S1_at	Unknown	TC99383	50.58	62.87	77.72	134.32	148.27	111.31	63.72	7.85	131.30	10.78	0.007	2.06
Mtr.9682.1.S1_at	Disease resistance response protein homolog F12L6.9	TC104060	75.13	55.91	68.58	119.09	135.29	156.96	66.54	5.64	137.12	10.97	0.005	2.06
Mtr.39535.1.S1_at	N-hydroxycinnamoyl/benzoyltransferase-like protein	TC105076	540.01	664.79	708.21	1238.49	1319.36	1395.02	637.67	50.41	1317.62	45.19	0.001	2.07
Mtr.23314.1.S1_at	Unknown	1666.m00045	74.39	54.98	65.05	160.70	107.13	135.38	64.81	5.61	134.40	15.47	0.013	2.07
Mtr.17470.1.S1_at	Unknown	IMGAG|1000.m00022	16.10	16.67	19.41	36.84	28.89	42.62	17.39	1.02	36.12	3.98	0.010	2.08
Mtr.41984.1.S1_at	Lanatoside 15'-O-acetylesterase precursor	TC110505	46.20	38.45	49.80	90.58	97.22	92.43	44.82	3.35	93.41	1.98	0.000	2.08
Mtr.39065.1.S1_at	3-oxo-5-alpha-steroid 4-dehydrogenase	TC104122	46.66	40.91	39.49	84.73	79.27	100.96	42.35	2.19	88.32	6.51	0.003	2.09
Mtr.52180.1.S1_at	Zn-finger, C2H2 type	IMGAG|780.m00022	206.31	143.73	146.31	359.45	319.87	356.86	165.45	20.44	345.39	12.78	0.002	2.09
Mtr.8585.1.S1_at	N3 like protein	TC100726	2317.79	2820.04	3220.05	5200.39	7457.31	4793.81	2785.96	261.02	5817.17	828.43	0.025	2.09
Mtr.39005.1.S1_at	Nitrate transporter	TC104008	864.29	780.27	849.20	1989.92	1571.67	1653.11	831.25	25.86	1738.23	128.02	0.002	2.09
Mtr.1424.1.S1_at	Unknown	AL375121	57.63	48.29	46.83	104.31	97.18	118.01	50.92	3.38	106.50	6.11	0.001	2.09
Mtr.39289.1.S1_at	Flavonoid 1-2 rhamnosyltransferase	TC104594	97.41	73.13	88.25	128.96	214.32	199.27	86.27	7.08	180.85	26.31	0.026	2.10
Msa.3151.1.S1_at	Unknown	TC427	631.47	587.60	636.47	1422.66	1145.96	1321.82	618.51	15.52	1296.81	80.85	0.001	2.10
Mtr.12742.1.S1_at	GAST-like gene product	TC95807	17.97	12.20	10.92	22.42	27.73	36.06	13.70	2.17	28.74	3.97	0.029	2.10
Mtr.11511.1.S1_at	Purple acid phosphatase	TC110155	244.53	160.66	127.96	326.47	421.49	371.79	177.72	34.72	373.25	27.44	0.012	2.10
Mtr.42256.1.S1_at	Major facilitator superfamily antiporter	TC111070	33.36	27.57	32.32	78.69	47.41	69.75	31.08	1.78	65.28	9.30	0.023	2.10
Mtr.8229.1.S1_at	Receptor protein kinase-like protein	CX530393	37.47	35.48	39.46	68.96	94.03	73.80	37.47	1.15	78.93	7.68	0.006	2.11
Mtr.23748.1.S1_s_at	C3HC4-type zinc finger protein family	1693.m00034	16.95	13.92	19.70	37.64	34.57	34.54	16.86	1.67	35.58	1.03	0.001	2.11

Table S4.1 *(continued)*. List of all induced genes in root absorption zone of *M. truncatula* seedlings under drought treatment (≥2-fold, $p \leq 0.05$).

Mtr.42918.1.S1_at	Protein disulfide isomerase	TC94110	176.39	156.82	166.40	377.00	345.58	338.02	166.53	5.65	353.53	11.94	0.000	2.12
Mtr.37046.1.S1_at	Anthranilate N-hydroxycinnamoyl/benzoyltransferase-like protein	TC111146	35.17	36.51	38.15	83.59	55.54	94.62	36.61	0.86	77.92	11.63	0.024	2.13
Mtr.27152.1.S1_at	Cytochrome P450 family protein	AW574247	110.60	118.90	137.53	285.68	240.04	258.31	122.34	7.96	261.35	13.26	0.001	2.14
Mtr.36378.1.S1_at	Apyrase-like protein	BF635526	1360.89	1425.22	1461.23	2962.89	3157.10	2956.04	1415.78	29.35	3025.34	65.91	0.000	2.14
Mtr.37342.1.S1_at	Probable mannitol dehydrogenase	TC100466	47.73	46.45	49.12	80.75	139.16	86.96	47.77	0.77	102.29	18.52	0.042	2.14
Mtr.6192.1.S1_at	PGPS/D10	BI273325	153.53	162.99	161.57	312.94	403.05	316.32	159.36	2.94	344.10	29.49	0.003	2.16
Mtr.42945.1.S1_x_at	Unknown	TC94166	1923.64	2053.40	1855.45	4373.80	4032.23	4200.21	1944.16	58.06	4202.08	98.61	0.000	2.16
Msa.897.1.S1_s_at	Unknown	gi|1592791|gb|X99099.1|MSAIPRP	13.99	18.61	15.33	26.44	39.05	38.13	15.98	1.37	34.54	4.06	0.012	2.16
Mtr.1647.1.S1_at	Unknown	AW684213	54.56	49.64	57.97	129.57	87.74	133.45	54.06	2.42	116.92	14.63	0.013	2.16
Mtr.43058.1.S1_at	Tfm5 protein	TC94445	431.35	319.35	322.19	862.81	719.17	738.98	357.63	36.87	773.65	44.94	0.002	2.16
Mtr.21953.1.S1_at	Glyoxal oxidase amine-terminal protein	1575.m00042	63.30	54.62	39.25	92.97	148.24	99.62	52.39	7.03	113.61	17.42	0.031	2.17
Mtr.37363.1.S1_at	CPRD46 protein	TC100514	82.87	82.78	90.98	205.75	176.37	174.46	85.54	2.72	185.53	10.13	0.001	2.17
Mtr.5168.1.S1_at	AT4g26540/M3E9_30	AW690301	61.21	49.28	45.11	111.60	115.70	110.27	51.86	4.83	112.52	1.63	0.000	2.17
Msa.1714.1.S1_at	Unknown	TC499	81.13	59.11	80.13	151.13	135.80	192.51	73.46	7.18	159.81	16.94	0.009	2.18
Mtr.13825.1.S1_at	Laccase	TC99276	85.13	81.46	82.63	173.83	175.96	194.00	83.07	1.08	181.26	6.40	0.000	2.18
Mtr.17167.1.S1_at	Methyladenine glycosylase	IMGAG|900.m00026	42.01	38.04	31.56	79.91	74.20	89.55	37.20	3.05	81.22	4.48	0.001	2.18
Mtr.38073.1.S1_at	Dihydroflavanol-4-reductase 1	TC102034	27.04	19.48	22.59	61.59	35.89	54.38	23.04	2.20	50.62	7.65	0.026	2.20
Mtr.44844.1.S1_at	Chalcone reductase	TC98216	106.55	106.96	108.04	246.03	262.42	199.76	107.18	0.44	236.07	18.76	0.002	2.20
Mtr.27068.1.S1_at	Unknown	AW257160	265.29	278.20	284.74	637.60	628.49	563.19	276.08	5.71	609.76	23.43	0.000	2.21
Mtr.24929.1.S1_at	NIP3	1778.m00042	64.09	57.01	58.47	123.33	107.83	167.26	59.86	2.16	132.81	17.80	0.015	2.22
Mtr.8436.1.S1_at	Lipoxygenase LoxN3	TC100175	2183.90	1921.04	1720.36	3718.54	4016.86	5199.79	1941.77	134.21	4311.73	452.31	0.007	2.22
Mtr.43937.1.S1_at	At1g60590/F8A5_12	TC96355	106.23	71.03	106.56	198.96	228.84	202.79	94.60	11.79	210.20	9.39	0.002	2.22
Mtr.42836.1.S1_at	Receptor protein kinase-like protein	TC112517	1043.84	895.02	862.56	2184.76	1897.74	2147.19	933.81	55.81	2076.56	90.07	0.000	2.22
Mtr.44300.1.S1_at	Bifunctional nuclease	TC97086	46.22	35.65	40.25	76.04	121.44	74.19	40.71	3.06	90.55	15.45	0.034	2.22
Mtr.21791.1.S1_at	Serine/Threonine kinase family protein	1565.m00048	12.29	9.68	8.31	24.16	23.80	19.66	10.09	1.17	22.54	1.45	0.003	2.23
Mtr.41655.1.S1_at	Unknown	TC109832	608.60	532.09	458.78	1258.97	1225.45	1090.44	533.16	43.25	1191.62	51.51	0.001	2.24
Mtr.14237.1.S1_at	Unknown	IMGAG|1216.m00015	21.31	35.99	19.27	46.48	56.84	68.66	25.53	5.27	57.33	6.41	0.019	2.25
Mtr.35240.1.S1_s_at	Xyloglucan endotransglycosylase hydrolase 1	CX539544	48.21	41.10	36.06	83.71	93.09	104.78	41.79	3.52	93.86	6.09	0.002	2.25
Mtr.45303.1.S1_at	Unknown	TC99322	152.78	138.81	126.29	310.41	213.66	415.96	139.29	7.65	313.34	58.42	0.042	2.25
Mtr.40844.1.S1_at	Diphosphonucleotide phosphatase 1 precursor	TC108163	63.10	67.39	70.99	139.64	165.49	148.10	67.16	2.28	151.08	7.61	0.000	2.25
Mtr.14668.1.S1_at	Nucleoside phosphatase GDA1/CD39	IMGAG|756.m00018	490.37	527.81	543.70	1117.88	1267.61	1128.96	520.62	15.81	1171.48	48.17	0.000	2.25
Mtr.33007.1.S1_at	Breast cancer protein 1	BF637067	66.90	67.24	70.54	142.08	145.53	174.23	68.23	1.16	153.94	10.19	0.001	2.26
Mtr.42102.1.S1_at	Unknown	TC110761	45.13	44.81	49.07	111.66	94.93	107.96	46.33	1.37	104.85	5.07	0.000	2.26
Mtr.12712.1.S1_at	Alpha-expansin	TC95685	186.17	138.08	159.19	354.84	314.00	425.88	161.15	13.92	364.91	32.69	0.005	2.26
Mtr.47022.1.S1_s_at	Wound-inducible protein	1705.m00036	511.92	409.42	476.24	1002.17	883.96	1283.56	465.86	30.04	1056.56	118.52	0.008	2.27
Mtr.13481.1.S1_at	P-glycoprotein	TC98132	23.87	23.97	18.99	42.86	55.57	53.21	22.28	1.64	50.55	3.90	0.003	2.27
Mtr.49432.1.S1_at	flavanone 3-hydroxylase-related	IMGAG|944.m00030	165.26	108.77	113.96	229.37	302.49	352.54	129.33	18.03	294.80	35.76	0.014	2.28
Mtr.42815.1.S1_at	N-hydroxycinnamoyl/benzoyltransferase-like protein	TC112471	7.16	6.13	7.16	13.17	20.24	13.62	6.81	0.34	15.67	2.29	0.019	2.30
Mtr.13653.1.S1_at	Laccase	TC98681	72.33	66.14	67.97	196.64	125.21	154.96	68.82	1.84	158.94	20.71	0.012	2.31
Mtr.23965.1.S1_s_at	Wound-inducible protein	1705.m00053	95.83	73.07	77.96	182.43	158.98	230.71	82.29	6.92	190.71	21.12	0.008	2.32
Mtr.15281.1.S1_at	Transferase	IMGAG|781.m00001	1415.28	1280.80	1310.30	2963.78	2880.21	3469.05	1335.46	40.81	3104.35	183.94	0.001	2.32
Msa.3182.1.S1_at	Unknown	TC64	36.00	28.77	26.71	53.47	65.93	94.01	30.50	2.82	71.14	11.99	0.030	2.33
Mtr.11698.1.S1_at	APETALA3	TC110754	75.40	60.52	57.32	165.13	174.13	118.98	64.41	5.57	152.75	17.08	0.008	2.37

Table S4.1 *(continued)*. List of all induced genes in root absorption zone of *M. truncatula* seedlings under drought treatment (≥2-fold, $p \leq 0.05$).

Mtr.48892.1.S1_at	BURP	IMGAG|820.m00016	16.66	17.00	14.98	38.91	31.77	45.39	16.22	0.62	38.69	3.93	0.005	2.39
Mtr.24264.1.S1_at	LOX1 Lipoxygenase	1726.m00040	103.17	103.68	110.18	228.77	347.45	184.57	105.68	2.26	253.60	48.63	0.038	2.40
Mtr.37470.1.S1_at	Unknown	TC100713	242.80	135.05	132.52	390.02	380.83	457.52	170.12	36.35	409.46	24.18	0.005	2.41
Mtr.42071.1.S1_at	GTP cyclohydrolase I	TC110696	101.88	121.18	115.05	261.49	284.27	277.03	112.71	5.69	274.26	6.72	0.000	2.43
Mtr.21809.1.S1_at	PB1 domain protein	1566.m00053	294.58	292.37	259.74	710.91	809.51	549.44	282.23	11.26	689.95	75.80	0.006	2.44
Mtr.9401.1.S1_at	High mobility group protein 2 (HMG-2)	TC103227	41.46	27.14	31.02	87.79	84.90	70.97	33.21	4.28	81.22	5.19	0.002	2.45
Mtr.10450.1.S1_at	genomic DNA, chromosome 1, PAC clone	TC106817	83.13	83.00	99.96	221.66	196.38	236.58	88.70	5.63	218.21	11.73	0.001	2.46
Mtr.24198.1.S1_s_at	Lipoxygenase	1721.m00031	1108.86	1014.87	881.21	2197.32	2264.22	2952.66	1001.65	66.05	2471.40	241.40	0.004	2.47
Mtr.10893.1.S1_at	Acid phosphatase type 5 precursor	TC108256	258.13	260.75	259.18	576.66	649.96	708.40	259.35	0.76	645.01	38.11	0.001	2.49
Mtr.16274.1.S1_at	Proteinase inhibitor I12	IMGAG|864.m00004	127.83	127.93	114.83	375.57	263.80	282.48	123.53	4.35	307.28	34.57	0.006	2.49
Mtr.35850.1.S1_at	Transcription factor WRKY44	TC97762	19.99	22.09	18.64	44.04	61.78	45.96	20.24	1.00	50.59	5.62	0.006	2.50
Mtr.19818.1.S1_at	Ferritin	IMGAG|1091.m00001	79.28	68.75	77.25	197.67	187.26	179.74	75.09	3.22	188.22	5.20	0.000	2.51
Mtr.18492.1.S1_at	Zinc-containing alcohol dehydrogenase superfamily	IMGAG|953.m00006	30.97	27.26	31.63	45.91	97.58	82.27	29.95	1.36	75.25	15.32	0.042	2.51
Mtr.20779.1.S1_at	Lipoxygenase	IMGAG|1123.m00005	55.87	39.82	38.33	109.25	114.96	113.07	44.67	5.61	112.43	1.68	0.000	2.52
Mtr.11503.1.S1_at	Cold acclimation protein	TC110135	63.77	71.63	53.20	196.94	175.13	104.14	62.87	5.34	158.73	28.01	0.028	2.52
Mtr.51214.1.S1_at	O-methyltransferase, family 2; SAM binding motif	IMGAG|755.m00003	66.27	63.16	49.01	157.28	104.19	191.71	59.48	5.31	151.06	25.46	0.024	2.54
Mtr.11694.1.S1_at	Albumin 1 C precursor (PA1 C)	TC110745	128.98	218.65	208.49	542.13	387.72	483.39	185.38	28.35	471.08	45.00	0.006	2.54
Mtr.20116.1.S1_s_at	ZIM	IMGAG|1101.m00011	39.15	18.22	35.52	101.80	51.96	83.47	30.96	6.46	79.08	14.55	0.039	2.55
Mtr.14934.1.S1_s_at	Gly rich structural protein	IMGAG|722.m00022	12.70	14.44	10.17	21.91	34.26	39.33	12.44	1.24	31.83	5.17	0.022	2.56
Msa.3042.1.S1_s_at	Unknown	TC54	96.32	84.76	69.49	210.68	175.19	262.93	83.52	7.77	216.27	25.48	0.008	2.59
Mtr.47151.1.S1_at	Glutathione S-transferase	1695.m00045	53.57	46.55	41.83	124.63	100.87	143.50	47.32	3.41	123.00	12.33	0.004	2.60
Mtr.14667.1.S1_at	Nucleoside phosphatase GDA1/CD39	IMGAG|756.m00016	87.95	74.05	94.13	240.31	204.76	220.82	85.38	5.94	221.97	10.28	0.000	2.60
Mtr.32803.1.S1_at	Alcohol oxidase p68	BE324295	21.10	24.52	19.96	66.96	32.95	71.19	21.86	1.37	57.03	12.11	0.045	2.61
Mtr.41934.1.S1_at	Pupal cuticle protein (Ecdysone-dependent protein 91)	TC110406	401.77	391.11	379.11	894.08	932.60	1239.23	390.67	6.54	1021.97	109.20	0.004	2.62
Mtr.33453.1.S1_at	Similarity to ATFP3	BG450887	36.82	33.72	39.12	116.28	87.78	83.72	36.55	1.57	95.93	10.25	0.005	2.62
Mtr.40518.1.S1_at	Glutathione S-transferase	TC107455	440.35	403.18	405.29	965.30	1107.02	1205.13	416.28	12.05	1092.48	69.61	0.001	2.62
Mtr.18406.1.S1_at	Sterile alpha motif homology	IMGAG|1031.m00005	57.41	45.19	48.01	141.59	124.29	131.28	50.20	3.69	132.39	5.02	0.000	2.64
Msa.3084.1.S1_at	Unknown	TC87	99.40	87.61	73.40	178.61	227.51	280.90	86.80	7.52	229.01	29.54	0.010	2.64
Mtr.16275.1.S1_at	Proteinase inhibitor I12	IMGAG|864.m00006	3042.62	2725.49	2419.68	7949.77	6059.29	7626.55	2729.26	179.84	7211.87	583.80	0.002	2.64
Mtr.12648.1.S1_at	Ovary protein induced by treatment with gibberellic acid	TC95463	510.96	373.06	338.02	937.63	981.55	1370.65	407.35	52.78	1096.61	137.60	0.009	2.69
Mtr.45103.1.S1_at	GTP cyclohydrolase I	TC98800	139.89	131.75	148.57	358.88	390.13	391.34	140.07	4.86	380.11	10.62	0.000	2.71
Mtr.23132.1.S1_at	Albumin 1 precursor	1654.m00039	669.16	527.46	460.40	1278.16	1396.46	1887.89	552.34	61.53	1520.84	186.68	0.008	2.75
Mtr.37288.1.S1_at	Beta-primeverosidase	TC100298	710.29	549.90	507.34	1667.97	1327.29	1877.64	589.18	61.79	1624.30	160.37	0.004	2.76
Mtr.7344.1.S1_at	Unknown	TC109497	427.04	328.74	326.75	690.80	1293.91	1044.11	360.84	33.10	1009.61	174.95	0.022	2.80
Mtr.43942.1.S1_s_at	Unknown	TC96362	87.57	76.38	76.92	191.52	306.90	176.23	80.29	3.64	224.88	41.24	0.025	2.80
Mtr.42113.1.S1_at	AP2 domain transcription factor-like	TC110781	30.15	29.13	32.89	106.03	65.92	86.43	30.73	1.12	86.13	11.58	0.009	2.80
Mtr.29537.1.S1_at	Unknown	TC105793	50.29	34.29	55.40	173.44	84.35	141.13	46.66	6.36	132.97	26.04	0.032	2.85
Mtr.23132.1.S1_s_at	Albumin 1 precursor	1654.m00039	955.47	881.63	736.90	2150.30	2160.76	3043.03	858.00	64.19	2451.36	295.85	0.006	2.86
Mtr.22601.1.S1_at	Endoxyloglucan transferase	1617.m00030	765.17	606.28	555.61	1459.61	1779.30	2303.00	642.35	63.13	1847.30	245.83	0.009	2.88
Mtr.37368.1.S1_at	At2g22590/T9I22.3	TC100520	115.96	92.13	92.77	191.66	363.79	316.79	100.29	7.84	290.75	51.37	0.021	2.90
Mtr.39873.1.S1_s_at	MYB-like protein	TC105935	23.63	20.58	20.07	43.47	68.23	74.71	21.43	1.11	62.14	9.52	0.013	2.90
Mtr.9227.1.S1_at	Nodulin homologous to narbonin	TC102760	108.94	84.32	49.60	267.00	289.47	149.87	80.95	17.21	235.45	43.28	0.029	2.91
Msa.3055.1.S1_at	Unknown	TC60	66.38	40.11	44.66	124.43	143.62	183.01	50.38	8.11	150.36	17.24	0.006	2.98

Table S4.1 *(continued)*. List of all induced genes in root absorption zone of *M. truncatula* seedlings under drought treatment (≥2-fold, $p \leq 0.05$).

Mtr.8470.1.S1_s_at	Strictosidine-O-beta-D-glucosidase	TC100295	425.62	329.17	255.46	1022.95	817.13	1182.00	336.75	49.27	1007.36	105.62	0.005	2.99
Mtr.5628.1.S1_s_at	Lipoxygenase	BF640256	137.15	140.63	157.45	431.67	467.86	458.34	145.08	6.27	452.62	10.83	0.000	3.12
Mtr.21370.1.S1_x_at	Glycine rich protein	IMGAG|1151.m00029	1580.75	1735.14	1290.24	4657.10	4989.95	5021.38	1535.37	130.42	4889.48	116.54	0.000	3.18
Mtr.5990.1.S1_s_at	Unknown	BG455728	44.06	28.76	29.72	78.43	125.97	125.07	34.18	4.95	109.82	15.70	0.010	3.21
Mtr.50426.1.S1_at	Lipoxygenase	IMGAG|970.m00007	481.10	506.26	508.34	1453.63	1750.06	1649.56	498.57	8.75	1617.75	87.04	0.000	3.24
Mtr.41019.1.S1_at	Specific tissue protein 1	TC108557	1443.12	1267.54	1119.63	4632.04	3339.40	4461.34	1276.76	93.50	4144.26	405.44	0.002	3.25
Msa.1651.1.S1_at	Unknown	TC3	158.03	163.29	111.38	380.52	440.22	594.29	144.23	16.50	471.68	63.68	0.008	3.27
Mtr.44449.1.S1_at	Patatin-like protein	TC97383	30.29	33.30	25.80	94.84	77.95	120.93	29.80	2.18	97.90	12.50	0.006	3.29
Mtr.17550.1.S1_at	Plant lipid transfer protein	IMGAG|1003.m00011	162.79	155.91	125.29	370.66	472.49	631.65	148.00	11.53	491.60	75.95	0.011	3.32
Mtr.29990.1.S1_at	MYB-related protein 306	AW776119	53.21	50.40	44.47	136.29	184.85	176.37	49.36	2.58	165.84	14.97	0.002	3.36
Mtr.38087.1.S1_at	Hyoscyamine 6 beta-hydroxylase	TC102060	143.05	102.29	83.88	285.41	386.96	454.49	109.74	17.48	375.62	49.14	0.007	3.42
Msa.3070.1.S1_s_at	Unknown	TC69	14.71	23.19	18.03	61.40	59.29	71.51	18.64	2.47	64.07	3.77	0.001	3.44
Mtr.13634.1.S1_at	CPRD12 protein	TC98607	69.61	70.38	73.77	278.91	237.18	221.69	71.25	1.28	245.93	17.09	0.001	3.45
Msa.1021.1.S1_at	Unknown	gi|50316683|gb|CO511809.1|CO511809	53.71	56.96	51.44	172.98	174.28	212.95	54.04	1.60	186.74	13.11	0.001	3.46
Mtr.48778.1.S1_x_at	Glycine rich protein	IMGAG|1151.m00030	3098.46	3248.29	2454.32	10022.18	10782.62	9747.34	2933.69	243.56	10184.05	309.63	0.000	3.47
Mtr.50430.1.S1_at	Lipoxygenase	IMGAG|970.m00002	1756.12	1934.30	1786.63	6236.96	6176.87	6956.60	1825.68	55.02	6456.81	250.49	0.000	3.54
Mtr.12256.1.S1_at	Nonspecific lipid-transfer protein precursor (LTP)	TC94138	1158.23	1202.46	902.90	3120.68	3673.19	4824.84	1087.86	93.36	3872.90	501.98	0.005	3.56
Mtr.36333.1.S1_at	Flavonoid 3'-hydroxylase	BE248436	12.03	15.60	14.82	60.54	35.69	57.65	14.15	1.09	51.29	7.85	0.009	3.62
Mtr.40156.1.S1_at	3-hydroxy-3-methylglutaryl coenzyme A	TC106633	54.68	37.73	37.12	177.97	113.25	180.51	43.18	5.76	157.24	22.01	0.007	3.64
Msa.2936.1.S1_at	Unknown	TC1	141.27	174.37	110.57	377.42	521.63	677.02	142.07	18.42	525.36	86.51	0.012	3.70
Mtr.37609.1.S1_at	Unknown	TC101042	32.25	30.35	31.92	130.09	99.23	128.90	31.51	0.59	119.41	10.09	0.001	3.79
Mtr.10364.1.S1_at	Ripening-related protein	TC106509	175.57	169.98	126.99	415.01	708.31	684.32	157.52	15.35	602.55	94.02	0.010	3.83
Mtr.5433.1.S1_at	Unknown	BE323853	137.55	113.97	150.28	369.63	599.58	580.46	133.93	10.64	516.55	73.67	0.007	3.86
Mtr.23130.1.S1_at	Albumin 1 precursor	1654.m00037	486.85	467.30	421.53	1596.87	1475.49	2268.56	458.56	19.35	1780.30	246.63	0.006	3.88
Mtr.44147.1.S1_at	Lipid transfer protein	TC96789	91.86	76.14	77.44	289.91	302.69	362.99	81.81	5.04	318.53	22.53	0.001	3.89
Mtr.8650.1.S1_at	Xyloglucan endotransglycosylase hydrolase 1	TC100920	57.75	49.29	44.47	183.63	172.84	233.49	50.50	3.88	196.65	18.68	0.002	3.89
Mtr.13942.1.S1_at	Polyphosphoinositide binding protein Ssh2p	TC99702	48.82	30.20	34.54	134.38	129.24	182.79	37.85	5.63	148.81	17.06	0.003	3.93
Mtr.5351.1.S1_at	Cuticle protein (YORE-YORE protein)	BE316021	163.55	150.26	148.40	548.76	573.76	695.46	154.07	4.77	605.99	45.31	0.001	3.93
Mtr.42933.1.S1_s_at	Nonspecific lipid-transfer protein precursor (LTP)	TC94143	2446.69	2625.96	2034.63	7171.63	9874.96	11272.21	2369.09	175.06	9439.60	1203.58	0.004	3.98
Msa.1746.1.S1_at	Glutathione S-transferase GST	TC6	187.13	144.63	156.77	564.03	677.83	846.26	162.84	12.64	696.04	81.98	0.003	4.27
Msa.2966.1.S1_s_at	Lipid transfer protein 5 precursor	TC2	1648.91	1742.24	1245.42	5055.17	6945.68	7821.79	1545.53	152.45	6607.55	816.35	0.004	4.28
Mtr.18492.1.S1_s_at	Zinc-containing alcohol dehydrogenase superfamily	IMGAG|953.m00006	19.86	20.36	22.31	62.69	108.36	98.93	20.84	0.75	89.99	13.92	0.008	4.32
Mtr.44034.1.S1_at	Unknown	TC96563	10.82	10.65	13.68	61.74	40.81	51.29	11.72	0.98	51.28	6.04	0.003	4.38
Mtr.28742.1.S1_at	Very-long-chain fatty acid condensing enzyme CUT1	BI312233	76.18	56.30	53.41	189.87	246.85	395.74	61.96	7.16	277.48	61.37	0.025	4.48
Mtr.8427.1.S1_at	Lipoxygenase	TC100141	698.51	629.82	793.96	2621.45	4052.77	2859.59	707.43	47.59	3177.94	442.79	0.005	4.49
Mtr.39293.1.S1_at	Unknown	TC104602	34.36	33.38	29.87	166.79	88.25	184.81	32.53	1.36	146.62	29.64	0.018	4.51
Mtr.28774.1.S1_at	Anthocyanidin synthase	BM812824	37.33	35.44	31.80	187.30	103.97	200.63	34.86	1.62	163.96	30.24	0.013	4.70
Mtr.42933.1.S1_x_at	Nonspecific lipid-transfer protein precursor (LTP)	TC94143	669.82	803.49	537.08	2142.05	3120.78	4627.95	670.13	76.91	3296.93	723.00	0.023	4.92
Msa.1549.1.S1_at	Unknown	gi|50321916|gb|CO517042.1|CO517042	62.89	62.07	42.80	181.28	306.10	354.10	55.92	6.56	280.49	51.51	0.012	5.02
Mtr.12258.1.S1_at	Nonspecific lipid-transfer protein precursor (LTP)	TC94140	678.93	604.50	488.52	2297.30	3603.72	4730.87	590.65	55.40	3543.96	703.15	0.014	6.00
Mtr.12797.1.S1_at	Family II lipase EXL3	TC95982	43.02	42.04	30.79	148.86	254.10	334.44	38.62	3.92	245.80	53.73	0.018	6.37
Mtr.39734.1.S1_at	Probable glutathione S-transferase (Heat shock protein 26A)	TC105598	450.02	365.12	312.26	2173.94	2277.87	2871.32	375.80	40.13	2441.05	217.22	0.001	6.50

Table S4.2. List of all repressed genes in root absorption zone of *M. truncatula* seedlings under drought treatment (≤0.5-fold, $p \leq 0.05$).

DOWN-REGULATED		CONTROL (C)			DROUGHT (D)			AVE C	SE C	AVE D	SE D	P-VALUE	Ratio (D/C)
Target Description	Representative Public ID	#1	#2	#3	#1	#2	#3						
Histidine decarboxylase (Serine decarboxylase)	BG448567	397.19	224.88	227.46	36.66	44.47	36.18	283.18	57.01	39.10	2.69	0.013	0.14
(-)-germacrene D synthase	TC100525	1020.38	1036.88	1096.04	141.60	234.59	169.79	1051.10	22.97	181.99	27.53	0.000	0.17
High affinity nitrate transporter	TC103501	61.48	51.93	42.34	8.41	9.73	12.68	51.92	5.53	10.28	1.26	0.002	0.20
Anther-specific protein	TC94767	4114.29	3829.35	3808.79	693.34	1088.29	572.01	3917.48	98.58	784.55	155.86	0.000	0.20
MtN15 protein precursor	TC99324	420.49	497.72	628.81	61.45	161.13	109.71	515.67	60.80	110.76	28.78	0.004	0.21
Non-cyanogenic beta-glucosidase	AL385713	163.67	193.37	222.82	36.73	56.76	36.82	193.29	17.08	43.44	6.66	0.001	0.22
Cytochrome P450 82A3 (P450 CP6)	TC98420	1739.16	1671.60	1624.92	308.65	504.31	331.27	1678.56	33.16	381.41	61.79	0.000	0.23
expressed protein and genscan	1584.m00048	741.43	572.29	587.11	141.54	194.77	157.76	633.61	54.08	164.69	15.75	0.001	0.26
(-)-germacrene D synthase	TC94781	849.15	718.48	687.64	133.36	313.90	189.67	751.76	49.50	212.31	53.33	0.002	0.28
Peroxidase 1	TC109303	114.15	83.96	90.96	25.71	34.82	23.27	96.36	9.12	27.93	3.52	0.002	0.29
1-deoxy-D-xylulose 5-phosphate synthase 2 precursor	TC95651	603.70	314.65	347.40	116.12	128.21	124.59	421.92	91.38	122.97	3.58	0.031	0.29
Unknown	TC107928	2145.77	1465.87	1310.36	448.58	448.93	537.81	1640.67	256.51	478.44	29.69	0.011	0.29
Sulfotransferase	IMGAG|1250.m00011	87.87	54.18	53.27	17.82	19.47	22.52	65.11	11.38	19.94	1.37	0.017	0.31
conserved hypothetical protein	IMGAG|745.m00023	133.29	119.54	141.20	28.63	52.34	42.52	131.34	6.33	41.16	6.88	0.001	0.31
Unknown	CX532741	39.54	20.25	20.44	8.25	8.60	8.80	26.74	6.40	8.55	0.16	0.047	0.32
Plant protein of unknown function	IMGAG|825.m00016	202.97	156.60	164.18	33.67	78.22	57.52	174.58	14.36	56.47	12.87	0.004	0.32
Unknown	CA920546	565.46	416.27	452.79	104.22	222.29	138.88	478.17	44.90	155.13	35.04	0.005	0.32
Cytochrome P450 71D9 (P450 CP3)	1660.m00069	727.65	636.13	603.36	167.07	259.22	212.19	655.71	37.19	212.83	26.60	0.001	0.32
Class Ib chitinase	TC106402	1521.05	1396.66	1284.30	458.10	443.79	505.89	1400.67	68.37	469.26	18.78	0.000	0.34
Class III peroxidase 70 precursor	TC109304	109.10	93.66	85.25	26.76	37.55	33.20	96.01	6.98	32.50	3.13	0.001	0.34
Hyoscyamine 6-dioxygenase	TC103111	461.79	495.23	512.09	121.27	230.41	152.91	489.70	14.78	168.20	32.42	0.001	0.34
(+)-delta-cadinene synthase isozyme A	AW774638	42.45	24.27	23.52	8.73	12.67	9.66	30.08	6.19	10.35	1.19	0.035	0.34
Cytochrome P450 monooxygenase	TC94158	719.01	648.13	608.23	214.47	212.27	270.94	658.46	32.39	232.56	19.20	0.000	0.35
Macrophage migration inhibitory factor (MIF)	1418.m00029	1841.02	1350.54	1294.34	472.99	603.79	513.96	1495.30	173.62	530.25	38.63	0.006	0.35
Exo70 exocyst complex subunit	IMGAG|1246.m00008	516.39	413.95	401.56	137.13	170.83	166.39	443.97	36.39	158.11	10.57	0.002	0.36
strong similarity to unknown protein	IMGAG|760.m00012	1476.57	876.86	757.08	289.13	464.67	389.48	1036.84	222.57	381.09	50.85	0.045	0.37
Thioredoxin M-type 4, chloroplast precursor	TC107795	2945.07	1723.57	1651.30	601.73	912.04	809.33	2106.64	419.73	774.37	91.27	0.036	0.37
Short-chain dehydrogenase Tic32	AJ503481	391.79	348.15	300.46	91.32	154.11	138.46	346.80	26.37	127.96	18.87	0.003	0.37
FAD linked oxidase, N-terminal	IMGAG|760.m00011	350.88	216.13	192.61	66.00	119.76	95.38	253.20	49.31	93.72	15.54	0.037	0.37
Iron/thiamine transport system	TC110574	68.17	49.92	49.30	16.15	26.73	19.17	55.79	6.19	20.68	3.14	0.007	0.37
D-arabinono-1,4-lactone oxidase-like protein	AJ846328	2305.00	1408.88	1240.79	486.44	735.43	631.23	1651.56	330.30	617.70	72.20	0.038	0.37
Metal transport protein	TC109158	1253.74	1007.94	1025.06	345.96	475.99	415.48	1095.58	79.24	412.48	37.57	0.001	0.38
Hexose transporter HT2	BE240339	635.91	463.10	472.02	142.09	256.20	201.05	523.68	56.18	199.78	32.95	0.008	0.38

Table S4.2 (*continued*). List of all repressed genes in root absorption zone of *M. truncatula* seedlings under drought treatment (≤0.5-fold, $p \leq 0.05$).

Cytochrome P450 71D9 (P450 CP3)	1660.m00069	456.36	411.75	395.25	147.15	178.45	157.90	421.12	18.25	161.17	9.18	0.000	0.38
DNA-binding WRKY	IMGAG|747.m00011	229.81	185.67	173.89	63.55	94.27	69.38	196.46	17.02	75.73	9.42	0.003	0.39
D-arabinono-1,4-lactone oxidase-like protein	AJ846328	1559.13	988.66	806.31	286.13	502.32	508.36	1118.03	226.74	432.27	73.09	0.045	0.39
Unknown	TC108029	419.96	437.79	415.87	159.79	159.49	177.10	424.54	6.73	165.46	5.82	0.000	0.39
Cytochrome P450	TC96912	411.10	379.96	389.42	134.29	186.15	141.21	393.49	9.22	153.88	16.26	0.000	0.39
Caffeoyl-CoA O-methyltransferase-like protein	BM814917	1010.53	849.05	833.71	329.27	331.49	392.51	897.76	56.55	351.09	20.72	0.001	0.39
Geraniol synthase	TC99779	1877.33	1479.11	1253.70	621.90	550.67	630.46	1536.71	182.32	601.01	25.29	0.007	0.39
RGC2-like protein	TC96613	272.77	194.67	204.44	81.13	110.63	71.29	223.96	24.57	87.68	11.82	0.007	0.39
Geraniol 10-hydroxylase	TC110034	846.57	648.37	644.80	253.63	301.53	289.63	713.25	66.67	281.60	14.40	0.003	0.39
Kunitz proteinase inhibitor-1	TC95067	71.41	57.73	75.60	24.74	33.07	23.31	68.25	5.39	27.04	3.04	0.003	0.40
Lipoxygenase	TC100240	4177.31	3058.49	3300.96	1162.79	1614.56	1438.73	3512.25	339.81	1405.36	131.48	0.004	0.40
Hexose transporter HT2	AJ845920	223.06	154.73	181.91	53.71	94.91	80.92	186.57	19.86	76.52	12.10	0.009	0.41
Narbonin	TC101001	3764.34	3446.36	4006.88	1504.69	2046.22	1063.45	3739.19	162.30	1538.12	284.19	0.003	0.41
Unknown	TC105887	71.92	79.27	65.92	26.11	31.59	31.91	72.37	3.86	29.87	1.88	0.001	0.41
Isopenicillin N synthase; 2OG-Fe(II) oxygenase	IMGAG|1112.m00009	192.83	148.55	159.77	56.35	84.77	65.81	167.05	13.29	68.97	8.36	0.003	0.41
T1N6.22 protein	TC104797	331.14	333.63	343.97	141.58	123.36	154.69	336.25	3.93	139.87	9.08	0.000	0.42
Unknown	TC105514	895.38	794.95	708.84	256.50	364.93	381.71	799.72	53.90	334.38	39.24	0.002	0.42
Lipoxygenase	TC100184	149.10	117.47	119.77	44.54	73.13	44.14	128.78	10.18	53.94	9.60	0.006	0.42
Acidic glucanase	TC96172	1157.07	1041.80	855.90	404.61	424.05	456.69	1018.25	87.73	428.45	15.19	0.003	0.42
Cytochrome P450	IMGAG|802.m00006	2606.55	1821.01	1788.40	590.94	1120.86	905.69	2071.99	267.45	872.50	153.87	0.018	0.42
Cytochrome P450	TC105774	259.72	249.23	248.33	78.78	138.64	102.89	252.43	3.66	106.77	17.39	0.001	0.42
Unknown	TC110633	121.96	131.35	116.71	52.29	51.19	53.73	123.34	4.28	52.41	0.73	0.000	0.42
Glutathione S-transferase GST 12	CX550152	4327.10	3176.97	3263.00	1131.18	1950.93	1494.98	3589.02	369.87	1525.70	237.14	0.009	0.43
Lectin-like protein kinase	AL367605	382.40	269.33	284.86	119.36	151.40	127.67	312.20	35.39	132.81	9.60	0.008	0.43
Unknown	TC97487	1220.40	1130.13	1178.99	424.79	609.91	469.35	1176.50	26.09	501.35	55.78	0.000	0.43
Alpha fucosidase precursor	1572.m00054	207.50	141.06	128.13	61.13	69.64	74.10	158.90	24.59	68.29	3.80	0.022	0.43
ADR6 protein	TC100948	5384.54	5648.46	5556.96	2110.58	2721.99	2302.58	5529.99	77.37	2378.38	180.52	0.000	0.43
Receptor-like protein kinase	TC105088	68.46	49.19	43.74	18.07	30.93	20.54	53.79	7.50	23.18	3.94	0.022	0.43
Cytochrome b5 DIF-F	BF635325	439.67	500.90	420.98	169.84	203.13	214.73	453.85	24.14	195.90	13.45	0.001	0.43
Wound-inducible P450 hydroxylase	TC104023	184.05	180.45	177.03	90.71	75.98	67.13	180.51	2.03	77.94	6.88	0.000	0.43
Multidrug resistance-associated protein-like protein	TC104059	79.62	64.04	48.11	22.17	34.55	26.09	63.92	9.10	27.60	3.65	0.021	0.43
Unknown	TC109529	291.69	228.08	194.31	78.96	121.83	107.70	238.03	28.55	102.83	12.61	0.012	0.43
Sulfate transporter protein-like	TC106463	2382.09	1890.71	1958.91	668.82	1225.00	805.14	2077.24	153.69	899.65	167.37	0.007	0.43
Cytochrome P450	BE943181	404.67	303.34	276.29	132.93	136.13	157.33	328.10	39.07	142.13	7.66	0.010	0.43
Protein kinase	BF647597	119.76	117.53	141.09	52.90	66.90	44.13	126.13	7.51	54.64	6.63	0.002	0.43
Unknown	TC97937	544.57	509.27	457.95	182.48	271.49	201.14	503.93	25.15	218.37	27.10	0.002	0.43
Peptidase M10A and M12B, matrixin and adamalysin	IMGAG|1025.m00010	2234.63	2119.30	1969.66	892.13	1015.60	842.67	2107.86	76.70	916.80	51.42	0.000	0.43

Table S4.2 (*continued*). List of all repressed genes in root absorption zone of *M. truncatula* seedlings under drought treatment (≤0.5-fold, $p \leq 0.05$).

Receptor-like protein kinase	TC109408	1923.76	1278.26	1246.05	510.94	803.64	622.38	1482.69	220.73	645.65	85.29	0.024	0.44
VQ motif protein	IMGAG|985.m00022	797.12	513.58	479.98	265.62	237.95	276.62	596.89	100.58	260.06	11.50	0.029	0.44
Galactinol synthase	BG451003	658.69	508.46	539.40	238.01	278.05	227.76	568.85	45.80	247.94	15.34	0.003	0.44
Class I helical cytokine receptor number 17	TC109721	815.59	609.34	582.49	234.48	356.10	288.32	669.14	73.63	292.96	35.19	0.010	0.44
Heavy metal transport/detoxification protein	IMGAG|825.m00011	599.57	466.34	462.96	166.16	299.87	203.63	509.62	44.99	223.22	39.82	0.009	0.44
Unknown	TC97862	113.54	119.52	113.39	54.14	49.94	48.00	115.48	2.02	50.69	1.81	0.000	0.44
GDSL-motif lipase/hydrolase family protein	TC103549	194.16	160.70	143.77	59.02	77.27	83.06	166.21	14.80	73.12	7.24	0.005	0.44
Amino acid transporter-like protein 1	TC100219	80.13	58.16	59.98	28.65	30.26	28.44	66.09	7.04	29.12	0.58	0.006	0.44
Predicted protein	TC110986	687.77	489.82	506.77	194.14	315.12	232.84	561.45	63.35	247.37	35.67	0.012	0.44
Heat shock protein HSP22.7	TC110284	42.01	45.80	38.23	20.38	18.49	16.87	42.01	2.18	18.58	1.01	0.001	0.44
Cytochrome P450	BG587076	208.06	162.94	144.63	77.22	65.43	85.93	171.88	18.85	76.20	5.94	0.008	0.44
2A6 protein	TC109276	611.96	513.96	519.20	215.93	282.24	234.06	548.37	31.83	244.08	19.79	0.001	0.45
Putative receptor-like protein kinase	1742.m00058	110.79	99.44	87.34	36.01	49.69	47.07	99.19	6.77	44.25	4.19	0.002	0.45
F3H-like protein	TC104677	1473.63	1446.79	1349.60	599.15	733.30	590.08	1423.34	37.67	640.85	46.30	0.000	0.45
O-methyltransferase	TC108939	119.39	81.70	74.08	39.40	36.06	48.96	91.72	14.01	41.47	3.87	0.026	0.45
F3H-like protein	TC112116	827.25	771.24	751.75	328.58	418.78	316.90	783.41	22.63	354.75	32.19	0.000	0.45
Cysteine proteinase inhibitor	TC107154	224.54	154.68	137.90	67.12	89.26	77.93	172.37	26.53	78.10	6.39	0.026	0.45
Lectin	BQ157378	51.97	47.19	37.60	18.77	21.49	21.72	45.59	4.23	20.66	0.95	0.005	0.45
Probable WRKY transcription factor 29	TC112282	465.22	311.30	298.69	143.91	188.39	156.03	358.40	53.53	162.78	13.28	0.024	0.45
Alcohol dehydrogenase I	BI263584	46.46	41.69	38.85	22.38	15.31	20.19	42.33	2.22	19.29	2.09	0.002	0.46
Protein kinase; Leucine-rich repeat	IMGAG|1106.m00002	21.58	16.88	14.94	8.65	8.28	7.46	17.80	1.97	8.13	0.35	0.008	0.46
Light repressible receptor protein kinase	TC99628	425.16	337.13	332.96	134.29	198.36	168.09	365.08	30.06	166.91	18.50	0.005	0.46
Cytochrome P450	IMGAG|1087.m00021	112.04	82.88	86.42	35.68	55.75	37.38	93.78	9.19	42.94	6.43	0.011	0.46
Glycine-rich protein	CX538135	120.17	131.63	150.61	39.03	91.81	54.19	134.14	8.88	61.68	15.69	0.016	0.46
MtN1 protein precursor	TC100789	45.98	25.85	30.26	16.03	15.45	15.70	34.03	6.11	15.73	0.17	0.040	0.46
Heat shock protein Hsp70	IMGAG|978.m00004	895.80	971.19	906.29	388.49	441.47	453.79	924.43	23.58	427.92	20.03	0.000	0.46
ABC transporter related	IMGAG|733.m00011	1519.19	1281.21	1376.30	581.51	740.21	618.29	1392.23	69.16	646.67	47.96	0.001	0.46
NBS-LRR-like protein	AJ504337	262.72	181.90	183.06	87.60	103.24	100.83	209.23	26.75	97.22	4.86	0.015	0.46
Glutathione S-transferase GST 19	TC102103	712.35	610.21	640.08	294.06	308.06	310.42	654.21	30.32	304.18	5.11	0.000	0.46
Glutathione S-transferase GST 12	TC95725	8143.39	6485.41	6012.91	2597.02	3829.06	3221.28	6880.57	645.98	3215.78	355.67	0.008	0.47
Flavonoid 3',5'-hydroxylase	BE248260	67.61	80.96	76.89	34.23	37.59	33.80	75.16	3.95	35.21	1.20	0.001	0.47
Pectin methylesterase 9	NP1130399	89.91	62.13	61.29	28.20	35.68	36.12	71.11	9.40	33.33	2.57	0.018	0.47
Cytochrome P450	TC97050	181.96	142.73	137.98	70.00	71.39	75.54	154.22	13.94	72.31	1.66	0.004	0.47
Cytochrome P450 93A3 (P450 CP5)	AJ500027	470.06	387.29	410.61	177.37	218.32	198.92	422.65	24.64	198.21	11.83	0.001	0.47
Alcohol dehydrogenase	TC111275	1524.73	1094.60	1020.23	475.46	650.30	587.59	1213.19	157.24	571.12	51.14	0.018	0.47
Nodulin 6	TC96169	42.83	39.73	38.45	16.34	21.32	19.37	40.34	1.30	19.01	1.45	0.000	0.47

Table S4.2 (*continued*). List of all repressed genes in root absorption zone of *M. truncatula* seedlings under drought treatment (≤0.5-fold, $p \leq 0.05$).

Unknown	TC112496	221.86	164.27	173.18	74.67	123.29	66.04	186.44	17.90	88.00	17.82	0.018	0.47
Trypsin/chymotrypsin inhibitor	TC105872	110.79	84.83	126.29	41.47	72.10	38.57	107.31	12.10	50.71	10.72	0.025	0.47
Flavonoid 3',5'-hydroxylase	CB894445	281.97	300.48	265.73	127.97	138.93	134.32	282.72	10.04	133.74	3.18	0.000	0.47
Tobacco W38/1 PR-1 pathogenesis-related protein	TC94626	139.20	145.87	125.29	81.13	51.09	62.15	136.79	6.06	64.79	8.77	0.003	0.47
Isoflavone synthase	TC106940	1335.86	1569.26	1418.04	658.02	665.78	726.37	1441.05	68.35	683.39	21.61	0.000	0.47
Corallocarpus bainesii 18S ribosomal RNA gene	TC106466	742.31	548.34	615.18	267.18	375.34	262.25	635.28	56.89	301.59	36.90	0.008	0.47
IDS4-like protein	1735.m00025	34.72	27.07	30.52	12.26	19.57	12.01	30.77	2.21	14.61	2.48	0.008	0.47
Unknown	CX533341	62.55	57.93	73.55	28.42	32.07	31.67	64.67	4.63	30.72	1.15	0.002	0.47
Cytochrome P450	TC96849	44.71	41.28	39.77	13.82	25.10	21.05	41.92	1.46	19.99	3.30	0.004	0.48
Kunitz proteinase inhibitor-1	TC95067	40.96	44.75	51.42	21.59	24.49	19.40	45.71	3.06	21.83	1.47	0.002	0.48
Methylesterase	TC112264	243.35	154.65	154.75	71.99	103.54	88.72	184.25	29.55	88.08	9.11	0.036	0.48
Unknown	TC100120	1699.17	1738.12	1754.46	629.52	1045.07	808.02	1730.58	16.40	827.54	120.36	0.002	0.48
X-linked retinitis pigmentosa GTPase regulator-interacting protein 1	MTUCU11TVC	394.90	424.04	384.09	161.54	211.08	203.29	401.01	11.93	191.97	15.38	0.000	0.48
Cytochrome P450	AW687530	606.15	633.96	619.54	324.57	273.32	293.10	619.88	8.03	296.99	14.92	0.000	0.48
NL27	BG585060	47.54	31.55	28.53	14.38	20.65	16.68	35.87	5.90	17.24	1.83	0.039	0.48
Conserved hypothetical protein	IMGAG|1091.m00029	206.43	236.07	229.06	98.33	118.72	105.61	223.85	8.94	107.55	5.97	0.000	0.48
Isoflavone synthase	TC106940	1748.73	1974.86	1807.37	861.64	863.29	933.50	1843.65	67.75	886.14	23.68	0.000	0.48
Unknown	IMGAG|1116.m00009	1254.98	918.05	915.63	450.47	516.63	517.98	1029.55	112.72	495.02	22.28	0.010	0.48
Heat shock protein Hsp20	IMGAG|1174.m00029	2153.24	2598.63	2540.59	893.13	1522.01	1100.00	2430.82	139.80	1171.71	185.05	0.006	0.48
Cytochrome P450 82A4 (P450 CP9)	TC98192	1389.56	1442.64	1411.18	767.57	624.01	662.39	1414.46	15.41	684.66	42.91	0.000	0.48
Cytochrome P450 93A3 (P450 CP5)	AW685151	74.79	62.54	68.85	33.29	38.64	27.99	68.73	3.54	33.31	3.07	0.002	0.48
Unknown	AJ548059	544.16	536.43	639.68	252.55	346.80	237.46	573.43	33.20	278.94	34.21	0.003	0.49
Unknown	TC110146	132.90	91.55	95.54	37.13	65.49	53.28	106.66	13.17	51.97	8.21	0.024	0.49
Unknown	IMGAG|846.m00025	200.60	182.42	215.71	90.24	118.96	83.13	199.58	9.63	97.44	10.95	0.002	0.49
Thaumatin-like protein 1 precursor	TC103744	176.88	131.68	117.57	75.79	43.23	89.28	142.04	17.89	69.43	13.67	0.032	0.49
Conserved hypothetical protein	IMGAG|1206.m00006	3091.46	2819.80	3014.97	1134.72	1786.88	1443.71	2975.41	80.88	1455.11	188.35	0.002	0.49
Dehydration-induced protein RD22-like protein 2	TC95843	797.61	1061.14	1053.15	376.52	714.41	333.31	970.64	86.54	474.75	120.48	0.029	0.49
Putative receptor-like protein kinase	1742.m00054	235.34	213.68	234.46	95.30	137.56	102.35	227.83	7.08	111.73	13.07	0.001	0.49
TIR-similar-domain-containing protein TSDC	TC109733	89.13	69.84	69.36	27.32	50.28	34.38	76.11	6.51	37.33	6.79	0.015	0.49
FAD-linked oxidoreductase family	1469.m00045	1365.07	931.08	852.27	487.64	478.31	582.64	1049.47	159.43	516.19	33.33	0.031	0.49
F1E22.7	TC98678	1854.18	1303.24	1287.16	591.34	923.72	671.12	1481.52	186.38	728.72	100.18	0.024	0.49
Heat shock factor RHSF2	TC95045	871.63	745.80	727.48	338.66	435.16	379.79	781.64	45.30	384.54	27.96	0.002	0.49
Unknown	BG586132	224.35	153.79	149.62	66.00	117.44	77.16	175.92	24.24	86.87	15.62	0.037	0.49
Naringenin-chalcone synthase; Type III	IMGAG|918.m00018	2590.36	2317.15	1977.45	1227.16	876.15	1305.31	2294.98	177.28	1136.21	131.97	0.006	0.50
Similar to GB At1g56300	BG452391	41.18	56.66	53.92	19.05	31.35	24.76	50.58	4.77	25.05	3.55	0.013	0.50
Similar to GB At5g49760	BG645819	454.07	361.41	345.00	153.70	241.39	180.35	386.83	33.95	191.81	25.95	0.010	0.50
Class I heat shock protein	TC100459	89.69	104.56	99.04	40.00	61.96	43.47	97.76	4.34	48.48	6.82	0.004	0.50
Zn-finger, CCHC type	IMGAG|924.m00003	116.80	110.96	119.63	53.98	66.79	51.81	115.80	2.55	57.53	4.67	0.000	0.50
Abscisic acid receptor PYL6	CX533517	916.79	804.90	748.27	411.07	423.22	392.90	823.32	49.51	409.06	8.81	0.001	0.50
TIR-similar-domain-containing protein TSDC	TC111675	153.71	127.04	118.08	60.13	74.22	64.22	132.94	10.70	66.19	4.18	0.004	0.50

Table S4.3. List of all GC-MS identified polar metabolites significantly regulated in root absorption zone of *M. truncatula* seedlings under drought treatment ($p \leq 0.05$).

METABOLITE (Name)	Retention time (min)	CONTROL (C)			DROUGHT (D)			AVE C	SE C	AVE D	SE D	P-VALUE	Ratio (D/C)
		#1	#2	#3	#1	#2	#3						
Canavanine	34.12	0.051	0.044	0.039	0.017	0.025	0.016	0.044	0.004	0.019	0.003	0.006	0.44
Citric Acid	30.68	2.459	2.251	2.154	0.969	1.091	0.973	2.288	0.090	1.011	0.040	0.000	0.44
Pipecolic Acid, N,O-	20.10	0.018	0.019	0.018	0.011	0.012	0.009	0.018	0.000	0.011	0.001	0.001	0.59
Norvaline, DL-	16.52	0.000	0.000	0.000	0.000	0.000	0.000	0.000	0.000	0.000	0.000	0.047	0.59
Fumaric Acid, O,O-	19.61	0.042	0.038	0.039	0.024	0.028	0.019	0.040	0.001	0.024	0.003	0.005	0.60
Malonic Acid, O,O-	15.53	0.178	0.165	0.152	0.110	0.101	0.086	0.165	0.007	0.099	0.007	0.003	0.60
Unknow	16.10	0.001	0.001	0.001	0.001	0.001	0.001	0.001	0.000	0.001	0.000	0.049	0.71
Daidzein (4',7-dihydroxyisoflavone), O,O-	51.45	0.008	0.008	0.008	0.005	0.007	0.006	0.008	0.000	0.006	0.001	0.017	0.73
Unknow	19.85	0.003	0.003	0.003	0.002	0.002	0.002	0.003	0.000	0.002	0.000	0.017	0.74
Unknow	41.22	0.067	0.068	0.062	0.051	0.059	0.045	0.066	0.002	0.052	0.004	0.033	0.79
Unknow	9.68	0.001	0.001	0.001	0.000	0.000	0.000	0.001	0.000	0.000	0.000	0.005	0.84
Unknow	34.21	0.023	0.024	0.023	0.021	0.020	0.020	0.023	0.001	0.020	0.000	0.013	0.88
Unknow	30.95	0.009	0.009	0.009	0.011	0.010	0.010	0.009	0.000	0.010	0.000	0.008	1.12
Pyroglutamic acid	24.12	0.186	0.159	0.161	0.206	0.190	0.208	0.168	0.009	0.201	0.006	0.032	1.20
Unknow	14.65	0.003	0.002	0.003	0.003	0.003	0.003	0.003	0.000	0.003	0.000	0.042	1.22
L-Methionine, N,O	24.02	0.701	0.612	0.619	0.841	0.793	0.730	0.644	0.028	0.788	0.032	0.028	1.22
beta-Galactopyranosyl-1,3-arabinose, D- (1MEOX)	43.64	0.029	0.033	0.030	0.035	0.041	0.037	0.031	0.001	0.038	0.002	0.028	1.23
Adenosine	45.23	0.006	0.005	0.005	0.007	0.007	0.007	0.006	0.000	0.007	0.000	0.031	1.24
Butanoic acid, 2,4-diamino-	28.32	0.051	0.043	0.042	0.059	0.061	0.056	0.045	0.003	0.059	0.002	0.015	1.29
Saccharic Acid, O,O,O,O,O,O-	34.88	0.011	0.012	0.011	0.014	0.016	0.015	0.011	0.000	0.015	0.001	0.008	1.33
Ethanol Amine, N,O,O-	16.34	0.013	0.011	0.014	0.018	0.018	0.015	0.013	0.001	0.017	0.001	0.019	1.34
Cysteine	24.84	0.014	0.013	0.012	0.019	0.018	0.016	0.013	0.001	0.018	0.001	0.014	1.34
Glucopyranose [-H20]	29.46	0.038	0.042	0.045	0.055	0.059	0.055	0.041	0.002	0.056	0.001	0.003	1.36
galactosyl glycerol	39.87	0.026	0.028	0.023	0.034	0.040	0.032	0.026	0.001	0.035	0.003	0.030	1.36
Putrescine	29.11	0.742	0.612	0.606	0.935	0.945	0.812	0.653	0.044	0.897	0.043	0.017	1.37
Unknow	24.65	0.002	0.002	0.002	0.003	0.002	0.003	0.002	0.000	0.003	0.000	0.049	1.40
Saccharic acid	34.57	0.039	0.044	0.042	0.056	0.064	0.063	0.042	0.001	0.061	0.003	0.003	1.46
Unknow	31.66	0.005	0.004	0.004	0.006	0.007	0.007	0.004	0.000	0.006	0.000	0.008	1.48
Ononitol, O,O,O,O,O-	34.34	0.030	0.027	0.026	0.040	0.046	0.038	0.028	0.001	0.041	0.002	0.007	1.49
L-Tryptophan, N,N-ene,O-	38.53	0.023	0.024	0.022	0.035	0.034	0.034	0.023	0.001	0.034	0.000	0.000	1.50

Table S4.3 (*continued*). List of all GC-MS identified polar metabolites significantly regulated in root absorption zone of *M. truncatula* seedlings under drought treatment ($p \leq 0.05$).

Unknow	11.60	0.001	0.001	0.001	0.001	0.001	0.001	0.001	0.000	0.001	0.000	0.004	1.52
Saccharic Acid, O,O,O,O,O,O-	35.14	0.031	0.035	0.034	0.046	0.053	0.054	0.034	0.001	0.051	0.003	0.003	1.52
L-Valine, N,O-	15.86	0.327	0.280	0.276	0.478	0.380	0.487	0.294	0.016	0.448	0.034	0.015	1.52
Unknow	30.29	0.120	0.133	0.137	0.200	0.196	0.202	0.130	0.005	0.199	0.002	0.000	1.53
n-Octyl-beta-D-glucoside, O,O,O,O	40.44	0.014	0.015	0.014	0.026	0.018	0.024	0.015	0.000	0.023	0.002	0.031	1.54
L-Alanine, N,O-	12.66	0.011	0.008	0.009	0.015	0.014	0.017	0.009	0.001	0.015	0.001	0.013	1.59
L-Asparagine	27.42	2.144	1.814	1.943	3.134	3.497	2.773	1.967	0.096	3.135	0.209	0.007	1.59
Unknow	20.27	0.012	0.010	0.010	0.019	0.018	0.016	0.011	0.001	0.018	0.001	0.003	1.61
Proline [+CO2]	25.58	0.005	0.004	0.004	0.008	0.006	0.006	0.004	0.000	0.007	0.001	0.026	1.61
L-Lysine, N,N,N,O-	32.90	0.004	0.004	0.003	0.006	0.007	0.005	0.004	0.000	0.006	0.001	0.016	1.62
L-Asparagine, N,N,O-	27.60	4.015	3.367	3.628	5.970	6.642	5.266	3.670	0.188	5.959	0.397	0.006	1.62
Cysteine, S-methyl-, DL-	21.54	0.003	0.003	0.003	0.005	0.005	0.004	0.003	0.000	0.005	0.000	0.001	1.63
Serine, O-acetyl-	20.73	0.006	0.006	0.006	0.009	0.011	0.009	0.006	0.000	0.010	0.001	0.003	1.63
Unknow	35.86	0.035	0.039	0.039	0.067	0.067	0.053	0.038	0.002	0.062	0.005	0.008	1.65
Trisiloxane, Octamethyl-	11.57	0.002	0.002	0.003	0.004	0.004	0.004	0.002	0.000	0.004	0.000	0.002	1.66
Histidine	32.91	0.394	0.381	0.331	0.646	0.644	0.545	0.368	0.019	0.612	0.033	0.003	1.66
Threitol	23.46	0.003	0.003	0.003	0.004	0.006	0.004	0.003	0.000	0.005	0.001	0.031	1.68
Threitol	23.27	0.002	0.003	0.003	0.004	0.005	0.004	0.002	0.000	0.004	0.000	0.024	1.68
Unknow	30.56	0.017	0.014	0.013	0.024	0.028	0.023	0.014	0.001	0.025	0.002	0.005	1.71
Isobutanoic acid, 3-amino-	22.48	0.003	0.003	0.003	0.006	0.006	0.005	0.003	0.000	0.006	0.000	0.000	1.74
Unknow	19.84	0.002	0.002	0.002	0.004	0.004	0.004	0.002	0.000	0.004	0.000	0.001	1.75
Unknow	24.98	0.013	0.013	0.013	0.022	0.023	0.022	0.013	0.000	0.023	0.000	0.000	1.76
L-Proline, O-	15.02	0.000	0.000	0.000	0.000	0.000	0.000	0.000	0.000	0.000	0.000	0.014	1.79
Unknow	33.22	0.016	0.008	0.009	0.019	0.023	0.017	0.011	0.002	0.020	0.002	0.042	1.80
Glycine, N,N,O-	18.44	0.157	0.119	0.131	0.253	0.233	0.247	0.135	0.011	0.244	0.006	0.001	1.80
L-Glutamine, N,N,O-	29.83	0.136	0.120	0.116	0.234	0.227	0.215	0.124	0.006	0.225	0.006	0.000	1.82
Unknow	32.98	0.039	0.041	0.040	0.070	0.081	0.067	0.040	0.001	0.073	0.004	0.002	1.82
L-Isoleucine, O-	14.94	0.006	0.004	0.006	0.010	0.008	0.011	0.005	0.001	0.010	0.001	0.019	1.83
Unknow	15.72	0.000	0.000	0.000	0.000	0.000	0.000	0.000	0.000	0.000	0.000	0.043	1.85
Allantoin, N,N,N-	34.49	0.008	0.009	0.009	0.018	0.016	0.015	0.009	0.000	0.016	0.001	0.001	1.87

Table S4.3 (*continued*). List of all GC-MS identified polar metabolites significantly regulated in root absorption zone of *M. truncatula* seedlings under drought treatment ($p \leq 0.05$).

L-Serine, N,O,O-	19.77	1.310	1.058	1.121	2.281	2.203	2.072	1.163	0.075	2.185	0.061	0.000	1.88
Unknow	32.56	0.093	0.048	0.052	0.109	0.156	0.108	0.064	0.014	0.124	0.016	0.049	1.93
L-Aspartic Acid, O,O-	21.59	0.006	0.002	0.004	0.010	0.008	0.008	0.004	0.001	0.008	0.001	0.038	1.95
D-(+)-Galactose, O,O,O,O,O- o-methyloxime 1	32.24	0.363	0.360	0.337	0.590	0.771	0.772	0.354	0.008	0.711	0.061	0.004	2.01
Allantoin, N,N,N,N,N-	32.05	0.009	0.008	0.007	0.019	0.016	0.013	0.008	0.001	0.016	0.002	0.010	2.01
D-(-)-Fructose, O,O,O,O,O-o-methyloxime 2	31.88	0.417	0.341	0.344	0.607	0.804	0.808	0.367	0.025	0.740	0.066	0.006	2.01
L-Phenylalanine, N,O-	26.65	0.156	0.131	0.135	0.324	0.253	0.293	0.141	0.008	0.290	0.020	0.002	2.06
D-(-)-Fructose, O,O,O,O,O- o-methyloxime 1	31.69	0.539	0.455	0.445	0.820	1.051	1.125	0.479	0.030	0.999	0.092	0.006	2.08
D-(+)-Galactose, O,O,O,O,O- o-methyloxime 2	32.65	0.051	0.049	0.046	0.084	0.111	0.110	0.049	0.001	0.102	0.009	0.004	2.09
L-Alanine, N,N,O-	19.90	0.004	0.004	0.004	0.008	0.006	0.011	0.004	0.000	0.008	0.001	0.045	2.09
Alanine, beta-	21.67	0.032	0.026	0.028	0.062	0.062	0.058	0.029	0.002	0.061	0.001	0.000	2.11
Unknow	37.55	0.052	0.051	0.047	0.106	0.127	0.097	0.050	0.002	0.110	0.009	0.003	2.19
Unknow	16.28	0.001	0.001	0.001	0.003	0.002	0.002	0.001	0.000	0.002	0.000	0.001	2.21
Unknow	20.07	0.001	0.001	0.001	0.003	0.002	0.002	0.001	0.000	0.002	0.000	0.013	2.22
L-Asparagine, N, O-	25.94	0.142	0.083	0.120	0.287	0.277	0.216	0.115	0.017	0.260	0.022	0.007	2.26
Ononitol	33.46	0.619	0.534	0.533	1.280	1.415	1.179	0.562	0.029	1.291	0.068	0.001	2.30
L-Serine, N,N,O,O-	25.21	0.001	0.001	0.001	0.002	0.002	0.003	0.001	0.000	0.002	0.000	0.013	2.35
Unknow	26.17	0.012	0.011	0.011	0.027	0.030	0.023	0.011	0.000	0.027	0.002	0.001	2.38
Unknow	30.46	0.518	0.483	0.546	1.171	1.352	1.281	0.516	0.018	1.268	0.052	0.000	2.46
Alanine [+CO2]	20.92	0.000	0.000	0.000	0.000	0.001	0.001	0.000	0.000	0.001	0.000	0.012	2.55
Unknow	37.67	0.014	0.013	0.013	0.033	0.045	0.026	0.013	0.000	0.035	0.005	0.018	2.58
Urea, N,N-TMS	16.85	0.019	0.017	0.016	0.046	0.041	0.046	0.017	0.001	0.044	0.002	0.000	2.61
Histidine	37.36	0.003	0.003	0.003	0.007	0.007	0.010	0.003	0.000	0.008	0.001	0.006	2.67
Ascorbic Acid TMS MEOX1	31.80	0.021	0.021	0.022	0.052	0.060	0.061	0.021	0.000	0.058	0.003	0.000	2.74
Unknow	33.75	0.226	0.224	0.234	0.541	0.664	0.677	0.228	0.003	0.628	0.043	0.001	2.75
Unknow	27.46	0.002	0.002	0.001	0.004	0.004	0.004	0.002	0.000	0.004	0.000	0.001	2.77
Ascorbic Acid TMS MEOX2	31.94	0.025	0.018	0.017	0.052	0.060	0.061	0.020	0.003	0.058	0.003	0.001	2.87
Pinitol, D-	30.89	0.011	0.010	0.010	0.029	0.035	0.026	0.010	0.000	0.030	0.003	0.002	3.03
L-Leucine, O-	14.30	0.003	0.002	0.003	0.010	0.007	0.008	0.003	0.000	0.008	0.001	0.006	3.08
L-Valine, trimethylsilyl ester	12.40	0.014	0.006	0.011	0.039	0.031	0.026	0.010	0.002	0.032	0.004	0.008	3.09
Asparagine [-H2O]	23.67	0.290	0.251	0.283	0.997	1.054	0.852	0.275	0.012	0.968	0.060	0.000	3.53
Unknow	30.62	0.109	0.113	0.126	0.346	0.432	0.473	0.116	0.005	0.417	0.037	0.001	3.60
L-Serine, O,O-	17.07	0.002	0.001	0.002	0.008	0.008	0.007	0.002	0.000	0.008	0.000	0.000	4.57
Unknow	19.45	0.000	0.000	0.000	0.001	0.001	0.001	0.000	0.000	0.001	0.000	0.001	4.97
Unknow	45.49	0.000	0.000	0.001	0.003	0.003	0.002	0.000	0.000	0.003	0.000	0.003	5.44

Table S4.4. List of all GC-MS identified nonpolar metabolites significantly regulated in root absorption zone of *M. truncatula* seedlings under drought treatment ($p \leq 0.05$).

METABOLITE (Name)	Retention time (min)	CONTROL (C)			DROUGHT (D)			AVE C	SE C	AVE D	SE D	P-VALUE	Ratio (D/C)
		#1	#2	#3	#1	#2	#3						
Unknow	48.23	0.0018	0.0017	0.0016	0.0010	0.0005	0.0010	0.0017	0.0001	0.0008	0.0002	0.011	0.50
Spinasterol-TMS from M.truncatula seeds	57.17	0.0657	0.0611	0.0573	0.0441	0.0250	0.0322	0.0614	0.0025	0.0338	0.0056	0.011	0.55
Unknow	37.81	0.0003	0.0004	0.0005	0.0003	0.0001	0.0002	0.0004	0.0000	0.0002	0.0000	0.048	0.56
Unknow	37.69	0.0007	0.0011	0.0009	0.0007	0.0005	0.0005	0.0009	0.0001	0.0005	0.0001	0.036	0.60
Tricosanoic acid methyl ester, n-	45.33	0.0061	0.0082	0.0064	0.0040	0.0042	0.0045	0.0069	0.0006	0.0042	0.0002	0.016	0.61
L-Serine, N,O,O-TMS	19.76	0.0085	0.0080	0.0059	0.0042	0.0051	0.0051	0.0075	0.0008	0.0048	0.0003	0.035	0.64
Unknow	26.33	0.0082	0.0092	0.0079	0.0057	0.0060	0.0061	0.0085	0.0004	0.0059	0.0001	0.003	0.70
Ethanolamine (3TMS)	17.31	0.3372	0.3291	0.2910	0.2396	0.2473	0.1946	0.3191	0.0142	0.2272	0.0164	0.013	0.71
Methyl 9,12-(Z,Z)-octadecadienoate	36.49	0.1241	0.1193	0.1037	0.0863	0.0830	0.0787	0.1157	0.0062	0.0827	0.0022	0.007	0.71
Methyl Tetracosanoate	46.80	0.0024	0.0025	0.0022	0.0020	0.0014	0.0018	0.0024	0.0001	0.0018	0.0002	0.039	0.74
Methyl hexadecanoate	33.18	0.0376	0.0353	0.0305	0.0272	0.0257	0.0241	0.0345	0.0021	0.0257	0.0009	0.018	0.75
Octadecatrienoic acid methylester, 9,12,15-(Z,Z,Z)-, n-	36.60	0.0382	0.0366	0.0326	0.0299	0.0259	0.0268	0.0358	0.0017	0.0275	0.0012	0.016	0.77
Pentadecanoic acid, methyl ester	31.12	0.0010	0.0010	0.0009	0.0007	0.0008	0.0007	0.0010	0.0000	0.0007	0.0000	0.022	0.77
Unknow	47.08	0.0076	0.0068	0.0065	0.0058	0.0056	0.0049	0.0070	0.0003	0.0054	0.0003	0.021	0.77
galactosyl glycerol 6TMS	39.88	0.0776	0.0878	0.0753	0.0635	0.0652	0.0578	0.0802	0.0038	0.0622	0.0022	0.015	0.77
Unknow	33.93	0.0046	0.0047	0.0039	0.0034	0.0034	0.0036	0.0044	0.0003	0.0035	0.0001	0.025	0.79
Umbelliferone, O-TMS	31.62	0.1643	0.1716	0.1642	0.1315	0.1388	0.1304	0.1667	0.0025	0.1336	0.0026	0.001	0.80
Cellobiose, MEOX (8-TMS) minor; Glu beta (1-4) Glu)	46.97	0.0138	0.0119	0.0117	0.0103	0.0103	0.0093	0.0125	0.0007	0.0100	0.0003	0.030	0.80
Galactopyranoside, 1-O-methyl-, alpha- (4TMS)	30.68	0.0162	0.0179	0.0149	0.0138	0.0141	0.0125	0.0163	0.0009	0.0135	0.0005	0.047	0.83
Unknow	40.56	0.0033	0.0036	0.0033	0.0054	0.0053	0.0044	0.0034	0.0001	0.0051	0.0003	0.009	1.49
Methyl Docosanoate	43.80	0.0118	0.0128	0.0115	0.0200	0.0199	0.0169	0.0120	0.0004	0.0190	0.0010	0.003	1.58
Cadaverine (4TMS)	31.24	0.1352	0.1545	0.1503	0.3081	0.2112	0.2636	0.1467	0.0059	0.2610	0.0280	0.016	1.78
Arachinyl Alcohol, O-TMS	40.88	0.0062	0.0047	0.0050	0.0140	0.0150	0.0119	0.0053	0.0005	0.0137	0.0009	0.001	2.58

Table S4.5. List of all UHPLC-QTOF-MS identified metabolites significantly regulated in root absorption zone of *M. truncatula* seedlings under drought treatment ($p \leq 0.05$).

METABOLITE (Name)	CONTROL (C)			DROUGHT (D)			AVE C	SE C	AVE D	SE D	P-VALUE	Ratio (D/C)
	#1	#2	#3	#1	#2	#3						
447.09276(6.732,Luteolin-4'-O-glucoside_AUT_QQQ)	0.004	0.001	0.002	0.000	0.000	0.000	0.0025	0.0008	0.0003	0.0001	0.0487	0.111
447.0919(6.7914,Kaempferol hexoseose (Put_YDS))	0.004	0.001	0.003	0.000	0.000	0.000	0.0025	0.0008	0.0003	0.0001	0.0498	0.111
492.1024(3.22,8-Methylsulfinyl-n-octyl glucosinolate (Put(Lit+emp)_DH))	0.000	0.001	0.000	0.000	0.000	0.000	0.0005	0.0001	0.0001	0.0000	0.0035	0.183
269.04502(6.87,7,3',4'-Trihydroxyisoflavone Precursor m/z267_AUT_QQQ)	0.073	0.071	0.068	0.018	0.021	0.006	0.0709	0.0015	0.0150	0.0044	0.0003	0.211
269.04502(6.87,7,3',4'-Trihydroxyisoflavone Precursor m/z269_AUT_QQQ)	0.073	0.071	0.068	0.018	0.021	0.006	0.0709	0.0015	0.0150	0.0044	0.0003	0.211
315.08689(12.546,5,6-dihydroxy-3',4'-dimethoxy-flavanone_AUT_QQQ)	0.001	0.001	0.001	0.000	0.000	0.000	0.0008	0.0000	0.0002	0.0001	0.0004	0.235
447.09276(4.624,Orientin (Luteolin 8-C-glucoside) m/z 445_AUT_QQQ)	0.001	0.001	0.001	0.000	0.000	0.000	0.0010	0.0001	0.0002	0.0001	0.0046	0.238
447.09276(4.624,Orientin (Luteolin 8-C-glucoside) m/z 447_AUT_QQQ)	0.001	0.001	0.001	0.000	0.000	0.000	0.0010	0.0001	0.0002	0.0001	0.0046	0.238
449.108(2.45,Pelargonidin-3-glucoside_AUT)	0.126	0.115	0.130	0.049	0.000	0.042	0.1237	0.0044	0.0304	0.0151	0.0040	0.246
297.07632(12.481,3(3',4'-Dimethoxyphenyl)-7-hydroxycoumarin_AUT_QQQ)	0.001	0.001	0.001	0.000	0.000	0.000	0.0006	0.0001	0.0002	0.0000	0.0050	0.258
297.0761(12.51,3,3',4'-Methoxy-phenylo-7-OH-Coumarin_AUT)	0.001	0.001	0.001	0.000	0.000	0.000	0.0006	0.0001	0.0002	0.0000	0.0050	0.258
445.079(6.51,Quercitrin_AUT)	0.013	0.014	0.012	0.003	0.004	0.003	0.0127	0.0006	0.0033	0.0003	0.0001	0.259
367.3582(35.8388,Lignoceric acid (Put_YDS))	0.024	0.028	0.012	0.008	0.006	0.006	0.0213	0.0048	0.0064	0.0007	0.0375	0.302
267.02937(10.187,Coumestrol_AUT_QQQ)	0.028	0.024	0.023	0.007	0.008	0.008	0.0249	0.0014	0.0078	0.0003	0.0003	0.314
255.0662(8.133,Liquiritigenin_AUT)	0.010	0.008	0.008	0.003	0.003	0.003	0.0087	0.0005	0.0028	0.0001	0.0003	0.327
255.0661(8.0839,Liquiritigenin (Put_MB))	0.010	0.008	0.008	0.003	0.003	0.003	0.0087	0.0005	0.0029	0.0001	0.0003	0.330
285.0398(10.61,Kaempferol_AUT)	0.000	0.000	0.000	0.000	0.000	0.000	0.0004	0.0000	0.0001	0.0000	0.0013	0.336
313.0713(15.84,Irisolidone_AUT)	0.000	0.000	0.001	0.000	0.000	0.000	0.0005	0.0001	0.0002	0.0000	0.0075	0.360
367.35763(36.051,Lignoceric acid_AUT_QQQ)	0.000	0.000	0.000	0.000	0.000	0.000	0.0005	0.0000	0.0002	0.0001	0.0077	0.389
447.12915(7.7,Sakuranin (4',5-Dihydroxy-7-methoxyflavanone 5-glucoside)_AUT_QQQ)	0.001	0.001	0.001	0.000	0.000	0.000	0.0009	0.0001	0.0004	0.0000	0.0017	0.402
447.0931(5.399,Luteolin-3'-7-di-O-glucoside (fragment)_AUT)	0.001	0.001	0.001	0.000	0.001	0.001	0.0014	0.0000	0.0006	0.0001	0.0003	0.409
577.15576(6.846,Isorhoifolin (Apigenin-7-O-rutinoside)_AUT_QQQ)	0.010	0.009	0.009	0.004	0.004	0.004	0.0096	0.0004	0.0039	0.0002	0.0002	0.411
593.1508(4.45,Saponari_AUT)	0.057	0.050	0.052	0.020	0.024	0.022	0.0533	0.0020	0.0219	0.0011	0.0002	0.412
358.0234(0.84,Sinigrin (2-Propenyl-glucosinolate)_AUT)	0.003	0.005	0.003	0.002	0.001	0.001	0.0034	0.0006	0.0014	0.0002	0.0396	0.413
577.1584(6.76,Isorhoifolin_AUT)	0.010	0.009	0.010	0.004	0.004	0.004	0.0095	0.0004	0.0040	0.0002	0.0002	0.414
445.1135(10.75,Sissotrin (Biochanin A-7-O-glucoside)_AUT_QQQ)	0.000	0.000	0.000	0.000	0.000	0.000	0.0002	0.0000	0.0001	0.0000	0.0416	0.471
445.1135(10.75,Sissotrin (Biochanin A-7-O-glucoside) Precursor m/z 505_AUT_QQQ)	0.000	0.000	0.000	0.000	0.000	0.000	0.0002	0.0000	0.0001	0.0000	0.0416	0.471
271.0606(6.83,Naringenin-7-O-glucoside - aglycone_AUT)	0.005	0.004	0.004	0.002	0.003	0.002	0.0042	0.0003	0.0021	0.0002	0.0041	0.511
973.4977(14.5488,Hexose-hexose-hexose-Bayogenin (Put_MB))	0.002	0.002	0.002	0.001	0.001	0.001	0.0019	0.0001	0.0010	0.0002	0.0204	0.515
381.0609(4.84,Scopoletin (dimer)_AUT)	0.005	0.005	0.005	0.003	0.003	0.002	0.0050	0.0002	0.0026	0.0003	0.0017	0.521
465.1035(1.96,Cyanidin-3-O-glucoside_AUT)	0.000	0.000	0.000	0.000	0.000	0.000	0.0002	0.0000	0.0001	0.0000	0.0009	0.523
253.0481(8.25,Daidzein_AUT)	0.001	0.001	0.001	0.001	0.001	0.000	0.0009	0.0001	0.0005	0.0000	0.0071	0.526

Table S4.5 (*continued*). List of all UHPLC-QTOF-MS identified metabolites significantly regulated in root absorption zone of *M. truncatula* seedlings under drought treatment ($p \leq 0.05$).

227.07084(6.95,Resveratrol_AUT_QQQ)	0.000	0.000	0.000	0.000	0.000	0.000	0.0002	0.0000	0.0001	0.0000	0.0272	0.542
283.0607(9.08,Glycitein_AUT)	0.035	0.034	0.032	0.016	0.020	0.019	0.0334	0.0010	0.0182	0.0012	0.0007	0.545
353.08728(2.375,Chlorogenic acid m/z351_AUT_QQQ)	0.000	0.000	0.000	0.000	0.000	0.000	0.0004	0.0001	0.0002	0.0000	0.0317	0.551
353.08728(2.375,Chlorogenic acid m/z353_AUT_QQQ)	0.000	0.000	0.000	0.000	0.000	0.000	0.0004	0.0001	0.0002	0.0000	0.0317	0.551
271.06067(9.906,Naringenin (+/-)_AUT_QQQ)	0.003	0.003	0.003	0.001	0.002	0.002	0.0029	0.0001	0.0016	0.0002	0.0046	0.559
271.0598(10.07,Naringenin_AUT)	0.003	0.003	0.003	0.001	0.002	0.002	0.0029	0.0001	0.0016	0.0002	0.0046	0.559
285.0389(1.96,Cyanidin-3-O-glucoside_AUT)	0.005	0.005	0.005	0.003	0.004	0.002	0.0052	0.0001	0.0029	0.0004	0.0045	0.563
267.06576(12.074,7-Hydroxy-4'-methoxyflavone (Pratol)_AUT_QQQ)	0.000	0.001	0.001	0.000	0.000	0.000	0.0005	0.0000	0.0003	0.0001	0.0188	0.565
455.3562(32.81,Boswellic acid, alpha_AUT)	0.000	0.000	0.000	0.000	0.000	0.000	0.0003	0.0000	0.0002	0.0000	0.0302	0.573
339.1241(18.64,Desmethylxanthohumol_AUT)	0.000	0.000	0.000	0.000	0.000	0.000	0.0001	0.0000	0.0001	0.0000	0.0188	0.594
267.0656(8.64,Ferulic acid)	0.024	0.022	0.023	0.012	0.016	0.014	0.0231	0.0005	0.0140	0.0013	0.0026	0.606
267.0663(8.47,Formononetin-7-O-glucoside_AUT)	0.024	0.022	0.023	0.012	0.016	0.014	0.0231	0.0005	0.0140	0.0013	0.0026	0.607
303.0505(4.93,Taxifolin (3,3',4',5,7-pentahydroxylflavanone) m/z 301_AUT_QQQ)	0.002	0.002	0.002	0.001	0.001	0.001	0.0016	0.0001	0.0010	0.0000	0.0007	0.609
303.0505(4.93,Taxifolin (3,3',4',5,7-pentahydroxylflavanone) m/z 303_AUT_QQQ)	0.002	0.002	0.002	0.001	0.001	0.001	0.0016	0.0001	0.0010	0.0000	0.0007	0.609
359.07672(12.051,5,7,4'-Trihydroxy-6,3',5'-trimethoxyflavone_AUT_QQQ)	0.000	0.000	0.000	0.000	0.000	0.000	0.0003	0.0000	0.0002	0.0000	0.0429	0.611
137.02389(2.101,Protocatechuic aldehyde (3,4-Dihydroxybenzaldehyde)_AUT_QQQ)	0.009	0.009	0.008	0.006	0.007	0.003	0.0087	0.0004	0.0053	0.0011	0.0495	0.614
253.05011(9.946,3',4'-Dihydroxyflavone_AUT_QQQ)	0.017	0.017	0.018	0.010	0.011	0.011	0.0171	0.0004	0.0106	0.0004	0.0003	0.618
253.0477(10,4',6-Dihydroxy aurone_AUT)	0.017	0.017	0.018	0.010	0.011	0.011	0.0171	0.0004	0.0106	0.0004	0.0003	0.619
319.21209(16.927,n-Decyl-beta-D-glucopyranoside_AUT_QQQ)	0.000	0.000	0.000	0.000	0.000	0.000	0.0002	0.0000	0.0001	0.0000	0.0206	0.623
114.01914(0.725,N-Hydroxysuccinimide_AUT_QQQ)	0.004	0.003	0.003	0.002	0.003	0.002	0.0036	0.0002	0.0023	0.0002	0.0084	0.627
128.07118(0.718,L-Pipecolic acid_AUT_QQQ)	0.000	0.000	0.000	0.000	0.000	0.000	0.0002	0.0000	0.0001	0.0000	0.0402	0.629
191.03446(4.713,Scopoletin_AUT_QQQ)	0.003	0.003	0.003	0.002	0.002	0.002	0.0030	0.0001	0.0019	0.0001	0.0009	0.634
191.0344(4.9,Scopoletin_AUT)	0.003	0.003	0.003	0.002	0.002	0.002	0.0030	0.0001	0.0019	0.0001	0.0009	0.634
461.07203(5.156,Scutellarein-7-glucuronide (scutellarin)_AUT_QQQ)	0.000	0.000	0.000	0.000	0.000	0.000	0.0003	0.0000	0.0002	0.0000	0.0192	0.667
471.13(9.7,formononetin_7_O_glucoside_malonate (-COO))	0.003	0.003	0.004	0.002	0.002	0.002	0.0032	0.0003	0.0023	0.0001	0.0413	0.703
111.01948(0.725,Uracil_AUT_QQQ)	0.078	0.080	0.081	0.054	0.063	0.054	0.0798	0.0012	0.0571	0.0028	0.0018	0.715
433.1121(3.824,Naringenin chalchone 4-O-glucoside (Put_MB))	1.621	1.547	1.514	1.241	1.211	1.130	1.5607	0.0315	1.1944	0.0331	0.0013	0.765
283.0603(7.3836,Biochanin A (Put_YDS))	0.013	0.016	0.016	0.010	0.012	0.013	0.0149	0.0007	0.0117	0.0009	0.0491	0.787
299.0566(10.894,Chrysoecin_AUT)	0.008	0.009	0.009	0.007	0.007	0.007	0.0085	0.0001	0.0071	0.0002	0.0017	0.836
299.057(11.07,Diosmetin_AUT)	0.008	0.009	0.009	0.007	0.007	0.007	0.0085	0.0001	0.0071	0.0002	0.0017	0.836
299.05559(11.097,Diosmetin_AUT_QQQ)	0.008	0.009	0.009	0.007	0.007	0.007	0.0085	0.0001	0.0071	0.0002	0.0017	0.836

Table S4.5 (*continued*). List of all UHPLC-QTOF-MS identified metabolites significantly regulated in root absorption zone of *M. truncatula* seedlings under drought treatment ($p \leq 0.05$).

299.05559(11.12,Hispidulin_AUT_QQQ)	0.008	0.009	0.009	0.007	0.007	0.007	0.0085	0.0001	0.0071	0.0002	0.0017	0.836
343.0826(15.48,Nevadensin_AUT)	0.000	0.000	0.000	0.000	0.000	0.000	0.0001	0.0000	0.0001	0.0000	0.9794	1.014
647.3766(14.5771,Hexose-Gypsogenic acid (Put_MB))	0.066	0.064	0.066	0.068	0.074	0.074	0.0652	0.0005	0.0719	0.0020	0.0285	1.104
973.4993(12.8304,Hexose-hexose-hexose-Bayogenin (Put_MB))	0.601	0.575	0.571	0.628	0.684	0.672	0.5824	0.0096	0.6616	0.0170	0.0152	1.136
973.5025(12.84,hexose-hexose-hexose-Bayogenin (Put_MB))	0.601	0.575	0.571	0.628	0.684	0.672	0.5824	0.0096	0.6616	0.0170	0.0152	1.136
811.4469(12.441,Glucose-glucose-Bayogenin (Put_DH))	0.421	0.419	0.409	0.461	0.496	0.523	0.4161	0.0036	0.4937	0.0179	0.0133	1.186
811.4475(12.47,Hexose-hexose-Bayogenin (Put_DH))	0.421	0.419	0.409	0.461	0.496	0.523	0.4161	0.0036	0.4937	0.0179	0.0133	1.186
811.4449(12.8105,Glu Glu Bayogenin Fragment to 973 (-162) (Put_MB))	0.421	0.419	0.409	0.462	0.496	0.523	0.4161	0.0036	0.4940	0.0177	0.0125	1.187
811.4505(13.2,Hexose-hexose-Bayogenin (Put_DH))	0.135	0.141	0.139	0.163	0.170	0.165	0.1381	0.0018	0.1664	0.0020	0.0005	1.205
809.4335(15.29,Hexose-hexoseA-Hederagenin (Put_DH))	0.028	0.030	0.030	0.033	0.039	0.037	0.0294	0.0005	0.0363	0.0018	0.0205	1.236
973.4997(10.2012,hexose-hexose-hexose-Bayogenin (Put_MB))	0.009	0.009	0.009	0.010	0.013	0.011	0.0090	0.0001	0.0111	0.0007	0.0442	1.244
287.0545(2.4,Catechin (fragment)_AUT)	0.002	0.002	0.002	0.003	0.002	0.002	0.0018	0.0000	0.0024	0.0001	0.0124	1.302
957.5018(12.4346,Hexose-hexose-Rha-Bayogenin (Put_MB))	0.020	0.025	0.023	0.028	0.033	0.029	0.0226	0.0015	0.0300	0.0014	0.0225	1.324
253.05011(7.709,7,4'-Dihydroxyflavone_AUT_QQQ)	0.014	0.013	0.014	0.020	0.016	0.019	0.0137	0.0003	0.0188	0.0012	0.0139	1.367
795.4526(19.819,Hexose-hexose-Hederagenin (Put_DH))	0.019	0.020	0.018	0.024	0.029	0.025	0.0193	0.0006	0.0263	0.0015	0.0115	1.367
939.4936(13.5333,Dehydrosoyasaponin (Put_MB))	0.012	0.014	0.013	0.018	0.018	0.018	0.0132	0.0007	0.0182	0.0003	0.0025	1.376
175.02429(0.718,D-Glucuronic Acid Lactone_AUT_QQQ)	0.021	0.018	0.019	0.028	0.027	0.025	0.0195	0.0008	0.0268	0.0011	0.0049	1.379
811.4434(16.6846,Hexose-hexose-Bayogenin (Put_MB))	0.179	0.158	0.159	0.213	0.239	0.234	0.1652	0.0068	0.2285	0.0081	0.0039	1.383
925.511(14.827,Rha-hexose-hexose-Soyasapogenol E (fragment of 1087) (Put_MB))	0.139	0.103	0.102	0.157	0.152	0.171	0.1145	0.0121	0.1598	0.0057	0.0278	1.395
647.3831(14.14,Hexose-New Aglycone (Put_DH))	0.014	0.021	0.019	0.023	0.028	0.024	0.0177	0.0020	0.0248	0.0014	0.0459	1.399
925.5173(14.86,Rha-hexose-hexose-SoyE (Put_DH))	0.136	0.103	0.102	0.157	0.152	0.170	0.1138	0.0114	0.1596	0.0054	0.0218	1.403
269.0452(10.4704,Apigenin (Put_MB))	0.013	0.012	0.012	0.017	0.020	0.016	0.0124	0.0004	0.0175	0.0011	0.0123	1.403
269.04502(10.291,Apigenin_AUT_QQQ)	0.013	0.012	0.012	0.017	0.020	0.016	0.0124	0.0004	0.0175	0.0011	0.0132	1.406
911.5005(18.303,Rha-Ara-GlcA-SoyB (Aut_DH))	0.001	0.001	0.001	0.001	0.001	0.001	0.0007	0.0001	0.0010	0.0001	0.0443	1.438
1103.564(14.0897,Hexose-Rha-hexose-hexose-Hederagenin (Put_MB))	0.037	0.037	0.036	0.051	0.056	0.052	0.0368	0.0002	0.0532	0.0016	0.0005	1.447
138.01914(0.925,3-Hydroxypicolinic acid_AUT_QQQ)	0.001	0.001	0.001	0.001	0.001	0.001	0.0007	0.0001	0.0010	0.0001	0.0247	1.455
138.01914(0.947,6-Hydroxynicotinic acid_AUT_QQQ)	0.001	0.001	0.001	0.001	0.001	0.001	0.0007	0.0001	0.0010	0.0001	0.0247	1.455
705.3849(18.28,3-Glc-Malonyl-MedicagenicAcid (Put_DH))	0.012	0.014	0.014	0.019	0.022	0.018	0.0133	0.0008	0.0198	0.0012	0.0105	1.492
987.4791(13.5266,GlcA-Glc-Glc--Bayogenin (Put_MB))	0.057	0.073	0.070	0.096	0.105	0.099	0.0667	0.0048	0.0998	0.0026	0.0038	1.497
633.4041(20.989,Hexose-Hederagenin (Put_DH))	0.006	0.005	0.005	0.006	0.008	0.008	0.0050	0.0003	0.0075	0.0005	0.0150	1.507

Table S4.5 (*continued*). List of all UHPLC-QTOF-MS identified metabolites significantly regulated in root absorption zone of *M. truncatula* seedlings under drought treatment ($p \leq 0.05$).

279.2367(30.6349,Linoleic acid (Put_YDS))	0.212	0.185	0.182	0.257	0.302	0.317	0.1932	0.0096	0.2917	0.0180	0.0085	1.510
663.3777(17.53,3-Glc-Medicagenic Acid (Aut_DH))	0.028	0.021	0.022	0.034	0.039	0.035	0.0237	0.0020	0.0358	0.0015	0.0082	1.512
141.0163(23.9785,18-Hydroxy-9-octadecenoic acid (Put_YDS))	0.000	0.000	0.000	0.000	0.000	0.000	0.0001	0.0000	0.0002	0.0000	0.0467	1.532
663.3756(15.49,Hexose-Medicagenic Acid (Put_DH))	0.022	0.021	0.020	0.031	0.036	0.031	0.0208	0.0007	0.0326	0.0018	0.0038	1.570
1117.5419(13.6447,Rha-hexose-hexose-hexose-Quillaic acid (Put_MB))	0.104	0.109	0.109	0.145	0.197	0.173	0.1074	0.0015	0.1716	0.0152	0.0138	1.597
607.1635(7.98,NeoDiosmin_AUT)	0.000	0.000	0.000	0.000	0.000	0.000	0.0001	0.0000	0.0002	0.0000	0.0066	1.597
957.5092(16.05,Rha-hexose-hexose-Bayogenin (Put_DH))	0.007	0.006	0.006	0.010	0.011	0.009	0.0061	0.0003	0.0097	0.0005	0.0041	1.602
167.0346(4.904,5-Methoxysalicylic acid_AUT)	0.002	0.002	0.002	0.003	0.003	0.003	0.0018	0.0001	0.0029	0.0002	0.0051	1.614
167.03446(4.964,5-Methoxysalicylic acid_AUT_QQQ)	0.002	0.002	0.002	0.003	0.003	0.003	0.0018	0.0001	0.0029	0.0002	0.0051	1.614
167.0346(5.01,2,4,6-Trihydroxyacetophenone_AUT)	0.002	0.002	0.002	0.003	0.003	0.003	0.0018	0.0001	0.0029	0.0002	0.0051	1.614
167.03446(5.046,2,4,6-Trihydroxyacetophenone_AUT_QQQ)	0.002	0.002	0.002	0.003	0.003	0.003	0.0018	0.0001	0.0029	0.0002	0.0051	1.614
649.394(17.44,Hex-Bayogenin (Put_DH))	0.093	0.090	0.085	0.143	0.161	0.136	0.0895	0.0025	0.1466	0.0073	0.0018	1.638
287.05559(4.513,3,7,3',4'-Tetrahydroxyflavanone (Fustin)_AUT_QQQ)	0.000	0.000	0.000	0.000	0.000	0.000	0.0003	0.0000	0.0004	0.0000	0.0026	1.662
501.3211(19.7996,Medicagenic Acid (Put_MB))	0.009	0.006	0.006	0.009	0.014	0.012	0.0069	0.0008	0.0116	0.0015	0.0478	1.685
563.14011(7.25,Apiin (Apigenin-7-apioglucoside)_AUT_QQQ)	0.001	0.002	0.001	0.002	0.003	0.003	0.0016	0.0001	0.0027	0.0002	0.0127	1.728
277.2173(28.606,Linolenic acid (Put_YDS))	0.154	0.144	0.145	0.231	0.279	0.271	0.1478	0.0033	0.2607	0.0149	0.0018	1.763
617.4049(22.001,Hexose-SoyE (Put_DH))	0.001	0.002	0.002	0.002	0.003	0.003	0.0016	0.0001	0.0028	0.0002	0.0078	1.782
973.50084(10.615,Madecassoside_AUT_QQQ)	0.009	0.009	0.009	0.016	0.017	0.014	0.0088	0.0002	0.0157	0.0010	0.0024	1.788
219.17492(13.716,2,6-Di-tert-butyl-4-methylphenol_AUT_QQQ)	0.000	0.000	0.000	0.000	0.000	0.000	0.0002	0.0000	0.0004	0.0000	0.0190	1.868
193.0492(5.37,3-Hydroxy-4-methoxycinnamic acid_AUT)	0.002	0.003	0.003	0.005	0.006	0.005	0.0028	0.0002	0.0053	0.0003	0.0027	1.870
1063.237(11.665,cyanidin_3_O_glucoside_malonate (Dimer))	0.000	0.000	0.000	0.000	0.000	0.000	0.0000	0.0000	0.0001	0.0000	0.0326	1.873
164.05726(1.064,6-Methylguanine_AUT_QQQ)	0.015	0.015	0.015	0.031	0.024	0.029	0.0148	0.0002	0.0277	0.0021	0.0037	1.880
423.42023(36.053,n-Octacosanoic acid_AUT_QQQ)	0.000	0.000	0.000	0.000	0.000	0.000	0.0002	0.0000	0.0003	0.0000	0.0385	1.913
130.08683(0.71,6-Amino-n-hexanoic acid_AUT_QQQ)	0.009	0.009	0.011	0.020	0.016	0.020	0.0097	0.0004	0.0188	0.0014	0.0030	1.934
237.05519(11.889,7-Hydroxyflavone_AUT_QQQ)	0.000	0.000	0.000	0.000	0.000	0.000	0.0001	0.0000	0.0002	0.0000	0.0354	2.002
939.4945(19.2447,Dehydrosoyasaponin (Put_MB))	0.030	0.036	0.032	0.060	0.061	0.076	0.0326	0.0017	0.0656	0.0051	0.0036	2.010
1205.5675(13.756,Gypsogenin (Put_MS/MS_JHS))	0.002	0.001	0.002	0.003	0.003	0.003	0.0016	0.0002	0.0033	0.0000	0.0017	2.023
481.1135(8.3,Silychristin_AUT_QQQ)	0.000	0.000	0.000	0.001	0.001	0.001	0.0003	0.0001	0.0007	0.0000	0.0204	2.036
795.4543(17.945,Gal-GlcA-SoyB (Put_DH))	0.012	0.009	0.012	0.022	0.021	0.023	0.0108	0.0011	0.0220	0.0004	0.0007	2.044
485.327(26.3936,Quillaic acid (Put_MB))	0.006	0.005	0.005	0.010	0.013	0.012	0.0054	0.0005	0.0116	0.0007	0.0022	2.134

Table S4.5 (*continued*). List of all UHPLC-QTOF-MS identified metabolites significantly regulated in root absorption zone of *M. truncatula* seedlings under drought treatment ($p \leq 0.05$).

407.18587(24.88,6,8-Diprenylnaringenin_AUT_QQQ)	0.000	0.000	0.000	0.000	0.000	0.000	0.0000	0.0000	0.0001	0.0000	0.0101	2.168
647.3793(16.8011,Hexose-Quillaic acid (Put_MB))	0.001	0.001	0.001	0.002	0.002	0.003	0.0011	0.0001	0.0025	0.0002	0.0052	2.203
301.0373(5.02,3,7,3',4',5'-Pentahydroxyflavone (Robinetin)_AUT)	0.000	0.000	0.000	0.001	0.001	0.000	0.0003	0.0001	0.0007	0.0001	0.0408	2.212
1205.5549(13.83,Many possible_3x Arab/xyl, 2x hexose (Put_MS/MS_JHS))	0.001	0.001	0.002	0.003	0.003	0.004	0.0014	0.0003	0.0032	0.0003	0.0103	2.292
451.1235(3.09,Epicatechin-3-Glucoside_AUT)	0.011	0.012	0.009	0.020	0.027	0.027	0.0107	0.0009	0.0246	0.0023	0.0048	2.300
1119.5621(12.64,Rha-hexose-hexose-hexose-Bayogenin (Put_DH))	0.001	0.001	0.000	0.001	0.002	0.002	0.0006	0.0001	0.0015	0.0001	0.0037	2.516
455.3565(28.83,Ursolic acid_AUT)	0.008	0.007	0.006	0.016	0.020	0.019	0.0071	0.0006	0.0181	0.0013	0.0014	2.569
455.3569(28.77,Oleanolic acid_AUT)	0.008	0.007	0.006	0.016	0.020	0.019	0.0070	0.0007	0.0181	0.0013	0.0014	2.579
455.3538(28.766,Soyasapogenol E (Put_MB))	0.008	0.007	0.006	0.016	0.020	0.019	0.0070	0.0007	0.0182	0.0013	0.0016	2.583
793.4408(19.62,Hexose-hexoseA (Put_DH))	0.001	0.001	0.001	0.003	0.003	0.002	0.0011	0.0002	0.0027	0.0004	0.0183	2.586
471.3485(23.0424,Hederagenin (Put_MB))	0.003	0.003	0.003	0.006	0.007	0.007	0.0026	0.0000	0.0067	0.0005	0.0015	2.617
471.3519(23.07,Hederagenin_AUT)	0.003	0.003	0.003	0.006	0.007	0.007	0.0026	0.0000	0.0067	0.0006	0.0022	2.619
471.3468(25.8634,Echinocystic acid (Put_MB))	0.002	0.002	0.001	0.003	0.005	0.005	0.0016	0.0001	0.0042	0.0005	0.0060	2.665
471.3486(26.543,Aglycone triterpene C30H48O4 (isomer of Hederagenin)(Put_MB))	0.005	0.005	0.005	0.013	0.016	0.016	0.0051	0.0002	0.0149	0.0011	0.0010	2.954
473.111(7.95,apigenin_7_O_glucoside_malonate (-COO))	0.000	0.000	0.000	0.000	0.000	0.000	0.0001	0.0000	0.0003	0.0001	0.0403	3.032
469.3342(24.75,Glycyrrhetinic acid, 18 beta_AUT)	0.000	0.000	0.000	0.001	0.001	0.001	0.0002	0.0001	0.0006	0.0000	0.0063	3.089
469.33181(24.769,Glycyrrhetinic acid, 18 beta-_AUT_QQQ)	0.000	0.000	0.000	0.001	0.001	0.001	0.0002	0.0001	0.0006	0.0000	0.0056	3.163
469.3339(24.82,Glycyrrhetinic acid, 18 alpah_AUT)	0.000	0.000	0.000	0.001	0.001	0.001	0.0002	0.0001	0.0006	0.0000	0.0056	3.163
1265.5499(11.315,Zanhic acid (Put_MS/MS_JHS))	0.000	0.000	0.000	0.001	0.001	0.002	0.0004	0.0000	0.0013	0.0003	0.0485	3.418
193.05011(4.92,Ferulic acid_AUT_QQQ)	0.002	0.001	0.001	0.005	0.002	0.005	0.0012	0.0003	0.0040	0.0010	0.0454	3.497
223.06067(5.208,Sinapic acid_AUT_QQQ)	0.000	0.000	0.000	0.001	0.001	0.001	0.0003	0.0001	0.0011	0.0001	0.0014	3.916
649.3969(17.47,hexose-Bayogenin (Put_DH))	0.005	0.090	0.004	0.143	0.160	0.137	0.0330	0.0287	0.1466	0.0071	0.0185	4.439
485.3257(22.7271,Gypsogenic acid (Put_MB))	0.002	0.005	0.002	0.012	0.016	0.014	0.0029	0.0011	0.0140	0.0010	0.0016	4.880